ORIGIN, MINERALOGY AND DIAGENESIS OF QUATERNARY SEDIMENTS FROM THE NOARLUNGA AND WILLUNGA EMBAYMENTS, SOUTH AUSTRALIA

A thesis submitted by

Richard Ian May

B.Sc. (Melb.)

to

The University of Adelaide

for the degree of

Doctor of Philosophy

Department of Soil Science

Waite Agricultural Research Institute

The University of Adelaide

February, 1992

TABLE OF CONTENTS

LIST OF FIGURES

LIST OF TABLES

LIST OF APPENDICES

SUMMARY

The Quaternary sequence from the Noarlunga and Willunga Embayments has been studied in coastal cliff sections south of Adelaide where excellent exposures enable detailed assessment of the mineralogy, stratigraphy and diagenesis of the Quaternary sediments. Previous investigations of Quaternary sediments in this area have been based on limited data, particularly with regard to mineralogical and diagenetic features and thus have had insufficient evidence to understand the landscape history of the region.

Underlying and interfingering with basal non-marine Quaternary sediments in the Noarlunga and Willunga Embayments is the Early Pleistocene Burnham Limestone of estuarine origin. Thin beds of mottled dolomite associated with smectitic clays overlie this unit and are thought to result from an interaction between continental Mg-rich groundwater and highly saline waters of marine origin reflecting the transition from marine to non-marine environments.

Overlying non-marine sediments have been divided into two newly named stratigraphic units; the Robinson Point and Ngaltinga Formations. The Robinson Point Formation comprises an interbedded sequence of gravels, sands, silts and clays. Upward fining sedimentary cycles grading from cross-bedded gravel and sand to silt or clay are commonly observed with fine-grained sediments in upper parts of these sedimentary cycles displaying thin vertical tubular structures, characteristic yellow-orange reticulate mottling patterns and columnar structures indicative of pedogenic modification of the sediments. The Ngaltinga Formation comprises dominantly massive clays with rare lens-shaped and tabular sand bodies, particularly in upper parts. Carbonate mottles within clays at some localities represent calcareous palaeosols and the increasing incidence of such features in upper parts of the Ngaltinga Formation and the presence of a thick blanket of calcareous material overlying the alluvial sequence indicates gradual change to a drier climate. Both sedimentary units are considered to be of fluvial origin with sands and gravels deposited in distributary channels and finer

sediments representing suspended load deposition in more distal parts of the alluvial plain as overbank sedimentation.

The clay mineralogy of the Quaternary sequence has been investigated in detail following work by Callen (1976; 1977) which showed that clay mineralogy was useful in determining the origins of Tertiary non-marine sediments from northern South Australia. Kaolinite, illite and randomly interstratified illite-smectite are the dominant clay minerals identified in Quaternary sediments from the Noarlunga and Willunga Embayments with lesser amounts of hydroxy interlayered smectite, smectite and halloysite. With the exception of the latter two minerals, all are considered to be of detrital origin and derived from the Mt Lofty Ranges to the east where they form the dominant clay mineral component of present-day soils and sediments. The proportions of clay minerals vary considerably through the sequence with the Robinson Point Formation and coarser sediments containing more kaolinite than illite or randomly interstratified illite-smectite and finer sediments, particularly those from the Ngaltinga Formation, containing higher proportions of illite and randomly interstratified illite-smectite. A study of the clay mineralogy of four size fractions <20μm indicates that illite and expanding clays are concentrated in finest fractions <0.2μm, while kaolinite occurs mostly in fractions >0.2μm. Thus the concentration of kaolinite in coarser sediments appears to reflect primary sedimentation. The increasing proportion of smectitic layers in randomly interstratified illite-smectite together with broadening of diffraction peaks for illite in fine-grained units reflects transformation in intervals with restricted drainage where interlayer K^+ is lost from illitic layers and replaced by hydrated cations. Where smectite is identified in fine-grained sediments from basal parts of the Robinson Point Formation which have been subjected to pedogenesis, a similar transformation reaction from illite and randomly interstratified illite-smectite is postulated. Thus the palaeosols formed on poorly drained parts of the alluvial plain where high water tables existed. Development of goethitic mottling reflects some fluctuation in the level of this water table.

Halloysite occurs in indurated sandy sediments near the base of the Robinson Point Formation where it is associated with elongate pods and thin seams of alunite. Both minerals are interpreted to be of diagenetic origin. In thin section, alunite and halloysite show evidence of stress and precipitation in cracks and such features are thought to represent formation during exposure and desiccation of the sediments. Support for this is given from a study of hydrogen isotopes by Bird *et al* (1989) who suggest that alunite precipitated in equilibrium with evaporated meteoric waters. Compared with surrounding sediments, randomly interstratified illite-smectite and illite are depleted in intervals where halloysite is identified and this suggests that halloysite has formed through diagenesis from these clays. High water tables on the alluvial plains and possibly a swampy environment created reducing conditions where H_2S could be generated from sulphate in groundwaters. Oxidation of the sediments initiated by a lowering of the water table due either to climatic changes, tectonic uplift or lower sea level led to acidic weathering conditions where sulphuric acid generated from H_2S reacted with clay minerals. The clays provided a source of K for alunite formation and Si and Al for halloysite formation.

Ferruginous mottling is present throughout much of the alluvial sequence with the largest, most prominent mottles developed in sandy intervals confined by clay-rich intervals where perched water tables could exist. Petrographic evidence shows that iron appears to precipitate at sites of localised oxidation either along cracks in finer-grained sediments or in pores of coarser sediments. Iron also replaces clay minerals in many samples. Mottling results from reduction and mobilisation of iron followed by oxidation and precipitation at localised sites and reflects fluctuating groundwater levels. Alteration of clay minerals under slightly acidic conditions would make iron available to form mottles. Some silica released during these reactions has precipitated in mottled intervals leading to induration of these zones. Silicification post-dates the initiation of mottle formation and possibly relates to drier local environments in order that Si concentrations in groundwaters were sufficiently high to enable precipitation to occur.

Thus a study of the sedimentary and diagenetic history of the Quaternary sequence from the Noarlunga and Willunga Embayments indicates that the sediments were deposited on alluvial fans eminating from the Mt Lofty Ranges. Variation in the nature of the sediments, their mineralogy and diagenetic components provide evidence for a gradual change in both the amount of sediment available in source areas and the climatic regime prevailing during the Quaternary period. Coarser sediments, particularly of the Robinson Point Formation, which dominate basal parts of the sequence indicate that there was an abundant supply of sediment in source regions due to uplift in these areas and/or a wetter climate than that which occurs in the region today. The dominance of finer sediments in upper parts of the sequence, particularly in the Ngaltinga Formation, and the increasing proportion of calcareous sediment suggests a declining supply of sediment from the Mt Lofty Ranges and an increasingly arid climate. Development and preservation of palaeosols in basal parts of the sequence indicate episodic deposition in an aggradational environment. The presence of smectite, alunite and halloysite in associated sediments suggests high water tables and a moist climate whereas palaeosols in the Ngaltinga Formation dominated by carbonate mottles and the preservation of detrital clay minerals with only minor transformation confirm conditions with limited leaching and lower water tables.

DECLARATION

This thesis contains no material which has been accepted for the award of any other degree or diploma in any university. To the best of the author's knowledge and belief, this thesis contains no material previously published or written by another person, except where due reference is made in the text of the thesis.

Richard May

February, 1992

NAME: RICHARD IAN MAY **COURSE:** PhD

I give consent to this copy of my thesis, when deposited in the University Library, being available for loan and photocopying.

SIGNED:

DATE: 23/2/92

ACKNOWLEDGEMENTS

I thank my two supervisors, Professor J. M. Oades of the Department of Soil Science and Dr A. R. Milnes from CSIRO, Division of Soils for their advice during the period of my study and encouragement to complete this work. Access to laboratory facilities was willingly provided on several occasions when I visited from Perth to continue my studies and this has made the task of completing this thesis much easier.

The staff and students in the Department of Soil Science and the staff at CSIRO, Division of Soils have willingly provided information and assistance when required. I also thank them for their friendship and good humour during my period in Adelaide. In particular, I have enjoyed many interesting and challenging hours in the field with Bob Bourman and Sally Phillips and gratefully acknowledge their contributions to this work. Mark Raven was of considerable assistance in completing XRD work and I thank him for his efforts. Neville Alley from the South Australian Department of Mines and Energy provided valuable assistance in looking for microfossils in some samples. The size fractionation and determination of clay minerals from several samples was undertaken by Balwant Singh from the Department of Soil Science and Plant Nutrition at the University of Western Australia and I thank him for his diligence at a time when he too was trying to complete his thesis.

Dr Marjorie Muir from CRA Exploration Pty Ltd, Canberra and Associate Professor Bob Gilkes of the Department of Soil Science and Plant Nutrition, University of Western Australia gladly reviewed earlier drafts of the manuscript and I thank them for their constructive advice. In addition, the laborious task of proof reading an earlier version of this thesis was undertaken with considerable enthusiasm by Lyn May, Chris May and Mary Fant.

My employer, CRA Exploration Pty Ltd has shown considerable patience in helping me complete this research. I thank the staff for their interest and, in particular, Stephan Meyer and Anne Hall for their encouragement and provision of a working environment conducive to finishing this thesis.

Finally, I thank my family for their unending interest in this project, for sharing the highs and lows with me and helping to instil in me the confidence necessary to continue the battle. Your support has been appreciated although not always acknowledged.

CHAPTER 1
INTRODUCTION AND LITERATURE REVIEW

Quaternary sediments are widely distributed throughout southern Australia. They have a conspicuous development in the major saline lake basins of the arid interior of the region, as well as on the margins of these depositional areas as an extensive blanket containing associated palaeosols and soils. In the southern regions, they occur as relatively thick, generally non-marine cappings over Tertiary sediments which were widely deposited in downfaulted basins marginal to the present coastline. Few detailed geological investigations of these Quaternary deposits have been attempted until recent times, due partly to their poor exposure and accessibility in most areas apart from some coastal cliff sections. On the other hand, pedologists generally have long been aware of the importance of these sediments as source materials for the contemporary soils and for an understanding of landscape evolution.

In the Murray Basin, recent investigation of groundwater problems by the BMR (Stephenson 1986; Stephenson & Brown 1989) and aridity in southern Australia during the Late Tertiary and Quaternary at ANU (Bowler 1982; Zhisheng *et al* 1986) has provided additional information regarding Quaternary sediments enlarging upon earlier work undertaken by Firman (1965) and Lawrence (1966; 1976) (see Figure 1.1 for general locations). Adjacent to the Flinders Ranges a comprehensive study of Cainozoic sediments from the Tarkarooloo Basin has been undertaken by Callen (Callen 1976; 1977; Callen & Tedford 1976) while Williams (1969; 1973) has described Quaternary sediments from piedmont regions east of Lake Torrens. Quaternary sediments are well represented in the St Vincent Basin where some of the most accessible outcrops are found in coastal cliffs. Exposures from eastern Yorke Peninsula were described by Crawford (1965) and Stuart (1970), from northern Kangaroo Island by Milnes *et al* (1983) and from the region south of Adelaide by Ward (1965; 1966), Stuart (1969) and Cooper (1985). In the Adelaide Plains Sub-basin and adjacent areas where exposure is poor, Quaternary sediments have been described mainly from drill holes and building excavations (Firman 1966; Lindsay 1969; Taylor *et al* 1974; Selby & Lindsay 1982).

1.1 Purpose of the Research

With an increasing interest in regolith studies within southern South Australia, in particular with regard to ferricretes and calcretes (Milnes *et al* 1985b; Milnes & Ludbrook 1986; Phillips 1988; Phillips & Milnes 1988; Bourman 1989), an understanding of the complex Quaternary sequences which contribute to the regolith is necessary. Some of the best examples of Quaternary sediments in southern South Australia are found in the Noarlunga and Willunga Embayments south of Adelaide where exposures in coastal cliffs provide an excellent starting point for detailed research.

The initial aim of this research was to map the distribution of Quaternary sediments in these coastal cliff sections to determine the relationship of these non-marine sediments with underlying marine units of Late Pliocene (Hallett Cove Sandstone; Crespin 1954) and Early Pleistocene age (Burnham Limestone; Firman 1976). An understanding of the vertical and lateral variation of Quaternary sediments obtained from preliminary mapping was used to give a broad understanding of the origins of the sediments. The mapping was also used as the basis for establishing a number of representative sections along the coastline where detailed sampling could be undertaken. The second aim of the research was to sample the chosen sites in detail and undertake sedimentological, mineralogical and stratigraphic studies of the sediments. Size analyses, clay mineralogical determinations and observation of heavy mineral suites were undertaken to confirm the validity of initial stratigraphic subdivisions made on the basis of field mapping and to provide data on which to assess the origins of the sediments. The third aim of the thesis was to identify features relating to the diagenetic alteration of the sediments and to determine the timing of these diagenetic events. Iron minerals, alunite, halloysite and palaeosols were identified and their detailed characteristics and distribution studied. Thus a comprehensive understanding of both the initial environments of deposition and post depositional changes was obtained. The landscape history determined for the study area provided the basis for comparison with work previously undertaken in the Noarlunga and Willunga Embayments and other nearby areas.

1.2 Geological Framework of the Region

Much of southern South Australia is dominated by Precambrian and Cambrian bedrock which forms the highlands of the Mt Lofty, Flinders and Gawler Ranges (Figure 1.1). The Gawler Ranges are part of Early Proterozoic basement volcanics, granites and gneisses which form the Gawler Craton and extend over most of Eyre and Yorke Peninsulas (Ludbrook 1980; Parker *et al* 1985). The structure of the bedrock underlying the Mt Lofty Ranges is essentially a broad-scale, overturned anticlinorium composed of a core of Early Proterozoic basement gneisses overlain by Late Proterozoic and Cambrian metasediments. The structure is overturned to the west with the normal limb on the east (Daily *et al* 1976). In the southern Mt Lofty Ranges, on Fleurieu Peninsula and Kangaroo Island the Proterozoic and Cambrian metasediments are of andalusite grade and have been extensively intruded by granites (Offler & Fleming 1968, Milnes *et al* 1977). To the north, the Mt Lofty Ranges extend into the Flinders Ranges which consist of equivalent folded but essentially unmetamorphosed sedimentary rock sequences with the Mt Painter Inlier of basement granites and metamorphics occurring in the far northeast (Ludbrook 1980; Preiss 1988).

No further record of sedimentation in southern South Australia is found until the Permian when there was widespread deposition of glacigene sediments. These sediments now crop out over much of Fleurieu Peninsula where they are preserved in valleys originally cut by the action of glaciers, or are preserved at depth in a number of basins in the region (Ludbrook 1980). Following the Permian, much of the region appears to have remained above sea level until the early Tertiary, during which time extensive weathering of the exposed land surface produced a deep regolith including a complex of soil materials and ferricretes (Milnes *et al* 1985b). Deposition during the Cretaceous was extensive in northern South Australia but to the south was confined to isolated areas such as the Eucla, Polda and Otway Basins and the Renmark Trough (Wopfner 1972).

During the Early Tertiary, widespread sedimentation commenced in intracratonic basins formed by downfaulting (Wopfner 1972; Ludbrook 1980; Falvey & Mutter 1981). In the Lake Eyre and Tarkarooloo Basins, the sediments were deposited exclusively under fluvial and lacustrine conditions. In basins marginal to the modern coasts such as the St Vincent, Eucla and Otway Basins, the sediments were initially fluvial clastics derived from the adjacent highlands, but later, in the Middle Eocene, marine conditions prevailed. The onset of marine deposition in the Murray Basin did not take place until the Oligocene. A widespread regression exposed most of the southern areas to continental conditions once more during the Middle Miocene while marine transgressions during the Early and Late Pliocene and the Early Pleistocene are recorded by thin fossiliferous marine limestones in the southern basins. Subsequently, however, the basins were sites of non-marine sedimentation widely represented by sands and clays (Daily *et al* 1976; Ludbrook 1980; Cooper 1985). In many near-coastal regions, extensive aeolian calcarenites form major dune sequences with associated calcretes and palaeosols. The blanket of carbonate silt which covers much of the adjacent continental area and obscures the older Quaternary and Tertiary sequences may have been derived from these calcarenite sequences (Crocker 1946; Milnes & Ludbrook 1986).

1.3 St Vincent Basin

The St Vincent Basin is one of the more important and well studied intracratonic sedimentary basins in southern Australia, occupying a region between the eastern edge of the Gawler Craton (Yorke Peninsula) and the Mt Lofty Ranges, and extending southwards onto the northern margins of Kangaroo Island (Figure 1.1). The eastern margins of the basin are marked by a series of arcuate faults which bound several embayments or sub-basins including the Adelaide Plains Sub-basin and the Golden Grove-Adelaide, Noarlunga and Willunga Embayments (Daily *et al* 1976). The basin has a long history of sedimentation which has been summarised by Cooper (1985), beginning in the Early Eocene with non-marine clastics followed by marine sediments of Eocene to Middle Miocene age. Further marine and estuarine limestones were deposited during the Late Pliocene and Early Pleistocene times, culminating in the deposition of relatively thick and extensive non-marine

clays and sands throughout the Pleistocene and Holocene. The sedimentary sequences are well exposed in the coastal cliffs of eastern Yorke Peninsula (Crawford 1965; Stuart 1970), parts of northern Kangaroo Island (Milnes *et al* 1983) and the region south of Adelaide (Ward 1966; Stuart 1969; Ludbrook 1980; Cooper 1985). The latter comprises the sequence investigated in the present study and was chosen on the basis of good exposure and access. Marine sediments of Tertiary and Early Pleistocene age are also well represented in these coastal exposures and hence provide recogniseable strata from which to define the overlying non-marine sediments.

1.4 Detailed Late Cainozoic Geology of the Eastern Part of the St Vincent Basin

A series of embayments or sub-basins mark the eastern margin of the St Vincent Basin (Fig 1.2). The present investigation deals with sedimentation in the Noarlunga and Willunga Embayments where there is best exposure of the Cainozoic sediments. As in other parts of the St Vincent Basin, sedimentation in these embayments commenced in the Early Eocene with deposition of non-marine sands and clays of the North Maslin Sand and subsequent marginal marine sediments of the South Maslin Sand (Daily *et al* 1976; Cooper 1985). Marine sediments of Late Eocene to Middle Miocene age followed and have been described from coastal cliff sections in the Noarlunga and Willunga Embayments (Reynolds 1953; Glaessner & Wade 1958; Lindsay 1967; 1970; Cooper 1985) and from drilling in the Adelaide Plains area (Lindsay 1969). Marine sedimentation re-commenced in the Pliocene with deposition of the Croydon Facies (Ludbrook 1963), the Hallett Cove Sandstone and Dry Creek Sands (Crespin 1954; Lindsay 1969) and Burnham Limestone of Early Pleistocene age (Firman 1976). Widespread non-marine deposition followed in the Quaternary and it is these sediments which form the basis of the present study.

1.4.1 Review of Marine Sedimentation of Pliocene and Early Pleistocene Age

Marine units of Pliocene and Early Pleistocene age immediately underlie Quaternary sediments in the Noarlunga and Willunga Embayments and hence define the base of the sequence discussed in this thesis. In order to understand the landscape development represented by these sediments, an understanding of the relationship between the final marine sediments and subsequent non-marine sequence is necessary. A review of sediments of this age has therefore been undertaken.

Early Pliocene sedimentation has been recognised from bores in the Adelaide Plains Sub-basin where shallow marine-bay deposits consisting of bryozoal silts and clayey quartz sands have been named the Croydon Facies (Ludbrook 1963; Lindsay 1969). They have not been reported from the Noarlunga or Willunga Embayments but sediments of similar age were recognised in outcrop on Kangaroo Island by Milnes *et al* (1983).

A warm, shallow sea extended into the St Vincent Basin during the Late Pliocene (Daily *et al* 1976) and shelly sands with bands of fossiliferous calcareous sandstone were deposited in the Adelaide Plains Sub-basin. These were named the Dry Creek Sands by Glaessner (1951) and their distribution and properties discussed in more detail by Lindsay (1969). They have not been reported from the Noarlunga or Willunga Embayments.

Fossiliferous quartz sandstones and sandy limestones commonly crop out in the Noarlunga and Willunga Embayments as thin remnants up to two metres thick and were named the Hallett Cove Sandstone (Crespin 1954). The sandstone is thought to be interbedded with and overlie the Dry Creek Sands in the Adelaide Plains Sub-basin (Lindsay 1969; Selby & Lindsay 1982). In coastal cliffs near Ochre Cove, Glaessner & Wade (1958) and Stuart (1969) reported Pliocene sediments consisting of a fossiliferous, ferruginous conglomerate containing the foraminifer *Marginopora vertebralis* and lamellibranch fragments. Stuart noted similar sediments at a number of isolated localities from Ochre Cove to Ochre Point where they are poorly exposed and unconformably overlain by unconsolidated sediments.

Ward (1966) also reported a conglomerate from Sellicks Beach and regarded it as a facies of the Hallett Cove Sandstone.

Fossiliferous calcareous sandstones were first reported to occur near the 91 metre contour about 1.5 km east of Hallett Cove and correlated with similar calcareous sandstones of Pliocene age which crop out at the coast by Howchin (1923). Sprigg (1942) again described the inland occurrences and correlated them with similar sediments which were exposed west of Hackham and northeast of Noarlunga, near the Noarlunga Trigonometrical Station (Noarlunga Trig). He proposed an aeolian environment of deposition for these sediments which he also considered may be post-Pliocene in age. Ludbrook (1963) observed that the fossils from this unit belonged to the *Anodontia* fauna and hence indicated a Pliocene age for the sediments and correlated them with the Hallett Cove Sandstone.

Ward (1965; 1966) rejected the palaeontological evidence and suggested that the fossiliferous beds were of Early Pleistocene age, because at their southernmost exposure they are overlain by mottled sands, gravels and conglomerates resembling his Ochre Cove Formation. Such an interpretation afforded good agreement with Ward's proposed sea level scheme. Twidale *et al* (1967) disagreed with Ward's interpretation and reiterated earlier evidence which suggested that these beds were deposited in a strandline environment during the Late Pliocene. Stuart (1969) concurred with Twidale *et al* and suggested that the underlying mottled sediments at Noarlunga Trig could also be of Pliocene age on the basis of the known stratigraphy of other Tertiary sediments.

Recently, remnants of the fossiliferous beds east of Hallett Cove have been resampled and preliminary micropalaeontological examination carried out by Ludbrook suggests an Early Pliocene age (Milnes *pers. comm.*). Sediments of this age have not previously been reported from the Noarlunga and Willunga Embayments, although Early Pliocene silts have been reported from bores in the Adelaide Plains Sub-basin (Croydon Facies of Lindsay 1969). Un-named Early Pliocene sediments are described from Kangaroo Island by Milnes

et al (1983) and the Bookpurnong Beds or basal Loxton Sands of the Murray Basin may also be of this age (Stephenson & Brown 1989).

Firman (1976) first named and described the Burnham Limestone from its type location at Kingston Park where it comprises pale grey micritic limestone with some manganese staining and includes clasts derived from the underlying Hallett Cove Sandstone. A supplementary section was defined at Port Willunga. Ludbrook (1983) studied the molluscan fauna of both the Burnham Limestone and the equivalent Point Ellen Formation from Kangaroo Island. She stated the the fauna were indicative of an intertidal environment of estuaries and sandy or muddy flats of sheltered bays and suggested an Early Pleistocene age on the basis of the molluscan fauna. Uncertainty still exists regarding whether the *Hartungia* species used by Ludbrook to define the age of the Burnham Limestone is restricted to the Early Pleistocene due to the position of the Plio-Pleistocene boundary being ill-defined (Lindsay *pers. comm.*). In addition to several sites in the Willunga Embayment, Ludbrook also reported the Burnham Limestone from Hallett Cove and O'Sullivan Beach in the Noarlunga Embayment. The Burnham Limestone has also been recognised from drill-holes in the Adelaide Plains Sub-basin (Lindsay 1969; Selby & Lindsay 1982). At Maslin Bay, Stuart (1969) reported that sediments subsequently assigned to the Burnham Limestone graded laterally into sands and clays of the Seaford Formation (defined by Ward 1966). Ward (1966) had interpreted these sediments to be equivalent to the Hallett Cove Sandstone, however Twidale *et al* (1967) suggested that at this locality an un-named limestone of Pleistocene age (the Burnham Limestone) occurred between the Hallett Cove Sandstone and Seaford Formation.

A review of available literature suggests that the final marine sediments prior to widespread non-marine deposition are of estuarine origin. There is also evidence to suggest a gradational change from the Burnham Limestone to subsequent non-marine sediments at Maslin Bay (Stuart 1969) and hence careful consideration should be given to defining the nature of this contact. Thus the identification of the Burnham Limestone at Maslin Bay

suggests that re-evaluation of Ward's conclusions regarding the origin and age of basal parts of the Quaternary sequence should be undertaken.

1.4.2 Stratigraphy of Sediments Overlying Pliocene Marine Deposits

Several studies of the non-marine Quaternary succession from the eastern margin of the St Vincent Basin have been undertaken. Such work has generally been of a descriptive and stratigraphic nature and is summarised in Table 1.1. As no fossils have been reported from the non-marine sediments, it is difficult to correlate units defined from the various studies. However, it is considered that the table represents a useful summary of the evolving stratigraphic concepts for the region.

Tate (1878) provided one of the first descriptions of sediments from the Port Willunga area in the Willunga Embayment as part of a broad study of Tertiary corals exposed in cliffs along the River Murray near Mannum and at Aldinga Bay. Fifteen metres of unfossiliferous clays overlying the marine sediments at Aldinga were considered by Tate to be of possible lacustrine origin and similar to clays he had studied along the River Murray.

Howchin (1923) described sediments exposed along 41 km of coastline south of Adelaide and distinguished two Quaternary units, separated by an erosional contact, which were continuous for much of the coastline surveyed. The older unit, which he named "Pleistocene Clays", was described as strongly mottled, red and grey, tough, plastic or argillaceous, sand rock. "Recent Clays" formed the younger unit, which was reddish in colour, less compact than the older clays and contained minor sand and gravel.

Segnit (1939), surveyed the coast south of Moana from Ochre Cove to Ochre Point and described the sequence of clays, sands and gravels to which he assigned a Late Tertiary to Early Pleistocene age near Ochre Point.

Sprigg (1942) described the geology of the Eden-Moana fault block and adjacent Noarlunga Embayment. Although he did not subdivide the Quaternary deposits, he suggested that they were a product of erosion of Oligocene and Miocene sediments which occurred to the north of the embayment. He reported that clays were dominant at the coast, but noted coarser sediments including well bedded sands towards the base of the deposits as well as in a northerly direction along the coast.

In the Willunga Embayment, Campana & Wilson (1953) and Reynolds (1953) described sediments equivalent to those discussed by Sprigg. At Sellicks Beach, adjacent to the Willunga Fault, coarse sub-horizontal alluvial formations considered to be Upper Pliocene to Pleistocene in age were recognised by Campana & Wilson (1953). Away from the Willunga Fault, Reynolds (1953) identified two fine-grained units of probable Pleistocene age which were similar to those of Howchin (1923). Reynolds also described a thin layer of calcrete overlying the uppermost clays and suggested that the calcrete mantled the landscape.

An overview of the geology of the whole St Vincent Basin was given by Glaessner & Wade (1958) who highlighted the lack of information then available on Quaternary events in the basin. The authors indicated that, in places, fossiliferous limestones were interbedded with unfossiliferous sands and gravels of probable non-marine origin which then passed upward into mottled sands and clays. A lack of fossils in these upper beds prevented a definite assessment of age, although Late Pliocene to Pleistocene was considered probable.

The most detailed work involving the Pleistocene successions of the study region was carried out by Ward (1965; 1966; 1967) in the context of a study of landscape history and soil development. Concurrently, Firman (1966) described and named Quaternary sedimentary units in the Adelaide Plains Sub-basin and developed stratigraphic terminology which differed from Ward. No attempts were made to establish a coherent approach to this problem.

Ward (1965; 1966, p.25) proposed one stratigraphic unit of Pliocene age; the Seaford Formation which he defined as "moderately well-bedded fluvial sandy clays and clays and variously consolidated sands interbedded with pebble beds, gravel beds and grits". White alunite was described interbedded with clays in lower levels of the formation. This unit was assigned a Pliocene age by Ward on the basis that Seaford Formation sediments interfingered with the Hallett Cove Sandstone at Maslin Bay, although several workers have since disagreed with this interpretation (Twidale *et al* 1967; Stuart 1969) (see Section 1.4.1). The sea level scheme proposed for the area by Ward (1966; 1967) required the Seaford Formation to be of Mid to Late Pliocene age. A younger age for this unit, such as the Early Pleistocene age suggested by Twidale *et al* (1967), indicates that a re-evaluation of the stratigraphy, eustatic, climatic and landscape history proposed for the area by Ward is necessary.

The Ochre Cove Formation of Early Pleistocene age was defined by Ward (1966) as thick, mottled, horizontally bedded alluvial sands containing lenses of grit and gravel and with an irregular erosion surface occurring between it and the Seaford Formation. Ward used the mottling pattern in sediments below the high level fossiliferous beds at Noarlunga Trig as a means of correlating these sediments with his Ochre Cove Formation. Twidale *et al* (1967) indicated that the mottling observed by Ward could be produced in a variety of sediments resulting in considerable confusion if stratigraphic correlations were attempted using the mottled sediments as marker units. A distinctive iron-mottled interval within Pleistocene sediments on eastern Yorke Peninsula and also from the study area has been named the "Ardrossan Soil" by Daily *et al* (1976) or the "Ardrossan Palaeosol" by Firman (1981).

Ward's Kurrajong Formation consisting of "compact fanglomerates" included both gravels and clay which were commonly mottled with iron oxides, cemented with silica and assigned a Late Pleistocene age. Twidale *et al* (1967) considered that the cemented and dissected nature of these sediments along the foot of the Willunga Escarpment suggested an older age and thus a post-Miocene but pre-Pleistocene age was postulated.

Ward defined the Ngaltinga Clay as grey to olive-grey plastic clays, partly calcareous and including occasional lenses of marl and sand. He suggested the clay to be of aeolian origin due to the unusual nature of a rare microfauna and heavy mineral assemblages, the presence of marls both as a blanket above and as lenses within the clays and the thinning of the unit toward the east. Twidale *et al* (1967) questioned the validity of the unit as defined by Ward and implied that the calcareous blanket should be considered as a separate unit to the clays beneath. Previous and subsequent workers have also considered the clays to be separate from the calcareous blanket (Howchin 1923; Reynolds 1953; Daily *et al* 1976; Phillips & Milnes 1988). The aeolian sediments referred by Ward to the Ngaltinga Clay have previously been thought of as lacustrine in origin by Tate (1878) and alluvial by Howchin (1923).

The four youngest units described by Ward (1966) are the Taringa, Christies Beach, Ngankipari Sand and Waldeila Formations, all believed to be of Late Pleistocene to Recent age. With the exception of the Ngankipari Sand all are defined as alluvial in origin and their distribution patterns are closely associated with modern stream courses. The Ngankipari Sand was defined as a calcareous sand, probably derived in part as aeolian material from erosion of the coastal dunes and in part from alluvial sands.

While Ward discussed the Quaternary sequence from the Noarlunga and Willunga Embayments, the sequences in the Adelaide area were principally investigated by Firman (1963; 1966; 1967; 1969a; 1969b; 1976) and to a lesser extent by Lindsay (1969), Williams (1969), Taylor *et al* (1974) and Selby & Lindsay (1982). Much thicker sequences, named the Hindmarsh Clay, are found in the Adelaide area with up to 130 metres of Quaternary sediments having been deposited west of the Para Fault (Firman 1966). The majority of these sediments are clays and sandy clays regarded as deposits of valley-flat environments. Nearer the fault escarpments, gravels and gravelly sands and clays, deposited in piedmont environments, predominated. A thinner unit which overlay the Hindmarsh Clay was named the Keswick Clay. Similar alluvial sediments have been described from Ardrossan on Yorke

Peninsula by Crawford (1965) and from Redbanks on the north coast of Kangaroo Island by Daily *et al* (1979).

Recent work to investigate the engineering properties of soils in the Adelaide area has critically assessed the Hindmarsh and Keswick Clays (Sheard & Bowman 1987a; 1987b). They interpret the deposits to be mostly of alluvial origin with minor fine-grained overbank deposition. Carbonate segregations representing B horizons of palaeosols are recognised in upper parts of the Hindmarsh Clay while small-scale ferruginous mottling is noted within fine-grained sediments of both the Hindmarsh and Keswick Clays. These are thought to result from fluctuating water tables within the sediments.

Three marine and marginal marine units including the Late Pleistocene Glanville Formation and the Holocene Lipson and St Kilda Formations were reported by Firman (1963; 1966; 1969b) to overlie the Hindmarsh Clay in the Adelaide Plains region. Belperio *et al* (1984) subsequently redefined the St Kilda Formation to include all sediments previously assigned to the Lipson Formation. In the Noarlunga and Willunga Embayments similar marine units have not been recognised apart from sediments deposited during a possible Holocene high sea level in the Onkaparinga River estuary (Bourman 1972) and a boulder beach deposit of probable Late Pleistocene age south of Sellicks Beach (May & Bourman 1984).

Over large areas of southern Kangaroo Island, Yorke Peninsula and Eyre Peninsula, thick calcarenite sequences composed of sand and shell material represent beach and backshore dune deposits. Large-scale cross-beds are found commonly in the calcarenites together with interbedded red palaeosols and calcretes and these sequences have been assigned to the Bridgewater Formation (Daily *et al* 1979; Milnes *et al* 1983; Parker *et al* 1985). On Figure 1.1 such sediments are shown as Cainozoic coastal dunes and represent the approximate position of ancient coastlines. Their age has not been positively determined, but on Kangaroo Island they are reported to overlie limestones of Early Pleistocene age (Milnes *et al* 1983). Milnes & Ludbrook (1986) have recently suggested that deposition of some of these coastal dune sequences may have begun as early as the Middle Miocene. In the present

study area such materials have not been identified, although Daily *et al* (1976) reported sediments of the Bridgewater Formation at Hallett Cove and also as a reef at the end of the Port Noarlunga jetty. It is evident from the literature that the Bridgewater Formation has not been sufficiently well defined and that its distribution and age range require further investigation.

There is disagreement amongst previous workers regarding their interpretation of the origin of non-marine Quaternary sediments which have been considered of lacustrine (Tate 1878), aeolian (Ward 1966) or alluvial origin (Howchin 1923; Campana & Wilson 1953; Ward 1966; Sheard & Bowman 1987a; 1987b). In addition, basal non-marine sediments are thought to interbed with or grade laterally into marine sediments equivalent to the Burnham Limestone at Maslin Bay (Stuart 1969) and parts of the Adelaide Plains Sub-basin (Lindsay 1969; Selby & Lindsay 1982). Apart from the recognition of probable palaeosols in upper parts of the Hindmarsh Clay (Sheard & Bowman 1987b) and the suggestion that mottled intervals within the sequence represent palaeosols (Daily *et al* 1976; Firman 1981), there is no discussion of landscape development during the Quaternary period which would help to clarify the origin of these sediments. Correlation of stratigraphic units between sites is difficult due to the lack of fossils present in the non-marine succession. Without an understanding regarding the origin of the palaeosol and other features and the environment in which the sediments were deposited, such correlation is potentially misleading.

1.4.3 Tectonic History of the Region During the Late Cainozoic

Ward (1965; 1966) attempted to determine the Quaternary history of the Noarlunga and Willunga Embayments by relating sea level fluctuations to high level terraces which he identified as being related to the various Quaternary sedimentary units. Eustatic models developed by Zeuner (1959) and Fairbridge (1961) in the northern hemisphere and Brothers (1954) in New Zealand were used as a basis for these correlations and to date the sedimentary units. This method of interpretation was considered valid as Ward believed that there had been no significant tectonic movements in the area during the Late Cainozoic. The

major point which led Ward to this conclusion was his interpretation that the Late Pliocene Hallett Cove Sandstone interfingered with horizontally bedded alluvial sediments. Subsequent work suggests that the Hallett Cove Sandstone identified by Ward is, in fact, the Burnham Limestone (Twidale *et al* 1967; Stuart 1969; Firman 1976). Ward also indicated that none of the formations defined by him were offset by the Eden or Clarendon Faults, however the Ochre Cove Formation, but not younger formations, were displaced by the Willunga Fault. As this movement was insufficient to displace his 183 metre terrace, Ward dismissed Quaternary tectonic movements as negligible. The uncertainty regarding Ward's approach indicates that the tectonic history of the area should be re-evaluated.

Wopfner (1972) argued that both Tertiary and Quaternary sedimentary patterns have been strongly influenced by the tectonic history of the St Vincent Basin. Stuart (1969) and Wopfner (1972) considered the St Vincent Basin to be intracratonic, the shape and extent of which had been strongly influenced by rejuvenation of ancient structural features developed during the Palaeozoic. The majority of workers have accepted this theory of block faulting along arcuate and steeply dipping normal faults to produce the main St Vincent Basin and a number of smaller sub-basins along its eastern margin (see for example Daily *et al* 1976; Ludbrook 1980; Cooper 1985).

Based on correlation of dinoflagellate suites over a wide area of southern Australia, Harris (1985) argued that the depositional events of Eocene age in the St Vincent Basin were controlled largely by eustatic rather than tectonic events. Glaessner (1953) also differed somewhat from the classical tectonic model for the St Vincent Basin when he suggested that there was no evidence for graben-style faulting in the St Vincent Basin. Instead, he produced a model based on hinge-faulting in which compression took place resulting in upwarping of sediments near the present coast. This movement was thought to be mostly post-Pliocene by Glaessner (1953).

In contrast to Glaessner (1953), Cooper (1985) suggested that evidence for crustal tension and normal faulting was abundant in the St Vincent Basin. At Sellicks Beach, Early

Miocene limestones of the Port Willunga Formation stand almost vertically, in unconformable contact with basement rocks (Cooper 1979), while at Ochre Cove, the Clarendon Fault has similarly deformed the Tertiary succession (Stuart 1969). Cooper (1985) also considered that at least two distinct faulting maxima could be discerned for the basin thereby supporting several previous workers hypotheses (Daily *et al* 1976; Ludbrook 1980; Selby & Lindsay 1982). Initial faulting was thought to have accompanied the formation of the basin during the Eocene and a second period followed in the Pleistocene.

The great majority of papers published on Late Cainozoic geology in the St Vincent Basin and, in particular, in the Noarlunga and Willunga Embayments, favour continued tectonic instability during the Quaternary (Sprigg 1942; 1946; Miles 1952; Glaessner 1953; Reynolds 1953; Campana & Wilson 1953; Glaessner & Wade 1958; Twidale *et al* 1967; Daily *et al* 1976; Ludbrook 1980; Selby & Lindsay 1982; Ludbrook 1983). Significant displacement of Tertiary sediments across most faults in the Adelaide area has been inferred by extensive drilling (Lindsay 1969; Twidale *et al* 1967; Daily *et al* 1976; Selby & Lindsay 1982).

A low-angle unconformity exists between mid-Tertiary and Pliocene sediments exposed in coastal cliffs between Tortachilla Trig and Snapper Point, indicating movement of the fault blocks in the intervening period. The Late Pliocene Hallett Cove Sandstone occurs at a variety of elevations above sea level in the study area, cropping out at 36 metres above sea level at Hallett Cove, and dipping below sea level at Snapper Point. Sprigg (1942) calculated a southerly dip of about 1° and assumed that this was due to tectonic movement, a point which Ward (1965) contested. Ward indicated that the dip was low and difficult to measure and since he believed the Hallett Cove Sandstone interfingered with horizontally bedded alluvium of the Seaford Formation he rejected the notion of tectonic movements tilting Late Pliocene sediments. Subsequent work reported above casts doubt on the interfingering relationship of the Hallett Cove Sandstone and Seaford Formation and suggests that tilting of Pliocene sediments has taken place.

Definition of the Burnham Limestone (Firman 1976) and a description of its distribution through the region (Ludbrook 1983) suggests that there has been tectonic movement following deposition of this unit in the Early Pleistocene. The Burnham Limestone crops out 30 metres above sea level at Hallett Cove then decreases in elevation, being 20 metres above sea level at Maslin Bay and below sea level near Snapper Point. A disconformable relationship between the Hallett Cove Sandstone and Burnham Limestone is evident from the exposures in coastal cliffs (Ludbrook 1983).

In the Adelaide Plains Sub-basin, sediments equivalent to the Burnham Limestone have been described from bores at depths of 52 to 62 metres below sea level on the down-thrown side of the Para Fault (Lindsay 1969) suggesting considerable displacement in this region. On Kangaroo Island, Ludbrook (1983) reported that the Point Ellen Formation crops out 10 metres above sea level at Cape Willoughby and less than 10 metres at Point Ellen while at Cape Jervis, on the tip of Fleurieu Peninsula, it occurs 50 metres above sea level. The Point Ellen Formation is equivalent to the Burnham Limestone from the study area and Ludbrook's data provide further evidence for some tectonic movement since the Early Pleistocene.

A number of workers have indicated that the sequence of sands, clays and gravels which overlies the Burnham Limestone and Hallett Cove Sandstone in the St Vincent Basin is the result of renewed earth movements beginning in the Early to Middle Pleistocene (Firman 1969b; Daily *et al* 1976; 1979; Milnes *et al* 1983; 1985b). Daily *et al* (1976) postulated three distinct periods of faulting during the Early, Middle and Late Pleistocene, thus conflicting with the hypotheses of Ward.

Campana & Wilson (1953) were the first to describe displacement of Pleistocene gravel beds in Mt Terrible Gully, south of Sellicks Beach. They further stated that younger gravels were also tilted and faulted and suggested that this indicated Late Pleistocene or Holocene faulting at this location. Although Twidale *et al* (1967) reported that similar Pleistocene sediments at

Marino were faulted against Precambrian rocks, Ward (1967) suggested that this exposure was not at the location of the Eden Fault but instead was a former sea cliff.

Continued tectonic instability in the region is indicated by seismicity and occasional earthquakes (Twidale *et al* 1967; Sutton & White 1968). The Adelaide earthquake of 1954 had its epicentre along the Eden Fault (Kerr-Grant 1956) although Ward (1967) has pointed out that as there was no movement identified along the fault, its significance should not be overrated.

A review of the literature would suggest therefore, that there has been tectonic movement in the study region during the Early and Middle Pleistocene whereas movements of Late Pleistocene and Holocene age are probable although not definitely substantiated. Such a conclusion conflicts with the contention of Ward (1965; 1966). As Ward based the age of sedimentary units defined by him on correlation with a eustatic model which assumed negligible tectonic activity, his conclusions must be re-assessed based on the tectonic evidence presented above. The model was also used in determining the origins of the sediments and the Quaternary history for the region. Thus the nature and origin of the Quaternary sediments from the Noarlunga and Willunga Embayments will be critically assessed in this study on the basis that tectonic movement has continued through this period.

1.5 Mineralogy of the Cainozoic Sediments

A review of literature dealing with the Late Cainozoic geology of the eastern margin of the St Vincent Basin (Section 1.4) identifies discrepancies regarding the origin of the sediments, their age and correlation between sites. Previous work relates almost exclusively to the stratigraphic and lithological properties of the sedimentary sequence with little information regarding the mineralogical composition. In determining the origin and provenance of the sediments and development of the landscape during the Quaternary, knowledge of the mineralogical component of the sequence would be of value.

Ward (1966) re-examined data provided in Aitchison *et al* (1954) for heavy minerals present in soils and sediments of the Adelaide area and concluded that some metamorphic minerals appeared to have been derived from non-local sources. Ward (1966) also noted the presence of alunite at a number of localities in the basal sediments of his Seaford Formation but did not determine its origin or significance. A number of workers have noted the development of red, brown or yellow mottles within these sequences (Crawford 1965; Ward 1966; Daily *et al* 1976; Firman 1981; Milnes *et al* 1985b) which Daily *et al* (1976) and Firman (1981) suggested were the product of soil formation and hence marked the position of former land surfaces. In contrast, Milnes *et al* (1985b) considered the mottles to be the result of mobilisation and precipitation of iron as a consequence of groundwater movement within the sediments.

In southern South Australia, studies of calcretes and associated calcareous sediments have provided some mineralogical information regarding carbonates and clay minerals (Hutton & Dixon 1981; Wilson 1981; Milnes & Hutton 1983; Phillips & Milnes 1988) while von der Borch (1976) and von der Borch & Lock (1979) discuss the formation of dolomite in Holocene sediments from southeastern South Australia. In particular, Phillips & Milnes (1988) note the presence of illite, randomly interstratified clays, kaolinite and minor smectite in clay fractions and calcite, dolomite, quartz and minor feldspars in coarser fractions from the carbonate mantle and underlying Quaternary sediments in the Noarlunga Embayment. A common mineralogical component suggests that both the carbonate mantle and underlying sediments may have been partly derived from the same source. Additional mineralogical investigation of the remaining portion of the Quaternary sequence in the Noarlunga and Willunga Embayments would be beneficial.

There is some limited mineralogical information reported for Quaternary sediments from the Murray Basin which have been used to elucidate the origins of these sediments. Lawrence (1976) described lacustrine sediments assigned to the Blanchetown Clay and reported abundant red-brown ferruginous sand in the basal Irymple Member which indicated deposition under dominantly oxidising conditions. In upper parts of the formation Lawrence

noted a clay mineral assemblage dominated by illite and iron-rich chlorite but with an absence of kaolinite and suggested that this clay mineral assemblage was the product of a fairly stagnant alkaline environment. Thin, isolated beds of gypsum occurring near the top of the sequence were the product of increased lake salinities during final stages of deposition. Zhisheng *et al* (1986) described several pedogenically altered horizons within the Blanchetown Clay at Chowilla and Lake Tyrrell which are expressed as mottling, chemical alteration and biotubules. These indicate periodic exposure of the lacustrine sediments which is important in developing an understanding of the history of the sediments.

One of the most comprehensive studies of mineralogical properties of Cainozoic sediments from South Australia is provided by Callen from the Tarkarooloo Basin in north eastern South Australia (Callen 1976; 1977; Callen & Tedford 1976). This work integrated stratigraphic and mineralogic data, particularly clay mineralogy, to elucidate the environments of deposition and ultimately the palaeoclimate and palaeogeography of the region.

Four distinct clay mineral associations were identified. Smectite dominated the clay fraction of Miocene sediments and was thought to be derived by the transformation of illites and chlorites eroded from adjacent highland areas. Since Grim (1968) proposed that smectite formed under conditions of restricted leaching, Callen suggested that this transformation took place in a swampy environment of low relief surrounding a freshwater lake and under a sub-tropical climate, rather than a semi-arid environment in which there could also be restricted leaching. He based this conclusion on sedimentological observations which suggested deposition of these sediments under lacustrine and floodplain conditions.

In central parts of the sequence, illite is the dominant clay mineral. Sedimentological observations indicated greater erosion during this period and probable uplift of the nearby Flinders Ranges. Illite and chlorite from basement sediments were therefore not being converted to smectite and Callen attributed this to the increased leaching of soils and

sediments in source regions brought about by changes in hydrology consequent to the renewed uplift. The fact that illite was not converted to smectite within the basin sediments also suggested increased leaching in these areas, possibly due to lowering of water tables under slightly drier climates. The dominance of kaolinite over illite at some sites was thought to be due to sediment from different source regions where erosion of Tertiary sediments and kaolinized basement could contribute kaolinite to the basin. Seasonality of climate continued to develop and led to the increasing alkalinity of lake waters and the precipitation of a palygorskite-dolomite assemblage.

Smectite again became the dominant clay mineral in upper parts of the sequence but its presence here was attributed to semi-arid weathering. Sediments in which this smectite assemblage occurs show very poor sorting, decreased mineralogical maturity and include large clasts of limestone and granitic rocks. A mudflow origin for these sediments at some sites was suggested by Callen which indicated increased erosion in conjunction with an arid climate at this time. Hence in both source regions and the Tarkarooloo basin, leaching was low and allowed transformation of illite to smectite. In both intervals where smectite was identified, low leaching, either in a dry climate or as a result of limited relief, appeared to be a major factor in determining its occurrence.

Aridity continued into the Pleistocene following a period of non deposition and uplift. Sediments deposited at this time were characterised by poorly crystalline clay minerals comprising mostly randomly interstratified clays, illites and kaolinites. These were thought to have been developed by weathering and degradation in soils, although Callen did not elaborate on this statement.

The study by Callen from the Tarkarooloo Basin shows the importance of a knowledge of mineralogical properties of the sediments in determining the origin of the sediments and the landscape history represented by the sequence. An integration of such information with detailed field observations in the Noarlunga and Willunga Embayments has the potential to unravel differences in interpretation regarding the origin, stratigraphic correlations and age of

the Quaternary sequence which are evident from previous studies. A review of the limited information available shows several important features which could be used to begin a mineralogical study. These include metamorphic minerals from the heavy mineral assemblage which may be derived from a non-local source (Ward 1966), the presence of alunite at the base of the sequence (Ward 1966), ferruginous mottling which may be related to pedogenesis (Daily *et al* 1976; Firman 1981) and calcareous palaeosols in the Hindmarsh Clay (Sheard & Bowman 1987b).

1.6 Summary

Previous studies of Quaternary sediments in the Noarlunga and Willunga Embayments and nearby areas have been conflicting in their interpretation of the origin of the sediments, their age and relationships. For example, the Ngaltinga Formation was defined by Ward as an aeolian deposit, however similar sediments described by Firman and others from the Adelaide Plains Sub-basin are considered to be of alluvial origin. In addition, Ward considered that there had been negligible tectonic movement along faults in the study area during the Late Cainozoic. This enabled him to propose a eustatic model for the region from which he extrapolated the age and relationships of the various sedimentary units which he defined. All other studies in the region indicate that tectonic activity continued into the Quaternary and hence have interpretations regarding the sequence which differ from those proposed by Ward.

Work by Callen from the Tarkarooloo Basin demonstrates the additional understanding of sedimentary sequences and environments of deposition that can be obtained by a study of the mineralogy, in particular clay mineralogy, when combined with detailed field observations. There is a lack of mineralogical information for Late Cainozoic sediments from the St Vincent Basin, although several observations in previous studies provide preliminary information. These suggest the presence of heavy minerals derived from a non-local source, development of alunite at the base of the sequence and pedogenic modification of some sediments.

In order to provide a sound basis for understanding the complex Quaternary sequence in the St Vincent Basin and enable comparison between sites, the present study is proposed to investigate these sediments in the Noarlunga and Willunga Embayments where they are best exposed in coastal cliff sections. An integrated approach using detailed field observations together with sedimentological and mineralogical studies is required to enable the origin of the sediments and their post depositional alteration to be determined. From this detailed information, the history of landscape evolution during the Quaternary can be determined and will allow stratigraphic interpretations and correlations between sites to be undertaken on a much sounder basis than has been previously possible.

CHAPTER 2
METHODS

2.1 Fieldwork

Excellent exposures of Quaternary sediments occur in coastal cliffs south of Adelaide between Hallett Cove and Sellicks Beach which provide a unique opportunity to begin to understand the complex Quaternary sequence. Initial reconnaissance fieldwork was undertaken to assess the distribution of existing stratigraphic units and interpretations of their origins. Mapping of the coastal sequences using 1:16,000 colour aerial photographs as a basis was carried out at this stage. Particular attention was paid to the lateral and vertical extent of stratigraphic units, the distribution of distinctive mineralogical components such as iron-rich mottles, seams of alunite and mottles of carbonate and the relationship of Quaternary sediments with underlying marine units. Collection of reconnaissance samples from the recognised stratigraphic units and other distinctive features was carried out in order to gain preliminary information regarding the mineralogy of the sediments.

The aim of the research was to undertake detailed mineralogical analyses of the Quaternary sequence in order to identify the various detrital and diagenetic components and to ultimately determine the environments of deposition of the sediments and the nature of any diagenetic changes. Thus, information from reconnaissance mapping and sampling was used to locate a number of sections along the coast which were representative of the stratigraphic, mineralogic and diagenetic features recognised within the Quaternary sequence. This enabled more detailed observations and sampling to be undertaken which could then be related back to the wider distribution of the various features. Four sites were chosen, located at Snapper Point (Yankalilla 1:50 000; 672933), Maslin Bay (Noarlunga 1:50 000; 697970), Onkaparinga Trigonometrical Station (Onkaparinga Trig) (Noarlunga 1:50 000; 691048) and Hallett Cove (Noarlunga 1:50 000; 718154). Bulk samples of between 0.5 and 1 kg were collected at 50 cm intervals through the vertical sections at each of the four sites with additional samples being collected where interesting features or frequent lithological changes

were noted. Sampling commenced immediately above limestones of either Tertiary or Early Pleistocene age and terminated just below the ubiquitous mantle of calcareous sediment occurring throughout the area. The limestones provided convenient basal marker beds while the overlying calcareous material was the subject of a separate study (Phillips 1988). Difficulty of access where cliff sections were steep meant that several juxtaposed profiles located within 10 metres of each other were necessary to sample the complete Quaternary succession at three sites (Maslin Bay, Onkaparinga Trig and Hallett Cove). Detailed descriptions were made of each sample together with a record of the location of the sample and its relationship with surrounding sediments.

2.2 Laboratory Studies

2.2.1 Particle Size Separation

For detailed clay mineralogical analyses of the samples collected as representative of the various stratigraphic intervals, the <2μm fraction was separated from coarse particles such as quartz and feldspars. Where necessary, air-dried samples were disaggregated by lightly crushing in a mortar and 15 g of <4 mm material was then dispersed in a solution of distilled water and 5 ml of both 10% Calgon (0.96M) and 1M NaOH using an ultrasonic probe. Following dispersal, each sample was washed through a 63 μm sieve, the material >63 μm being retained, oven dried and then further split by dry sieving through a 250 μm sieve. The proportion of coarse sand (>250 μm) and fine sand (63-250 μm) was calculated with the ratio of coarse sand to fine sand being subsequently determined. Collection of the <2 μm fraction from most samples was accomplished by centrifuging at 500 rpm for 12.6 minutes using an Heraeus Christ centrifuge. To flocculate the clay following separation, the clay fractions were Mg saturated by adding 15 ml of 1M $MgCl_2$ and excess chloride removed by repeated centrifugation in distilled water. For some reconnaissance samples the <2 μm fraction was collected by sedimentation for 8 hours at 20°C in 1250 ml cylinders. Clay fractions collected by both methods were freeze-dried for storage in the manner used by Brindley & Brown (1980), to ensure that no hydrolysis or cation exchange processes took place. Determination of the proportion of clay (<2μm) and silt (2-63μm) in each sample was

through sedimentation with 20 ml sub-samples being collected from 10 cm depth after 2 minutes (silt + clay) and 8 hours (clay) based on the methods described by Day (1965).

2.2.2 Mineralogical Analyses

The mineralogical composition of samples was determined by X-ray diffraction (XRD) using a Philips PW1710 diffractometer with graphite monochromator and Co Kα radiation. Cu Kα radiation with a Philips PW1710 diffractometer was used during investigation of the clay mineralogy of clay and silt fractions of eight samples from Maslin Bay and Onkaparinga Trig as this work was undertaken in Perth rather than in Adelaide. In most cases data was collected by analogue techniques. More recently however, collection has been undertaken digitally using the control programs of Self (1989) and the analytical program XPLOT developed by Raven (1990) at CSIRO Division of Soils. In this method XRD patterns of samples were recorded with a Philips PW1800 microprocessor-controlled diffractometer using Co Kα radiation, variable divergence slit and a graphite monochromator. The diffraction patterns were aquired in steps of 0.05° 2θ with 0.5 second count time per step. Data were logged to permanent files on an IBM PC/XT and subsequently analysed using the software package developed by Raven (1990).

Sub-samples of the bulk samples were finely ground using an agate mortar and pestle and lightly pressed into aluminium holders for determination of carbonate, iron and sulphate minerals. Continuous scans were run from 3° to 60° 2θ at a speed of 2° per minute with output recorded on chart paper running at 10 mm per minute. The composition of the clay fraction was determined by sedimenting the <2 μm fraction onto a flat, porous, ceramic plate using a suction technique to achieve maximum preferred orientation (Gibbs 1967). XRD traces from 3° to 40° 2θ were collected from the oriented samples which had been variously Mg saturated, Mg saturated with the addition of glycerol, K saturated and heated to 350°C and K saturated and heated to 500°C. Saturation and heating of the oriented clay samples before X-ray analysis was undertaken to allow discrimination of the various clay minerals, in particular the components making up interstratified clays. Further discussion of the effects

of these techniques can be found in Chapter 4. All peaks in the XRD traces were identified by comparison with ASTM cards and the data given in Brindley & Brown (1980).

2.2.3 Clay Mineral Abundance

Semi-quantitative determinations of clay mineral abundances have been undertaken using the technique described by Norrish & Pickering (1977; 1983). This method involves sedimenting a small amount of dispersed clay onto a porous ceramic plate, then saturating the sample with Ba using 1M $BaCl_2$ before measuring Ba, Cl and K by X-ray fluorescence spectrometry (XRF). The Ba content is a measure of cation exchange capacity of the clay (CEC) while the K percentage is used as a guide to the approximate proportion of illite or mica in the sample. Determination of Cl is made to check that excess $BaCl_2$ had been washed out of the sample. Peak heights above background of the 7.15 Å and 10.0 Å diffraction peaks were used to calculate the ratio of kaolinite to illite. To allow for stronger diffraction effects from the kaolinite lattice when compared to illite, the illite peak height was multiplied by a factor of 2 in all calculations. This factor is the result of extensive comparative work using known proportions of various standard clay minerals (J.G.Pickering *pers. comm.*). Using the proportions of kaolin and illite calculated from diffraction traces, the maximum possible CEC was determined using CEC values based on those given in Grim (1968). Excess CEC not accounted for by kaolin and illite was then proportioned to the other clay minerals identified from XRD traces according to the values given in Table 2.1.

Halloysite is identified from some samples in both the 7Å and 10Å forms causing broadening of peaks at these positions. Confirmation of halloysite and estimation of the relative proportions of halloysite and kaolinite using intercalation with formamide followed the methods of Churchman *et al* (1984) and Theng *et al* (1984).

Clay mineral abundances obtained using the method of Norrish & Pickering (1983) were compared to those obtained using a method developed by Avery & Bullock (1977) which

measured the area under the diffraction peak. Proportions of clay minerals calculated by both methods are similar apart from kaolinite and illite where Avery & Bullock advocate a weighting factor of 3 rather than 2 as used by Norrish & Pickering.

Table 2.1

Ranges of CEC (me/100 g) for Clay Minerals

Clay Mineral	Grim (1968)	May (this study)
Kaolinite	3-15	10
Smectite	80-150	110
Vermiculite	100-150	130
Mica/Illite	10-40	30
Chlorite	10-40	25
Interstratified	No figure given	110

2.2.4 Crystallinity Index

An indication of the crystallinity of kaolinite and illite was determined by measurement of the widths of the strong (001) diffraction peaks. This method is based on work by Foscolos & Kodama (1974) who described the degree of diagenesis in Lower Cretaceous shales of northeastern British Columbia in terms of sharpness ratio (SR) and crystallinity index (CI) of illitic clay minerals. Weaver (1960) and Kubler (1967) had earlier defined these terms and used them when describing the degree of metamorphism in sediments. A broadening of the diffraction peak is indicated by a decrease in sharpness ratio and also by an increase in the crystallinity index. In the present study, the crystallinity index has been calculated for both illite and kaolinite and the effects of variable crystallite size and crystal disorder on these measurements are discussed in Chapter 4.

2.2.5 Sand Fraction Mineralogy

The mineralogy of the coarse sand fraction of 44 samples collected from Onkaparinga Trig has been determined using a binocular microscope and optical techniques developed at CRA

Exploration, Belmont for assessing heavy mineral concentrates of samples collected during diamond exploration. In addition, the sand fraction of eight samples from Onkaparinga Trig and Maslin Bay was separated using wet seiving techniques during collection of clay and silt fractions and the mineralogy of the sand determined using the above methods. Light components of the sand fraction such as quartz and feldspar were removed using tetrabromoethane (TBE) which has a specific gravity of 2.96. The method of reporting adopted is given in Table 2.2. Results have been compared with the summary provided by Ward (1966) of heavy minerals present in a number of soils from the study area.

Table 2.2

Convention used in Reporting Mineral Abundances from Sand Fractions

Reporting Term	Estimated %
Prevalent (P)	>50 %
Abundant (A)	20-50 %
Common (C)	10-20 %
Some (S)	3-10 %
Often (O)	1-3 %
Few (F)	0.1-1 %
Rare (R)	2-10 grains
Trace (T)	1 grain

2.2.6 X-ray Fluorescence Spectrometry (XRF)

The major element composition of bulk samples was determined by XRF. Samples were ignited for 1 hour at 1000°C with mass losses due to volatile emission being determined. The ignited samples were fused into glass borate discs with a Li-tetraborate and La oxide flux using the method of Norrish & Hutton (1969). Analyses were undertaken on a Philips PW1400 spectrometer. Minor element analyses for 28 elements were also carried out using an experimental low dilution fusion technique developed at CSIRO Division of Soils (Norrish *pers. comm.*). A nominal 1.2 g of sample which had been ignited at 1000°C was fused with 2.8 g of 1222 flux (Li-tetra-meta-borate in the ratio of 12 to 22). The clay

fraction (<2μm) of eight samples were analysed using this technique and results are presented in Appendix 7.

2.2.7 Electron Microprobe Analyses

Detailed mineral chemistry of samples containing alunite and halloysite were undertaken using an electron microprobe due to the very fine grain-size and intimate relationships of these minerals. Analyses were carried out on polished thin sections with a Cambridge "Geoscan" wavelength dispersive electron probe microanalyser using an excitation voltage of 20 kV, a beam current of 20 nA and short counting time of ten seconds. Moving beam rather than stationary beam analyses were used to minimise the loss of sulphur from alunite which had been detected after several seconds when using a stationary focussed beam.

2.2.8 Thin Sections

Thin sections of selected samples were prepared from air-dried materials impregnated with epoxy or polyester resins following the methods of Cent & Brewer (1971) and Riley (1973). Due to the very fine grain size of many samples some difficulty was experienced in impregnating using epoxy resins. Several experiments altering vacuum settings, the temperature of the resin prior to impregnation and increasing the standing time of sample and resin before curing were therefore undertaken. In general, epoxy resins remained too viscous for complete impregnation of fine-grained samples and Escon polyester resin was selected as providing the best results. The method adopted involved slow impregnation of the sample with Escon polyester resin under vacuum at room temperature. The sample was then left to stand for 7 days before final curing at 110°C. Impregnated blocks were cut, ground, mounted on glass slides with Araldite and then ground and polished until 25 to 30 μm thick.

The thin sections were subsequently studied using an optical microscope in transmitted light at magnifications ranging from 10 to 80 times.

2.2.9 Ammonium Oxalate Extraction

A number of samples from horizons where alunite and/or halloysite occurred were tested for allophane-like minerals using acid ammonium oxalate extraction techniques. SEM studies had identified a number of thin wispy forms in several samples which could not be categorised using the EDS system. A study of the literature suggested that allophane had been noted in association with both alunite and halloysite, hence tests for allophane were undertaken on these samples. Published results in Mitchell *et al* (1964) and Schwertmann (1964) suggested that acid ammonium oxalate should extract amorphous materials with allophane being identified from a comparison of the amounts of Si and Al present in the extracts. The samples were extracted using a procedure modified from that of McKeague & Day (1966) with Si determinations made spectrophotometrically using the method of Webber & Wilson (1964) and Al determined using atomic absorption spectroscopy.

2.2.10 Scanning Electron Microscopy

Scanning electron microscopy (SEM) using a Cambridge Stereoscan 250 Mk III instrument fitted with a Link energy dispersive X-ray analysis system (EDS) was undertaken on fragments of whole samples mounted on aluminium stubs and sputter coated with gold at the Electron Optical Centre of The University of Adelaide. Samples were selected from alunite/halloysite intervals and mottled carbonate beds in order to assess the *in situ* relationships of the mineral components and help determine modes of formation. Later SEM studies of clay-rich samples which were undertaken to look for possible diagenetic clays, were carried out at CSIRO Division of Soils using a Cambridge Stereoscan 250 Mark III fitted with a Link System EDS.

Features identified by optical transmission microscopy from thin sections were often difficult to relate to morphologies observed on small fragments using the SEM. To overcome this, impregnating resin from some thin sections was removed by etching with methylene chloride

before observation using the SEM. Norton *et al* (1983) had previously successfully applied a similar technique to micromorphological studies.

2.2.11 Transmission Electron Microscopy

The <2μm fraction of some clay and alunite-rich samples were dispersed in distilled water using an ultrasonic probe and sedimented onto carbon-coated grids for observation using transmission electron microscopy (TEM). A JEOL 100S TEM operating at 80 kV was used to photograph these samples providing a record of particle shape and size.

CHAPTER 3
FIELD OBSERVATIONS

3.1 General Statement

Sediments of Quaternary age are well exposed in coastal cliffs between Hallett Cove and Sellicks Beach. Detailed fieldwork in this area was undertaken to identify, describe and map the distribution of sedimentary units and to locate sites which were representative of these sediments where more detailed observations and sampling could be undertaken. In general, Quaternary sediments from coastal exposures within the Noarlunga and Willunga Embayments comprise a basal coarser unit overlain by much finer sediments. Lateral variation in the distribution of these units occurs and is discussed in this Chapter.

Quaternary non-marine sediments which are the focus of the current work are underlain by marine units in most sections of the coastline and the relationship between the two has been investigated to help understand the origin of the basal Quaternary sequence. A greater marine influence occurred during the Late Tertiary and Early Pleistocene in the Willunga Embayment than within the Noarlunga Embayment. In the latter embayment only isolated remnants of a fossiliferous and calcareous sandstone thought to be deposited in shallow marine conditions (Lindsay 1969), the Late Pliocene Hallett Cove Sandstone, are found. Much thicker and continuous deposits of this unit crop out along the coast in central parts of the Willunga Embayment. In addition, a lateral facies change in the Hallett Cove Sandstone can be identified in northern parts of the Willunga Embayment from limestone at Maslin Bay through fossiliferous sands to a fossiliferous conglomerate at Ochre Point (Stuart 1969). No similar sequence can be identified in the Noarlunga Embayment.

The Early Pleistocene Burnham Limestone is a soft, fossiliferous marl considered to have been deposited in lagoonal or near-shore marine and marginal marine environments (Ludbrook 1983). It has not been positively identified in the Noarlunga Embayment during the present study. At Hallett Cove however, there are small carbonate mottles within sands

of the coarse basal Quaternary unit and these are tentatively correlated with the Burnham Limestone due to their similarity with carbonate mottles associated with this unit in parts of the Willunga Embayment. In contrast, there is continuous exposure of the Burnham Limestone in central parts of the Willunga Embayment with additional outcrop in the south at Sellicks Beach. Sandy sediments at the base of the Quaternary sequence in central parts of the Willunga Embayment are frequently mottled with white dolomite. These mottled sediments overlie or show a lateral gradation from massive limestone of the Burnham Limestone.

Non-marine Quaternary sediments overlie the Hallett Cove Sandstone and Burnham Limestone marine sediments in both embayments. Sandy and gravelly sediments occupy basal parts of the non-marine sequence in the Noarlunga Embayment and northern parts of the Willunga Embayment. In central parts of the Willunga Embayment the coarser basal sediments are absent and clays of the upper fine-grained unit directly overlie the marine units. The basal non-marine Quaternary sediments exposed in the Noarlunga Embayment are more complex than equivalent sediments from the Willunga Embayment with numerous upward fining sedimentary cycles and more frequent and extensive gravel beds. A thick sequence of gravels and sandy clays at Sellicks Beach forming an alluvial fan adjacent to the Willunga Fault escarpment provides the only example of coarse gravelly sediments in the Willunga Embayment. The upper fine-grained unit has similar characteristics in both embayments with thickest sequences occurring in central parts of the embayments such as at Onkaparinga Trig and between Port Willunga and Snapper Point. These are the only areas where carbonate beds are found within the clay-rich unit and also where an upper sandy unit is best developed. Towards the embayment margins (except the southern margin of the Willunga Embayment), the fine-grained unit thins and contains sandy sediments mostly in the form of poorly defined sand sheets rather than as lenses within the clays.

Carbonate-rich sediments which include calcrete layers together with unconsolidated carbonate silt overlie the Quaternary sequence as a blanket throughout the Noarlunga and Willunga Embayments. Vertically oriented mottles and discontinuous beds of carbonate are

frequently observed in upper parts of the sequence immediately below the main carbonate mantle and suggest a gradational contact between these intervals. Where Quaternary sediments are not present, the calcareous sequence mantles a wide variety of Precambrian and Tertiary rocks.

3.2 Description of Sites Along the Coastline

Following reconnaissance fieldwork along the coastline to map the distribution of sedimentary units and identify significant features within the sequence, more detailed observations were made at a number of sites to enable lithological breaks to be closely examined. Features such as the occurrence of alunite in basal parts of the sequence, the presence of mottled carbonate within upper fine-grained units and the development of iron-rich mottles within sandy intervals were also described in detail. Reconnaissance sampling of these features and the sedimentary units identified was also undertaken at many of these sites so that the mineralogical composition of the Quaternary sequence could be determined. Based on these data, several sites were selected for more detailed investigations and sample collection. The sites in which reconnaissance studies were undertaken were chosen because of ease of access and to span the two embayments from south to north. Except where a specific feature was identified for study, sites were selected to be representative of the full Quaternary sequence with marine Tertiary or Precambrian sediments cropping out and defining the base of the non-marine sequence. Locations of all sites mentioned are shown on Figure 1.2.

3.2.1 Sellicks Beach

(Yankalilla 1:50 000, 676862)

Sellicks Beach lies on the southern margin of the Willunga Embayment where a thick sequence of gravels and sandy clays occurs adjacent to the Willunga Fault escarpment. In the vicinity of Sellicks Trig, limestones of the Miocene Port Willunga Formation have been warped into a slight anticlinal structure forming a resistant base to the cliffs up to 6 metres

high. The limestones have a karst-like and calcreted surface with a relief of up to 4 metres and several small silicified, cylindrical root-like features have been observed on this surface.

Within the basal sequence of clays and sandy clays a soft, friable and marly carbonate rock (Fig 3.1) containing a rich marine fauna has been identified as the Early Pleistocene Burnham Limestone (May & Bourman 1984) because of its lithology and the presence of the Early Pleistocene gastropod *Hartungia dennanti chavani* (identified by Dr Ludbrook). There is a 10 cm layer of soft white dolomite interbedded with laminated grey (10YR 8/2) clays approximately 1 metre above the limestone and several small, isolated pods of dolomite also occur between the limestone and main layer of dolomite. Similar occurrences of dolomite have been noted in association with the Burnham Limestone at many localities. Minor, small, yellow to orange (10YR 6/6) mottles occur within the limestone and also in sands and clays immediately below the limestone. Several poorly sorted gravel layers which crop out between the Port Willunga Formation and the Burnham Limestone include pebble-sized, sub-angular clasts of quartzite and grey, purple and red siltstone (Fig 3.2).

A maximum of 50 metres of interbedded gravels and sandy clays overlie the interval containing the Burnham Limestone (Fig 3.3). Gravel units are up to 3 metres thick and contain poorly sorted, angular to sub-rounded clasts of quartzite, siltstone and limestone, mostly of pebble and cobble size, in a clayey and sandy matrix. The intervening sandy clays can be up to 5 metres thick and contain isolated pebbles. Gravel units occur most frequently in central portions of the sequence and underlie a friable, yellow-grey, clay-rich unit which appears similar to clays from upper fine-grained units observed elsewhere in the study area. The steepness of cliffs in this area has precluded detailed observation and sampling of this unit. Immediately below this clay-rich unit, the coarse sediments display vertically oriented, red, ferruginous mottles up to 25 cm in size with iron oxides impregnating the fine matrix and coating large clasts. Capping the sequence is a thin gravelly calcrete composed of angular clasts of quartzite and siltstone cemented by carbonate.

To the north of Sellicks Trig the stratigraphy has been considerably disrupted by a large landslump which is discussed by May & Bourman (1984). Evidence for older phases of slumping can also be found to the south of Sellicks Trig.

3.2.2 Snapper Point

(Yankalilla 1:50 000, 672933)

Marine sediments of the Hallett Cove Sandstone and Burnham Limestone are exposed just above beach level at Snapper Point and are overlain by a thick clay-rich sequence (Figs 3.4 and 3.5). A disconformable contact between the Hallett Cove Sandstone and the Burnham Limestone is suggested by the incorporation of boulders of calcareous sandstone up to 20 cm in size within basal parts of the Burnham Limestone and also the presence of calcified roots on the exposed upper surface of the Hallett Cove Sandstone. The roots vary from thin, isolated cylindrical forms up to 2 cm in diameter to massive, matted and twisted structures up to 20 cm in diameter (Fig 3.6).

Massive grey-green clay which displays rare columnar structure and small yellow mottles is the dominant lithology in the Snapper Point area. Isolated sand-filled channels in upper parts commonly show horizontal planar bedding while laminated sand and clay occurs just above the Burnham Limestone. The bed of mottled carbonate which occurs between 7 and 8.5 m above the beach at Snapper Point crops out intermittently at the same stratigraphic position for several kilometres north of this location and varies in thickness from 1 to 2 m. To the north of Snapper Point a sand-filled channel has eroded into the underlying clays truncating the mottled calcareous bed and suggesting that development of this calcareous unit pre-dates deposition of the overlying sandy sediments (Fig 3.7).

3.2.3 Port Willunga

(Yankalilla 1:50 000, 688949)

Overlying the Miocene Port Willunga Formation at this location is a similar sequence to that observed at Snapper Point (Figs 3.8 and 3.9). The Hallett Cove Sandstone is up to 4 metres thick and is overlain by 1 to 2 metres of rubbly limestone (identified as the Burnham Limestone) which incorporates occasional boulders of calcareous sandstone reworked from the underlying Hallett Cove Sandstone. Large, vertical fractures in the upper surface of the Burnham Limestone are filled with green sandy clay. Green-yellow clay with several thin sandy intervals (<1 cm) overlies the limestone. A discontinuous band of soft, white dolomite occurs approximately 20 cm above the Burnham Limestone. Additional, isolated dolomitic mottles, a maximum of 15 cm high and 7 cm across, are found within the clays up to 1 metre above the limestone.

Clay-rich sediments at this site are up to 12 metres thick with lower clays a yellow-green colour and upper clays a red-green colour. The presence of small iron-rich mottles which are yellow near the base and red in upper parts appears to explain these colour differences. Columnar structure is noted occasionally within the clays, however they are usually massive with isolated sand-sized quartz grains scattered randomly throughout the clay. A thin, discontinuous sandy lens which is mottled red or orange and in places contains gravel beds up to 10 cm thick and 2 metres long separates the two different coloured clays. Clasts in the gravel beds include shale, quartz and ferricrete up to 4 cm in size and are generally sub-angular to sub-rounded.

3.2.4 Chinaman Gully

(Yankalilla 1:50 000, 690956)

Quaternary sediments form the upper part of cliffs at this locality and overlie Tertiary sediments which include the Hallett Cove Sandstone, the Port Willunga, Chinaman Gully and Blanche Point Formations (Figs 3.10 and 3.11).

Sediments identified as the Burnham Limestone at this site are 1 metre thick but, unlike other locations where this unit occurs, there is no mottled dolomite in the overlying clays. Instead, a sequence 6 cm thick of thinly interbedded yellow-green (5Y 6/3) clays and sands is observed below a 2 metre interval of clay. Seventy cm above the Burnham Limestone, a 20 cm thick horizon containing small alunitic pods is present, and extends laterally for 100 metres. The pods of alunite are up to 8 cm across and have sharp lower but diffuse upper boundaries with the surrounding clays.

A central sand-rich unit comprising mostly fine sand and silt is present at the Chinaman Gully site and has a maximum thickness of 2.6 metres. The contact with underlying clays is generally sharp, however fine sand extends into these clays along vertical fissures up to 30 cm deep and 8 cm wide. Red, iron-rich mottles are common within the sands and occasionally exhibit yellow skins of jarosite. A gradational change to the overlying green-red (5Y 6/3 with mottles 7.5R 3/6) sandy clays occurs at this site although several hundred metres to the north, the boundary is sharp with laminated clay filling small, vertical tubular structures 4 cm long by 1 cm wide. Similar structures have been observed at Ochre Cove and Onkaparinga Trig where they are thought to be due to burrowing fauna.

3.2.5 Blanche Point

(Noarlunga 1:50 000, 690963)

The basal 20 to 25 metres of coastal cliffs in this area are formed by Tertiary limestones with Quaternary sediments comprising the upper 15 metres. At Blanche Point a thick sequence of massive clay is exposed above sediments correlated with the Burnham Limestone. The lower clays are a yellow-green colour and the upper clays red (Fig 3.12). The perceived colour difference is due mainly to the presence of small ferruginous mottles which are yellow-orange (10YR 6/8) in basal parts and red (7.5R 3/6) in upper parts. The clay itself remains an olive-yellow colour (5Y 6/3). To the south, prominent sand-rich units occur which are up to 100 metres long and 3 metres thick and separate the two different coloured

clays. However at several locations the sands rest directly on the Burnham Limestone. Within the thicker sandy units, thin beds of clay are common. Red-brown to green clays overlie the sandy units and an undulating, erosional contact is displayed at several sites (Fig 3.13). Minor red mottling occurs at the base of clays adjacent to the sandy units but prominent ferruginous mottling similar to that observed at Chinaman Gully is not widespread near Blanche Point.

3.2.6 Maslin Bay

(Noarlunga 1:50 000, 697970)

A site between Tortachilla Trig and the access path has been sampled and described at Maslin Bay (Figs 3.14 and 3.15). At the base of the sampled section a 1 metre interval of grey-green sandy clay contains abundant large, soft mottles which are often dolomitic and frequently coalesce into large masses. Similar carbonate mottles have been observed at various localities along the coastline associated with limestones of the Burnham Limestone. It is considered that the mottles at Maslin Bay are also related to the Burnham Limestone as they can be traced laterally to the south occurring intermittently for approximately 150 metres with massive limestones identified in the same stratigraphic position at the southern end of Maslin Bay. To the north, near Tortachilla Trig, mottled carbonate overlies several metres of interbedded grey, white and yellow fossiliferous quartz sand and calcareous sandstone which have been correlated with the Hallett Cove Sandstone (Crespin 1954; Reynolds 1953; Stuart 1969) (Fig 3.16).

An interval of yellow to orange sand up to 1 metre thick overlies the carbonate which is in turn overlain by 11.5 metres of interbedded sand, sandy clay and minor clay. Several interesting features are present within this sequence. Immediately above the orange sand is a thin accumulation of manganese oxide which impregnates the sandy sediment and imparts a grey-black colour to this interval. Between 2 and 4 metres above the mottled carbonate are several bands where the sand is impregnated by halloysite to form grey, waxy bulbous masses. Several, thin, elongate pods of white alunite also occur within the halloysite-rich

zone. Alunite is more common to the north near Tortachilla Trig where it forms thin discontinuous seams.

Approximately 5.5 metres above the mottled carbonate is a 1.5 metre interval comprising sand and silt which is indurated and contains large, red, vertical, ferruginous mottles. Such prominently mottled intervals are not continuous in this area but occur within a thin band near the southern end of Maslin Bay, reappear at the site sampled and also occur northward past Tortachilla Trig. Intervening sections consist of sandy clays and minor clays with no coarser, sandy mottled intervals.

In the upper 9 metres of the sampled section, there are massive grey-green clays. These are overlain by several metres of calcareous sediment with the surface indurated to form a calcrete. This fine-grained sequence is common throughout the Maslin Bay area.

3.2.7 Ochre Point

(Noarlunga 1:50 000; 696995)

The type section for Ward's (1966) Seaford and Ochre Cove Formations and Ngaltinga Clay is located at Ochre Point (Figs 3.17 and 3.18). The Quaternary sequence overlies either basement rocks comprising interbedded siltstones and sandstones of the Precambrian Umberatana Group or a ferruginised conglomerate which was correlated with the Hallett Cove Sandstone by earlier workers (Glaessner & Wade 1958; Ward 1966; Stuart 1969). This unit has been traced north as far as Ochre Cove and southwards for a further 300 metres where it contains fossil fragments in sandy pockets within the otherwise conglomeratic deposits. The thickness of this bed is extremely variable with sandy sections 20 cm thick grading to intervals containing large boulders of quartzite up to 60 cm in diameter.

The basal 12.5 metres of Quaternary sediments are dominantly interbedded grey and light yellow fine sand and sandy clay with the more clayey units being up to 25 cm thick. Coarser sediments dominate the central 1.5 to 2 metres where a succession of thin gravel lenses up to

30 cm thick fill shallow channels eroded into the underlying finer sediments. Minor planar cross bedding is displayed by the gravel lenses with clasts being sub-angular to sub-rounded and including quartz, quartzite and siltstone. Exposure within the vicinity of Ochre Point is not always good, but it is evident that the coarser, gravelly sequence occurs discontinuously. North of Ochre Point, yellow-orange (10YR 8/2 to 10YR 7/8) mottled sandy units which exhibit a vertical, prismatic structure with bleached upper portions are occasionally observed (Fig 3.19). These discontinuous sequences up to 60 cm thick and generally more resistant than surrounding sediments are interpreted as probable palaeosols.

Massive grey-green clays which contain isolated sand-sized quartz grains dominate the upper 8 metres of section at Ochre Point with the colour tending toward red-brown near the top of this unit. Several isolated 1 metre thick lenses of indurated white to grey-coloured sand occur and contain large, red, vertical mottles of iron oxide. Calcareous silty sand overlies the clay and is capped by a calcrete layer.

3.2.8 Seaford

(Noarlunga 1:50 000, 694028 to 693035)

Coastal cliffs in the Seaford area, particularly near Robinson Point, provide excellent exposures of Quaternary sediments (Fig 3.20). However the base of the sequence is not always exposed above beach level. Miocene Port Willunga Formation crops out as isolated remnants on the beach and also forms wave-cut platforms. The Quaternary sequence in this area comprises a basal sequence of interbedded sands, sandy clays and gravels with minor clay and an upper unit composed dominantly of grey-green to red clays. Isolated sandy lenses occur within the upper clays and the sequence is capped by a blanket of calcareous sediment which includes a calcrete.

A section 600 metres south of Robinson Point (Noarlunga 1:50 000, 694028) illustrates the nature of the sediments in the area (Figs 3.21 and 3.22). Bedding of sand and clay units, particularly in the basal 3 metres of the section near Robinson Point, is generally horizontal

with thicker clay units traceable for several hundred metres at roughly the same elevation. Thick gravels form lenses and also fill shallow channels eroded into underlying sands. Low-angle cross-beds can also be observed in a number of the gravel lenses but are seldom seen in sandy beds. Clay-rich sediments in upper parts of the sequence are generally massive. Rare intervals occur where the clay breaks preferentially into blocky peds up to 12 cm high and 5 cm across. Staining by iron and manganese oxides is common on the surfaces of peds, as is evidence of remobilisation of clay to form laminated coatings.

Six upward fining sedimentary cycles, comprising angular to sub-angular gravels which grade through sands to clays, are evident within the Robinson Point Formation near Robinson Point. Most sedimentary cycles have been truncated by variable amounts of erosion prior to the deposition of gravels which form the subsequent unit, however clay and silt-rich beds are still present in upper parts of most sequences. Some 400 metres to the south, up to nine upward fining cycles can be observed below the gravel lenses. Each cycle is coarsest at the base and gradually grades from coarse, often gritty sands to micaceous silty and clayey sediments. Thin gravel beds are frequently included at the base of such cycles and consist mostly of small sub-angular pebbles of quartz, siltstone and ferricrete. Sharp undulating contacts are observed at the base of each cycle, with a relief of up to 10 cm (Fig 3.23). Isolated, larger hollows appear to have an erosional origin and are filled by coarse sands and grits of the overlying unit. The finest sediments are buff to grey in colour and display small, vertical mottles of yellow goethite. Coarser sediments nearer the base of each cycle are redder in colour, with hematite being present as well as goethite. Mottling in the coarser sediments takes the form of large, irregular blotches, up to 10 cm in size and appears to form by selective bleaching of the dominantly orange-red coloured sediments.

Numerous small vertically oriented tubes up to 0.5 mm in diameter penetrate the silt and clay-rich beds and have circular cross sections. Occasionally larger tubules, up to 1 cm in diameter, are observed which have been infilled by further deposition. Such structures are interpreted as burrows made by small organisms and suggest that bioturbation has been active in these sediments.

Mottles present within sands from the lower 1.5 metres of cliffs throughout the Seaford area display an unusual orange-pink colour which appears to be due to hematite, the dominant iron oxide present in these mottles. The colours are associated with thin, discontinuous seams of white alunite which broadly conform to local bedding. Seams are up to 6 cm in thickness, have a sharp basal contact and a diffuse upper contact with the surrounding sandy sediments and are generally free of impurities such as quartz grains. Occasional isolated pods of alunite up to 10 cm across are also found (Fig 3.24).

3.2.9 Onkaparinga Trig

(Noarlunga 1:50 000; 691048)

Between Seaford and the Onkaparinga Trig Station, exposure of Quaternary sediments is generally poor due to vegetation cover and surface wash. Immediately south of the Trig Point however, up to 20 metres of unconsolidated sediments of Quaternary age overlie the Tertiary Port Willunga Formation which forms a low bench behind the beach (Fig 3.25). A karst-like surface is evident with solutional hollows up to 75 cm deep and 2 metres diameter.

A section through the Quaternary sequence has been sampled approximately 150 metres south of the Trig Point (Figs 3.26 and 3.27). Sediments are similar to those observed in the Seaford area with the exception that the upper clay-rich unit is much thicker at this location.

A thin green-yellow clay immediately overlies Tertiary limestones and often includes small, rounded masses of soft, chalky alunite. Further alunite occurs as thin, elongate pods up to 3 cm thick and 25 cm long in the overlying 1.3 metres of interbedded sand and sandy clay. Rounded, waxy pods which are halloysite-rich and up to 15 cm across also occur in this interval. A 10 cm band of yellow-brown sand cemented by iron oxides (dominantly goethite) overlies the halloysite followed by pink (10R 5/6 to 2.5YR 5/6) and white, unconsolidated fine sands. Several gravel units comprising sub-angular to sub-rounded

clasts of quartz, quartzite, siltstone and weathered schist (0.5 to 2 cm size) occur in the next 3 metres and grade upward into fine micaceous sand and silt (Fig 3.28).

The upper 13 metres at this site are dominated by massive clays which display occasional blocky peds giving a columnar appearance. Brownish clays occur in the upper 4 metres with several thin, sandy interbeds. A white, micaceous, sandy to silty unit which occasionally contains small ferruginous mottles occurs about 8 metres above the Robinson Point Formation. Immediately below this unit is a 2 metre thick interval where large, white, calcareous mottles up to 30 cm in size are present. Carbonate also impregnates the surrounding green-grey clay. The carbonate unit is discontinuous but can be traced intermittently northward to the mouth of the Onkaparinga River.

3.2.10 Onkaparinga River Mouth

(Noarlunga 1:50 000; 696058)

Seven samples have been collected from an erosion gully developed as a result of outflow from a stormwater drain just east of the mouth of the Onkaparinga River (Figs 3.29 and 3.30). At the base of the gully, 50 cm of sub-rounded gravels up to 10 cm in size overlie Tertiary limestones of the Blanche Point Formation. The gravels grade upwards into sands which are up to 50 cm thick and overlain by grey-green clays exhibiting a pronounced vertical prismatic structure. A 40 cm thick band of mottled carbonate similar to that described from the Onkaparinga Trig site occurs within the clay unit. Sandy, and in places silty and micaceous sediments overlie the clays and grade upward to brown and grey sandy clays with long vertical columns of soft white carbonate penetrating these sediments from the overlying thick calcareous mantle.

3.2.11 Port Noarlunga/Witton Bluff

(Noarlunga 1:50 000; 691074 to 691078)

Only limited sampling has been undertaken in this area and is confined to a lower interval where alunite occurs just north of Port Noarlunga and also to upper clay-rich sediments near Witton Bluff. Quaternary sediments overlie thick Tertiary Limestones of the Blanche Point Formation and, as at many sites in the study area, comprise gravels, sands and sandy clays. Red-brown clays which in this area are not more than 4 metres thick overlie the coarser sediments (Figs 3.31 and 3.32). In the cliff face at Witton Bluff, a massive to platy carbonate bed of variable thickness (up to 60 cm) occurs between the sandy sediments and red-brown clays. Further carbonate mottles and blotches occur in upper parts of the clay-rich unit immediately below a calcrete layer.

Several beds of chalky, white alunite occur at the base of the Quaternary sequence with 2 to 3 horizontal bands up to 3 cm thick observed in gritty basal sands (Fig 3.33). The lowermost band of alunite is unusually thick (20 cm) and continuous for several hundred metres. Small, rounded, bulbous masses are found on the underside of this bed and protrude into the underlying clays (Fig 3.34).

Gravel lenses up to 30 cm thick are common immediately above the alunite interval and grade into a sequence of interbedded sands and sandy clays where gravels are rare. Sandy units are generally horizontally bedded and often indurated although rare tabular cross-beds are observed. South of Witton Bluff these sediments have been considerably disturbed. Blocks of planar bedded sand up to 1.5 metres across are often steeply tilted and occur randomly within otherwise massive sands and sandy clays (Fig 3.35). Bedding within the blocks cannot be traced laterally into surrounding massive sands, nor are adjacent blocks obviously related. Underlying sediments which are of similar lithology and overlying clays remain undisturbed. Intraformational slumping of well bedded and cohesive sandy sediments within a 5 metre sequence of incompetent sandy clays may account for the disrupted nature of these sediments.

3.2.12 Hallett Cove

(Noarlunga 1:50 000; 718154)

Up to 20 metres of Quaternary sediment are exposed in the Amphitheatre at Hallett Cove overlying unconsolidated Permian sediments and a thin remnant of the Hallett Cove Sandstone. A section adjacent to the Sugarloaf has been sampled (Figs 3.36 and 3.37).

Overlying the Hallett Cove Sandstone immediately east of the Sugarloaf are 70 cm of grey-green sandy clays including a discontinuous zone of mottled, white carbonate in the upper 15 cm. The carbonate is considered to be equivalent to the Burnham Limestone based on the presence of mottled carbonate associated with this unit at other locations in the study area. Where samples were collected, some 100 metres further east, carbonate is not present at the base of the section. Instead, grey-green, horizontally bedded sand occurs which includes minor gravel beds containing sub-angular clasts of quartz, siltstone, sandstone and ferruginous material. Grey-green to yellow clays or sandy clays which tend towards red-brown colours continue for 3 to 4 metres underlying a thick, sandy to silty and indurated unit in which prominent, vertical, ferruginous mottles have formed. A further 4 metres of sands and sandy clays with rare gravel beds and thin clay units crop out above the mottled interval and are in turn overlain by massive red-green clay.

Lateral variation of sedimentary units within the Amphitheatre is apparent (Fig 3.38). The central mottled sandy interval is absent towards the north where upper red-green clays thicken and directly overlie grey-green to yellow clays. As at many sites in the region, the colour of the clays reflects the ferruginous mottling with yellow mottles (10YR 6/8) giving yellow colours and red mottles (7.5R 3/4) a redder colour. Isolated sandy lenses which are mottled and sometimes indurated are observed within upper clays at the northern end of the Amphitheatre but are not stratigraphically equivalent to more pronounced mottled sediments further south.

North of the Amphitheatre, Quaternary sediments are thin and poorly exposed with up to 1 metre of gritty and sometimes gravelly sand overlying isolated remnants of the Hallett Cove Sandstone. Isolated pods and thin beds of alunite sometimes occur within these sands. Beds and small lenses of gritty green-grey clay containing angular grains of quartz, feldspar and rock fragments overlie the basal sands. Occasional, small mottled sandy lenses are observed in upper parts of the Quaternary sequence. However poor exposure prevents correlation of these occurrences with those within the Amphitheatre.

3.2.13 Railway Cutting, O'Sullivan Beach Road

(Noarlunga 1:50 000; 716108)

While the railway cutting described here is located 2.3 km from the coastline, several samples were collected at this site as part of mineralogical investigations, particularly in relation to the development of ferruginous mottles. An alluvial channel approximately 100 metres wide and 6 metres deep has been cut in Precambrian bedrock and filled with Quaternary non-marine sediments (Fig 3.39). Coarse, channel-fill sands are thickest in the channel base, thinner toward the margins and show horizontal planar bedding in several sections. Vertically oriented iron mottling is pronounced within the basal sands which are otherwise a white-grey (7.5Y 7/2) colour. The sands are overlain by several metres of massive green-red (5Y 6/2 to 7.5R 3/4) clays. A thin calcrete and associated soft calcareous silt overlie the clays with calcareous material partially filling small vertical fractures in the clay.

3.3 Proposed Sedimentary Units

Based on field observations described in this Chapter, a stratigraphic scheme for Quaternary sediments exposed in coastal cliffs in the Noarlunga and Willunga Embayments is proposed (Table 3.1). Overlying the Hallett Cove Sandstone of Late Pliocene age and the Burnham Limestone of Early Pleistocene age are two newly named units; the Robinson Point and Ngaltinga Formations. The Robinson Point Formation is proposed for generally coarse-

grained sediments at the base of the Quaternary sequence while the Ngaltinga Formation covers mostly fine-grained sediments forming the upper parts of the sequence. Within the Ngaltinga Formation two members are recognised; the Neva Clay and Snapper Point Sand Members. All new names have been approved by the Stratigraphic Nomenclature Sub-committee of the Geological Society of Australia (South Australian Division) and definitions have been published by May *et al* (1991).

3.3.1 Robinson Point Formation

A type section for the Robinson Point Formation has been nominated in coastal cliffs at the section described just south of Onkaparinga Trig (Noarlunga 1:50 000; 691048) (Figs 3.26 and 3.27). The name is derived from Robinson Point (Noarlunga 1:50 000; 694034) which is located 1.4 km south of the type section.

The Robinson Point Formation consists of an interbedded sequence of clays, sandy clays, sands, grits and gravels. Basal sediments and those near the top of the formation are dominantly sands and sandy clays with rare thin gravel beds while discontinuous gravel lenses are common in central parts. Gravels comprise mostly angular to sub-rounded clasts of quartz, quartzite, siltstone and ferricrete which vary in size from a few mm to 10 cm. In the Noarlunga Embayment between Witton Bluff and Port Noarlunga, coarse gravels which have a similar appearance to those from central parts of the formation elsewhere in the region, occur at the base of the unit. There are no underlying sands or clays. Much coarser gravels are found in a thick sequence adjacent to the Willunga Fault Escarpment at Sellicks Beach (see section 3.2.1). Planar bedding is commonly exhibited in sandy and gravelly intervals with cross-beds occasionally preserved in these sequences. Cross-beds are more frequent in coarse sand to grit units which occur mostly in basal parts of the formation. In contrast with the coarser intervals, interbedded sandy clay units show no bedding structures. Basal parts of the formation are characterised by cycles of deposition up to 1 metre thick commencing with poorly sorted, angular to sub-rounded gravels and fining upwards to silty and clayey beds. These finer units often display a coarse, prismatic structure which masks

any original sedimentary structure. Evidence of bioturbation in the form of 2 to 10 mm diameter, vertically oriented, cylindrical tubes, some of which have been infilled by clay is also common in the finer units. Thin beds and isolated, rounded masses of white alunite often occur in basal sandy sediments and are generally associated with hardened, nodular masses of the surrounding sandy sediment. The development of alunite is usually associated with an interval up to 2 metres thick which displays an unusual pink-red colour not seen in any other sediments in the region. Prominent ferruginous mottling is common in central parts of the formation within indurated sandy sediments which are sandwiched between fine-grained beds. Smaller, less prominent yellow-orange mottling is associated with fine-grained units while unconsolidated red-orange sands and grits are often selectively bleached. A coarse rectangular pattern of bleaching is common.

Sediments of the Robinson Point Formation are exposed almost continuously along the coastline between Hallett Cove and Sellicks Beach apart from areas adjacent to modern drainages where they have been removed by erosion and between Blanche Point and Aldinga Beach where sediments of the Ngaltinga Formation directly overlie the Burnham Limestone (Fig 3.40). Thickest sequences are found at Sellicks Beach adjacent to the Willunga Fault escarpment where up to 50 metres of poorly sorted gravels and interbedded sandy clays are exposed. Elsewhere, the formation is generally between 5 and 10 metres thick.

At the coast, the Robinson Point Formation directly overlies marine sediments of Tertiary age or the Early Pleistocene Burnham Limestone. However, at several locations such as Sellicks Beach, Maslin Bay and Hallett Cove, the Burnham Limestone is interbedded with basal sands of this formation. As no fossils have been identified from the Robinson Point Formation, these observations provide the only evidence for the age of the sediments and suggest that they can be no older than Early Pleistocene.

3.3.2 Ngaltinga Formation

The Ngaltinga Formation comprises clays and sandy clays forming the upper part of the Quaternary sequence but the definition excludes the layer of calcareous material which forms a blanket over a wide variety of sediments in the study area. A type section is located in coastal cliffs just south of Snapper Point (Yankalilla 1:50 000; 672933) (Figs 3.4 and 3.5). The Ngaltinga Formation at Snapper Point and also at other locations can be divided into the Neva Clay and Snapper Point Sand Members which reflect the frequent occurrence of coarser sediments in upper parts of the formation.

The Neva Clay Member comprises massive, grey-green clay with rare, very thin interbeds (up to 1 mm thick) of fine sand near the base. Rounded, fine sand-sized quartz grains are scattered randomly through the clay but generally form less than 10% of the sediment. The clay often breaks into blocky peds where exposed at the surface with slickensides and manganese staining developed on many ped surfaces. Small orange-yellow blotches are common in parts of the Neva Clay Member but blotches tend to be red-coloured in some central and upper portions of the unit. Discontinuous intervals of mottled carbonate up to 2 metres thick occur in the upper half of the Neva Clay Member at several localities in central parts of both the Noarlunga and Willunga Embayments.

Coarse sands filling isolated channels eroded into clays of the Neva Clay Member often mark the base of the Snapper Point Sand Member. Planar bedding is common in these sandy channel deposits but gravels and cross-beds are rare. The channels generally form broad troughs up to 40 metres across while slightly higher in the sequence, smaller, U-shaped channels are sometimes observed. Induration of the sands is common. Large red-yellow ferruginous mottles occur frequently at the base of the channels and also at the gradational contact with overlying clayey sediments. Upper parts of the Snapper Point Sand Member usually consist of interbedded clayey sands and clays with occasional sandy interbeds and rare gravel layers comprising pebble-sized, sub-rounded clasts of quartzite and siltstone. A gradational contact with the overlying blanket of calcareous material is recognised with thin

beds and mottles of carbonate penetrating the upper metre of the Snapper Point Sand Member. Within the Noarlunga Embayment, sand bodies in upper parts of the Ngaltinga Formation are poorly defined and not confined to isolated channels as is the case in the Willunga Embayment. These sands have similar textural characteristics to the channel-fill sands in the Willunga Embayment and are occasionally mottled with iron oxides but tend to be unconsolidated and devoid of bedding structures. The sand sheets are upward fining and frequently interbedded with finer sandy clay units. While differences exist between the two types of sand body recognised in the area, they are both considered to represent the Snapper Point Sand Member due to their textural similarities and occurrence at the same stratigraphic interval.

Sediments of the Ngaltinga Formation are exposed almost continuously in coastal cliffs between Hallett Cove and Sellicks Beach, apart from several sections where erosion by modern drainage has removed the older sediments. Thickest exposures occur near the type section and also Onkaparinga Trig where the Ngaltinga Formation is up to 14 metres thick (Fig 3.40). At other localities the thickness rarely exceeds 10 metres.

The Ngaltinga Formation overlies the Robinson Point Formation with sharp contact and lithological differences usually make the distinction clear. Between Blanche Point and Aldinga Beach, the Ngaltinga Formation rests directly on the Burnham Limestone and carbonate mottles often occur within basal clays immediately above the limestone. In the vicinity of Blanche Point and also at Hallett Cove, sandy sediments of the Robinson Point Formation lens out and therefore the basal sediments of this formation, which are yellow-green clays, immediately underlie grey-green to red clays of the Ngaltinga Formation. The slight colour difference between the clays at these locations enables a distinction to be made between the formations.

3.4 Features of Diagenetic Origin

The presence of several features which relate to post depositional alteration of the sediments have been observed at numerous localities and include:

1. Conspicuous development of alunite and halloysite near the base of the Quaternary succession.
2. Iron oxide mottling which is common and very pronounced in sandy units of both the Robinson Point and Ngaltinga Formations.
3. Induration of many sandy units within the sequence, particularly those associated with conspicuous iron mottling.
4. The presence of root structures on unconformity surfaces associated with upper parts of the Port Willunga Formation, the Hallett Cove Sandstone and gravels of the Robinson Point Formation.
5. The identification of tubular and columnar structures and distinctive goethitic mottling patterns associated with materials that are interpreted to be incipient soils in parts of the Robinson Point Formation.
6. Development of mottled and rubbly carbonate within clays and sandy clays of the Ngaltinga Formation.

These features are described and discussed in more detail in later sections but are recognised on the basis of field observations detailed in this Chapter as being significant in the post depositional modification of sediments in the Noarlunga and Willunga Embayments.

3.5 Selection of Sites for Detailed Work

Four sites were selected for detailed sampling and results of this sampling are discussed in later Chapters. The sites were chosen to be representative of the differences which exist between the Noarlunga and Willunga Embayments. They also show the full range of characteristics of the sedimentary units and diagenetic features including alunite deposits at

the base of the sequence, mottled carbonate within clays of the upper fine-grained unit and ferruginous mottles within sandy sediments. The four sites are listed below.

Locality	Map Reference
1. Snapper Point	Yankalilla 1:50 000, 672933
2. Maslin Bay	Noarlunga 1:50 000, 697970
3. Onkaparinga Trig	Noarlunga 1:50 000, 691048
4. Hallett Cove	Noarlunga 1:50 000, 718154

CHAPTER 4
DETAILED CHARACTERISTICS OF THE QUATERNARY SEDIMENTS

Detailed characteristics of the Quaternary sediments have been investigated at each of the four sites selected on the base of fieldwork presented in Chapter 3. Characteristics which are considered to represent primary depositional features are covered in this Chapter while those interpreted as diagenetic in origin are discussed in Chapter 5.

4.1 Particle Size Analyses

Particle size data have been obtained for samples collected from each of the four major sites at Snapper Point, Maslin Bay, Onkaparinga Trig and Hallett Cove in addition to several sites which were sampled in a reconnaissance manner such as Sellicks Beach, Aldinga Beach, Port Willunga, Seaford, Onkaparinga River Mouth and the Railway Cutting at O'Sullivan Beach Road. Four size fractions have been used; the coarse sand (>250μm), fine sand (63-250μm), silt (2-63μm) and clay fractions (<2μm). All data for samples from these sites are presented in Appendix 2.

4.1.1 Clay Content

Graphs showing the % <2μm in samples from Snapper Point, Maslin Bay, Onkaparinga Trig and Hallett Cove are presented as Figures 4.1 to 4.4. At Snapper Point (Fig 4.1), where only the Ngaltinga Formation is identified above the Burnham Limestone, the Neva Clay Member has a fairly uniform and high clay proportion (averaging 75%) which decreases sharply at the base of the Snapper Point Sand Member. Two separate sedimentary cycles are evident within the Sand Member with the base of the upper cycle occuring at 12 m (25% <2μm) and containing slightly more clay than the lower cycle (19% at 10.5 m).

At the Onkaparinga Trig site (Fig 4.2), the Ngaltinga Formation displays similar characteristics to those observed at Snapper Point with a fine-grained Neva Clay Member overlain by a coarser, but variable Snapper Point Sand Member. At both Snapper Point and Onkaparinga Trig a mottled carbonate unit is present within the Neva Clay Member, however the carbonate is not associated with any change in the proportion of clay-sized sediment. The Robinson Point Formation at Onkaparinga Trig shows extremely variable clay content, with values in the basal 3.5 m varying from 50% <2μm at 0.0 m to 7% at 1.0 m and this reflects the interbedding of thin gravel, sand and silty clay units. Clay content is much less than in the Neva Clay Member but some fine-grained interbeds near the base of the Robinson Point Formation have clay contents (50% <2μm) comparable with sediments from parts of the Snapper Point Sand Member (35-55% <2μm).

At the other two sites, the Snapper Point Sand Member of the Ngaltinga Formation is not present and plots of clay content show little change throughout the formation. At Maslin Bay (Fig 4.3) the lower 2.5 m has approximately 70% <2μm with a slight drop to about 60% in the upper 3 m. A transitional zone 2 m thick occurs between these zones. There is more fluctuation at Hallett Cove (Fig 4.4) with clay maxima of 68%, 59% and 60% occuring at 12.5, 15.5 and 17.5 m respectively with the total range in the Ngaltinga Formation at this location being from 51% to 68%.

The Robinson Point Formation at Maslin Bay shows considerable variation in clay content with several local maxima at 6.0 (46%), 9.0 (27%) and 11.9 m (57%) and a rapid fluctuation in the basal 2.5 m. Lowest clay contents of 11% and 15% occur within an indurated and mottled zone from 6.5 to 7.5 m and this is located between clay maxima at 6 and 9 m. Gradual changes in clay content are observed within the Robinson Point Formation at Hallett Cove with a central coarse bed separating fine-grained units and this contrasts to the variability existing at both Maslin Bay and Onkaparinga Trig. The mottled zone at Hallett Cove from 5 to 7.7 m has clay contents ranging from 16% to 23% and occurs between clay-rich zones centred at 2 and 10.5 m (69% and 47% <2μm respectively).

4.1.2 Summary of Particle Size Data

Triangular plots have been used to summarise particle size data for the four sites which have been sampled in detail. Two plots are presented for each, using firstly total sand %, silt % and clay % as vertices and secondly coarse sand %, fine sand % and silt % + clay % (Figs 4.5 to 4.12). Summary plots which include all samples from the four sites are also included (Figs 4.13, 4.14).

Data from Snapper Point (Figs 4.5, 4.6) show that samples from the Neva Clay Member cluster tightly toward the clay or clay + silt end-member with samples for the Snapper Point Sand Member forming two distinct groups. The group plotting with highest sand content (Group A) represents channel-fill sand at the base of the member and also the coarse basal sample of the second depositional cycle (RM218 at 12 m). The intermediate group (Group B) arises from finer-grained sediments deposited following the initial influx of coarse sediment.

At Maslin Bay three major clusters can be seen on the plots (Figs 4.7, 4.8) with Group A comprising samples from the Ngaltinga Formation and also two clay-rich samples from the Robinson Point Formation (RM262, 6 m; RM275, 11.9 m). Group B consists of samples with about 50% sand and 20 to 30% silt which come from the Robinson Point Formation, mostly in the 3.5 metres overlying the ferruginous mottled interval. Samples from below the mottled zone cluster as Group C with samples from the basal 2 metres showing considerable variation.

The Neva Clay Member at Onkaparinga Trig is tightly clustered in contrast to most other samples from this site which scatter widely across the plots (Figs 4.9, 4.10). Samples from the Robinson Point Formation, in particular, show considerable variation with upper parts of this formation having high silt contents and hence plotting with samples from the Neva Clay Member in Figure 4.10 but on their own toward the silt end-member in Figure 4.9 (RM306, RM307). The Snapper Point Sand Member at this site shows similar trends to those evident

at Snapper Point with samples from coarser beds plotting together as Group A and intervening samples plotting as Group B. The composition of Group B tends toward that of samples from the Neva Clay Member.

At Hallett Cove the lower clay unit from the Robinson Point Formation (RM340-RM345, 1.0-3.5 m) plots in a similar position to samples from the Ngaltinga Formation (Figs 4.11, 4.12) with a slightly higher ratio of coarse sand to fine sand being the major difference (Fig 4.12). The remainder of samples from the Robinson Point Formation plot with higher but variable sand contents and are more typical of sediments from this formation at other localities.

Plots of all samples from the four sites are given in Figures 4.13 and 4.14 and show similar trends with coarse sand to fine sand ratios of about 0.4 and silt to clay ratios of about 0.28. The Ngaltinga Formation at both Maslin Bay and Hallett Cove is not clustered as tightly as the Neva Clay Member from Snapper Point or Onkaparinga Trig and is also slightly coarser-grained. Coarser sediments from the Snapper Point Sand Member at Snapper Point and Onkaparinga Trig (Group A) have similar textures to parts of the Robinson Point Formation at Maslin Bay (Group B) and also upper parts of this formation at Hallett Cove. Similarly, samples RM340 to RM345 from the Robinson Point Formation at Hallett Cove and sample RM262 and RM275 from Maslin Bay have textures approaching those commonly occurring in samples from the Ngaltinga Formation. In general, sediments of the two formations show distinctive textural characteristics, however some overlap is evident. This suggests that depositional conditions and/or sediment sources may not have altered greatly during deposition of the Quaternary sequences within the Willunga and Noarlunga Embayments. The greatest variation may, in fact, be a reflection of distance to source areas with finer-grained sediments of the Ngaltinga and Robinson Point Formations being deposited further into the embayments.

4.1.3 Sand Ratios

Ratios of coarse to fine sand have been calculated for all samples from the Snapper Point, Maslin Bay, Onkaparinga Trig and Hallett Cove sections (Figs 4.15 to 4.18 and also Appendix 2). Data for reconnaissance samples collected from other sites are also included in Appendix 2.

At Snapper Point (Fig 4.15), values are low (average 0.25) in the basal 7 metres of the Neva Clay Member with very little variation. Above the carbonate interval the ratio shows greater fluctuation with maximum values of 0.84 (RM226, 8.0 m) and 0.54 (RM224, 9.0 m) just below the sharp boundary with the Snapper Point Sand Member. Ratios in this member are significantly higher than in the Neva Clay Member and also show greater variation. Peaks occur at 9.5 m (RM223, 0.87) and 12.0 m (RM218, 1.26) and these samples also correspond closely to clay content minima (Fig 4.1).

The Ngaltinga Formation at Maslin Bay (Fig 4.16) shows a very gradual increase in sand ratio from 0.13 for sample RM279 (14.0 m) to 0.33 for RM290 (20.5 m). This is in contrast to samples from the Robinson Point Formation where sand ratios vary considerably and, with the exception of two samples, are always higher than the Ngaltinga Formation. Greatest variation occurs in the basal 4 metres of the Robinson Point Formation with a maximum value of 1.86 for RM255 at 2.7 m. An association of high values for the sand ratio and low clay contents which was suggested from data from the Snapper Point Sand Member at Snapper Point does not appear to exist at Maslin Bay. No data is provided for the iron mottled interval between 6 and 8 metres as the samples were incompletely dispersed due to the indurated nature of these sediments, but above this interval variation in sand ratios is less than below the mottled zone.

Data for the Robinson Point Formation at Onkaparinga Trig is also incomplete due to the difficulty in dispersing silty sediments between 1 and 4 metres (8 samples). The data which are available (Fig 4.17) show values less than 0.25, apart from two gravel beds which have

sand ratios of 3.6 (RM298, 2.3 m) and 10.0 (RM300, 2.65 m). Many of the sediments from the Robinson Point Formation at Onkaparinga Trig are silty with abundant fine grains of angular quartz and muscovite observed under the microscope and the sand ratios reflect the abundance of this material. At the base of the Neva Clay Member, values are identical to those of upper parts of the Robinson Point Formation but gradually increase from 0.15 at 6.7 m (RM308) to 0.29 at 10.2 m (RM315) just below the mottled carbonate unit with a maximum of 0.45 at 12.0 m (RM320). A second maximum (0.47, RM324, 13.5 m) occurs in the upper 1.5 metres of the Neva Clay Member just below the Snapper Point Sand Member which has a silty and micaceous basal interval with sand ratios similar to upper parts of the Neva Clay Member. Central parts of the Snapper Point Sand Member from 15.8 m to 16.8 m (RM329 to RM331) have the highest ratios (0.83) with a gradual decrease to 0.37 just below the carbonate mantle.

It has previously been noted that basal parts of the Robinson Point Formation at Hallett Cove have a similar appearance and clay content to the Ngaltinga Formation at this location. Data for sand ratios (Fig 4.18) indicate that basal sediments below the iron mottled interval have higher values (ave 0.85 from 2.0 to 5.0 m) than the Ngaltinga Formation (ave 0.54). Several samples immediately above the basal sandy and gravelly unit in the Robinson Point Formation have significantly higher values ranging from 1.58 to 2.34. Data are incomplete through the indurated mottled interval but above the mottles, sand ratios remain fairly constant (ave 0.57) and marginally higher than those from the Ngaltinga Formation. At most sites along the coastline sand ratios within the Ngaltinga Formation are generally low (<0.5), apart from some sections of the Snapper Point Sand Member. Values calculated for the basal 5 metres of the Robinson Point Formation at Hallett Cove are therefore more akin to those from this formation at other sites in the region, particularly the Maslin Bay section.

The most obvious difference in sand ratios between the Robinson Point and Ngaltinga Formations is in terms of the amount of variation which occurs. Gradual changes take place within much of the Ngaltinga Formation whereas considerable fluctuation is seen in the Robinson Point Formation. This fluctuation is particularly evident in basal parts of the

Robinson Point Formation which also correlates with the zone where there is constant change in the proportion of clay-sized material. A plot of sand ratio against clay content shows that there is no direct relationship between these variables (Fig 4.19) hence coarser sediments with little clay content (< 2μm) do not imply higher proportions of coarse sand with respect to fine sand. For example, basal parts of the Snapper Point Sand Member have similar sand ratios to upper parts of the Neva Clay Member despite having considerably less clay-sized material.

Within the Neva Clay Member, a slight change in both the value of and the amount of variation which takes place in the sand ratio occurs where the mottled carbonate unit has formed. Such a change is not evident at the Hallett Cove and Maslin Bay sites where no carbonate occurs and at these locations the sand ratio shows similar trends to lower parts of the Neva Clay Member at Snapper Point and Onkaparinga Trig. The carbonate interval may therefore represent a local hiatus with the nature of sedimentation being different following formation of the carbonate.

Data for the amount of fine and coarse sand in samples collected from the Quaternary sequence show that the Ngaltinga Formation generally has higher proportions of fine sand compared with the Robinson Point Formation. The amount of variation of the ratio of coarse to fine sand is greater for sediments from the Robinson Point Formation compared with the Ngaltinga Formation and reflects a more episodic depositional environment. Sharp changes which occur within the Neva Clay Member where mottled carbonate occurs may represent hiatus during sedimentation. Absolute values of the sand ratio and the degree of variation which occurs in samples from the Snapper Point Sand Member fall part-way between and also overlap those values calculated for the Neva Clay Member and the Robinson Point Formation. This supports the idea, evident from particle size data (Sections 4.1.1; 4.1.2), that the Snapper Point Sand Member represents a depositional environment which is transitional between the Neva Clay Member and Robinson Point Formation and also that sediment sources are unlikely to have altered markedly during deposition of the Quaternary sequence.

4.2 Mineralogy of Particle Size Fractions of Sediments

4.2.1 Sand Mineralogy

4.2.1.1 X-Ray Diffraction

The mineralogy of fine sand fractions (63 to 250 μm) from some samples collected at Sellicks Beach, Aldinga Beach, Port Willunga, Ochre Point, Seaford, Hallett Cove and O'Sullivan Beach Road Railway Cutting has been determined using X-ray diffraction techniques (XRD) and results are summarised in Appendix 3A. Quartz dominates the mineralogy of all these samples with minor potassic and plagioclase feldspars and trace amounts of hematite, calcite, dolomite, alunite and possibly ilmenite in some samples. Counts for the major quartz peak at 3.34Å (approx 10 000) are always 50 to 100 times more than counts for the largest feldspar peaks at 3.24Å and 3.19Å (mostly within the range 50 to 300). Minerals detected in trace quantities are often related to nearby concentrations of these minerals within Quaternary sediments and therefore have limited value in assessing changes in sediment source which may have taken place. Hematite, for example, generally occurs adjacent to sediments mottled with iron oxides and calcite and dolomite are detected from samples associated with limestones.

4.2.1.2 Optical Assessment

Use of XRD techniques discussed in Section 4.2.1.1 proved to be insufficiently sensitive to identify minerals present in trace amounts. In order to obtain more conclusive data, the coarse sand fraction (>250 μm) of samples from the Onkaparinga Trig section have been studied using a binocular microscope and optical petrological techniques to determine their mineralogy. These techniques were developed by CRA Exploration in Perth to assess heavy mineral concentrates obtained during diamond exploration. Minerals identified are summarised in Appendix 3B.

Quartz, feldspar, tourmaline and iron oxides occur in almost all samples and hence are present in samples from both the Robinson Point and Ngaltinga Formations. Similarly rutile, although identified in only 10 samples, occurs in both stratigraphic units. A much greater range of heavy minerals has been identified from the Snapper Point Sand Member with 10 minerals occurring in this unit which have not been observed in older units.

To help determine whether there is a different suite of heavy minerals present in the Ngaltinga Formation compared with the Robinson Point Formation, the heavy mineral fraction (>2.96 SG) of several additional samples from both the Maslin Bay and Onkaparinga Trig sites has been separated from 0.5 kg sub-samples used for detailed size separation (see Section 4.3). The increased weight of heavy minerals available for observation from these eight samples confirms the distribution evident from coarse sand fractions discussed above. Staurolite, iron oxides, tourmaline and rutile are present in all samples (Appendix 3B). A greater range of minerals is present in samples from the Snapper Point Sand Member and Robinson Point Formation compared with the Neva Clay Member. Rare or trace amounts of amphibole, corundum and spinel are identified from the Snapper Point Sand Member but not from other stratigraphic units while all other minerals which have been identified occur in more than one stratigraphic unit.

4.2.2 Clay Mineralogy

The clay mineralogy of Quaternary sediments from the Noarlunga and Willunga Embayments has been investigated and results are presented in this section. Halloysite, which is considered to be a diagenetic mineral, is discussed together with alunite in Chapter 5.

4.2.2.1 Identification of Clay Minerals Present in Sediments

Clay minerals have been identified and described using techniques discussed in sections 2.2.2 to 2.2.4. Details of the clay mineralogy at all four major sites together with many reconnaissance sites are tabulated in Appendix 4. Kaolinite, illite/mica, smectite and

randomly interstratified layer lattice silicates are the dominant clay minerals in sedimentary units from the Noarlunga and Willunga Embayments and X-ray diffraction (XRD) responses from these minerals are discussed in the following sections.

4.2.2.1.1 Kaolinite

Kaolinite is identified by a diffraction peak at 7.15Å which is not altered by subsequent intercalation with various cations or organic solvents but which disappears on heating the sample to 500°C (Brindley & Brown 1980). All samples collected from the study area contain kaolinite with the 7.15Å peak being moderately sharp and showing little change in peak width or shape. Measurements of peak width at half height are within the range 0.4 to 0.65 °2θ (Appendix 4; these values have not been corrected for the effects of instrument broadening) suggesting some consistency in crystal size, thickness and ordering within kaolinites from the Quaternary sediments. In comparison, two samples of weathered Woolshed Flat Shale of Precambrian age collected from an old quarry at Bradbury in the Adelaide Hills, gave peak widths of 0.3 °2θ (Fig 4.20). The sharper kaolinite peaks from these samples could be due to either larger particles being present in the Precambrian sediments and/or that kaolinite present in the Quaternary sequences is more disordered.

4.2.2.1.2 Illite/Mica

Illite has been defined as clay mica (Brindley & Brown 1980). Apart from a difference in particle size, illite often has decreased K_2O and increased H_2O and cation exchange capacity compared with mica due to the removal of some interlayer potassium and replacement with hydrated exchangeable cations (Brindley & Brown 1980; Norrish & Pickering 1983). More recently, Srodon & Eberl (1984) have defined illite as a non-expanding, dioctahedral, aluminous, mica-like mineral with a particle size of <4μm. Fanning *et al* (1989) indicate that particle size is not part of the definition but that lower layer charge brought about by substitution of Al by Fe and Mg in octahedral sites and additional Si in tetrahedral sites are critical factors. Both illite and mica can be identified by a diffraction peak at 10Å which is

not altered following various saturation and intercalation experiments or by heating samples to 300°C or 500°C. While flakes of muscovite have been observed in both the fine and coarse sand fractions from many samples, the term illite will be used when discussing clay minerals from <2μm fractions giving a 10Å basal spacing following the definition of Srodon & Eberl (1984).

It might be expected that the decrease in crystal size and removal of interlayer potassium from illite compared with mica (muscovite) would result in changes to the basic diffraction pattern and in particular the shape of the basal (001) peak at 10Å. Illite is identified in all samples studied and shows considerable variation in the nature of the 10Å peak with width at half height varying from 0.35 to 1.2 °2θ due to variable broadening on the low-angle side of the diffraction peak. The shape of this illite peak has been frequently used to determine the degree of crystallinity of illite (or muscovite), particularly in studies of diagenesis and metamorphism where an increase in crystallinity (and hence sharpness of the 10Å peak) of authigenic illite takes place as a result of dehydration and potassium fixation (Kubler 1967; Kisch 1980; 1983). Studies by Brill (1988) of illite crystallinity from weakly metamorphosed sediments in the Cobar region of NSW gave values ranging from 0.21 to 0.37 °2θ which are much sharper than those identified for illite peaks from the Quaternary sediments discussed here. Samples of weathered shale from Bradbury in the Adelaide Hills have peak widths of 0.2 °2θ (Fig 4.20) which are similar to those from the Cobar area. In soils, a reverse reaction to diagenesis takes place where cation exchange occurs and potassium is leached from interlayers to produce poorly crystalline illite and interstratified clay minerals (Norrish 1973; Norrish & Pickering 1983; Eberl 1984; Fanning *et al* 1989). Illite from much of the Quaternary sequence has characteristics similar to those of soil-derived illite (Fig 4.21). Some illites have been considered as authigenic in origin (eg Muloorina illite from South Australia; Norrish & Pickering 1983), having formed in Tertiary lakes. Porrenga (1968) has also described authigenic illite occurring in green clays from the USA and Europe which are non-marine in origin and have formed in lacustrine environments. Norrish & Pickering (1983) indicate that as soil solutions in semi-arid and

arid environments can resemble those from saline lakes it is probable that authigenic illite could form in these soils.

Srodon (1984) discusses illite crystallinity in relation to illite/smectite mixed-layer minerals and suggests that broadening of the basal 10Å illite peak is caused by interstratification of expansible smectite layers within the illite structure. Diffraction characteristics can also be influenced by crystallite size and the degree of orientation of the sample on the ceramic disc (Fanning *et al* 1989). With peak widths for illites from the Quaternary sequences varying from 0.35 to 1.2 °2θ, this therefore illustrates a wide range in either the proportion of expansible interlayers and/or size of crystals. The implications of changes in the nature of illite through the Quaternary sequences will be discussed in a later section.

4.2.2.1.3 Smectite

Smectite is recognised from XRD traces by a peak at approximately 15Å when saturated with Mg and air-dried which expands to 17.8Å when Mg-saturated and glycerol solvated. Heating smectite to 300°C collapses the structure to 10Å. Where interstratified clays contain smectite layers in addition to a non-swelling component, the swelling component will be expanded to 17.8Å on addition of glycerol and hence the identification of pure smectite rather than a swelling component of interstratified clay is dependent on the recognition of integral spacings of higher order basal reflections (Brindley & Brown 1980). Reynolds & Hower (1970) have investigated the nature of interstratification in mixed-layer illite-smectites and demonstrated a complete range of compositions from 100% illite to 100% smectite. Tomita *et al* (1988) have also calculated curves for the estimation of interstratified components. The Reynolds & Hower (1970) method has been used as a basis to help identify both smectites and interstratified clays during the present study.

Smectite has been identified in 27 samples from the study area, however numerous other samples display evidence for a variable smectitic component in interstratified clays. Those samples considered to include smectite are listed in Table 4.1 together with the position of the

first 4 order basal reflections which allow the degree of interlayering of non-expandible illite layers to be calculated. All samples except two (RM119, RM299) give diffraction data which differ slightly from calculated ideal basal spacings and hence must contain a minor non-expandible component of up to 20% (Fig 4.22). Complete collapse to 10Å takes place for all samples on heating to 300°C indicating that there is no chloritic component in the dominantly smectitic clays (Fig 4.22). Of the 27 samples in which smectite has been identified, 16 are from silty and sandy sequences from the Robinson Point Formation, 8 occur in sandy or clayey sediments associated with the Burnham Limestone and 3 are related to fine-grained sediments from upper parts of the Tertiary sequence. There appears to be no relationship between the proportion of non-expandible interlayers within the smectite and the stratigraphic position of the samples.

4.2.2.1.4 Interstratified Clay Minerals

Interstratified clay minerals are common in both soils and sediments with considerable variety occurring in the component minerals and the way in which they are interlayered. Reynolds (1980) has reviewed these minerals concluding that interstratifications are either random, with no discernable pattern in the sequence of layer types, or ordered, showing periodic stacking of layers. Despite the large number of possibilities, a relatively small number of interstratified clay types occur and while two component systems are most common, three component interstratifications have been reported (Weaver 1956; Foscolos & Kodama 1974; Sawhney 1989).

Identification of interstratified clay minerals using XRD techniques is often difficult and relies upon recognition of non-integral basal diffraction spacings. Interlayering by small amounts of one component may produce subtle responses which are not recognised (Reynolds 1980). Individual components can be identified by their responses to the usual range of heating and intercalation techniques.

Many diffraction traces for <2μm fractions from the present study show an elevated "background" in the range 10 to 20Å with no definite peaks. These suggest the presence of poorly defined clay minerals in addition to the kaolinite, illite and smectite already identified (Fig 4.23). Following addition of glycerol, the elevated region remains, however it shows a shift toward lower angles leaving a broad illite peak centred on 10Å but which broadens on the high angle side due to the presence of the (002) smectite + glycerol peak (Fig 4.23). Such a shift indicates the presence of an expandable smectitic component. On heating to 300°C and 550°C, the broad, elevated background collapses giving a single peak at 10Å and confirming the presence of interstratified illite/smectite. Comparison with XRD traces given by Reynolds & Hower (1970) suggests smectite proportions varying from 10% to 50% (Fig 4.23).

In some samples, heating to 300°C and 550°C does not completely collapse all clay material to give a 10Å basal spacing and instead the 10Å peak is quite broad on the low angle side with elevated diffraction between 10Å and 15Å (Fig 4.24). Unlike smectite and vermiculite, the basal spacing of chlorite does not collapse from 14Å to 10Å on heating to 300°C (Brindley & Brown 1980; Barnhisel & Bertsch 1989) and hence a chlorite-like clay may be present in these samples with Al(OH) ions replacing hydrated cations within the clay structure. Assymetry of the 10Å peak can also be caused by very small crystal size. Such hydroxy interlayers in expansible layer silicates have been discussed by Rich (1968) and are known under varying names (eg dioctahedral chlorite, chloritised vermiculite, hydroxy interlayered vermiculite, hydroxy interlayered smectite) (Norrish & Pickering 1983; Barnhisel & Bertsch 1989). As smectite and not vermiculite peaks are identified in samples from the Quaternary sequence, the term hydroxy interlayered smectite (HIS) will be used in this study following the terminology proposed by Barnhisel & Bertsch (1989).

Both types of interstratified clays identified here are randomly interlayered based on their poorly defined diffraction characteristics and non-integral basal spacings. Many researchers consider that regularly interlayered clays are most common in sediments and form during diagenesis while the more randomly interstratified clays are formed in weathering

environments and soils (eg Wilson & Nadeau 1985; Sawhney 1989). Identification of randomly interstratified illite-smectite and hydroxy interlayered smectite in Quaternary sediments from the Noarlunga and Willunga Embayments and variations which take place in the components may therefore be useful indicators of the weathering and depositional history of the sediments.

4.2.2.2 Detailed Clay Mineralogy at Selected Sites

4.2.2.2.1 Snapper Point

Kaolin, illite, halloysite and interstratified clay minerals have been identified at Snapper Point and the proportion of these clay minerals in samples from this site is shown in Figure 4.25. Illite is the dominant mineral throughout the Neva Clay Member (average 40-50% but increasing to 50-60% above the carbonate interval) with lesser interstratified clays (average 30-40%) and kaolinite (average 20-30% then 10-20% above the carbonate interval). While the proportion of interstratified clays shows little change, both kaolinite and illite proportions change abruptly immediately above the carbonate interval at 7 m and this can be seen from a graph of kaolinite to illite ratios (Fig 4.26). The proportion of <2μm material is similar throughout the Neva Clay Member although an influx of coarser sand is evident in upper parts of this unit (Section 4.1.3, Fig 4.15). This suggests that the carbonate unit marks the boundary between two slightly different clay-rich sequences which may have resulted from minor changes in depositional conditions or source regions.

The Snapper Point Sand Member is immediately distinguished by the sudden increase in kaolinite content (50-60%) and a similar decrease in illite and interstratified clays. Both illite and interstratified clays gradually increase toward the top of the Snapper Point Sand Member while kaolinite shows a corresponding decrease. The proportions of all clay minerals in upper parts of the Snapper Point Sand Member approach those identified from parts of the Neva Clay Member. Kaolin to illite ratios gradually decrease in three distinct stages which correlate with similar fluctuations in the proportion of <2μm material in the sample. This

data suggests therefore that kaolinite is most abundant in the coarsest sediments with illite and to a lesser extent interstratified clays following a reverse trend.

Measurements of peak widths at half height of both the 7Å kaolinite and 10Å illite diffraction lines have been undertaken as a simple assessment of the crystallinity of these clay minerals and results are presented in Figure 4.27. Apart from an increase in peak width in sample RM223 associated with the presence of both 7Å and 10Å halloysite, there is very little change in the shape of diffraction peaks for either mineral, apart from minor broadening of the illite peak for samples from the Neva Clay Member above the carbonate interval. In all samples, the illite peak is much broader than that for kaolinite. This suggests either the loss of some interlayer K^+ from the illite structure and replacement by hydrated cations causing minor interstratification, or that illite occurs as smaller particles compared with kaolinite.

Cation exchange capacity (CEC) of the clay fractions of samples from Snapper Point shows little variation with the exception of basal samples of the Snapper Point Sand Member where values decrease due to the presence of lower proportions of illite and interstratified clays (Appendix 4). The CEC has been used together with diffraction data and K_2O contents to estimate clay mineral proportions using techniques discussed in Chapter 2. K_2O values are lowest in the basal 5 metres of the Snapper Point Sand Member but show little variation in other parts of the sequence, averaging 3% and reflecting the high proportion of illite, both as part of interstratified clays and as discrete illite (Fig 4.26; Appendix 4).

Interstratified clays comprise both illite and smectite components and based on work by Reynolds & Hower (1970) the proportion of expansible smectitic clays ranges from 15% to 40% (Appendix 4). Interstratified clays from the Neva Clay Member have uniform but low smectitic components (ave 20%), however clays from the Snapper Point Sand Member show much greater variation with lowest proportions (15%) occurring within coarser sediments and highest proportions (up to 40%) forming in clayey interbeds. On heating samples to 300°C and 550°C, most show incomplete collapse to 10Å indicating the presence of hydroxy interlayered smectite. Basal samples from the Snapper Point Sand Member which are sandy

and contain low proportions of interstratified clays show almost complete collapse on heating and hence are thought to contain only small amounts of hydroxy interlayered smectite.

Other minerals which are identified in minor amounts in clay fractions from this site include quartz, feldspar, goethite and dolomite (Appendix 4). Quartz is present in all samples, feldspar exclusively within the Snapper Point Sand Member and dolomite in several samples from within the carbonate interval. Goethite is identified from six fine-grained samples, all but one being from the Neva Clay Member, and appears to be related to development of small, yellow-orange mottles.

Clay mineralogy at the Snapper Point site clearly delineates the stratigraphy determined from field observations. The variability within the Snapper Point Sand Member is distinctive of that unit when compared with the Neva Clay Member. A subtle change in clay mineralogy also occurs within the Neva Clay Member above the carbonate interval in what is otherwise a very uniform sequence of fine-grained sediments.

4.2.2.2.2 Maslin Bay

Details of clay minerals identified in samples from Maslin Bay are tabulated in Appendix 4 and mineral proportions shown graphically in Figure 4.28. Kaolin, illite and randomly interstratified clays are the major clay minerals identified, with smectite and halloysite recorded from the basal 5 metres of the section.

Kaolin content is low at the base of the Robinson Point Formation where smectite is identified and also in samples where significant amounts of halloysite are recorded. In finer grained intervals within this zone (RM251, RM254), where neither smectite nor halloysite occur, kaolinite contents increase to 40-50%. Above 3.5 m (RM257), the amount of halloysite decreases and there is a corresponding increase in kaolinite content to a peak of 60% in sample RM260. Mottled, sandy sediments which occur between 6.5 and 8.0 m have much lower kaolinite contents (average 30-40%), however above this interval, the proportion

of kaolinite increases to 50-60% in samples RM273, RM274 and RM277. A clay-rich band which occurs between samples RM274 and RM277 has a lower kaolinite content. Within the Ngaltinga Formation, kaolinite contents are considerably lower than those recorded for most parts of the Robinson Point Formation and show little variation apart from a gradual decrease in the upper 3 metres.

In the lower 5.5 metres and upper 4.0 metres of the Robinson Point Formation, illite content varies little and averages 30%. No change in the proportion of illite is seen through the smectitic and halloysitic interval, however a large increase occurs within the iron mottled zone with a maximum of 70% in sample RM266. Within the Ngaltinga Formation, illite is the dominant clay mineral averaging 40% in the basal 2.5 metres then gradually increasing to 60% just below the overlying carbonate blanket. Potassium contents reflect these variations in illite content, being highest for samples within and adjacent to the mottled interval and from the Ngaltinga Formation (Fig 4.29). Kaolin to illite ratios (Fig 4.29) also reflect the variable proportion of illite and confirm the higher proportions of kaolinite in most of the Robinson Point Formation and lower amounts in the Ngaltinga Formation.

In the Robinson Point Formation, interstratified clays show a positive relationship with the proportion of clay-sized sediment and maximum proportions occur in samples RM251, RM254, RM258, RM263, RM269 and RM275 (Fig 4.30). Only minor amounts of interstratified clays occur within the iron mottled interval and none was identified where halloysite or smectite are abundant. Illite and smectite are identified as components of interstratified clays from the Robinson Point Formation with the smectitic component varying from 10% to 50%. Maximum smectite components are recorded in samples from clay-rich intervals (RM251, RM262, RM263 and RM272 to RM275). Interstratified clays form a higher proportion of samples from the Ngaltinga Formation compared with the Robinson Point Formation, emphasising the association of these clays with the finest sediments. In samples from the Ngaltinga Formation, the smectite component of the interstratified clays is relatively constant at 20 to 30% apart from several samples at the base of this formation which increase to 40%. Heating samples to 300°C and 550°C indicates that not all material

collapses to 10Å and hence, as at Snapper Point, hydroxy interlayered smectite is present in samples from the Ngaltinga Formation. In contrast, little hydroxy interlayered smectite is present in samples from the Robinson Point Formation as these show almost complete collapse on heating.

A graph of the width at half height of (001) peaks for both kaolinite and illite indicate little change for kaolinite throughout the sequence (Fig 4.31). There is an increase in illite for samples from the Ngaltinga Formation and also from the Robinson Point Formation between the halloysite-rich interval and the iron mottled zone. This suggests that illite from the Ngaltinga Formation and occasionally from the Robinson Point Formation is not as well ordered as in other samples and may have lost some interlayer potassium leading to minor interstratification within illite crystals. Alternatively, the change in diffraction peak widths for illite may reflect a smaller particle size in these intervals.

Minor amounts of quartz occur in the <2μm fraction of all samples at Maslin Bay with feldspar a common component of most samples from the Robinson Point Formation (Appendix 4). Goethite forms a minor component of both smectitic samples at the base of the Robinson Point Formation and also in one sample at the base of the iron mottled zone. Dolomite and calcite occur in two samples immediately below the carbonate blanket and are derived from isolated carbonate mottles which have formed in the upper parts of the Ngaltinga Formation.

The clay mineralogy at Maslin Bay indicates a clear difference between the Ngaltinga and Robinson Point Formations with kaolinite dominant over illite in most parts of the Robinson Point Formation and illite dominant over kaolinite in the Ngaltinga Formation. Hydroxy interlayered smectite is present in the Ngaltinga Formation but not the Robinson Point Formation and this may have implications for the source of the clays and subsequent post depositional modification. Within the Robinson Point Formation, variations from the standard kaolinite-dominated clay mineral suite occur at the base of the formation where smectite and halloysite are identified and also from within the iron mottled interval where the

illite proportion increases markedly at the expense of both kaolinite and interstratified clays. It is noted from this study that such variation always occurs in coarser sediments which suggests that coarser intervals within the sequence may preferentially allow alteration of clays following deposition.

4.2.2.2.3 Onkaparinga Trig

Five clay minerals are identified from the Onkaparinga Trig section. The proportions of kaolinite, illite, smectite, halloysite and interstratified clays are shown in Figure 4.32 and tabulated in Appendix 4 together with several other parameters related to the clay mineralogy.

Both smectite and halloysite are found only in the Robinson Point Formation at Onkaparinga Trig but do not occur together. Halloysite occurs in sandy interbeds in the basal 3 metres while smectite is identified from the overlying 3.5 metres comprising interbedded gravels, sands and silts. Illite and kaolinite occur throughout the Robinson Point Formation with kaolinite averaging 50% and illite 25 to 30%, except where halloysite is abundant and then both illite and kaolinite proportions are low. Interstratified clays were identified from only two clay-rich samples near the base of the formation (RM144, RM293) and these are random interstratifications of illite and smectite with smectite contents of 40 to 50% and 20 to 30% respectively. Complete collapse to 10Å of expansible clays is observed on heating these samples to 300°C and 550°C. The smectite contains a small non-expandable (illitic) component of up to 20% (Table 4.1), and hence even these clays could be strictly classified as interstratified illite-smectite. They are classified as smectite in this study to distinguish them from interstratified illite-smectite identified in other samples from the Quaternary sequence which contain less than 50% smectitic interlayers.

Only kaolinite, illite and randomly interstratified clays were identified from the Ngaltinga Formation. Within the Neva Clay Member, two zones were identified which are separated by an interval of mottled carbonate. Below the carbonate, kaolinite and interstratified clays comprise about 30% each of the sample and illite 35 to 40% while from the base of the

carbonate interval, the illite proportion increases markedly and both kaolinite and interstratified clay contents decrease sharply. This alteration can be seen from a graph of kaolinite to illite ratios (Fig 4.33). Illite crystallinity, which is lower in the Ngaltinga Formation than the Robinson Point Formation as measured by the width of the 10Å peak at half height, also shows a marked decrease at the base of the carbonate interval (Fig 4.34). As at Snapper Point, the carbonate interval appears to mark a change in clay mineralogy which may reflect the prevailing depositional conditions.

Basal parts of the Snapper Point Sand Member are coarse-grained and the dominant clay mineral is kaolinite with lesser amounts of illite and interstratified clay. Samples RM326 to RM328 all have low proportions of interstratified clay and higher illite crystallinity compared with the underlying Neva Clay Member. As the % <2μm increases near the top of the Snapper Point Sand Member, illite crystallinity decreases toward values similar to those found within parts of the Neva Clay Member. The proportions of the three clay minerals in this upper part of the Snapper Point Sand Member show some fluctuation, however the overall trend is toward less kaolinite and more illite with randomly interstratified clays showing little change. No clear association of these clay mineral fluctuations can be found with the amount of clay-sized sediment as was observed at Snapper Point, although the two samples containing the highest % <2μm also contain high proportions of illite compared with surrounding samples.

Interstratified clays from the Ngaltinga Formation show incomplete collapse on heating except for samples RM326 and RM327 from the base of the Snapper Point Sand Member where the small amount of interstratified clay present makes it difficult to ascertain this parameter. In contrast to interstratified clays from the Robinson Point Formation which are a mix of illite and smectite, those from the Ngaltinga Formation therefore include some hydroxy interlayered smectite. The smectitic component of the interstratified clays varies between 20 and 40% with highest proportions in the Neva Clay Member below the carbonate interval and also from the basal 2.5 metres of the Snapper Point Sand Member (Appendix 4).

Quartz is present as a minor component of the <2μm fraction of all samples at Onkaparinga Trig with feldspar noted in several samples from the Robinson Point Formation. Goethite is identified in all samples where smectite is also present. Calcite and dolomite occur in several samples near the top of the sequence just below the calcrete and in one sample from the carbonate interval within the Neva Clay Member (RM316).

The clay mineralogy at Onkaparinga Trig can again be used to distinguish between the stratigraphic units. Smectite is identified from the Robinson Point Formation with higher proportions of illite and interstratified clays occurring in the Ngaltinga Formation. Coarser samples from the base of the Robinson Point Formation are dominated by halloysite which does not occur in adjacent fine-grained samples. Similarly, the clay mineralogy in coarser sediments from the Ngaltinga Formation (base of the Snapper Point Sand Member) also differs from surrounding fine-grained sediments with kaolinite being the dominant clay mineral. The general decrease in crystallinity for illites from the Ngaltinga Formation and the presence of a hydroxy interlayered smectite component in the interstratified clays is consistent with observations of the Ngaltinga Formation from other sites.

4.2.2.2.4 Hallett Cove

At Hallett Cove, kaolinite, illite and interstratified clays are identified from diffraction traces and the clay mineral proportions are shown in Figure 4.35 with details documented in Appendix 4. In contrast to the Maslin Bay and Onkaparinga Trig sites, no halloysite or smectite is recorded at Hallett Cove.

Kaolinite is generally the dominant clay mineral within the Robinson Point Formation with illite dominant in the overlying Ngaltinga Formation. The kaolinite to illite ratio reflects this change (Fig 4.36). Sandy clays with occasional gravel bands occur in the basal 2 metres of the section and within this interval, kaolinite content increases to 35% while the interstratified clay proportion decreases from 40-50% to 20-30%. Illite remains relatively constant through this interval. Throughout the remainder of the Robinson Point Formation, kaolinite content

is about 40-50% with a sharp increase to 50-60% at the top of the mottled interval. Local minima occur in samples RM347 and RM361 which correlate with clay-rich interbeds and RM350 and RM356 which are on either side of the mottled interval. Illite content is fairly constant both above and below the mottled interval (ave 25 to 35%) but increases sharply within the iron mottled interval. Interstratified clays average 25 to 30% throughout the Robinson Point Formation except in the basal metre and within the mottled interval where only minor amounts are identified. With the exception of RM361 where some hydroxy interlayered smectite is present, all interstratified clays from the Robinson Point Formation collapse on heating and comprise illite and smectite. Smectite content of the interstratified clays is mostly in the range 20 to 30% except for sample RM338 at the base of the unit and several clay-rich intervals (RM347, RM356, RM357, RM361) where the expansible content increases to 40-50% (Appendix 4).

Within the Ngaltinga Formation, the proportion of interstratified clay is similar to upper parts of the Robinson Point Formation averaging 25 to 30%. All samples however show incomplete collapse on heating indicating the presence of hydroxy interlayered smectite in addition to randomly interstratified illite-smectite which are the components within the Robinson Point Formation. Smectite content of the interstratified clays is mostly about 30% except for several samples near the base of the unit (RM364, RM365, RM368) where smectite content increases to 30-40%. The similarity of interstratified clay from upper parts of the Robinson Point Formation (RM361) with those of lower parts of the Ngaltinga Formation suggests that while a sharp lithological break can be distinguished between the two formations, the mineralogical break is not as distinct. This is supported by the gradual increase shown by the illite proportion from upper parts of the Robinson Point Formation and a gradual decrease in kaolinite content in the same samples. Above this transitional zone, the proportions of all three clay minerals are relatively constant except in the upper 2 metres of the Ngaltinga Formation where the illite content increases while the kaolinite proportion shows a gradual decrease. Illite crystallinity also shows a gradual decrease in the upper metre of the Robinson Point Formation which continues into the Ngaltinga Formation. Peak width at half height of the illite (001) peak remains between 0.8 and 1.0 °2θ for the

remainder of the Ngaltinga Formation (Fig 4.37). There is little change in this measurement within the Robinson Point Formation.

Minor amounts of quartz are present in the <2μm fraction of all samples from Hallett Cove with feldspar noted in 50% of samples from the Robinson Point Formation. No other minerals are identified in the clay fractions.

4.3 Clay Mineralogy of Size Fractions <20μm

Eight samples were selected from the Maslin Bay and Onkaparinga Trig sites for detailed investigation of the relationship between clay mineralogy and particle size (RM259, RM262, RM265, RM304, RM312, RM323, RM326, RM334). The samples were selected as being representative of the different clay mineral assemblages recognised within the Quaternary sequence and also to cover all stratigraphic units identified from both the Noarlunga and Willunga Embayments. Separation into four size classes was undertaken (<20μm, <5μm, <2μm and <0.2μm) followed by identification of clay mineralogy using XRD techniques discussed in Section 4.2. Although the use of four open-ended size fractions does not allow a quantitative assessment of the proportions of clay minerals in each size class (eg 5 to 20μm), it does enable an estimate to be made of the size distribution of clay mineral species. Details of clay mineral proportions, kaolinite to illite ratios and widths at half height for the kaolinite and illite (001) peaks are given in Appendix 5.

Kaolinite, illite, randomly interstratified illite-smectite, hydroxy interlayered smectite, smectite and halloysite have been identified in the samples. Halloysite is present in very minor amounts in sample RM259 which lies immediately above the halloysite-alunite interval at the base of the Robinson Point Formation. This mineralogy is discussed in Section 5.1. Expansible clays such as smectite and randomly interstratified illite-smectite occur in highest proportions in the finest fraction (<0.2μm) and are present in all samples in this size range (Fig 4.38). Very little expansible clay appears to be present in coarser size fractions. Kaolinite is present in all size fractions although in the <0.2μm fraction the proportion of this

mineral decreases by comparison with other clay minerals (Fig 4.38). In samples RM262 and RM304, such a decrease is masked by the fact that illite is less abundant in the <0.2μm fraction but a large increase in the proportion of expansible clays means that the amount of kaolinite is still low. Illite is also present in all size fractions but most abundant in the finest fractions. There are several exceptions to this generalisation. In samples where smectite is abundant in the <0.2μm fraction (RM262, RM304), the proportion of illite is much less than would be expected when compared with other samples and this decrease is shown by changes in the kaolinite to illite ratio. In contrast, there are two samples (RM304, RM326) which show a bimodal distribution of illite based on variation in the kaolinite to illite ratios with concentrations occurring in fractions >2μm and also <0.2μm. Hydroxy interlayered smectite is identified in small amounts mostly in the finest fractions but is not present in all samples. Those samples with high proportions of randomly interstratified illite-smectite appear to also include hydroxy interlayered material, but this clay mineral is not identified in samples containing smectite.

Kaolinite to illite ratios have already been mentioned in relation to the bimodal distribution of illite which is suggested for two samples and also the reduction of illite which occurs in association with smectite. Ratios for each sample are shown in Figure 4.39 and apart from those samples already mentioned there is little change in silt-sized fractions but with illite increasing in the clay fractions. Widths at half height for the (001) peak of kaolinite and illite have also been measured (Fig 4.40). Kaolinite generally has sharper peaks than those for illite with little change occurring except in the <0.2μm fraction where kaolinite peaks have widths up to 0.2 °2θ wider than in silt and coarse clay fractions. Illite peak widths show a similar trend toward broader peaks in the <0.2μm fraction. In silt and coarse clay fractions there is considerable variation in peak characteristics for illite with those from the Ngaltinga Formation being broader than those from the Robinson Point Formation. This observation confirms previous measurements made on the <2μm fractions of all samples reported in Section 4.2.

Non clay minerals identified in these eight samples include quartz, feldspars, goethite and alunite. Goethite is only present in sample RM304 where it occurs mostly in the clay fractions (<2μm) while alunite is identified in minor amounts from the 0.2 to 5μm fraction of sample RM259. Quartz and feldspars are identified from all samples with feldspars mostly confined to the silt fractions (>2μm) and quartz to fractions >0.2μm.

4.4 Morphology of Clay Minerals using the SEM

Eight samples were selected from the Maslin Bay and Onkaparinga Trig sites for scanning electron microscopic study of the morphology of and relationships between the clay minerals. The samples were chosen as being representative of the various clay mineral assemblages identified from the four major sites.

4.4.1 Discussion

The clay minerals in all samples form dense masses in which the morphology of individual clays is almost impossible to distinguish. The very small size of most clays increases the difficulty of determining morphological features. In samples where skeletal grains such as quartz form a major component (eg RM265, RM326), clays form a thick skin coating the larger grains (Fig 4.41). In detail, individual clay aggregates appear to orient within the skins along the surface of the quartz grains suggesting movement of clay following deposition (Fig 4.42).

In clay-rich samples individual clay crystals are often small platelets up to 0.4μm in maximum dimension (Fig 4.43). Shape is irregular with a tendency toward rounded edges. On exposed surfaces of the more massive or tabular clay, thin, irregular and curled clays are often noted. These are mostly observed in samples having a high proportion of randomly interstratified illite-smectite or smectite as determined by XRD (eg RM304, RM334) and hence such morphology may represent these phases. Alternatively, the slightly curled nature

of these clays may be the result of dehydration of thin particles under the vacuum of the SEM.

Silt-sized grains of muscovite form a major component of sample RM304 in which smectite is reported as an important mineral in the <2μm fraction (based on XRD observation). Fine clays coat and infill the gaps between silt-sized particles with thin, curled clay common on edges of muscovite grains and also the more massive clay accumulations. X-ray spectra of the curled clays suggest that they may be smectite as they give Si to Al ratios of approximately 2:1 but with negligible K. A spectrum for silt-sized muscovite grains shows similar Si to Al ratios but with an appreciable K peak. Under the operating conditions used, the volume of sample contributing X-rays to the detectors is approximately 4μm deep and 8μm in diameter, hence spectra from such small and thin particles must be treated with considerable caution. Nevertheless, the absence of K in spectra from the curled clays suggests that it is smectite. In some locations, very fine, almost hair-like morphologies protrude from the edges of muscovite grains. They are too small for X-ray analyses, but are likely to be authigenic clays formed in the pore space surrounding the muscovite grains (Fig 4.44).

Apart from the clays described from RM304, few euhedral grains of possible authigenic origin have been noted. In sample RM323, three elongate, flat to rounded rods were identified on the surface of a quartz grain (Fig 4.42). These are up to 1.5μm long and 0.2μm wide and resemble halloysite seen in other samples. The remaining clay in this sample comprises dominantly massive clay or small oriented platelets with rare larger grains up to 1μm in diameter.

A completely different morphology was observed in sample RM265 which comprises quartz grains with clay skins and clay bridges between grains. On the surface of several quartz grains and adjacent to the broken edge of a clay skin are numerous small spheroidal particles which are quite uniform in size and up to 0.25μm in diameter (Fig 4.45). X-ray spectra suggest that these are composed of Si although the presence of a quartz grain beneath the

spherules indicates caution in interpreting the spectra. The absence of other elements in the spectra support the interpretation that Si is the major component of the spherules.

4.4.2 Summary

The very fine size of clays in these samples makes it difficult to assess the morphology of the clay minerals. Nevertheless, where individual particles are observed, there appear to be no gross differences in the size or shape of the particles between samples apart from the presence of thin, irregular and curled particles associated with samples RM304 and RM334. Such morphologies may represent smectite and randomly interstratified clays which are shown to be present in these samples using XRD techniques. Evidence for euhedral grains crystallised in pore space or associated with other mineral phases is limited to fine fibrous material in RM304, very rare halloysite in RM323 and spherules of silica in RM265. Such observations suggest that authigenic phases with distinct morphology are rare in these samples. Movement of clay following deposition is indicated by clay skins coating large grains of quartz and the orientation of particles in some of these clay skins.

4.5 Summary

There are distinct differences in particle size and mineralogy which support the field subdivision of Quaternary sediments into the Robinson Point and Ngaltinga Formations. The Ngaltinga Formation tends to be dominantly fine-grained and has low proportions of coarse sand relative to fine sand, while the Robinson Point Formation is more variable in particle size and generally coarser-grained.

A detailed assessment of the clay mineralogy at four sites in the Noarlunga and Willunga Embayments clearly supports the stratigraphic subdivision proposed from field and other laboratory observations. Kaolinite to illite ratios are consistently higher for samples from the Robinson Point Formation than for those from the Neva Clay Member of the Ngaltinga Formation. Values for basal sands of the Snapper Point Sand Member are high and similar

to those from parts of the Robinson Point Formation. Illite crystallinity shows a similar trend, being significantly lower in the Ngaltinga Formation than the Robinson Point Formation. The nature of the interstratified clay also differs with smectite and illite being components within the Robinson Point Formation but hydroxy interlayered smectite being additionally present in the Ngaltinga Formation.

Studies of the heavy mineral suites of the sediments suggest that there is little difference between the two formations and hence there was no change in the dominant source regions during the Quaternary. Similarities in terms of texture and mineralogy which exist between some parts of the Snapper Point Sand Member and the Robinson Point Formation provide further evidence that major changes in source have not taken place.

At sites where the Snapper Point Sand Member occurs, similarities are noted between this unit and parts of the Robinson Point Formation. Variation in particle size occurs in both units whereas the Neva Clay Member of the Ngaltinga Formation is a very uniform clay-rich deposit. Triangular plots show that the texture of the Snapper Point Sand Member is similar to that of the Robinson Point Formation, although some intervals from the Robinson Point Formation plot with higher clay contents and approach the composition of the Neva Clay Member.

Thicker sequences of coarser basal sediments of the Robinson Point Formation are often found toward the embayment margins and these locations have clay mineralogies characterised by higher proportions of kaolinite relative to illite or interstratified material. In central parts of the embayments, finer sediments of the Ngaltinga Formation thicken and become more complex with interbedding of sandy lenses from the Snapper Point Sand Member and occasional discontinuous carbonate beds such as at Onkaparinga Trig and Snapper Point. Illite and interstratified clays dominate the clay mineralogy at these sites relative to kaolinite. The lateral thinning of the Robinson Point Formation occurs in both embayments but is more pronounced in the Willunga Embayment where the Robinson Point

Formation disappears just south of Blanche Point and the sequence between here and Aldinga comprises clays and isolated sandy lenses of the Ngaltinga Formation.

The dolomitic intervals immediately above occurrences of the Burnham Limestone have a clay mineralogy dominated by smectite, whereas clays associated with the Burnham Limestone comprise illite, randomly interstratified clays and kaolinite. A similar suite to that which occurs in the Burnham Limestone is found in the Robinson Point Formation but with kaolinite more abundant than either illite or randomly interstratified material. Apart from occurring in silty sediments of the Robinson Point Formation in the vicinity of Onkaparinga Trig, smectite is only identified in these dolomitic intervals.

Clay-rich intervals within the Robinson Point Formation at Maslin Bay and Hallett Cove often have clay mineral suites which are similar to those from the Ngaltinga Formation. The major differences occur in the proportion of expansible clays which occur within the randomly interstratified illite-smectite. Those from the Robinson Point Formation contain up to 50% smectitic layers while those of the Ngaltinga Formation generally comprise only 20 to 30% and also include some hydroxy interlayered material. Differences in the interstratified clays may be due to diagenetic processes.

Detailed fractionation of material <20μm in size indicates that expansible clays such as smectite and randomly interstratified illite-smectite occur mostly in the finest fractions <0.2μm. Illite also tends to concentrate in this fraction except where smectite is common. Several samples indicate that a second concentration of illite occurs sometimes in silt fractions (2 to 20μm). Kaolinite is less common in the <0.2μm fraction but tends to be concentrated in coarse clays (0.2 to 2μm). SEM observations confirm XRD and particle size data which indicate that the majority of clays are present as very small particles. No morphological differences can be seen between clays from different stratigraphic units, although development of clay skins coating large grains is more common in samples from the Robinson Point Formation.

CHAPTER 5
FEATURES OF DIAGENETIC ORIGIN

Following detailed fieldwork in coastal regions of the Noarlunga and Willunga Embayments, several features which occur commonly in the Quaternary sediments were interpreted as being of probable diagenetic origin. These features are discussed in detail in this Chapter.

5.1 Alunite and Halloysite

5.1.1 Distribution in the Late Cainozoic Sequence

Both alunite and halloysite occur in intimate association in thin beds, generally less than 10 cm thick, often laterally extensive for tens of metres and broadly conformable to local bedding. Most outcrops are white to off-white in colour with some red-brown to pink staining from iron oxides (mostly hematite). Isolated bulbous masses are common, often elongated in a vertical direction and generally up to 15 cm in greatest dimension. Large pods are also occasionally observed, in which the long axis is oriented parallel to bedding and with the pods entirely enclosed by the host sediment. Such pods are more common in sediments of Tertiary age compared with those of Quaternary age (for example; the South Maslin Sands along the Onkaparinga River estuary).

Within the Quaternary sequence, alunite is usually identified only from basal sandy sediments of the Robinson Point Formation and is always associated with occurrences of halloysite. Apart from one location at Chinaman Gully, alunite has not been identified in sediments of the Ngaltinga Formation. In central parts of the Willunga Embayment between Port Willunga and Snapper Point where the Robinson Point Formation is not identified, alunite has not been observed. Halloysite is also generally absent from this unit apart from one occurrence at Snapper Point where the <2μm fraction at the base of the Snapper Point Sand Member contains approximately 20% halloysite. An association of alunite and

particularly halloysite with sandy intervals of the Robinson Point Formation is often demonstrated.

5.1.2 Distribution in the Noarlunga and Willunga Embayments and Nearby Areas

Many previous workers in South Australia have commented on the occurrence of alunite in a wide variety of sediments and Table 5.1 lists a number of these reported alunite occurrences together with the age and lithology of the host sediments. This list is by no means exhaustive but provides some idea as to the frequency with which alunite is found. At a number of localities alunite was reported as occurring in association with silica and/or kaolinite (Ward 1917; Dickinson 1943; King 1953; Callen 1977). During the present study, halloysite has frequently been identified in association with alunite and many of the earlier references to kaolinite may, in reality, be halloysite, as it is generally difficult to distinguish between these two clay minerals in the field or laboratory.

Alunite and/or halloysite have been identified within sediments of Late Cainozoic age at many localities from the St Vincent Basin (Fig 1.2). A number of sites where alunite occurs outside of the Noarlunga or Willunga Embayments have been included in the present investigation to help develop models for the formation of alunite and halloysite in the two embayments. Alunite is also noted in Cambrian sediments of the Kanmantoo Group at several localities in the Adelaide Hills.

The occurrence of alunite and halloysite is more prevalent in the Noarlunga Embayment than the Willunga Embayment. Apart from development at Maslin Bay in northern parts of the Willunga Embayment, alunite has only been identified at Chinaman Gully and halloysite at Snapper Point in this embayment. In contrast, development of these minerals in southern and central parts of the Noarlunga Embayment is almost continuous from Witton Bluff to Moana with isolated occurrences further north at O'Sullivan Beach, various localities south of the Field River and Hallett Cove. In addition to these coastal sites, there is extensive

development of alunite within Tertiary sediments of the South Maslin Sand along the Onkaparinga River.

Outside the Noarlunga and Willunga Embayments, an intensive search for sites where alunite and halloysite has developed has not been undertaken. In the course of a general assessment of Quaternary sediments outside these embayments alunite has been noted at Redbanks, north of Adelaide, and several coastal locations on Yorke Peninsula including Ardrossan, Stansbury, Port Moorowie and Port Rickaby. Only the occurrence at Port Moorowie has been studied in detail.

5.1.3 Field Observations

5.1.3.1 Onkaparinga Trig

Alunite and halloysite are found in the basal 1.5 metres of the Quaternary Robinson Point Formation at Onkaparinga Trig. The occurrences include elongate pods of alunite and halloysite as rounded pods and disseminated through sandy host sediments. Figure 5.1 shows this interval which comprises orange-brown (7.5YR 5/6) to green (5Y 7/2) clay at the base with minor manganese staining and isolated clasts of limestone up to 30 cm in diameter derived from the underlying Tertiary Port Willunga Formation. Between 30 and 60 cm from the base of the sequence, several thin bands of pale yellow (5Y 7/3) fine sand up to 2 cm thick are interbedded with the clays. The remaining sediments tend to be composed of buff-coloured fine sand with frequent coarse and gritty intervals where sub-rounded quartz grains of up to 4 mm diameter are observed. In central coarser parts of this sequence isolated pods of white to buff, waxy halloysite occur which are up to 30 cm across, rounded and include visible grains of quartz scattered randomly throughout. Halloysitic pods often have white or pale coloured cores but with margins stained yellow (10YR 7/8) or pink-red (10R 5/6) by iron oxides. Surrounding sandy sediments display similar colours. A further halloysitic interval which has a nodular appearance occurs 15 to 20 cm above the first and comprises tough, pink-red halloysite impregnated clayey fine sands and minor coarse sand. This

interval is more extensive than the first and overlain by a thin, 8 cm layer of black-purple (7.5R 2/1) to orange-yellow (10YR 6/6) indurated fine sand which weathers to form small ferruginous biscuit-shaped fragments. Up to 50 cm of unconsolidated yellow to pink-red halloysitic fine sand forms the uppermost part of this sequence and is overlain by gravel lenses and silty sediments.

Alunite is comparatively rare at Onkaparinga Trig. It is confined to a thin discontinuous bed of white, chalky material within clays filling solutional hollows in limestones of the Port Willunga Formation and isolated, sub-horizontal pods within central halloysite impregnated sands. The alunite pods are 3 to 4 cm thick and up to 25 cm long. They show sharp irregular contacts with the surrounding sandy sediments and diffuse upper contacts (Fig 5.2).

The sequence described here can be traced with little variation for several hundred metres to both the north and south.

5.1.3.2 Other sites in the Noarlunga Embayment

Between Moana and Witton Bluff, alunitic and halloysitic sediments are common at the base of the Robinson Point Formation, with alunite often more abundant than its rare occurrence at Onkaparinga Trig. At Port Noarlunga, to the north of the jetty, an unusually thick bed of alunite, up to 25 cm thick, is continuous for several hundred metres and overlies green-yellow clay at the top of the Tertiary Blanche Point Formation. On the underside of this bed of alunite, which has a sharp contact with the underlying clays, a number of small, rounded bulbous masses up to 10 cm across are observed (Fig 3.34). These appear similar to load structures but have not been recognised at other localities. In the overlying fine to gritty sands of the Robinson Point Formation, several further bands of alunite can be seen (Fig 3.33). Up to three bands, 1 to 5 cm thick and separated by 5 to 10 cm, occur intermittently between Port Noarlunga and Witton Bluff. They are conformable to bedding of the Robinson Point Formation. Alunite dominates the mineralogy of these beds with halloysite

forming a minor but variable component. Halloysite also occurs as part of the matrix in surrounding sandy sediments.

At Robinson Point an interval of yellow, white and pink sands and fine gravels is up to 50 cm thick and often overlies a thin brownish-red sand and weathered Tertiary limestones of the Port Willunga Formation. Above this is a 50 cm zone of fine sand which is relatively tough and compact for the first 25 cm where sediments are impregnated with halloysite. Sands from the upper 25 cm are softer and include pods up to 15 cm across and discontinuous seams up to 4 cm thick of white alunite (Fig 5.3). The soft pods are often elongate to a maximum length of 25 cm and include visible quartz grains. Very sharp lower contacts with surrounding sediments but diffuse upper contacts are observed for many pods (Fig 5.4). Fine sands which display colour banding of white, grey, yellow and orange interbed with green-grey clays and overlie the alunite-rich material.

Alunite is also identified in association with sediments other than the Robinson Point Formation. Immediately south of the Port Stanvac Oil Refinery near O'Sullivan Beach, two bands of white, nodular alunite, conformable to bedding, occur both just above and below remnants of the Hallett Cove Sandstone within sandy clays (Fig 5.5). Adjacent to the Onkaparinga River, approximately 2 km upstream from the mouth, several thin bands of alunite, conformable to bedding, occur within sands of the Eocene South Maslin Sand (Fig 5.6). Small, rounded pods are also common and often coalesce to form discontinuous seams of alunite.

5.1.3.3 Sites within the Willunga Embayment

Within the Willunga Embayment, occurrences of alunite and halloysite are less frequent than in the Noarlunga Embayment. At Maslin Bay, halloysite is common in basal sandy sediments of the Robinson Point Formation. One metre of fine yellow-orange (10YR 6/8) sand overlies the Burnham Limestone at this site with a clay mineralogy dominated by smectite. In the overlying 3 metres, halloysite is the dominant clay mineral and occurs

disseminated through fine pink-red (2.5YR 5/6) to yellow-green (2.5Y 6/4) fine sands and clayey sand. Halloysite is not identified from several clayey interbeds, nor is alunite identified as part of the matrix of any sample in this interval. In upper parts of the interval, white to grey sandy and waxy pods of halloysite occur in several discontinuous massive beds. These pods are 10 to 20 cm in size and commonly show pink-red staining on the margins. Alunite is identified as a rare component of these pods but horizontally oriented, chalky pods of alunite several cm thick and up to 10 cm long are occasionally observed within the same interval. Grey-white clayey sands in which neither alunite nor halloysite is identified overlie the interval described here.

Just south of Chinaman Gully discontinuous seams and elongate pods of alunite occur in a 20 cm thick zone lying some 60 cm above the Early Pleistocene Burnham Limestone in green (5Y 6/3) clays of the Ngaltinga Formation. The pods are up to 10 cm in diameter and as at several other sites display sharp lower contacts and diffuse upper contacts with surrounding clays. No halloysite has been identified at this locality.

At Snapper Point, halloysite is identified in the clay fraction of a sample from the base of the Snapper Point Sand Member (RM223) and forms part of the clayey matrix in sandy sediments. Alunite is not identified at this site.

5.1.3.4 Sites outside the Willunga and Noarlunga Embayments

Alunite and/or halloysite have been identified in samples from several localities outside the immediate study area but only the occurrence at Port Moorowie on the southern coastline of Yorke Peninsula has been studied in any detail. At Port Moorowie, 1.3 metres of brown-grey (2.5YR 5/6 to 5Y 7/2) mottled clay and sandy clay of Quaternary age overlie mottled Permian sand. Up to 1.5 metres of soft calcareous silty clay and calcrete cap the sequence. In the upper half of the Quaternary sediments, several discontinuous seams, 2 to 5 cm thick, of soft, white, waxy material are found (Fig 5.7). This zone is continuous along the coast for almost one km. XRD shows that both alunite and halloysite occur in the seams but with

halloysite the dominant mineral. Larger, vertically elongated pods up to 15 cm in size are common and show mostly sharp contacts with surrounding clays. Minor disseminated alunite and halloysite together with rare small pods of alunite-rich material several mm in size are found within the surrounding clays. Neither alunite nor halloysite occur in clays immediately overlying the Permian sequence or calcareous clays below the calcrete interval.

5.1.3.5 Other Sulphate Minerals

Alunite is not the only sulphate mineral in the Quaternary sediments of the region. Adjacent to both Chinaman Gully and Onkaparinga Trig, a fine-grained, pale yellow (2.5Y 7/3) mineral, which XRD identifies as jarosite, is frequently observed in association with iron-rich mottles which have formed in sandy sediments from the Snapper Point Sand Member of the Ngaltinga Formation. The jarosite occurs as coatings, up to 5 mm thick, on large iron-rich, hematitic mottles and also fills fissures and pores within the mottles (Fig 5.8). It appears that the jarosite formed by alteration of iron oxides in the mottles. At both sites where jarosite has been identified, alunite is also present, but crops out near the base of the Quaternary sediments, up to 8 metres below the mottled zone.

Barite has been identified in Permian sediments in a railway cutting just south of the Field River where it occurs in several thin colourless seams. These are up to 1 cm thick, several metres in length and conformable with bedding. Barite has also been observed in Permian sediments from other localities such as Hallett Cove as reported by Mawson (1907) and Howchin (1923). It is possible that formation of sulphate minerals such as barite, jarosite and alunite in these sediments is the result of a common source of sulphate.

5.1.4 Laboratory Analyses

5.1.4.1 X-ray Diffraction

Selected bulk samples have been analysed using XRD techniques and the mineralogy of these samples is summarized in Table 5.2. Alunite is present in most samples and XRD

peaks correspond closely to those for end-member $KAl_3(SO_4)_2(OH)_6$. This suggests that very little Na^+ has replaced K^+ in the structure and that natro-alunite is not present (Fig 5.9). Peaks are very sharp indicating that the alunite is well crystallised. Halloysite occurs in most samples together with variable amounts of alunite, but rarely as the sole mineral (Fig 5.9). Peaks for halloysite are much broader and less intense than those for alunite and both 10Å and 7Å forms of halloysite occur. It is possible however, that 7Å halloysite forms as a result of dehydration of the sample during storage in the laboratory and that when sampled all halloysite was present in the 10Å form. For example, samples from Port Moorowie which initially indicated the presence of only the 10Å form of halloysite showed diffraction peaks of both 7Å and 10Å forms after three months storage in the laboratory (Fig 5.10).

There are few other minerals evident in the bulk XRD traces. Quartz occurs in a number of samples together with minor amounts of K-feldspar. Traces of halite are present (identified by an XRD peak at 2.82Å) and interpreted as contamination from sea spray producing salt-rich interstitial waters. Subsequent crystallisation within pore spaces results from evaporation on exposure of the sediments or during drying in the laboratory.

Clay-sized fractions (<2μm) were separated from a number of samples for both mineralogical examination and transmission electron microscopy. XRD analyses of oriented samples confirmed the presence of halloysite in the clay fractions of most samples with alunite present in several samples. Halloysite is identified from samples due to broadening on the low angle side of the 7.15Å kaolinite peak and also occasionally on the high angle side of the 10Å illite peak (Fig 5.11). Detection in this manner of very small amounts of halloysite (up to 5%) from samples containing abundant kaolinite would be difficult and hence all samples containing halloysite may not have been identified. Where broadening of the 7.15Å peak was suspected, the presence or absence of halloysite was confirmed using intercalation with formamide (Churchman *et al* 1984; Theng *et al* 1984) which expands the halloysite structure giving a peak at 10.4Å. Formamide does not react rapidly with kaolinite which will continue to give a diffraction peak close to 7Å. Heating to 100°C collapses all

kaolinite and halloysite minerals to 7Å but does not affect the illite/mica peak which remains at 10Å thereby allowing the relative proportions of kaolinite and halloysite to be estimated.

Halloysite was identified in the <2μm fraction of samples from three of the four major sites at Snapper Point, Maslin Bay and Onkaparinga Trig and these sites provide information on the relationship between halloysite and other clay minerals identified in the Quaternary sequence. At Snapper Point, halloysite was identified from sample RM223 at the base of the Snapper Point Sand Member within coarse sediments. Kaolinite is the dominant clay mineral in this sample with minor amounts of illite and randomly interstratified illite-smectite. Halloysite was not detected in any other sample from this location.

At the Maslin Bay section, halloysite is recorded in most samples near the base of the Robinson Point Formation between 1.5 and 5.0 metres (see Figure 4.28). Between 0 and 1.5 metres, samples are rich in smectite with no halloysite identified. Interstratified clays are not observed in samples where halloysite is common with kaolinite and illite being the only associated clay minerals. Illite proportions change little through the halloysitic interval and hence the formation of halloysite appears to be at the expense of interstratified clays and some kaolinite. Several clay-rich bands were identified during fieldwork within the halloysitic zone and no halloysite was identified in samples from these bands (RM251, RM254). This suggests that the formation or preservation of halloysite in this sequence requires porous, coarse-grained sediments or alternatively that deposition of halloysite only took place in coarser sediments.

Similar clay mineral associations were observed near the base of the Robinson Point Formation at Onkaparinga Trig. Halloysite was identified in sandy sediments from the basal 3 metres together with kaolinite and illite (see Figure 4.32). No interstratified clay minerals were detected in these halloysite-rich samples, although two fine-grained bands within this interval contain no halloysite (RM144, RM293). Illite, kaolinite and randomly interstratified illite-smectite were recorded in these two samples.

5.1.4.2 Optical Microscopy

Thin sections were made of twelve samples collected from the alunite-halloysite interval at five sites and observed using normal optical petrologic techniques. Details of thin sections are given in Appendix 6. Where fine-grained material was present and individual grains could not be resolved under the optical microscope, the mineralogy of these areas was later confirmed using the electron microprobe.

Most thin sections show a fine-grained matrix filling areas between widely scattered skeletal grains up to 1 mm in size and comprising dominantly quartz with rare feldspar (Fig 5.12). Quartz grains are sub-angular to sub-rounded and commonly show embayed edges while feldspar grains are more angular and often etched along cleavages.

Both alunite and halloysite occur as part of the matrix with individual grains rarely resolved. Alunite-rich samples such as RM142 and parts of RM63 contain small lozenge-shaped grains of alunite up to 1μm in size (Fig 5.13). These often occur as clusters within a fine-grained, dark-coloured matrix which consists of both cryptocrystalline alunite and halloysite (Fig 5.14). The clusters of alunite lozenges may be replacements of previous minerals, although they form no particular shape such as may be expected if replacing a mineral such as pyrite. In most samples, both alunite and halloysite appear to form an intimate mixture, but with variable birefringence patterns. The speckled fabric displayed in parts of RM63 (Fig 5.15) may be due to tiny alunite crystals which can occasionally be resolved, while the coarser interlocking pattern (left hand edge) resembles halloysite-rich material from other samples. Such segregation suggests that there have been several phases of formation of both alunite and halloysite. The undulose extinction pattern displayed in Figure 5.15 may be related to stress during deformation of the sediments possibly as a result of drying and desiccation of the sediments. Fractures cutting through the sediments are likely to have a similar origin and have been filled by late-stage halloysite (RM167, Fig 5.16) or cryptocrystalline alunite (RM120, Fig 5.12).

Apart from alunite lozenges which form clusters in some samples, there is no evidence of alunite or halloysite replacing previous minerals or organic matter. Oxidation of the sediments during diagenesis would however, be expected to have destroyed any organic matter originally present. The embaying of quartz grains and etching of feldspars suggests that diagenetic processes have been active in these sediments and K^+ and Al^{3+} from feldspars may have contributed to subsequent formation of alunite.

Because of the intimate mixing of both alunite and halloysite in many samples and the desire to relate the various optical birefringence patterns observed to actual mineralogy, the use of SEM techniques to enable observation at higher magnifications was proposed. Several thin sections from sample RM63 (Port Moorowie) were fractured and edges of these fragments placed in the SEM for observation. While some crystal forms can be identified, in particular small rhombohedra which are probably alunite crystals and small platelets which could be clay minerals such as kaolinite or illite (Fig 5.17), impregnating media severely restrict the usefulness of the SEM to obtain 3-dimensional views. Following the ideas of Norton *et al* (1983), selective etching of the impregnating material was attempted. Portions of thin sections from RM63 were subjected to immersion in Epoxysolve or methylene chloride for varying periods of time from 30 seconds to 5 minutes. Methylene chloride was found to be better at etching the Escon polyester resin used as an impregnating medium with Epoxysolve merely loosening the thin section from the glass slide by dissolving the Araldite used as the adhesive. Examples of scanning electron images obtained from these experiments clearly show rhombohedral-shaped crystals characteristic of alunite and small laths which are thought to be halloysite crystals (Fig 5.18). Unetched quartz grains remain as flat-topped mesas (Fig 5.19). These images confirm the cryptocrystalline nature of both alunite and halloysite in matrix material but do not allow determination of the exact relationship between the two mineral phases.

5.1.4.3 Scanning and Transmission Electron Microscopy

In addition to the etching experiments described above, normal SEM procedures were adopted to look at small fragments of alunite and halloysite-rich material. TEM techniques were used to determine the nature of these minerals and also other clay minerals which occurred in these samples.

Transmission electron micrographs indicate that the halloysite occurs as thin tubes of variable size; length varying from 0.4μm to 3μm and width from 0.03μm up to 0.1μm. For example, tubes in sample RM166 (Port Moorowie) are typically short and stubby (Fig 5.20) while those from sample RM141 (Port Noarlunga) are much longer and slender (Fig 5.21). A few tubes of halloysite appear to be slightly bent while others exhibit sharp and irregular terminations suggesting breakage of the tubes probably during dispersal of the samples which was carried out using an ultra-sonic probe. The wide variety of sizes exhibited by halloysite suggest variations in the local environment during formation although even samples from the same locality often differ widely in crystal morphology. There is no obvious relationship between diffraction data which show the presence of both 7Å and 10Å forms of halloysite and observed crystal morphology. The 7Å halloysite phase therefore appears to be partly related to dehydration of the samples during storage as described earlier.

Where alunite has been recognised, for example in sample RM138 (Robinson Point), it occurs as small euhedral rhombs with the largest dimension seldom exceeding 1μm nor being less than 0.5μm (Fig 5.22). XRD analyses indicate that small amounts of kaolinite and illite are present in many samples and these minerals can be clearly seen using the TEM (Fig 5.23, RM167). The clay particles take two forms. One group includes large grains ranging in size from 0.5μm to 2μm and generally showing irregular to rounded shapes and the second comprises particles mostly less than 0.2μm in size. The smallest clays are more regular in shape with many being euhedral and hexagonal and suggesting the possibility that some of the very small clay is of authigenic origin. Larger, irregular grains of the first group are most likely to be of detrital origin.

Scanning electron micrographs confirm the mineral forms identified in the transmission electron micrographs. Alunite crystals tend to be blocky, often diamond-shaped and commonly occur massed together (Fig 5.24, RM142). Halloysite crystals are clearly identified occurring individually and also as matted tubes. Nested within the halloysite-rich areas are rare rhombs of alunite (Fig 5.25, RM69). Zalba (1982) termed the matted tubular form of halloysite a "wet-grass structure" and identified rough hexagonal shapes for some matted tubes which he suggested were formed from hexagonally shaped kaolinite crystals. In this study "wet-grass structure" has been observed in some samples but pseudo-hexagonal shapes were not noted. A number of mineral forms observed in the micrographs are difficult to identify due partly to their small crystal size. Aluminosilicate clay minerals appear to account for many of these crystals which are often present as small, etched and irregular thin plates and frequently associated with tubes of halloysite (Fig 5.26, RM165). The morphology of these clay minerals suggests that they have undergone some alteration, possibly during the formation of alunite and halloysite.

Thin, wispy forms were noted in a number of samples but the mineralogy of this material could not be identified using the SEM (for example RM165, Fig 5.26). Allophane had been previously reported to occur in association with halloysite (Ross & Kerr 1934; Keller *et al* 1967) hence it was thought that the wispy material may also be allophane. Oxalate extractions were carried out to determine the amount of amorphous Si and Al present in the samples and the results of these procedures for the eight samples analysed are shown in Table 5.3. Only minor amounts of Si and Al were extracted from these samples indicating that amorphous phases such as allophane, while possibly present, form a very small component of the sample. Additional SEM studies indicated that the wispy material occurred only in pore spaces and was not preferentially associated with any other mineral phase. Chloride was also detected in these samples. Additional observations in coastal cliffs where the samples had originally been collected identified small crystals of a white to colourless material which occurred as crusts and filling small fractures. X-ray diffraction analyses determined this material as halite. The thin, wispy material may therefore be halite,

crystallised recently in pore spaces within the sediments as a result of their close proximity to the sea.

5.1.4.4 Electron Microprobe Analyses

Electron probe analyses have been carried out on polished thin sections. Despite the careful selection of operating conditions, one of the problems encountered while using the probe was damage to the sample caused by the focussed beam. A considerable drop in the counts being registered for most elements analysed could be detected within a second or two of the beam being focussed on the sample. Two methods of analysis were thus employed to obtain definitive data for the samples; one method used a stationary beam and the other a moving beam. Results from both analytical methods have been plotted on the triangular diagram shown in Figure 5.27. Far greater sulphur losses are indicated for stationary beam analyses and hence a moving beam analysis was employed for all subsequent determinations.

The remaining data gathered from the probe analyses have been plotted on the triangular diagram in Figure 5.28. The majority of plotted points tend to lie along the alunite-halloysite tie line. It would appear that despite the problems discussed above, careful analysis utilising a moving beam has not seriously influenced the mineralogical interpretations made using the chemical data obtained from the probe. A number of points plot to the left of the alunite-halloysite tie line toward the SiO_2 end-member. Other than quartz, no other silicon-rich phase was evident in the XRD traces, however during analyses, care was taken to avoid including quartz clasts in the areas being investigated. It is possible that Si exists within the sample either as microcrystalline particles of quartz or in an amorphous state, neither of which would be optically resolvable but which could result in higher SiO_2 measurements. The three samples in which no silica was detected from ammonium oxalate extractions (RM135, RM138A, RM142; Table 5.3) all plot along the alunite-halloysite tie-line in Figure 5.28, while other samples which had measurable silica contents, apart from RM167, all plot toward the SiO_2 end-member. Goldbery (1978; 1980), while discussing the formation of alunite, proposed a model in which SiO_2 was formed as a product of the reaction. The

displacement of some data points from microprobe analyses away from the alunite-halloysite tie line and the presence of amorphous silica in ammonium oxalate extracts from these samples suggests that the model invoked by Goldbery may also be applicable to the present study.

5.1.5 Summary

Alunite has been described at numerous locations within South Australia from widely varying strata but such occurrences have not been studied in detail. Recent field observations have shown a common occurrence of both alunite and halloysite in Quaternary sediments of the Noarlunga and Willunga Embayments. Halloysite occurs mostly in waxy, sandy masses which are often indurated while alunite forms softer bulbous masses, elongate pods and stringers which are conformable to bedding and show sharp lower contacts with surrounding sediments and diffuse upper contacts. Where halloysite occurs, there is depletion in smectite and randomly interstratified clays compared with surrounding sediments suggesting that halloysite may have been transformed from these minerals. Transmission and scanning electron micrographs show that both alunite and halloysite occur as euhedral crystals and hence are most likely to be of diagenetic origin rather than sedimentary. Thin sections show several phases of alunite and halloysite which often occur as intimate mixtures and show evidence of formation under conditions of stress and dehydration. No evidence of replacement structures or organic material have been observed.

5.2 Iron Mottling

5.2.1 Distribution in the Late Cainozoic Sequence

A most striking feature of Quaternary sediments in the Noarlunga and Willunga Embayments is the spectacular mottled patterns developed as a result of the redistribution of iron oxides during post-depositional alteration. Mottling is observed within sediments of both the Robinson Point and Ngaltinga Formations. The most prominent concentrations occur within

coarse sandy intervals from parts of the Robinson Point Formation and Snapper Point Sand Member. These sandy lenses are frequently enclosed above and below by finer-grained, often clay-rich sediments. Mottles from these intervals are indurated, as is the host sediment.

In contrast to the large indurated mottles, many fine-grained sediments from both the Robinson Point and Ngaltinga Formations display minor concentrations of iron, rarely greater than 1 cm in largest dimension. Such mottling is often developed in finer sediments immediately adjacent to larger mottles in the indurated sandy lenses but can also be observed in lesser densities in most fine-grained sequences.

A third mottling pattern is generally observed in interbedded gravel, sand and silt sequences from basal parts of the Robinson Point Formation. Vertically oriented mottles are coarsest in sandy units and finer in silty units and are highlighted by the vertical and horizontal patterns of associated bleaching. Such mottling patterns have not been observed in sediments from the Ngaltinga Formation.

In summary, mottling can be observed throughout the Late Cainozoic sediments with the nature of the mottles varying according to the lithology of the host sediment. The most striking mottling is confined to coarse lenses which occur within parts of both the Robinson Point and Ngaltinga Formations.

5.2.2 Distribution in the Noarlunga and Willunga Embayments and Nearby Areas

The iron mottling described from Late Cainozoic sediments can be found in both the Noarlunga and Willunga Embayments. Large, prominent and indurated mottles occur in both the Robinson Point and Ngaltinga Formations in the Noarlunga Embayment. In the Willunga Embayment, they are confined to the Snapper Point Sand Member apart from an occurrence within the Robinson Point Formation at Maslin Bay near the northern margin of the embayment. This variation in the host unit for these indurated mottles is determined by the distribution of the stratigraphic units within each embayment with the Robinson Point

Formation being confined to basin margins in the Willunga Embayment but being more widespread in the Noarlunga Embayment. The mottles are always developed in sandy sediments within a finer-grained sequence regardless of the stratigraphic unit which is present. Similarly the coarse, rectangular mottling patterns observed in basal parts of the Robinson Point Formation are widespread through the Noarlunga Embayment. They are rarely observed in the Willunga Embayment due to the limited distribution of the Robinson Point Formation in the southern area and also the fact that similar interbedded gravel, sand and silt sequences do not occur as part of the Ngaltinga Formation.

Prominent iron mottling is not confined to Late Cainozoic sediments of the Noarlunga and Willunga Embayments but can be observed at numerous locations on Yorke Peninsula such as at Ardrossan and Port Moorowie, in the Adelaide region at Mitcham and Redbanks and on Kangaroo Island at Redbanks. Mottles are also developed in sediments of Tertiary and older ages particularly in the Mt Lofty Ranges and on Fleurieu Peninsula. Many of these older occurrences have been discussed in relation to development of ferricretes and weathering zones by Milnes *et al* (1985b) and Bourman (1989).

5.2.3 Field Observations

Some form of iron mottling within Quaternary sediments can be observed at most locations along the coastline in the Noarlunga and Willunga Embayments. Observations presented in this section are confined mostly to the four major sections at Hallett Cove, Onkaparinga Trig, Maslin Bay and Snapper Point which have been used for detailed study of other aspects of the sediments. Additional sites are discussed where such observations add to an understanding of the iron mottling or where a different type of mottling occurs.

5.2.3.1 Sites Within the Noarlunga Embayment

5.2.3.1.1 Hallett Cove

The most prominent mottling at Hallett Cove is confined to a central sandy interval in The Amphitheatre within the Robinson Point Formation (Fig 5.29). The mottles are large, red (10R 3/6) and indurated, up to 50 cm long and 20 cm across and generally vertically oriented. Occasionally a lighter, yellow-orange zone (10YR 6/8) is developed around part of the dark red core. The pale-coloured host sandy sediments are also indurated and include rare stone lines and occasional planar bedding. Immediately above the indurated zone, in light grey, more clay-rich intervals of the Robinson Point Formation, soft mottles up to 25 cm in size and less intense in colour (10R 4/6) are found. Clay-rich sequences with up to 50% <2μm occur both above and below the indurated interval. To the north of The Amphitheatre, small, indurated sandy lenses forming the Snapper Point Sand Member occur in clays of the Ngaltinga Formation and these display similar bright red mottling.

Finer-grained sediments of the Robinson Point Formation near the base of the sequence are a fairly uniform brown-red colour (7.5YR 5/6) but do display rare yellowish mottles (10YR6/6). In contrast, clays from the Ngaltinga Formation are frequently mottled with small concentrations of iron up to 2 cm in greatest dimension. The density of mottling however is not great with often 10 cm of pale-coloured clay between mottles. They are confined to surfaces of clay peds or along fractures which are frequently developed within the clays. Fine-grained sediments of the Ngaltinga Formation are mostly grey to olive-coloured (5Y 6/2 to 5Y7/3), while the small mottles are either yellowish (10YR 6/8 to 10YR 6/4) or reddish (7.5R 3/4). Yellow mottling is most common in basal clays of the Ngaltinga Formation with reddish mottles confined mostly to areas adjacent to slightly coarser sediments and upper parts of this sedimentary unit.

5.2.3.1.2 Onkaparinga Trig

At Onkaparinga Trig, large red mottles are rare and confined to a sandy interval at the base of the Snapper Point Sand Member. These mottles are less indurated and smaller in size (up to 30 cm) than those observed at Hallett Cove but retain a similar red colour (10R 4/6). Rare coatings of yellow jarosite (2.5Y 7/3) are found on some mottles at this location, while in thinner sandy units within the Snapper Point Sand Member, the mottles tend toward an orange-yellow colour (10YR 6/8). Fine-grained intervals of the Ngaltinga Formation are mottled in a similar manner to that observed at Hallett Cove with small red (7.5R 3/4) or yellow (10YR 6/8) blotches on ped or fracture surfaces. Red mottles predominate throughout the Ngaltinga Formation at this site with yellow mottles occasionally observed in upper parts.

Mottling in the Robinson Point Formation is confined to silty intervals within gravel, sand and silt sequences. The silty sediments are light grey in colour (10YR 8/2) with a columnar structure and have broad orange-yellow (10YR 7/8) vertically oriented mottles, 1 to 3 cm wide and up to 5 cm in length. This mottling is not developed in underlying coarse gritty or gravelly sediments and is truncated where overlying gravels fill shallow channels eroded into the silty sediments (Fig 5.30). Where alunite and halloysite have formed near the base of the Robinson Point Formation, an unusual pink-red colour (10R 5/6 to 10R 6/4) is observed in surrounding sediments. While this is not in the form of mottling, the presence of a laterally extensive zone with distinctly different colour to surrounding sediments suggests mobilisation and precipitation of iron oxides in this interval.

5.2.3.1.3 Other Sites Within the Noarlunga Embayment

Between Port Noarlunga and Witton Bluff, basal sediments of the Robinson Point Formation comprise a series of interbedded gravels, grits, sands and silty clays. Gravels and grits are not mottled, however grey silty sediments display numerous small, yellow (10YR 7/8) vertical mottles up to 4 cm in length. Sandy intervals are broadly mottled with large irregular

red to orange patches (10R 4/8). Intervening sediments are white to grey coloured and these bleached zones often form a roughly rectangular pattern (Fig 5.31). Induration of the sandy zones is common and hence these beds often form small benches in the cliff face.

Quaternary sediments exposed in a railway cutting adjacent to O'Sullivan Beach Road fill a channel eroded into underlying Precambrian bedrock. Sandy sediments which display horizontal bedding trends are mottled near the base of the channel but not in upper parts where they are overlain by clays (Fig 3.39). Induration of the mottles and surrounding white to grey sands is common. The mottles are dominantly red-coloured (10R 4/6) with yellow colours (10YR6/8) often forming an outer margin. Both vertically and horizontally elongate mottles are present with a maximum size of 30 cm. In upper parts of the sandy channel-fill sediment just below the clay-rich sequence, small, soft yellow mottles (10YR 6/6) up to 5 cm in size are occasionally developed. These do not extend into the overlying clays.

5.2.3.2 Sites Within the Willunga Embayment

5.2.3.2.1 Maslin Bay

Large, vertically oriented mottles are common at Maslin Bay within a 2 m thick, white, sandy unit from central parts of the Robinson Point Formation. This interval is strongly indurated and stands out in coastal cliffs as a resistant bench (Figs 3.14; 3.16). Mottles are up to 40 cm long and generally red-coloured (10R 3/6) but with significant development of yellow colours (10YR 6/8) on the edges of the mottles. Softer and smaller red mottles (10R 4/6) extend from the indurated interval into the surrounding more clayey sediments. The remainder of the Robinson Point Formation at Maslin Bay comprises greyish sandy clays (7.5Y 7/2) with occasional clay-rich beds and these sediments commonly display broad, irregular orange-brown patches (2.5YR 5/6).

Mottling in clay-rich sediments of the Ngaltinga Formation comprises small yellow (10YR 6/8) or red (2.5YR 5/6) patches up to 2 cm in size on the surfaces of clay peds. Yellow

mottles are most common in the basal metre and upper 2 m of this unit while red mottles dominate the central 4 m.

5.2.3.2.2 Snapper Point

Mottling is less pronounced at Snapper Point than at Maslin Bay with large mottles confined to horizontally bedded sandy sediments at the base of the Snapper Point Sand Member (Fig 3.4). The vertically oriented mottles are red to orange in colour (10R 4/6 to 10YR 7/8) and up to 20 cm in length. They are confined to either the base of sand-filled channels or upper parts of the sandy interval where a transition takes place to more clay-rich lithologies. Central parts of the sand unit which is up to 2 m thick, are rarely mottled. In the overlying clays and sandy clays, small red mottles (7.5R 3/6) are commonly developed. These are up to 5 cm in size and decrease in abundance toward the overlying carbonate unit. Green clays (5Y 6/3) of the Neva Clay Member which form the basal 9 m at the Snapper Point section display small yellow mottles (10YR 6/8) on ped surfaces along with occasional manganese staining.

5.2.3.2.3 Other Sites Within the Willunga Embayment

Near Blanche Point, the Quaternary sequence often comprises red-green clays overlying yellow-green clays. Occasional sandy intervals occur between these clay units which are strongly mottled in a manner similar to the Maslin Bay section (Fig 5.32). In places, this sandy interval is indurated and the mottles are extremely dark red (7.5R 2/1), weathering to a lighter red on the margins (10R 3/4). Where thinner, slightly clayey intervals occur, the mottles are soft, smaller and light coloured (10R 4/6). Clay sediments from the upper and lower units have the same olive-yellow base colour (5Y 6/3). The perceived difference when looking at these two units from a distance is due to the colour of the small ferruginous mottles which are common in the clay-rich sediments. Mottles from the lower clay are dominantly yellow-orange (10YR 6/8) while those from the upper clay unit are mostly red (7.5R 3/6).

At Ochre Point, isolated sandy intervals which are prominently mottled and indurated occur within the Ngaltinga Formation. Surrounding sediments are olive-green clays which display minor small red mottles similar to clay-rich units from other locations. Grey sandy sediments of the Robinson Point Formation are broadly mottled with orange-red colours which are similar to mottling developed throughout much of this formation at Maslin Bay. In central parts of the Robinson Point Formation in the Ochre Point area, some sandy beds are indurated, displaying a columnar structure and a broad red vertical mottling pattern (Fig 3.19). Bleached zones between mottles have a rectangular pattern similar to that developed in equivalent sediments near Witton Bluff.

5.2.4 Laboratory Observations

Mottles from Quaternary sediments in the region were sampled to collect material representative of the variation in the nature of mottles which had been observed in the field. The mineralogy and chemistry of the mottles was subsequently determined and is discussed in the following sections.

5.2.4.1 X-Ray Diffraction (XRD) and X-Ray Fluorescence (XRF)

Colour variations in mottles from dark red through to yellow suggest that there are differences in the iron mineralogy associated with mottles developed in these sequences. Examination of XRD traces indicates that the darkest mottles have hematite as the dominant iron mineral while yellow colours are generally associated with goethite. Such an association of mineralogy with colour is in agreement with previous work by Schwertmann (1985) who indicated that yellow colours were associated with goethite and reddish colours with hematite. Most mottles however, have an iron mineralogy composed of various proportions of both hematite and goethite and this is shown in Table 5.4. Ratios of the height of the goethite (110) and hematite (110) peaks are a crude measure of the relative proportion of

these two minerals in the samples and it is evident that low values of this ratio correlate well with samples having a strongly red colour.

No other iron-rich minerals have been identified from XRD traces and tests using a hand-held magnet indicate that no samples contain detectable magnetic minerals. Quartz and clay minerals are the major non-ferruginous minerals present in all samples with various amounts of feldspar and halite also present. These minerals occur in both the mottled samples and adjacent non-mottled material (Table 5.4).

Both hematite and goethite give XRD peaks of variable sharpness with widths at half height for both the hematite (110) and goethite (110) peaks varying from 0.3°2θ to 0.7°2θ (Table 5.4). Similar sharpness values are recorded for each mineral in the same sample. Comparison of diffraction peak positions for goethite and hematite from the present study with calculated positions given by Brown (1980) show that there is very little difference (Table 5.4). Norrish & Taylor (1961) discussed the isomorphous substitution of Fe by Al in soil goethites and the effect of this substitution on peak positions. This information, together with the position of goethite (110) and (111) peaks from samples studied in this thesis have been used to estimate the degree of Al-substitution in these samples. Most samples show negligible Al incorporated in the goethite structure, however four samples have between 2 and 6 mole % Al (Table 5.4).

Iron contents (% Fe_2O_3) as measured by XRF of bulk mottled and non-mottled material are highly variable. Mottles have between 10 and 45% Fe_2O_3 while associated non-mottled sediments have iron contents varying from 1.6 to 2.7% Fe_2O_3 (Table 5.4, Appendix 7). No association can be seen between iron mineralogy and total iron content although the highest Fe_2O_3 value in sample RM62-2 corresponds with the lowest goethite to hematite ratio.

5.2.4.2 Associated Clay Mineralogy

Where intensely mottled and indurated intervals occur within the Robinson Point Formation at Maslin Bay and Hallett Cove, clay minerals from the <2μm fraction have been studied. At Maslin Bay, there is a decrease in the proportion of both randomly interstratified clays and kaolinite with illite showing a strong increase compared with surrounding sediments of the Robinson Point Formation. Similarly, at Hallett Cove randomly interstratified clays are depleted in the mottled zone with the kaolinite proportion also decreasing and illite increasing at the base of this zone compared with surrounding sediments. From the bottom to the top of the 2.5 m thick mottled interval, there is then a gradual increase in the proportion of kaolinite and a decrease in illite. Randomly interstratified clays remain a minor proportion throughout the interval compared with surrounding sediments. In contrast, mottling at the Snapper Point and Onkaparinga Trig sections within sandy sediments of the Snapper Point Sand Member is associated with an increase in the proportion of kaolinite and decreases in the proportion of both illite and randomly interstratified clays.

5.2.4.3 Micromorphology

Data obtained from XRD and XRF analyses of bulk samples can provide only limited information regarding the processes involved in the formation of mottles in the Quaternary sediments. Observations of the distribution of iron oxide minerals in thin sections enable relationships with host sediments to be determined and form the basis for understanding the origin of the mottled sequences.

Field studies indicate that in a macro sense, the nature of mottling is strongly dependant on the host lithology. Thin sections have been grouped and observed using this as a basis for interpretation. Sandy sediments which are generally broadly mottled with orange-red to yellow colours comprise rounded to sub-rounded sand-sized grains of quartz with very rare feldspars and opaques. Considerable porosity is often present and only partially filled by clays and iron oxides. Clays form thin coatings around skeleton grains and also small

bridges joining adjacent grains. A mixture of iron oxides and clays partially fill some pore spaces and form thicker skins around the clay coated quartz grains (Fig 5.33, RM134). Iron oxide mineralogy is a mixture of hematite and goethite.

Fine-grained clay and sandy clay sediments such as those forming much of the Ngaltinga Formation have small blotches of iron which are generally visible in the field on fracture or ped surfaces. Thin sections of such sediments indicate that iron has usually accumulated in elongate zones which are often recognised as present or former fracture zones (Fig 5.34, RM80). The mineralogy is a mix of both hematite and goethite with yellow goethite colours frequently found on the margins of the iron accumulation.

Well developed mottles from sandy and sometimes indurated intervals often show complete impregnation of intergranular space, with hematite being the dominant iron oxide (Fig 5.35, RM349). Precipitation of iron oxides is commonly through the replacement of existing clay minerals and where remnant clays are identified they occur as isolated pockets within an iron-rich matrix (Fig 5.36, RM349). Partial replacement of clay minerals which coat many quartz grains in the mottled sediments is also frequently observed (Fig 5.37, RM264). On a larger scale, the partial disintegration of a mica lath by iron crystallising between cleavage planes indicates the extent of clay mineral alteration and also suggests that the clays themselves may be a potential source for some of the iron forming mottles (Fig 5.38, RM40). Iron oxides can also be seen replacing and etching feldspars and quartz in some samples (Fig 5.39, RM41).

In fractures leading toward ferruginous zones iron oxides are often concentrated along the margins of such fractures (Fig 5.40, RM264). Preferential precipitation of iron oxides along fractures within the sediment is supported by observations of thin sections from mottled carbonate within the Neva Clay Member. In sample RM170, hematite precipitation clearly marks the edge of a fracture through microcrystalline carbonate with secondary crystallisation of carbonate following development of carbonate (Fig 5.41). While most iron-rich material observed in thin section is an intimate mix of hematite and goethite, there are several

examples of multiple phases of iron oxide precipitation. In sample RM264, precipitation of iron oxides along a fracture was initially composed of goethite with a subsequent phase of hematite (Fig 5.40). Iron oxides filling intergranular pore space in sample RM40 show several phases of precipitation of hematite within a lighter coloured goethite-clay material. Very small crystallites of hematite occur within the goethite-clay matrix and in places these coalesce to form larger aggregates (Fig 5.42).

Opaline silica has been identified in several thin sections occurring as an isotropic material infilling voids (Fig 5.43, RM264). Samples in which this material is observed are mostly from indurated intervals within either the Robinson Point Formation or the Snapper Point Sand Member. XRD traces of bulk material and the <2μm fraction from these intervals often show a broad region of high background centred on 4.1Å and comparison with the work of Jones & Segnit (1971) suggests that such diffraction effects are due to the presence of minor opaline silica.

5.2.5 Summary

Mottling of Quaternary sediments from the Noarlunga and Willunga Embayments by iron oxides is commonly observed. The nature of the mottling varies, being dependant on the nature of the host sediment. Coarse sandy sediments are often indurated and display large, red, hematitic mottles. In contrast, finer sediments have smaller, soft mottles of lighter colour with goethite rather than hematite forming a larger proportion of the iron mineralogy. Thin section studies show iron filling pore spaces and replacing clay minerals in coarser sediments and precipitating along present or former fractures in finer sediments, at sites of local oxidation. Silica released from clay minerals during replacement by iron oxides may form opaline silica which has been identified in some thin sections. Reduction in the proportion of randomly interstratified clays and kaolin in mottled zones compared with adjacent sediments indicates the potential importance of mineral transformations in the formation of iron-rich mottles and the possible effect of local groundwater conditions.

5.3 Palaeosols

The recognition and description of fossil soils (palaeosols) in sedimentary sequences has been undertaken by many researchers (eg Allen 1974; Buurman 1975; 1980; Leeder 1976; Retallack 1976; 1977; 1988; Wright 1986). A number of features indicative of palaeopedogenesis have been identified from this previous work which include the presence of root traces, marked colour changes associated with development of soil horizons, evidence of soil structure, intensive bioturbation and mineral accumulation horizons (Blodgett 1988; Retallack 1988). There is also a tendency for the upper boundary of the unit to be sharp due to erosion, whilst the lower boundary is gradational (Retallack 1988). Using these criteria, palaeosols in Quaternary sequences from the Noarlunga and Willunga Embayments have been identified and are discussed in this section.

5.3.1 Field Observations

5.3.1.1 Robinson Point Formation

In basal parts of the Robinson Point Formation at the Onkaparinga Trig site, a series of upward fining intervals have been described (Section 3.2.9). Such intervals begin with gravel and gritty or coarse sandy sediment which often show remnant cross bedding structures. A gradual decrease in particle size is observed to a grey silty to clayey interval which is then overlain with an erosional contact by the next coarse gravel or sand unit. Such intervals are of variable thickness depending on the degree of truncation prior to deposition of the next unit but have been observed up to 1 m thick. At Onkaparinga Trig, four upward fining units are identified, however in the vicinity of Seaford a maximum of nine units have been observed.

Several features which are identified within silty to clayey units of the upward fining sequences suggest these to be palaeosols. Firstly, there are abundant small pores of circular cross-section which penetrate the silty sediments forming thin tubes of between 0.5 and 2

mm in diameter and with a vertical or sub-vertical orientation. Many of the tubular structures have a very thin red-brown (7.5YR 5/6) clay coating the walls which is a different colour to the rest of the grey (10YR 8/2) silt and clay-rich sediment. Occasional larger tubes with a diameter of between 5 and 10 mm are also observed and these are usually filled with red-brown clay. None of the tubular structures can be traced for more than 5 cm and branching structures have not been observed. These tubules are interpreted to be biogenic structures most likely to have been created by burrowing insects or worms. Similar structures described by Retallack (1976; 1977) from the Triassic Narrabeen Group in NSW were postulated to be formed by cicada-like insects, however insufficient information is available to allow such a detailed conclusion for tubular structures from the Robinson Point Formation.

The second feature of significance is the development of a columnar structure in the upper half to two thirds of the silty units (Fig 5.44). These are sub-rounded aggregates up to 3 cm in diameter and elongated in a vertical direction for up to 7 cm. No primary sedimentological structures are noted within these silty units.

Finally, a vertical pattern of iron mottling is common within the silty units having a diameter of up to 2 cm and length to 5 cm. The mottles are a yellow to orange colour (10YR 7/8) in contrast to the unmottled material which has a grey colour (10YR 8/2) and they often impart an overall yellow hue to the units. This is in contrast to adjacent sediments which do not normally display iron-rich mottling.

Features such as those described from the Robinson Point Formation at Onkaparinga Trig are commonly observed in coastal cliffs between Witton Bluff and Moana. They have not been observed from sediments in the Willunga Embayment.

In other parts of the Noarlunga Embayment to the north of Witton Bluff and south of Moana, more subtle features suggesting the presence of palaeosols are seen within predominantly sandy sequences from middle parts of the Robinson Point Formation. In the vicinity of

Ochre Point, there are a number of indurated intervals up to 1 m thick and continuous for up to 10 m (Fig 3.19). These sometimes overlie cross bedded gravels and comprise sand to clayey sand with rare isolated gravel clasts. A coarse, vertical columnar structure is always present with peds up to 20 cm in length and 5 cm diameter. No primary bedding structures are observed. The beds are red to orange coloured with broad vertical and rarely horizontal bleached zones which extend for up to 50 cm. Yellow, goethitic colours are common on the margins of bleached zones which grade into red-orange coloured zones. Many sites exhibit a complete bleaching in the upper 5 to 10 cm, similar to that observed in A_2 horizons of soil profiles. Within upper parts of these units, very rare tubular structures are observed, generally about 1 cm in diameter and 5 to 10 cm in length. They are vertically oriented and often filled with more clay-rich sediment.

Sandy intervals displaying features described here have not been observed in sediments from areas south of Ochre Point. To the north, in the Noarlunga Embayment, isolated examples have been identified near Hallett Cove, O'Sullivan Beach, Port Noarlunga and Seaford, all within sediments of the Robinson Point Formation.

Just south of Blanche Point there are several isolated locations where small, vertical tubular structures up to 1 cm in diameter have been noted at the boundary between the Robinson Point and Ngaltinga Formations. These occur within sandy sediments and are filled with laminated clay which has a concave upward orientation. This infill material is thought to be derived from the overlying clays of the Ngaltinga Formation due to similarity in colour. No distinctive mottling or soil structures are noted in association with the infilled tubular structures.

5.3.1.2 Ngaltinga Formation

Within sediments of the Ngaltinga Formation, tubular structures of possible biogenic origin have only been noted at the Onkaparinga River Mouth site. Micaceous, silty sediments form the basal part of the Snapper Point Sand Member at this locality and several vertically

oriented tubes, up to 1 cm in diameter occur within this unit. They are filled with more clay-rich sediment derived from overlying units.

A carbonate bed of variable thickness and lateral extent has been noted within olive-green clay-rich sediments of the Neva Clay Member at several localities along the coast. At Snapper Point this bed is up to 1.5 m thick and comprises irregularly shaped white masses of carbonate which are usually soft and friable but occasionally indurated. The carbonate tends to have a vertical, blocky structure similar to that developed in the surrounding clays (Fig 5.45). Individual carbonate masses are separated by up to 15 cm of clay and fine sand and have sharp edges which are commonly smooth with development of slickensides. Very rare thin tubes, several mm in diameter are observed in some carbonate masses and may represent rhizoliths. In the vicinity of Snapper Point, the carbonate bed is intermittently exposed for at least 400 m and in general has a relatively sharp upper contact with clays of the Neva Clay Member. The base of the bed is more diffuse with small isolated carbonate masses occurring up to 30 cm below the main carbonate bed. Just north of the Snapper Point section a sand-filled channel of the Snapper Point Sand Member has eroded into the underlying Neva Clay Member and removed the carbonate bed which continues to be exposed on either side of the channel (Fig 3.7). This indicates that the development of the carbonate bed pre-dates sedimentation of the Snapper Point Sand Member.

In the Noarlunga Embayment, a carbonate bed is noted within the Neva Clay Member at the Onkaparinga Trig and Onkaparinga River Mouth sites. At Onkaparinga Trig, a discontinuous bed of carbonate masses up to 2 m thick can be traced intermittently for up to 50 m (Fig 5.46). The masses are very similar to those described from the Snapper Point site and, in addition, often show small hollows and fractures within the carbonate masses which are filled with clay. At the Onkaparinga River Mouth site, the vertical section eroded by stormwater clearly displays the strongly vertical structure and sharp upper surface of the carbonate bed (Fig 5.47). A more irregular basal contact is apparent with isolated masses extending into the underlying clays below the 1 m thick main carbonate bed.

Further north, about 100 m south of Witton Bluff, a carbonate bed of variable thickness but up to 1 m is exposed in the cliff face at the boundary between the Robinson Point and Ngaltinga Formations (Fig 5.48). Due to the shear nature of the cliff face at this location the carbonate bed is inaccessible but appears to be well consolidated and have a platy structure in contrast to the blocky structure of previously described carbonate beds from the Neva Clay Member. Thin carbonate blotches appear to extend into the underlying sands of the Robinson Point Formation. A carbonate bed is not recognised at this stratigraphic position at any other location in the study area.

A carbonate unit mantles Quaternary sediments throughout the Noarlunga and Willunga Embayments and the relationship between this mantle and underlying sediments has been discussed by Phillips & Milnes (1988) and Phillips (1988). They describe a complex transition between the units with isolated blotches of carbonate and/or several discontinuous horizontal carbonate beds occurring within upper parts of the clay or sand-rich Ngaltinga Formation. Carbonate rhizoliths are recognised within carbonate in this transitional zone as well as in the overlying carbonate mantle.

5.3.1.3 Burnham Limestone

Isolated masses of carbonate occur within the metre of sediments overlying the Burnham Limestone at several locations in the Willunga Embayment between Snapper Point and Maslin Bay and also at Sellicks Beach (Fig 5.49). These masses are up to 20 cm in size and tend to occur in discontinuous beds which can be traced laterally for tens of metres. The masses have sharp boundaries and include many thin veins which are filled with clays or sands from the surrounding sediment. While there are no obvious features which enable these carbonate beds above the Burnham Limestone to be thought of as palaeosols, their similarity with carbonate beds from other parts of the sequence indicate that such an origin should be considered.

5.1.3.4 Preserved Root Structures

At several places along Sellicks Creek, indurated and mottled gravels which are thought to be part of the Robinson Point Formation are exposed in the creek bed. On several of these horizontal surfaces small, white cylindrical structures up to 5 mm wide and 10 cm long are preserved. Similar features are observed on indurated benches composed of Quaternary gravels in a quarry at Mitcham (Adelaide 1:50 000; 825257). These structures are interpreted as preserved roots.

More extensive preservation of root structures occurs on the shore platform at Snapper Point where a mat of twisted and gnarled cylindrical structures up to 80 cm in length and 20 cm in width is observed (Fig 3.6). These roots are preserved on the Hallett Cove Sandstone and cover an area of approximately 100 by 50 m. Similar, but isolated features have also been noted on the shore platform to the north of Snapper Point. The observation of preserved root structures at various stratigraphic positions and geographic locations within Late Cainozoic sediments from the Noarlunga and Willunga Embayments indicates that hiatus in sedimentation have occurred at numerous times in the past. This supports the interpretation that features described from the Robinson Point and Ngaltinga Formations represent palaeosols.

5.3.2 Laboratory Observations

5.3.2.1 Clay Mineralogy

Information regarding the clay mineralogy related to palaeosol features identified in the Quaternary sequence is taken from the Snapper Point and Onkaparinga Trig sites. These data show that silty units near the base of the Robinson Point Formation at Onkaparinga Trig have a clay mineralogy dominated by kaolinite but with appreciable amounts of smectite and illite (Fig 4.32). Smectite is not commonly present within Quaternary sediments from the Noarlunga and Willunga Embayments and at the Onkaparinga Trig site the silty units are the only sediments containing smectite. Reconnaissance samples collected from similar silty,

mottled and bioturbated sediments in the Seaford area have the same clay mineralogy. No smectite was identified from sandy units above the palaeosols at Seaford.

At both Onkaparinga Trig and Snapper Point, a carbonate bed occurs within clays of the Neva Clay Member. Clay mineralogy of this member is dominated by illite with lesser amounts of kaolinite and randomly interstratified illite-smectite. While these three clay minerals are all present within the carbonate bed, the proportion of each shows a sudden change associated with the carbonate bed. At Snapper Point the proportion of illite rises from 40-50% to 50-60% immediately above the carbonate bed. The kaolinite proportion drops from 20-30% to 10-20% at the same position while the proportion of interstratified clay remains constant (Fig 4.25). There is a similar change in clay mineral proportions at Onkaparinga Trig with illite increasing from 40-50% to 50-60% at the base of the carbonate interval. Both kaolinite and randomly interstratified clay show a decrease in their proportions at the same position from 30-40% to 20% for kaolinite and 30% to 20% for the interstratified clays (Fig 4.32). At both sites, the trend to higher illite and lower kaolinite contents is the same, although the position at which the change takes place differs between the locations. No change in particle size is evident through the carbonate beds at either site with the % <2μm averaging 70% throughout the Neva Clay Member at Onkaparinga Trig and 75% at Snapper Point. Triangular diagrams summarising particle size data show that all samples from the Neva Clay Member cluster tightly toward the clay apex.

5.3.2.2 Carbonate Mineralogy

The nature of the carbonate mineralogy within the carbonate bed at Onkaparinga Trig has been studied in detail with 12 samples collected through a 1.5 m interval. Numerous carbonate masses 10 by 20 cm in size occur in this interval with gaps of up to 20 cm between the carbonate accumulations (Fig 5.50). Dolomite is the only carbonate mineral identified from several samples at the base of the interval with dolomite and minor calcite present in most other samples below the top 50 cm. Calcite is the dominant mineral in uppermost parts of the interval (Fig 5.50). This variation from dolomite to calcite in an upward direction is

also shown in the carbonate bed at Snapper Point. At this site three samples were collected with the basal sample containing only dolomite, the middle sample approximately equal proportions of dolomite and calcite and the upper sample calcite with rare dolomite.

The discontinuous interval of carbonate above the Burnham Limestone has a mineralogy dominated by dolomite with only rare samples exhibiting small amounts of calcite (Table 5.5). This is in contrast to samples collected from the Burnham Limestone at Sellicks Beach, Snapper Point, Port Willunga and Maslin Bay where all samples have a carbonate mineralogy dominated by calcite. Only minor amounts of dolomite are recorded from these samples.

In samples where dolomite has been recorded either associated with the Burnham Limestone or the Neva Clay Member, examination of XRD traces shows only minor substitution of Mg by Ca (Table 5.5). Similarly, calcite XRD peaks are not displaced from expected positions and hence the composition of calcite in these sediments is close to the ideal $CaCO_3$.

5.3.2.3 Micromorphology

Thin sections from silty palaeosol sequences at Onkaparinga Trig show sub-angular to sub-rounded silt-sized quartz grains and mica laths within a clay matrix. Where small, hollow tubular structures have been sectioned, a thin dark brown to black layer is observed coating the holes (Fig 5.51). This material appears to be organic and stained by dark iron oxides with the clay matrix elsewhere showing pale yellow to orange colours. Apart from some preferred orientation around biogenic structures, the silty sediment is thoroughly mixed.

Carbonate from beds within the Neva Clay Member is shown to be microcrystalline with occasional silt and fine sand-sized quartz grains scattered randomly throughout. Isolated pockets of carbonate-free clay occur infrequently and are often stained red or yellow by iron oxides (Fig 5.52). Red hematite can also be seen forming small, isolated accumulations within the microcrystalline carbonate. Fractures which cut across the sediments are

discontinuous and these voids are generally partially filled by coarser, secondary carbonate which has precipitated following mobilisation and deposition of several generations of iron oxides (Fig 5.41). Scanning electron micrographs of carbonate from the voids show it to consist of euhedral-shaped crystals up to 4μm in size which are often embedded in a microcrystalline matrix (Fig 5.53).

5.3.3 Summary

Within silty members of upward fining cycles of sedimentation from the Robinson Point Formation several features such as biogenic alteration, distinctive iron mottling and columnar soil-like structure have been identified. Such features suggest the presence of palaeosols within these sequences and indicate an environment of intermittent deposition and limited erosion. The presence of smectite within these sediments may be related to the local conditions which enabled soil formation to proceed. Similar, but less pronounced features are present within other parts of the Robinson Point Formation and suggest more widespread development of soils at this time. Such sedimentary sequences are not part of the Ngaltinga Formation, however accumulations of irregular masses of carbonate showing vertical blocky structure and rare tubular forms are considered to represent former soils. Changes in the proportion of kaolin and illite associated with the carbonate intervals also suggest that these represent the position of sedimentary breaks.

CHAPTER 6
SEDIMENTARY HISTORY OF THE QUATERNARY SEQUENCE

Field observations and laboratory data which have been gathered for Quaternary sediments from the Noarlunga and Willunga Embayments provide the basis for understanding the origins of the sediments, the depositional environments and diagenetic changes which have taken place. Marine units of Tertiary and Early Pleistocene age provide suitable data points from which to describe the overlying non-marine sequence which, due to a lack of fossil evidence, cannot be dated. Diagenetic features which have been identified within the sequence and discussed in Chapter 5 provide evidence of continuing change following deposition and also support conclusions regarding environments of deposition. The following discussion draws together this information together with detailed clay mineralogy to develop a Quaternary history of these sediments. Sedimentary features are discussed in this Chapter while diagenetic changes are considered in Chapter 7.

6.1 Origin of Sedimentary Features

6.1.1 Burnham Limestone

The Burnham Limestone was interpreted by Ludbrook (1983) to have been deposited in the intertidal environment of estuaries and sandy or muddy flats of sheltered bays. It is thought to be of Early Pleistocene age on the basis of the fossil assemblage identified. As this unit provides a datable marker unit at the base of the Quaternary non-marine sequence, the distribution and relationship of this unit with younger sediments has been investigated in this study.

Significant differences in the distribution of the Burnham Limestone are recognised between the Noarlunga and Willunga Embayments. Extensive deposits are found along the coast in the Willunga Embayment from Sellicks Beach northward to Maslin Bay where a gradual

change from limestone to dolomitic mottles within basal sandy sediments of the Robinson Point Formation can be observed. The only possible occurrence of the Burnham Limestone in the Noarlunga Embayment is at Hallett Cove where dolomitic mottles occur at the base of the Quaternary sequence similar to occurrences at Maslin Bay. These observations suggest a gradual waning of the marine influence in a northerly direction.

Identification of the Burnham Limestone at Sellicks Beach (May & Bourman 1984) and the identification of the marine gastropod *Hartungia dennanti chavani* suggests a strong correlation with the Early Pleistocene Point Ellen Formation of southern Fleurieu Peninsula and Kangaroo Island in which *Hartungia* had previously been found. This gastropod is indicative of more exposed coasts (Ludbrook 1983) and hence suggests that not all limestone of the Burnham Limestone in the St Vincent Basin was deposited in estuarine environments. The Sellicks Beach site also indicates that the Burnham Limestone represents a marine incursion within non-marine sandy and clayey sediments of the Robinson Point Formation.

Thin, discontinuous beds and larger blotches of dolomite frequently occur within clayey or sandy sediments immediately overlying the main limestone bed. Dolomite is only a very rare component of the main limestone. In sediments associated with the dolomite, smectite is commonly found in the <2μm fraction and as this clay mineral is uncommon within the Quaternary sequence it is suggested to be of diagenetic origin and related to dolomite formation. The origin of such dolomite is discussed in Section 7.3.2 and is thought to be related to interaction of continental groundwaters with saline waters following regression of the sea. Smectite formation would be favoured in such a Mg-rich environment with high groundwater levels and limited leaching.

The rare occurrence of the Burnham Limestone within the Noarlunga Embayment indicates that non-marine deposition was dominant in this region during the marine incursion into the Willunga Embayment. The Burnham Limestone is also recognised within the Adelaide Plains Sub-basin to the north (Firman 1976; Selby & Lindsay 1982). Mottled dolomite

within basal sediments of the Robinson Point Formation at Hallett Cove which has been tentatively correlated with the Burnham Limestone indicates that at the most, only marginal marine conditions existed within the Noarlunga Embayment.

This data indicates that the Burnham Limestone is an Early Pleistocene unit which represents a marine incursion at the base of the Quaternary sequence but is not present throughout the study area. Basal Quaternary sediments in parts of the Noarlunga Embayment where the Burnham Limestone does not occur may therefore be older than Early Pleistocene as non-marine sedimentation was taking place in these areas at the time of marine deposition in southern areas. Subsequent to primary deposition, groundwater reactions have modified the sequence forming dolomite and smectite.

6.1.2 Robinson Point Formation

Basal non-marine sediments from the Noarlunga and Willunga Embayments have been assigned to the Robinson Point Formation. This formation comprises an interbedded sequence of gravels, sands, silts and clays with sand and sandy clay sediments predominating. Horizontal, planar bedding is exhibited in some sandy units with planar cross-bedding common in gritty sand and gravel units. Most sediments from the formation however, have no sedimentary structures preserved. Gravels frequently fill broad channel structures eroded into underlying units but also occur as tabular bodies which can be traced for several hundred metres. Upward fining sequences from gravels or sands to silts and clays occur commonly, particularly in central parts of the Noarlunga Embayment, and many of these show pedogenic modification of the finer-grained sediments. There is no evidence of organic-rich layers within the sequence and hence it is likely that deposition took place in predominantly oxidising conditions.

6.1.2.1 Depositional Environments

The features present in sediments of the Robinson Point Formation indicate that a fluvial origin is probable for this unit. Such an origin is consistent with examples described in the literature which show interbedding of gravels, sands and clays, channel and sheet structures and cross bedding (Allen 1965; Jackson 1976; Collinson 1978; Friend 1978; 1983; Galloway & Hobday 1983; Bridge 1985). Allen (1965) illustrated four models for common alluvial facies which included piedmont formed of alluvial fans, braided streams, low sinuosity streams and strongly meandering streams. The overall proportion of coarse to finer-grained sediment has been used as a means to distinguish braided from meandering deposits with braided systems considered to contain abundant coarse-grained sediment (Friend & Moody-Stuart 1972). More recently, Friend (1978; 1983) has indicated that the proportion of fine-grained sediment can not, by itself, be used as an indicator of channel pattern. This is due to the common introduction of coarse-grained sediment into an area of fine-grained sedimentation through short term flood events brought about for example by crevasse splays. Hence, such sand or gravel bodies need not represent fixed channel deposits. Grain size however, is a useful indicator of bed-load (gravel, coarse and medium sand) versus suspended load (silt and clay) deposits (Friend 1983).

Both bed and suspended load deposits are recognised in sediments of the Robinson Point Formation. Bed-load deposits comprising gravels and sands fill broad and generally shallow channel structures in which both planar cross-bedding and horizontal bedding is recognised. Upward fining of sediments within the channel deposits is common. Tabular, sheet-like bodies with rare cross bedded gravels are also present in a dominantly sandy or gritty upward fining sequence. Pedogenic modification of finer sediments from these sequences is frequently noted and indicates a period of stasis following vertical accretion. The presence of channel and sheet-like bodies suggest that these deposits accumulated in channel and point bar sequences with some flood events contributing sediment by way of crevasse splays (Allen 1965; Friend 1983; Galloway & Hobday 1983).

Fine-grained suspended load deposits are rarer in the Robinson Point Formation and confined to upper parts of channel and sheet deposits. Erosion of finer grained sediments prior to deposition in subsequent fluvial cycles is evident at numerous localities and may partly explain the general lack of fine sediment. Bedding structures are not observed in silts and clays of the Robinson Point Formation, particularly where pedogenesis has occurred. Suspended load deposits represent deposition in distal areas from channels and also the final sedimentation following flood events (Galloway & Hobday 1983).

Coarsest sediments which occur at Sellicks Beach are adjacent to the Willunga Fault Escarpment and comprise numerous lenses of poorly sorted, often cross-bedded gravels which fill channels. Upward fining to sands and clays is observed with many gravel units having a muddy matrix. Williams (1973) described alluvial sediments of Late Quaternary age forming piedmonts draining the Flinders Ranges in northern South Australia which have similar characteristics to those identified at Sellicks Beach. Such comparison, together with the proximity of the Sellicks Beach sequence to a steep escarpment suggest that the Robinson Point Formation at this locality was deposited as an alluvial fan.

Smith & Putnam (1980) provide criteria for identifying different fluvial systems including anastomosed, meandering and braided regimes. Anastomosed systems which occur in actively aggrading basins have multistorey channel deposits with common splays and avulsions separated by fine-grained sediment. Braided systems occur in areas of high sediment input and high gradient while meandering systems rarely have multistorey channel deposits or crevasse splays but commonly show evidence for extensive lateral channel migration. Evidence from sediments of the Robinson Point Formation suggest that there are features from both anastomosed and meandering systems present with the sediments at Sellicks Beach possibly representing a braided system. Thus depending on the position in the embayment, the nature of the fluvial sedimentation varied with a continuum of styles present. Braided systems occurred on embayment margins where steep escarpments

provided a plentiful supply of sediment while in more central parts, as stream gradients and sediment supply decreased, a combination of anastomosed and meandering systems prevailed.

6.1.2.2 Sediment Sources

A fluvial origin for the Robinson Point Formation implies that higher ground to the east forming the Mt Lofty Ranges was the probable source for the sediments deposited in the Noarlunga and Willunga Embayments. Granule, pebble and cobble-sized clasts from the Robinson Point Formation comprise quartz, siltstone, quartzite, ferricrete, schists and rare limestone fragments. All rock types occur in the Precambrian sequence, or as weathering products in the case of ferricrete, in the Mt Lofty Ranges. This suggests that this area forms the provenance for the Robinson Point Formation.

Ratios of coarse to fine sand for sediments of the Robinson Point Formation are quite variable with a tendency for coarsest sands to be deposited with the coarsest bed load sediments. Fine-grained units generally have little coarse sand and such a relationship suggests that depositional processes have influenced the proportion of coarse and fine sediment deposited at any site. No conclusions can be drawn regarding sediment source from the sand ratio data given that depositional processes may have influenced the grain size distribution.

Heavy mineral assemblages (>2.96 SG) have been determined for all samples from the Onkaparinga Trig site and several samples from Maslin Bay. While the number of different minerals identified is greatest in samples from the coarsest sediments, there are several minerals such as tourmaline, rutile, staurolite and iron oxides which occur throughout the formation. Other minerals occur sporadically in samples from throughout the unit and do not concentrate in upper or lower parts of the Robinson Point Formation. This limited data therefore suggests that there has been no major change in provenance during deposition of

the Robinson Point Formation. Furthermore, comparison with data provided by Aitchison *et al* (1954) for heavy minerals from soils and basement rocks in the Adelaide region indicate that all heavy minerals identified in the Robinson Point Formation could have been derived from the Precambrian sequence and soils developed on such rocks.

Clay minerals identified from the Robinson Point Formation support the thesis that the provenance for the Quaternary sediments was Precambrian and Tertiary sequences from the Mt Lofty Ranges and soils developed on these sediments. Kaolinite, illite and randomly interstratified illite-smectite are the dominant clays identified from the Robinson Point Formation with lesser amounts of smectite recorded in fine-grained sequences near the base of the formation. Data from Norrish & Pickering (1983) for soils from the Adelaide area are summarised in Table 6.1 and show that kaolinite, illite and randomly interstratified clays are common in most soils from the region with rare occurrences of other clays such as smectite, chlorite and hydroxy interlayered vermiculite. Hence the clay mineral assemblage identified from the Robinson Point Formation is most likely to be of detrital origin. The origin of smectite is discussed in sections 5.3 and 7.3 and is thought to be related to pedogenic modification of fine-grained sediments. Further discussion of the clay mineral assemblage can be found in Section 6.2.

The Robinson Point Formation is thought to be of fluvial origin based on the sedimentary features identified in the sequence. Alluvial fans forming piedmonts adjacent to fault escarpments on basin margins grade to anastomosing and meandering alluvial deposits further into the embayments. Both gravel and clay components of the sediments suggest a provenance in the Mt Lofty Ranges to the east and this source remained unchanged throughout the period of deposition.

6.1.3 Ngaltinga Formation

The Ngaltinga Formation comprises a basal massive, grey-green clay with rare fine sandy interbeds assigned to the Neva Clay Member and an upper coarser unit consisting of channel-fill sands and interbedded sand and clay units termed the Snapper Point Sand Member. Small yellow to red mottles are common in clay-rich sediments while sandy units generally show larger, vertical mottles. Sediments from the Neva Clay Member display no sedimentary structures apart from very thin interbeds of fine sand in basal parts at several localities. In contrast, the Snapper Point Sand Member is often recognised by broad channels cut into clays of the Neva Clay Member and filled by planar bedded sands with very rare gravel lines. The channel deposits grade upwards to clays with upper parts of the Snapper Point Sand Member comprising an interbedded sequence of poorly defined sands and clays. Where channel structures are not recognised, the Snapper Point Sand Member is represented by laterally extensive tabular sand bodies which normally have a gradational upper boundary to clays and a poorly defined lower contact with clays of the Neva Clay Member. Rarely, the lower boundary is gradational and coarsens upward, as at Port Willunga.

6.1.3.1 Depositional Environments

Bands of carbonate occur within both the Neva Clay and Snapper Point Sand Members. A 1 to 2 metre thick interval of large, irregular blotches of carbonate occurs within upper parts of the Neva Clay Member in central parts of the Noarlunga and Willunga Embayments and has been interpreted as a palaeosol (Section 5.3). Thin beds and isolated blotches of carbonate are also observed in upper parts of the Snapper Point Sand Member immediately below the carbonate mantle and are also thought to be pedogenic in origin.

The presence of channel structures and upward fining of sediment filling these channels suggest that sediments of the Snapper Point Sand Member are of fluvial origin. The isolated

nature of the channels and lack of vertical stacking of the channel deposits indicates that the channels were frequently abandoned and probably represent meandering rather than anastomosing or braided stream deposits (Allen 1965; Smith & Putnam 1980; Bridge 1984). Poorly defined, upward fining, tabular sand bodies contain very rare gravel layers and may represent sheet flood or crevasse splay deposits. Intermittent deposition of sands and occasional gravel is generally short-lived in these environments and occurs overlying fine-grained flood plain sediments (Allen 1965; Galloway & Hobday 1983). Non-deposition between flood events allows palaeosols to develop and intermittent beds and mottles of carbonate in upper parts of the Snapper Point Sand Member record such periods of stasis. Palaeosols are considered to be a normal phenomenon in fluvial systems with carbonate-rich palaeosols, in particular, often described (Williams 1973; Wright 1982; Atkinson 1986; Retallack 1986). Rare examples where upward coarsening sequences are observed in basal parts of the Snapper Point Sand Member are considered to represent crevasse splay deposits by comparison with Smith (1983). Splay deposits transport coarse bed-load sediment onto surrounding fine-grained sequences and coarsen upward from silt to coarse sand and rarely gravel as the depositional event progrades away from the main channel. A waning of the flood event will often see a gradual upward fining of sediment and this is recognised for many sheet-like sand deposits from the Snapper Point Sand Member.

A depositional environment for the Neva Clay Member is more difficult to interpret due to the lack of sedimentary structures present in these fine-grained deposits. However the close association of the unit with overlying fluvial sediments of the Snapper Point Sand Member suggests that the Neva Clay Member is also of fluvial origin with deposition of suspended load as floodplain or overbank sediments (Allen 1965; Galloway & Hobday 1983). Where the base of the Snapper Point Sand Member is not defined by sand-filled channels, the sand sheets record an upward coarsening sequence from massive fine-grained sediments of the Neva Clay Member. Such sequences are interpreted as crevasse splay deposits following the work of Smith (1983) and indicate that a continuum of depositional environments existed between the Neva Clay and Snapper Point Sand Members.

An alternative hypothesis for deposition of the Neva Clay Member is that it is of lacustrine origin. Picard & High (1972; 1981) discuss various criteria for the recognition of lacustrine deposits and while there are no criteria by themselves which are sufficient for such identification, the presence of a number of related features is diagnostic. Such features include palaeontological evidence, bedding and sedimentological structures such as laminations, ripples or varves, the presence of authigenic minerals, particularly those from evaporitic environments, the identification of limestones, regressive patterns of sedimentation with narrow shoreline facies and regional settings enclosed by fluvial sediments or disconformities. Features such as these are not recognised from the Neva Clay Member. In addition, preliminary micro-palaeontological work on fine sand and silt fractions separated from eight samples collected from the Robinson Point Formation and Neva Clay and Snapper Point Sand Members of the Ngaltinga Formation at the Onkaparinga River Mouth and Onkaparinga Trig sites did not identify a micro-fauna or flora in these sediments (samples RM197 to RM204, Dr N. Alley, *pers. comm*). In regions adjacent to major saline playas in northern South Australia, lacustrine sediments of Tertiary age are well developed and have lacustrine features that are well preserved (Callen 1976; 1977; Callen & Tedford 1976). There seems no reason why similar features should not be preserved in Pleistocene to Recent lake sequences from the St Vincent Basin if such environments prevailed at this time. Thus the lack of lacustrine features and an association with fluvial sediments of the Snapper Point Sand Member suggests that the Neva Clay Member is also of fluvial rather than lacustrine origin.

6.1.3.2 Sediment Sources

A fluvial origin for the Ngaltinga Formation suggests that the provenance for this unit may have been rocks and soils of the Mt Lofty Ranges as is the case for the Robinson Point Formation. Very few gravels are present within the Ngaltinga Formation with siltstone and

quartzite being identified as clasts. Both rock types could be sourced comparatively locally. They also occur within the Robinson Point Formation.

Only a limited suite of heavy minerals is identified within the Neva Clay Member with tourmaline, iron oxides, staurolite and rutile present in most samples together with several other minerals which occur more sporadically. A much larger heavy mineral suite is recorded from the Snapper Point Sand Member, but with tourmaline, iron oxides, staurolite and rutile being common throughout. This data suggests that a similar source was present during deposition of both the Neva Clay and Snapper Point Sand Members. The larger range of minerals present in the Snapper Point Sand Member is often related to higher proportions of coarse material and hence, as was the case in the Robinson Point Formation, depositional processes may effect the range of heavy minerals deposited. However, even in finer-grained units of the Snapper Point Sand Member, a larger range of minerals is recorded compared with the Neva Clay Member suggesting the possibility of an additional source at this time. The data is insufficient to allow a definite conclusion to be drawn on this matter. The fact that almost all heavy minerals identified within samples from the Snapper Point Sand Member are also recorded in at least one sample from the Neva Clay Member suggests however, that an additional source is unlikely. It may be that processes during deposition of the Snapper Point Sand Member were better at concentrating heavy minerals compared with those operating whilst the Neva Clay Member was deposited.

Clay minerals identified within the Ngaltinga Formation include illite, kaolinite, randomly interstratified illite-smectite and hydroxy interlayered smectite. While the proportion of each mineral varies considerably between the Neva Clay and Snapper Point Sand Members, the same clay minerals are identified throughout the Ngaltinga Formation. Kaolinite dominates coarser samples while illite and randomly interstratified clays are present in higher proportions in finer-grained samples. Similar clay minerals are present in the Robinson Point Formation where they are thought to be mostly of detrital origin. A similar origin for clay minerals from the Ngaltinga Formation is probable.

Carbonate, which is identified within parts of both the Neva Clay and Snapper Point Sand Members, is thought to have been derived during pedogenic modification of the sediments. The frequency of occurrence of carbonate intervals increases in upper parts of the Snapper Point Sand Member with a thick but variable mantle of carbonate overlying sediments of Quaternary age as well as older sediments. Phillips & Milnes (1988) and Phillips (1988) argue that the carbonate represents material derived from an external source, unrelated to the provenance of fluvial sediments of the Robinson Point and Ngaltinga Formations. Such an external source has not been identified, however the carbonate was thought to be deposited by aeolian means. Hence the increasing frequency of carbonate palaeosols in upper parts of the Snapper Point Sand Member represents a transition from a fluvial dominated environment to one characterised by aeolian deposition. A change to a more arid climate is the most logical explanation for this marked alteration in depositional regime and climatic variation during the Pleistocene with increasing aridity has been documented from many parts of Australia (Bowler *et al* 1976; Bowler 1982).

Textural parameters of samples from the Snapper Point Sand Member suggest that it is transitional between the Neva Clay Member and Robinson Point Formation. Coarser beds from the Snapper Point Sand Member plot on triangular diagrams in similar positions to most samples from the Robinson Point Formation while finer beds from this member plot toward samples from the Neva Clay Member. Rare clay-rich beds from the Robinson Point Formation also plot close to most samples from the Neva Clay Member suggesting similarities in depositional processes and the probability that the provenance of sediments had not changed. Such similarities between parts of the Ngaltinga and Robinson Point Formations is not surprising given that both formations are considered to be of fluvial origin and that both had a local provenance in the Mt Lofty Ranges.

The distribution of the Ngaltinga Formation in the Noarlunga and Willunga Embayments shows that it is thickest in central parts of the embayments in areas furthest from the Mt Lofty

Ranges. These dominantly fine-grained sediments were deposited on more distal parts of the alluvial fans draining from the ranges. An increased supply of sediment into the embayments following deposition of the Neva Clay Member led to deposition of coarse channel and sheet-sand sediments of the Snapper Point Sand Member. This supply was of limited duration however, as aeolian contributions represented by carbonate palaeosols increased dramatically during later stages of deposition under an increasingly arid climate.

6.2 Origin of Clay Minerals

Clay minerals identified within the Quaternary sequence from the Noarlunga and Willunga Embayments include kaolinite, illite, randomly interstratified illite-smectite, hydroxy interlayered smectite, smectite and halloysite. Due to their rare occurrence and confinement to several intervals within the sequence, both halloysite and smectite are considered to be of diagenetic origin. The remaining clay minerals are most likely to be of detrital origin although variations in the proportions of these minerals through the sequence may reflect minor diagenetic modification of the detrital clay mineral suite. A discussion of these issues is presented below.

6.2.1 Detrital Minerals

Sediments from both the Robinson Point and Ngaltinga Formations are considered to be of fluvial origin (Section 6.1) and hence the dominant source is likely to be Precambrian and Tertiary sediments and soils of the Mt Lofty Ranges. Table 6.1 summarises data for the clay mineralogy of soils from this region provided in Norrish & Pickering (1983) and indicates that kaolinite, illite, randomly interstratified clays and hydroxy interlayered clays occur commonly. Thus these minerals could readily be derived from source regions and form a detrital component within the Quaternary sediments. Smectite is an uncommon component of soils from the Adelaide region although small areas of smectite-rich black clay soils occur in poorly drained parts of the Mt Lofty Ranges. Smectite would therefore be expected as a

minor component within Quaternary sediments. Its concentration within several restricted intervals within the Quaternary sequence suggests that a simple detrital source is unlikely for this clay mineral.

Data for clay minerals present in sediments from the Mt Lofty Ranges are more difficult to obtain. Several samples from an abandoned quarry in the Precambrian Woolshed Flat Shale at Bradbury in the Mt Lofty Ranges show that kaolinite and illite are present in various proportions. Samples from mottled and weathered sandy clay of probable Tertiary age from a railway cutting at Blackwood also contain both kaolinite and illite. Bourman (1989) reports various proportions of kaolinite, illite, randomly interstratified clays, smectite, chlorite and vermiculite from samples associated with ferricretes in the Mt Lofty Ranges. Analyses of samples from a 104 m deep borehole at Willunga Hill (Willunga 1:50 000; 804916) presented by Bourman (1989) showed that minor randomly interstratified clays and smectite were present throughout the sequence of clays, shales and slates. Kaolinite was present in high amounts in the upper 30 m and then decreased while illite showed a reverse trend. Rare vermiculite was identified in upper parts of the sequence while moderate amounts of chlorite were present in the lower half of the hole. These data confirm that both illite and kaolinite are readily available in source regions for the Quaternary sediments, with weathered Precambrian rocks providing a limited source of other clay minerals.

6.2.2 Variability of Clay Mineral Proportions Within the Sequence

Given that many of the clay minerals identified within the Quaternary sequence are likely to be dominantly of detrital origin, the variation in proportions of these minerals within the sequence requires explanation. Similar clay mineral proportions would be expected throughout the sequence if there were no other factors to consider besides provenance. The fact that variation occurs within and between stratigraphic units suggests that processes of erosion and deposition may be preferentially concentrating some clays in certain parts of the

sequence. Alternatively, diagenetic processes may modify the detrital components with such diagenesis taking place in particular intervals.

Kaolinite is the dominant clay mineral in coarse-grained units within both the Robinson Point and Ngaltinga Formations with illite and randomly interstratified illite-smectite being dominant in fine-grained units. To investigate whether such a distribution may be a primary depositional feature, detailed size separations of the <20μm fraction were undertaken for eight samples and clay mineralogy of each of the four size fractions determined. XRD data from these samples indicate that illite and expansible clays such as smectite and randomly interstratified illite-smectite are concentrated in the finest fractions (<0.2μm). Previous studies from soils have found a similar size distribution. Micas are thought to occur preferentially in the 0.2 to 2μm fraction due to physical breakdown while mica present in finer fractions has often undergone partial interstratification with exchangeable cations (Fanning *et al* 1989). Similarly, studies by Fanning & Jackson (1965) and Borchardt *et al* (1966) show that smectite is most common in the <0.08μm fraction while mica occurs most frequently in the 0.08 to 0.2μm fraction. In contrast to illite and expandable clays, kaolinite in Quaternary sequences from the Noarlunga and Willunga Embayments appears to be concentrated in the coarse clay fraction (0.2 to 2μm). Dixon (1989) indicates that while kaolinite in soils can occur in a wide range of sizes from tenths of microns to several microns, the most common size range is from 0.2 to 2μm.

In several samples (eg RM304, RM327), two phases of micaceous material are identified. The first occurs in coarsest fractions (2 to 20μm), gives sharp peaks and is thought to represent muscovite, as flakes of muscovite can be seen in hand specimens of these samples. In finer fractions (<2μm) the 10Å material gives rise to broader peaks which are similar to illite recognised from other samples. These data therefore suggest that two types of detrital mica co-exist within the Quaternary sequence. The first represents coarse mica derived through erosion of Precambrian meta-sediments and young soils developed on these rocks. The second represents fine-grained illite derived through erosion of soils where illite formed

through transformation reactions from muscovite and chlorite. Data provided by Fanning *et al* (1989) suggests a similar size relationship for micas in many soils.

Kaolinite to illite ratios for size fractions from the eight samples analysed support the conclusion that illite is more common than kaolinite in the <0.2μm fraction compared with the 0.2 to 2μm fraction. The absolute value of this ratio is highest for samples which have the least amount of material <2μm in size as measured by sedimentation techniques (eg RM259, RM326). Such samples would also have the least amount of material in the <0.2μm fraction and hence minerals such as illite and expandable clays which occur preferentially in the finest fractions would not be present in these samples in large amounts. Thus the higher kaolinite to illite ratios for these samples are the result of the particle size distribution of the sediment. Such a distribution is most likely to reflect primary sedimentation.

An alternative explanation for the variable kaolinite to illite ratio through the Quaternary sequence is that diagenetic reactions have transformed illite to kaolinite in coarser-grained units or conversely kaolinite to illite in fine-grained intervals. Diagenesis may also have contributed to randomly interstratified clays being more common in finer-grained units. Scanning electron microscopy was undertaken on the same samples as those used for detailed size separations to look for evidence of authigenic minerals which would suggest that diagenetic processes were important in determining clay mineral proportions. For the most part, clays occur as very fine particles which have aggregated into dense masses where morphology of individual clays is impossible to determine. Possible authigenic minerals with distinct morphology were detected in three samples. Small rods of halloysite were noted in RM323, fine hair-like material protruding from the edges of muscovite grains in RM304 and tiny spherules of silica on the surface of quartz grains in RM265. These observations indicate that authigenic minerals have formed within the sequences, however no evidence of these reactions contributing to a significant change in the proportion of kaolin or illite is recognised. Fine-grained authigenic clays could be present in the matrix. As

authigenic illite is reported to form in lacustrine environments (Porrenga 1968; Norrish & Pickering 1983), the possibility remains that some illite could be formed in fine-grained units of the Neva Clay Member given that these sediments are interpreted as poorly drained floodplain deposits. The data presented here do not enable the proportion, if any, of this type of illite to be determined.

6.2.3 Interstratified Clay Minerals

Many clay mineral changes take place not through re-crystallisation reactions but through transformations which need not alter the morphology of the crystal (Millot 1970; Eberl 1984). Such transformations may only require a change in interlayer material and little re-organisation of the crystal structure. The conversion of illite to halloysite discussed in Section 7.1 represents a transformation which leads to a morphological difference, however the conversion of mica to hydroxy interlayered material requires only that the interlayer material changes.

Interstratified clay minerals identified within the Quaternary sequence include randomly interstratified illite-smectite and hydroxy interlayered smectite. Both minerals occur in higher proportions in fine-grained units with randomly interstratified illite-smectite having a variable expandable component and hydroxy interlayered clay minerals being almost totally confined to sediments of the Ngaltinga Formation. A study of the distribution and possible origins of these minerals may therefore contribute to an understanding of possible diagenetic reactions within the sequence.

Hydroxy interlayered clay minerals are generally considered to be a product of intense weathering in an acidic environment such as that found in many highly leached soils (Rich 1968; Barnhisel & Bertsch 1989). They form following replacement of interlayers with Al-hydroxy polycations most commonly through removal of K from dioctahedral mica. Alternatively, the Al polycations can fit into interlayer regions of vermiculite and smectite

(Schulze 1989). Intense weathering is required to form hydroxy interlayered clay minerals so that Al is released during this weathering process. It is difficult to envisage such intense weathering occurring within the Quaternary sequence and hence it is more probable that the hydroxy interlayered clay minerals recorded in these sediments are derived from soils of the Mt Lofty Ranges. Norrish & Pickering (1983) record hydroxy interlayered clay minerals in soils from this region and many of these soils are considered to be products of prolonged weathering (Northcote 1976; Twidale 1976).

The concentration of hydroxy interlayered clay minerals in sediments of the Ngaltinga Formation is more difficult to explain. If it is a detrital component then it would be expected in both the Robinson Point and Ngaltinga Formations. It is difficult to measure the proportion of the clay fraction formed by hydroxy interlayered material, but even in samples from the Ngaltinga Formation, this clay mineral is not present in large amounts. Hydroxy interlayered clay minerals are detected by incomplete collapse of clays to 10Å on heating to 300 and 550°C and the degree of non-collapse approximates the proportion of this material in the sample (Barnhisel & Bertsch 1989). Where only a small proportion of the clay fraction is accounted for by interstratified clay mineral, as in many coarser-grained samples from the Robinson Point Formation, a small amount of hydroxy interlayered material would be difficult to detect. The apparent concentration of hydroxy interlayered clay minerals in the Ngaltinga Formation is therefore most likely to be due to the much greater proportion of interstratified material in this unit.

Randomly interstratified clay minerals are a common clay mineral identified in soils and frequently form through loss of interlayer K from micas or illites or through loss of interlayer hydroxides from chlorite (Norrish & Pickering 1983; Sawhney 1989). In both cases interlayer material is replaced by hydrated exchangeable cations. Chlorite is a common component of Precambrian sediments from the Adelaide region (Aitchison *et al* 1954) but is not often identified within soils of this region due to its instability in the weathering environment (Norrish & Pickering 1983). It is most likely that chlorite alters to vermiculite

and randomly interstratified clay minerals in the soil environment (Barnhisel & Bertsch 1989). Randomly interstratified clay minerals are mostly formed in weathering environments and soils, with regularly interlayered clay minerals generally forming in sediments during diagenesis (Wilson & Nadeau 1985; Sawhney 1989). No evidence of regularly interstratified clay minerals exists within the Quaternary sequence and hence all interstratified clay minerals are most likely derived from a weathering environment. Norrish & Pickering (1983) report randomly interstratified clay minerals in most soils from the Adelaide area while Bourman (1989) reports them from weathered sediments and ferricrete profiles in the Mt Lofty Ranges. These soils and sediments provide the most likely source of randomly interstratified illite-smectite in the Quaternary sediments.

Comparison with the work of Reynolds & Hower (1970) shows that the proportion of expandable smectitic layers within the randomly interstratified illite-smectite from the Quaternary sequence varies from 10 to 50%. The majority of samples have smectitic proportions in the range 20 to 30%, however increases to 40 and 50% occur within clayey interbeds of the Robinson Point Formation and also the Snapper Point Sand Member. Basal parts of the Ngaltinga Formation also sometimes show increased smectite layers within the interstratified clay. The increase in expandable layers described for some intervals within the Quaternary sequence suggests modification of the randomly interstratified illite-smectite following deposition. Smectite forms where leaching is limited due to low precipitation, a restrictive layer in the profile or a high water table and hence cations are retained within the system (Allen & Hajek 1989; Borchardt 1989). Thus, where smectite interlayers increase within the Quaternary sequence, similar conditions would have prevailed. The association with clay-rich intervals from the Robinson Point Formation and Snapper Point Sand Member indicates that in such intervals, water movement through the sediments may have been restricted enabling hydrated cations to enter layer lattices, thereby producing a more smectitic interstratified clay. It is interesting to note that one of only two occurrences of smectite in the Quaternary sequence occurs in clay and silt-rich units in which high water tables are postulated and pedogenesis took place. Randomly interstratified illite-smectite is not present

in this interval and it is postulated that smectite formed through transformation of detrital illite-smectite.

A second transformation probably taking place within the Quaternary sediments involves illite. Measurement of the width at half height of the (001) peaks indicates that illite from the Ngaltinga Formation has much broader peaks than illite from most of the Robinson Point Formation. Peak characteristics are determined by size of the diffracting crystals and the degree of ordering within these crystals with smaller and less ordered crystals giving rise to broader diffraction peaks (Fanning *et al* 1989). Size fractionation studies have indicated that kaolinite tends to occur preferentially in the silt and coarsest clay fractions and hence exists as larger crystals when compared with other clay minerals. Measurement of the kaolinite (001) peak shows that kaolinite generally has sharper peaks than illite and this is a reflection of the coarser size of kaolinite compared with illite. Therefore the broader diffraction peaks identified for illite from the Ngaltinga Formation may be partly explained by finer-sized clay minerals being present. In addition, such diffraction effects could be due to less well ordered crystals. Loss of interlayer K from illite crystals would result in broadening of the diffraction peaks as the K was replaced by hydrated cations. In the same way that smectite contents of randomly interstratified illite-smectite were increased in fine-grained units where through flow of water has been restricted, so too could illite gradually become interstratified within the fine-grained Ngaltinga Formation.

6.2.4 Smectite

Although a greater proportion of expandable smectitic layers occur in interstratified clays from various intervals within both the Robinson Point and Ngaltinga Formations, relatively pure smectite is only identified from two intervals. The first occurrence is associated with fine-grained sediments from the Robinson Point Formation which have been interpreted as palaeosols while the second is related to dolomitic mottles immediately above or laterally

equivalent to the Burnham Limestone. Both occurrences are discussed in Sections 5.3 and 7.3.

The formation or preservation of smectite is favoured in environments where leaching is at a minimum and there is a high proportion of available Si and basic cations (Jackson 1965; 1968). A transformation from muscovite to smectite is commonly observed due to similarities in the structures of both minerals and this takes place through loss of interlayer K (Crawford *et al* 1983). A loss of Al from octahedral sheets and a gain of Si in tetrahedral sheets results in a lowering of layer charge (Komarneni *et al* 1985). Such a transformation requires $Si(OH)_4$ concentrations to be high (Huang 1966) and Al concentrations to be low as would occur in soils of pH >6. Where the pH is <6 smectite weathers to vermiculite which subsequently tends toward kaolinite (Ismail 1970). Thus the evidence suggests that restricted drainage is an extremely important factor leading to the formation of smectite (Borchardt 1989).

Where smectite is a major component of the clay mineralogy of the Quaternary sequence, illite and randomly interstratified illite-smectite are either not present or identified in greatly reduced amounts compared with overlying or underlying sediments. This suggests that smectite is forming at the expense of these clay minerals following the transformation reaction suggested by Crawford *et al* (1983). Restricted drainage in alluvial sediments exposed on floodplains and undergoing pedogenic alteration provided ideal conditions for the transformation of illite and randomly interstratified clays to smectite.

Similar transformations are reported in soils of the Swan Coastal Plain in Western Australia (McArthur & Bettenay 1974). Parent materials for soils of the Wellesley System were deposited in low lying areas subject to periodic ponding of surface water and poor drainage. The clay mineralogy of these soils is dominantly smectite with lesser kaolinite whereas other soils on the Swan Coastal Plain which are better drained have a clay mineralogy comprising kaolinite and lesser illite. Meyer & Pena Dos Reis (1985) also report smectite forming in

swampy floodplain sediments from western Portugal at the expense of both kaolinite and illite. A number of upward fining fluvial depositional units have undergone pedogenic alteration in upper fine-grained sections and the formation of smectite is associated with silicification and later precipitation of alunite. Transformations identified within the Robinson Point Formation are similar to this example from Portugal.

Smectite occurring with dolomitic mottles associated with the Burnham Limestone must also have formed in a poorly drained environment. The formation of dolomite suggests an alkaline environment in which basic cations were available and these conditions would enable the transformation of other clay minerals to smectite. Following regression of seas in which the Burnham Limestone was deposited an interaction between continental Mg-rich groundwaters and saline marine-derived waters took place. Such an environment would favour the formation of both dolomite and smectite.

6.2.5 Summary

Clay minerals identified from Quaternary sediments in the Noarlunga and Willunga Embayments are mostly detrital in origin and derived from weathered sediments and soils of the Mt Lofty Ranges. Kaolinite, illite, randomly interstratified illite-smectite and minor hydroxy interlayered smectite are derived in this manner. Variations in the distribution of these clay minerals through the sequence are related to depositional factors brought about by the particle size of each clay mineral. Kaolinite occurs mostly as particles with a size range from 0.2 to 2μm while illite and randomly interstratified clays are present in the finest fraction <0.2μm. Thus kaolinite was deposited most readily with the coarsest sediments leading to highest ratios of kaolinite to illite in these intervals and lowest ratios in units containing abundant material <2μm. In several coarse-grained units there is an increased amount of clay giving a diffraction peak at 10Å in the >2μm fraction. This corresponds to muscovite derived from weathered Precambrian sediments and gives rise to much sharper diffraction peaks than fine-grained illite derived from soils in the same areas.

Diagenetic reactions have transformed detrital clays in some intervals leading to the formation of smectite and halloysite and these are discussed in Chapter 7. While many of the clays discussed in this study are of detrital origin and hence assist in determining a provenance for the sediments, the identification of diagenetic clays allows a better understanding of depositional environments and the subsequent history of the sediments.

CHAPTER 7
DIAGENETIC HISTORY OF THE QUATERNARY SEQUENCE

It is argued in Chapter 6 that sediments of Quaternary age from the Noarlunga and Willunga Embayments were deposited in a fluvial environment on alluvial fans built out from the Mt Lofty Ranges to the east. A number of features such as the development of alunite and halloysite within parts of the sequence, mottling of the sediments by iron oxides and identification of palaeosols at numerous localities do not appear to be related to initial sedimentation. The identification of these diagenetic features provides information on the subsequent modification of the alluvial sediments and the environments under which these changes may have taken place. Such interpretations are discussed in this chapter.

7.1 Formation of Alunite and Halloysite

7.1.1 Previous Studies

Jack (1914; 1918) in his investigations of alunite in South Australia preferred to explain many occurrences as the result of the introduction of solutions of deep-seated origin. This was an alternative to the then generally held view that alunite was formed by volcanic activity in association with feldspathic rocks. In discussing a deposit near Stansbury, Jack (1918) thought that the introduction of deep-seated solutions probably accompanied late Tertiary faulting in the St Vincent and Spencer Gulfs areas; pathways for alunite-bearing solutions being provided by fault planes. Many of the deposits in South Australia however, remained unexplained.

King (1953), in discussing the Pidinga deposit, stated that alunite was almost universally accepted as being of secondary origin and related to the alteration of potassium feldspar and kaolinite in host materials. Sulphur was introduced through volcanic agencies or by the oxidation of pyrite or other sulphides. At Pidinga, while potassium was available in the host

clay-rich sediments, the sulphur was interpreted as coming from oxidation of sulphide minerals present in lignites which were interbedded with the clays in nearby areas.

Many occurrences of alunite have been described in the international literature and these have been summarised by Hemley *et al* (1969) and also Hall (1978). Most deposits show a clear relationship to intrusive bodies, volcanic activity or hydrothermal mineral deposits and are thus interpreted as resulting from hydrothermal alteration. However, Goldbery (1978; 1980), while studying Na-alunites from Jurassic flint clays in Israel could find no evidence to support an hydrothermal mode of formation. Instead, he proposed that the alunite was early-diagenetic and related to the environmental conditions prevailing at the time of deposition of the host sediments either in a swampy environment (Goldbery 1978) or in organic-rich lagoonal sediments and algal mat facies (Goldbery 1980). Where non-hydrothermal alunite has previously been described, its genesis has generally been attributed to the reaction of sulphuric acid, generated locally from oxidation of pyrite, with clay minerals (King 1953; Keller *et al* 1967; Ross *et al* 1968).

Any model proposed for the formation of alunite in Quaternary sediments from the Noarlunga and Willunga Embayments must account for its co-existence with halloysite in these areas. Some previous studies have reported alunite occurring together with halloysite (Ross & Kerr 1934; Keller 1964; Zalba 1982; Patterson & Murray 1984) while other work has shown alunite or halloysite occurring separately or in association with other minerals (Dana 1951; Goldbery 1978; 1980; Slansky 1983). Ross & Kerr (1934) suggested that halloysite formed as a result of weathering or supergene processes and postulated the action of sulphate-bearing solutions to transform kaolinite to halloysite. Some subsequent work concurs with this hypothesis (Keller 1964; Zalba 1982; Patterson & Murray 1984). Zalba (1982) termed this a desilicification process in which aluminium-rich phases such as alunite, halloysite and diaspore are formed. Both Keller (1964) and Zalba (1982) agree that the presence of sulphate ions and acidity are important in influencing the alteration of kaolinite minerals to halloysite. Keller *et al* (1971) when discussing the formation of halloysite from

rhyolitic volcanic rocks by the action of hot spring waters also noted the need for sulphate as the solvent ion in addition to high amounts of Si and Al in solution and a low pH of 3.5.

In the soils literature, halloysite is considered to be a product of acid weathering (Dixon 1989) which occurs primarily in youthful soils developed from volcanic deposits (Dixon & McKee 1974; Dudas & Harward 1975; Dixon 1989). In some cases halloysite is thought to be an intermediate product of weathering feldspars or other minerals such as amphiboles and chlorites to kaolinite (Deer *et al* 1962; Anand & Gilkes 1984; Anand *et al* 1985). A dehydration process in which tubular kaolinite forms from tubular halloysite and with prolonged weathering eventually transforms to gibbsite is proposed in lateritic weathering profiles over granites and dolerites in Western Australia (Churchman & Gilkes 1989).

7.1.2 Consideration of a Sedimentary or Diagenetic Origin

Alunite and halloysite have been identified occurring mostly within Quaternary sediments interpreted to be of fluvial origin as well as adjacent Tertiary sediments. The sediments exhibit some planar horizontal bedding with rare cross beds in gravel lenses and frequent upward-fining sequences. Unbedded silty and clay-rich intervals are typically light grey in colour with development of a goethitic, yellow-orange, rectangular mottling pattern. They also show evidence of pedogenic modification in the form of small burrows and a coarse prismatic structure. Smectite is often the dominant clay mineral in these fine-grained sediments while alunite and halloysite are best developed in sandy and clayey sediments immediately below the pedogenically modified sediments.

While there are many thin white seams of alunite which are conformable with bedding, at numerous localities the alunite and halloysite occur as large pods and blebs of material which cut across pre-existing sedimentary structure (for example at Port Moorowie, Chinaman Gully and in the vicinity of Seaford). Sharp lower and diffuse upper contacts with surrounding sediments are noted from many pods of alunite which are also free of visible quartz in contrast to the generally sandy host sediment. Goldbery (1978) described similar

contacts for early diagenetic alunite from Israel and suggested that colloidal segregation during dehydration of the sediments may have contributed to such structures. Alunite, and in particular halloysite, also occur disseminated through predominantly sandy sediments for several metres above zones where alunite has been concentrated into pods and thin beds. Such observations suggest that it is unlikely that the alunite or halloysite are of primary sedimentary origin.

It is also considered that the alunite and halloysite are of non-hydrothermal origin. While many occurrences of alunite reported in the literature are thought to be of hydrothermal origin (see Hemley *et al* 1969; Hall 1978), in all such cases they show clear relationships to intrusive bodies, volcanic activity or other hydrothermal deposits. No such relationships can be inferred for the deposits described here. Similarly, weathering of carbonaceous, sulphide-bearing sediments (Keller *et al* 1967; Meyer & Pena Dos Reis 1985) is unlikely to have contributed to alunite formation in the Quaternary sediments described here which are considered to be free of sulphide minerals.

The description from Port Noarlunga of thicker beds of alunite which exhibit loading on the underlying fine-grained sediments, suggests that the formation of alunite took place prior to, or at the time of consolidation and dewatering of the sediments. While none of the sediments of Quaternary age in which alunites occur are strongly lithified, it would seem unlikely that such loading structures could have been produced very recently. Two other possibilities exist. Firstly, the alunite could have replaced previously loaded components of the sediments and secondly, the structures could have formed during precipitation of alunite from a gel-like phase following compaction of the main body of sediment. No replacement structures have been recognised in thin section studies and hence the first scenario is the least likely explanation of these features. Goldbery (1978) postulated the colloidal segregation of alunite from kaolinite to form pods of alunite and noted that Nemecz & Varju (1967) had suggested a similar origin for nodular aggregates within flint clays. In addition to pods and seams of alunite similar to those described by Goldbery (1978), zones of nodular halloysite

are present within the Quaternary sequences, particularly in the vicinity of Onkaparinga Trig, and segregation during drying is most likely to have formed these features.

Thin section observations show an intimate relationship of alunite with halloysite and indicate a complex history for the formation of the two minerals. In addition, later phases of both alunite and halloysite have precipitated in cracks which cross-cut earlier phases (Figs 5.12; 5.16). Some crystallisation of the two minerals evidently took place prior to the development of cracks which are probably related to shrinkage and dehydration of the sediments, possibly as a result of exposure and desiccation. Undulose extinction patterns exhibited by mixtures of alunite and halloysite (Fig 5.15) are further evidence of stress arising from this dehydration.

A study of stable isotope ratios of surficial alunites from Australia has been made by Bird *et al* (1989) and several samples from Quaternary sediments in the Noarlunga Embayment formed part of this research (RM142, RM178, RM208). The high δD values recorded in this work indicate that the alunite formed in equilibrium with evaporated meteoric waters and hence support the hypothesis that alunite formation took place on dehydration of the sediments during early diagenesis.

7.1.3 Source of Sulphate

Formation of alunite requires a source of sulphur. Most workers have determined that non-hydrothermal alunite is the result of oxidation of pyritic sediments (see Section 7.1.1). In contrast, Goldbery (1978; 1980) suggested that oxidation of H_2S produced in anaerobic sediments contributed to alunite formation while King (1953) postulated that regional groundwaters contributed to the source of sulphate. The fluvial sediments which host the alunite in the Noarlunga and Willunga Embayments show no evidence of being organic-rich, although such evidence could easily be destroyed on oxidation of the sediments. No sulphide minerals have been identified in any of the Quaternary sediments from the study area, nor have pseudomorphs after sulphides been recognised in thin section. It is also

difficult to envisage the reducing conditions necessary for formation of H_2S in these sediments although a reducing environment could occur as a result of high water tables on river floodplains. An alternative source for the sulphate in these sediments may have been regional groundwaters following the ideas presented by King (1953), who proposed an early diagenetic formation for alunite which occurred in Eocene lacustrine clays at Pidinga. The clays provided sources of K^+ and Al^{3+} for the alunite while sulphate was thought to be derived from both the regional groundwaters and oxidation of abundant pyrite and free sulphur contained in lignite beds which were interbedded with the lacustrine clays at this location (King 1953). A similar sulphate source was postulated for gypsum which also occurs in the Pidinga area.

In the St Vincent Basin, carbonaceous and pyritic sands and clays of the Middle to Late Eocene South Maslin Sand are described occurring subsurface in the Adelaide Plains Sub-Basin and Willunga Embayments (Lindsay 1969). Carbonaceous clays with lignites are reported in the Clinton Formation of similar age from the Noarlunga Embayment (Cornelius 1927) and Adelaide Plains area (Lindsay 1969). A small outcrop of the Clinton Formation is reported by Daily *et al* (1976) immediately south of the Noarlunga township and indicates the possibility of groundwaters in this area being supplied with sulphate. Ludbrook (1980) indicates that the lignite deposit in the Noarlunga area has proven reserves of 1.5 million tonnes.

Bird *et al* (1989) have studied the stable-isotope composition of surficial alunite in Australia including three samples from the present study. The $\delta^{34}S$ value for these samples is high (+15.6‰ for RM142, +17.7‰ for RM208, +20.6‰ for RM178) and not strongly negative as would be expected if derived from oxidation of biogenic sulphur which would have formed part of sulphur derived from the lignite deposits. In fact, sample RM178 has a composition identical to that of modern seawater, suggesting that the source of sulphate was most probably seawater sulphate blown in from the sea and subsequently incorporated into the groundwater system. It would be interesting to determine the $\delta^{34}S$ composition of alunite occurring in the South Maslin Sand approximately 2 km upstream from the mouth of

the Onkaparinga River and within 2 km of the outcropping Clinton Formation to see whether there is an influence of biogenic sulphur at this site.

7.1.4 Origin of Alunite

It appears quite likely that groundwaters in the Noarlunga and Willunga Embayments at the time of formation of alunite were rich in sulphate. Bird *et al* (1989) suggest from $\delta^{34}S$ analyses that such sulphate was derived by aeolian means from seawater. Locally, where alunite has developed in sediments of the South Maslin Sands, nearby Tertiary carbonaceous sediments may have been an important additional source of sulphate.

The Quaternary Robinson Point Formation which hosts the most conspicuous development of alunite in the region is of fluvial origin. A series of interbedded, upward-fining sequences comprising gravels, sands, silts and clays reflect deposition in both channels and adjacent floodplains. Pedogenic alteration of silty sediments indicated by bioturbation, mottling patterns and mineralogical alteration took place in this environment. The presence of smectite as a major clay mineral component in fluvial sediments near where alunite is common suggests that these sedimentary sequences were generally poorly drained (see Chapter 6). Under such conditions, a reducing environment may have developed within the floodplain sediments and generation of H_2S would have contributed an additional source of sulphur to that already present in the groundwater. Experimental work by Brophy *et al* (1962) on the alunite-jarosite system indicates that under the low temperature and pressure conditions prevailing during the formation of alunite, Fe^{3+} is more likely to be incorporated in the crystal structure than Al^{3+}. The formation of alunite and not jarosite suggests either that iron was not present in the sediments or that it remained in a reduced state (Fe^{2+}) while alunite developed. This supports the contention that reducing conditions were present in floodplain sediments.

Clay minerals and possibly feldspars are the most likely sources of K^+ and Al^{3+} for the formation of alunite with acid weathering of the sediments allowing decomposition of these

components. Goldbery (1978) provides a reaction pathway for the transformation of illite to alunite which is given below.

$$KAl_3(OH)_2Si_3O_{10} + 4H^+ + 2SO_4^{2-} \longrightarrow 3SiO_2 + KAl_3(SO_4)_2(OH)_6$$

illite alunite

Oxidation of sediments containing sulphate-rich groundwater and possibly H_2S generated from reducing conditions would enable acid weathering to take place. Generation of sulphuric acid within soils or sediments of drained swamps similar to those envisaged for parts of the Robinson Point Formation could result in pH values as low as 2.5 (Bear 1964, p87). The presence of broad pink-red mottles within the host sediments, a thin ferruginous crust above this interval at Onkaparinga Trig and a zone of manganese oxide accumulation at Maslin Bay indicate that previously reduced components precipitated following oxidation of the sediments.

Oxidation must have been initiated by a lowering of the water table in the floodplain sediments and this could have occurred for a variety of reasons. Lowering of the local baselevel would reduce the water table and may be due to a marine regression or uplift of the sediments following movement along faults in the region. A more arid climate leading to lower stream discharge could also result in lower water tables in floodplain sediments. There is no evidence to suggest that any one of these theories is more probable than another. Tectonic instability in the region is thought to have continued into the Quaternary (Daily *et al* 1976), while this period is also characterised by climatic fluctuations (Bowler 1982) and sea level variations. The association of alunite formation with dehydration of the host sediments, possibly related to lowering of water tables is suggested by thin section studies. These show secondary alunite and halloysite filling cracks within the sediments, birefringence patterns suggestive of stress at the time of mineral formation and possible colloidal segregation of mineral phases.

7.1.5 Origin of Halloysite

Acid weathering of clay minerals and feldspar would make available Si and Al in addition to K and Al to form alunite. Halloysite is essentially an hydrated kaolinite and it would be expected that the Si and Al would be more likely to form kaolinite than halloysite given that alunite formation took place under conditions of oxidation and dehydration of the sediments. Bailey (1989) discusses the structure of halloysite and concludes that the water layer is present to minimise repulsion between layer surfaces and to coordinate exchangeable cations which are present to compensate for small charge imbalances which occur in the tetrahedral layer due to substitution of Si by Al. The presence of water molecules ensures that tetrahedral layer rotation which accommodates lateral misfit between the octahedral and tetrahedral layers in most layer silicates does not occur in halloysite. This results in the structure rolling up. In the kaolinite structure, there is no water layer and hence rotation of the tetrahedral layer is not restrained. A sheet-like, platy structure is therefore most common for kaolinite. SEM studies show that halloysite from the Quaternary sequences studied has a tubular morphology and hence the model discussed by Bailey (1989) is applicable to this work.

Detailed clay mineralogical studies show that where halloysite is present at the Onkaparinga Trig site, randomly interstratified illite-smectite is absent and illite present in reduced amounts compared with surrounding sediments. The proportion of kaolinite remains relatively constant throughout the interval. At Maslin Bay, randomly interstratified illite-smectite is again absent where halloysite occurs, however a decrease in the proportion of illite is not obvious. These observations suggest that randomly interstratified illite-smectite and to a lesser extent illite, have been transformed to halloysite through acid weathering. Kaolinite is not likely to have been involved in these reactions, possibly due to it being present as larger particles (see Section 4.3) and also to its greater stability in the acidic weathering conditions envisaged.

It is most probable that 2:1 clay minerals have been transformed to halloysite rather than 1:1 clay minerals and this observation is critical to understanding why halloysite may form in preference to kaolinite during diagenetic alunite formation. As suggested by Bailey (1989), halloysite forms due to the need to balance layer charges. Negative layer charges in 2:1 layer lattice silicates arise due to various substitutions in octahedral and tetrahedral layers, with replacement of some Si by Al in tetrahedra being quite common (Bailey 1980). If 2:1 clays have been transformed during acid weathering conditions as postulated above, it is possible that the resultant 1:1 clay mineral will inherit some of the substituted Al tetrahedra. Remnant layer charges brought about in this style of transformation would create the structural relationships which Bailey (1989) considers important in halloysite. Thus halloysite and not kaolinite forms.

The acid weathering of 2:1 clay minerals to form alunite also produces an excess of SiO_2 as indicated by the reaction proposed by Goldbery (1978). While much of this is subsequently utilised during formation of halloysite, electron microprobe analyses indicate that a number of samples have excess SiO_2. This enrichment in SiO_2, which could not be accounted for by any of the identified mineral phases, may be amorphous silica produced by the reaction described above. At Port Moorowie on Yorke Peninsula, there are a number of hard, cemented zones in the Permian sediments which immediately underlie the alunite and halloysite-rich zone. XRD shows that these zones include significant opal which may have originated as amorphous silica in the overlying sediments (Milnes, *pers. comm.*).

7.1.6 Summary

The formation of alunite and halloysite in fluvial sediments of the Robinson Point Formation is the result of acid weathering and transformation of randomly interstratified illite-smectite, illite and possibly smectitic clays. Sulphate derived through aeolian processes from the sea contributed to sulphate-rich groundwater. Poorly drained floodplain sediments which, in places, favoured formation of smectite were oxidised during the early diagenetic history of

the sediments when sea level, climatic or tectonic changes took place allowing a lowering of the water table. Alunite subsequently formed in response to dehydration of the sediments.

A study of the mineralogical changes represented by the occurrence of alunite and halloysite in the Quaternary sediments shows them to be related to the early diagenetic history of the sediments. As such, they provide a better understanding of palaeoenvironments soon after deposition and the importance of groundwater chemistry on the stability of detrital components within a sedimentary system.

7.2 Ferruginous mottles

Iron, in the form of oxides, has accumulated in a wide variety of lithologies and stratigraphic units within sediments of Quaternary age deposited in the Willunga and Noarlunga Embayments. However the most concentrated forms of iron appear in coarser-grained sediments where the iron has infilled pores and voids within the sediments. Resulting mottles are often indurated, composed of both hematite and goethite and have a variable Fe_2O_3 composition. In contrast, mottles from fine-grained sediments are much smaller and develop along fissures within the sediments or on ped surfaces. The proportion of hematite and goethite and total iron content are highly variable.

7.2.1 Comparisons with Previous Studies of Iron Oxides

Most data regarding the occurrence and form of iron oxides in weathering environments comes from the soil science literature. Schwertmann (1985) states that hematite and goethite are the most common iron oxides and oxyhydroxides in weathering environments, particularly soils, and that they have similar thermodynamic stabilities. It is not surprising then that both minerals occur within mottles from the Quaternary sequences south of Adelaide. The relative abundances of hematite and goethite in pedogenic environments are strongly influenced by the initial valence of the iron source and the concentration of iron in solution. In addition, factors such as temperature, water activity, pH, Eh, presence of

organic matter, the activity of Al in solution and rate of release of iron during weathering have some effect (Schwertmann & Taylor 1989). Goethite forms from solutions containing Fe^{3+}, $Fe(OH)_4^+$ and $Fe(OH)_2^-$ and is favoured by low temperatures, high water activity and high organic matter content. Hematite forms through dehydration and structural rearrangement of ferrihydrite particles which precipitate by rapid oxidation of Fe^{2+} solutions in the presence of high concentrations of organic matter and/or silicates. Higher temperatures and lower water activity favour formation of hematite in preference to goethite (Schwertmann & Taylor 1989).

Little Al-substitution occurs in goethite from the Quaternary sediments. Schwertmann (1985) has reviewed the effect of pedogenic environments on the degree of Al-substitution in goethite and concludes that amounts above 10 to 15 mole % are typical of highly weathered soils. Low substitution reflects formation in weakly acidic soils and hydromorphic environments. He also indicates that the concentration of Si in the local environment may affect the degree of Al-substitution. The identification of opaline silica within some mottled intervals would therefore suggest a high activity of Si in solution and preclude significant Al substitution in the Quaternary sediments.

Micromorphological studies indicate that iron has precipitated at sites of localised oxidation. Hematite can be seen as scattered small crystallites within a clay matrix, which coalesce into larger masses. In coarse sediments, iron has also filled voids and replaced clay minerals while in more clayey sediments iron has precipitated along the margins of fractures developed within the sediments. As a major accumulation of iron is approached, the fractures leading toward this area become more and more concentrated with iron, suggesting that such fractures provide pathways for the movement of iron through the sediments. Milnes *et al* (1985a) identified similar relationships in their petrological study of ferricretes from southern Australia and southern Africa.

The variability of iron mineralogy between mottles and occasionally within mottles suggests that fluctuations in local environmental conditions have occurred. When water activity was greater, possibly at times of higher water tables, formation of goethite was favoured. Torrent *et al* (1982) investigated the effect of relative humidity on the formation of goethite and hematite and found that at constant temperature, goethite formed more readily than hematite in the most humid environments. In fine-grained sediments where humidity within pore spaces would be higher than coarse sediments, goethite should be more abundant than hematite. This is supported by thin section observations which indicate that mottles from finer-grained sediments are less intensely red and hence contain less hematite and by field observations which suggest that the reddest mottles occur within sandy sediments. As clay-rich sediments became dehydrated, particularly adjacent to fractures, conditions would have been more conducive to formation of hematite.

7.2.2 Association with Clay Mineralogy

Iron oxides are frequently observed replacing clay minerals. This alteration would release Si, Al and alkalies into solution. Opaline silica is identified in association with mottled sequences in the Noarlunga and Willunga Embayments and probably formed from silica released by alteration of clay minerals during mottle formation. The indurated nature of many mottled intervals is most likely due to the presence of opaline silica. Halloysite is recorded from a mottled interval at Snapper Point forming up to 20% of the <2μm fraction and in electron micrographs from other samples associated with iron mottles within the Quaternary sequence. Diagenetic formation following alteration of existing clay minerals during development of mottles is also thought to account for these occurrences of halloysite.

Tardy & Nahon (1985) studied the mechanisms of concretion formation in bauxites and ferricretes and concluded that hematite tended to form through replacement of kaolinite in areas of small pore size. While data on clay mineralogy obtained at the Maslin Bay site support this concept, changes in clay mineralogy through mottled intervals at other sites suggest that kaolinite, in fact, increases in relation to other clay minerals. A discussion of the

manner in which clay mineralogy is influenced by particle size distribution indicates that in many coarse intervals kaolinite is the dominant clay mineral because it is present as larger particles (Section 4.3). This suggests that the high proportion of kaolinite present in the mottled zones is related to primary depositional processes rather than reflecting alteration during mottle formation. Such observations do not discount the possibility that hematite subsequently replaces kaolinite within the mottled zone.

Micromorphological observations which show that iron oxides frequently replace clay minerals, are in agreement with the work of Tardy & Nahon (1985) who state that iron accumulation takes place in small-sized pores. It is easier to reach saturation of solutions in small pores and hence precipitation takes place at these sites. While the water activity is fairly high, goethite will precipitate but as the size of the pore decreases, water activity also diminishes and hematite becomes the dominant mineral formed. Observation in thin sections of hematite forming a final coating along fractures, often following deposition of goethite, supports the importance of water activity in determining the iron oxide mineral formed. Even within the coarsely mottled sandy intervals which are prominent in the Quaternary sequence, there are small patches of clay which can be observed in thin sections and these may have acted as nucleii for mottle formation. In contrast, clean, sandy sediments often have only thin skins of clay and iron oxide coating skeleton grains with large intergranular pores.

7.2.3 Source of the Iron

There are several possible sources for the iron which has accumulated in the form of mottles. Firstly, iron may have been introduced in a reduced state by groundwaters. Secondly, weathering of ferro-magnesian or other similar iron-rich minerals within the Quaternary sequence may have contributed Fe^{2+} to groundwater circulating through the sediments. Finally, clay minerals within the sequence may have contributed iron. Norrish & Pickering (1983) indicate that illite can contain up to 10% Fe_2O_3 while Rengasamy *et al* (1975) suggest that substitution of Al by Fe in soil kaolinites does not exceed 3 mole %. Hence it is likely that the clay minerals in the Quaternary sequence are a sufficient source of iron for the

mottles. The replacement of clays by iron oxides as observed in thin section, would release iron and other cations and precipitation of iron oxides could take place virtually *in situ* in response to local environmental conditions. Therefore large scale lateral movement of iron in solution is not essential for mottle formation.

7.2.4 Summary

Iron mottling within the Quaternary sequence has developed through the local mobilisation and possible introduction of iron in a reduced state in groundwaters flowing through confined aquifers or along fractures within the sediments. Mottles form at localised sites of oxidation with variations in the mineralogy and crystallinity of the oxides reflecting fluctuating local environments. The lack of Al-substitution in goethites suggests formation in slightly acidic and/or hydromorphic conditions. Alteration and replacement of clay minerals by iron oxides would be favoured under slightly acidic environments and iron released from clay minerals could contribute to mottling of the sediments.

7.3 Palaeosols

Comparison of the features identified and discussed in this Chapter with those generally used to suggest the modification of sediments by pedogenesis (Blodgett 1988; Retallack 1988) indicate that there are several intervals within the Quaternary sequence which may have undergone pedogenic alteration. A succession of silty intervals that are devoid of sedimentary structures but which show biogenic alteration, iron mottling and soil-like structure are the most likely palaeosols in the sequence. The presence of up to nine such intervals in the Seaford area in various states of preservation suggests that periods of non-deposition and soil formation were common within basal parts of the Robinson Point Formation in this area. The lack of lateral continuity of these palaeosols over distances greater than 200 metres and the fact that the number of palaeosols preserved at any site is extremely variable indicates considerable fluctuation in the nature of the depositional environment during this time.

7.3.1 Palaeosols in the Robinson Point Formation

The presence of smectite in the clay fraction of intervals interpreted to be palaeosols and not in other sediments at Onkaparinga Trig suggests that unique conditions prevailed within these intervals to allow either the preservation of smectite or its formation through diagenesis from previously deposited clays. Within the Quaternary sequence from the Noarlunga and Willunga Embayments, smectite is only recorded from the palaeosol sequences discussed above and from clays and sands immediately above the Burnham Limestone at several localities in the Willunga Embayment. Smectite is commonly reported from soils where leaching is limited due to low precipitation, a restrictive layer or a high water table and under such conditions smectite can form pedogenically or alternatively be preserved if inherited (Borchardt 1989). The silty palaeosols are formed in a sequence believed to be of fluvial origin and hence periodic exposure of fine-grained components of these sediments, possibly on floodplains, would enable pedogenesis to occur. High water tables and limited leaching would be common in such environments and hence the formation of smectite could take place. The sediments have a general grey colour with mottling being of yellow-orange goethitic colours. Goethite forms preferentially over hematite in conditions of high water activity and low temperature (Schwertmann & Taylor 1989) and this supports the hypothesis that these diagenetic changes took place in a poorly leached environment. Thus the presence of smectite in silty sequences of the Robinson Point Formation supports other observations which suggest that these units are palaeosols.

In other parts of the Robinson Point Formation there are sandy indurated intervals displaying columnar structure, a rectangular bleaching pattern and rare tubular structures. Such features suggest that these intervals have undergone pedogenesis but to a lesser degree than silty sequences from other parts of the Robinson Point Formation. Complete bleaching of the upper 20 cm of some sections suggests affinities with A_2 horizons of soils where clays and iron oxides are leached from this zone and illuviated to lower horizons. The preservation of upper parts of the soil profile in the sedimentary sequence indicates that only limited erosion

has taken place between successive depositional cycles and hence an aggradational environment can be postulated. A vertical and horizontal trend to bleaching within the sandy sediments may be related to prior sedimentary structure in the case of horizontal bleaching or to removal of iron adjacent to roots in the case of vertical bleaching. No organic remains are identified, nor do these sandy units display horizontal bedding trends although rare gravel accumulations in basal parts show a general horizontal orientation. The sandy palaeosols are generally present in central to upper parts of the Robinson Point Formation and most common in areas to the north and south of the greatest development of silty palaeosols.

7.3.2 Palaeosols in the Ngaltinga Formation

Several features suggest that the carbonate bed within the Neva Clay Member is a palaeosol. There are rare examples of tubular, calcified structures which are interpreted as remnant burrows or roots. The beds have a sharp upper boundary suggesting erosion prior to further deposition and a lower gradational boundary characteristic of mineral accumulation horizons in soils (Retallack 1988). Thin sections show that the carbonate impregnates existing clay-rich sediments leaving occasional angular blocks of clay within the carbonate matrix. Changes in the proportion of kaolinite and illite occur in association with the carbonate beds implying a sedimentary break at this level. Such changes in clay mineralogy do not occur at any other position within the Neva Clay Member and elsewhere in the Ngaltinga Formation only occur in association with changes in lithology. Mineralogy within the carbonate beds shows a characteristic increase in calcite towards upper parts of the carbonate interval with lower parts dominated by dolomite and such variation is typical of many calcrete profiles in southern South Australia (Milnes & Hutton 1983).

The presence of dolomite within parts of the carbonate beds suggests that comparison with other Quaternary sediments containing dolomite should be made to ascertain it's origin. The presence of dolomite in calcrete profiles has already been noted. Dolomite also occurs extensively in lacustrine environments where association with hypersaline playas and marginal marine ephemeral lakes is noted (Last 1990). Within southern Australia the best

documented example is the Coorong lake system where interaction between continental Mg-rich waters and highly saline marine-derived waters allows precipitation of dolomite (von der Borch 1965; 1976; von der Borch *et al* 1975; von der Borch & Lock 1979). Sediments of the Neva Clay Member do not exhibit sedimentary structures such as mud cracks, teepee structures, intraclast breccias or pseudomorphs after evaporite minerals such as would be expected from saline, ephemeral lacustrine environments. Nor is there an association with marine or marginal marine sediments. Hence carbonate beds within the Neva Clay Member most likely represent the preserved B_{Ca} horizons of soils.

Dolomite is also noted immediately above the Burnham Limestone at several locations in the Willunga Embayment. At none of these locations are the blotches of carbonate associated with features characteristic of palaeosols and hence a different mode of formation for this dolomite is probable compared with carbonate from the Neva Clay Member. The spatial association of dolomite with the Burnham Limestone of marine origin suggests an interaction of groundwaters of marine origin with less saline continental waters may have taken place. A Coorong-type model may be appropriate for dolomite associated with the Burnham Limestone with regression of the sea allowing marginal marine conditions to develop as continental sedimentation became increasingly important.

7.3.3 Significance of Palaeosols for Interpreting Depositional Environments

Palaeosols developed in the Robinson Point Formation are more frequent and distinctly different to those identified from the Ngaltinga Formation. Thus the depositional regime of the Robinson Point Formation was episodic allowing sufficient time between depositional events for soil formation to take place. Additionally, erosional events were not severe enabling the preservation of many of the soils which had developed. Soils identified from the Ngaltinga Formation are calcareous suggesting an environment with limited leaching and as intervening sediments between the carbonate palaeosols are non-calcareous, there must have been an additional external source to provide the carbonate. Increasing numbers of carbonate palaeosols preserved in upper parts of the Quaternary sequence and the presence of

a thick carbonate mantle overlying the sequence is taken by Milnes & Phillips (1988) and Phillips (1988) to indicate a gradual change in environmental conditions and an increasing importance of an external sedimentary source.

While the nature of palaeosols within the Ngaltinga Formation is identical in both the Noarlunga and Willunga Embayments, the same is not true for the Robinson Point Formation. The best developed, silty palaeosol sequences are only identified from the Noarlunga Embayment between Witton Bluff and Moana. This region is adjacent to the modern position of the Onkaparinga River and hence silty palaeosols may relate to deposition associated with the palaeo Onkaparinga River. Palaeosols from other parts of the Noarlunga Embayment are sandy and less well developed. Apart from several sandy palaeosols identified on the northern margin of the Willunga Embayment at Ochre Point, no palaeosols have been identified from the Robinson Point Formation in this embayment. This reflects the limited extent of this unit in the Willunga Embayment and also the gradual change in depositional regime which takes place within the Robinson Point Formation in a southerly direction away from central parts of the Noarlunga Embayment.

The nature of palaeosols preserved in Quaternary sediments of the Noarlunga and Willunga Embayments therefore reflect changes in the nature of the depositional environment and are useful in determining the history of sedimentation in this region during the Quaternary.

7.4 Summary of diagenetic clays

The clay mineralogy of the Quaternary sediments from the Noarlunga and Willunga Embayments has been discussed in Sections 4.2, 4.3, 4.4 and 6.2. Many clay minerals are considered to be of detrital origin, however in this chapter formation of some clays through diagenesis has been proposed. Diagenetic reactions have transformed detrital clays in some intervals leading to the formation of smectite and halloysite. Halloysite forms in an acidic environment following the lowering of water tables in floodplain sediments in conjunction with development of alunite (Section 7.1). Illite and randomly interstratified illite-smectite

are considered to be precursors of halloysite. Smectite also forms from illite and randomly interstratified illite-smectite following pedogenesis in poorly drained floodplain sediments (Section 7.3). In fine-grained intervals within parts of the Robinson Point and Ngaltinga Formations, increases in the proportion of smectitic layers within interstratified illite-smectite suggest that a similar transformation toward smectite has taken place. Such clay-rich intervals were evidently zones of restricted drainage but there is insufficient additional evidence to indicate whether this transformation is related to pedogenesis. Similar reactions also altered illite in these fine-grained intervals with broader diffraction peaks indicating replacement of interlayer K with hydrated cations. Intensely iron-mottled zones from both the Robinson Point Formation and Snapper Point Sand Member show some evidence for a loss of kaolinite relative to illite. Following studies by Tardy & Nahon (1985) replacement of kaolinite by hematite is suggested to account for this.

While many of the clays discussed in this study are of detrital origin and hence assist in determining a provenance for the sediments, the identification of diagenetic clays allows a better understanding of depositional environments and the subsequent history of the sediments. Deposition of some sediments in areas of restricted drainage is indicated by the identification of smectite while subsequent exposure and desiccation of the sediments is suggested by the formation of both halloysite and alunite. Such clay mineralogy confirms the presence of palaeosols within the Quaternary sequence which was suggested by field observations at many sites.

CHAPTER 8
COMPARISON WITH PREVIOUS STUDIES OF QUATERNARY SEDIMENTS FROM THE NOARLUNGA AND WILLUNGA EMBAYMENTS AND NEARBY AREAS

Studies of clay and sand-rich deposits of Quaternary age from the eastern margin of the St Vincent Basin have been undertaken by a number of scientists. Early work such as that by Tate (1878; 1882; 1890) and Howchin (1923; 1935; 1936) was mostly descriptive. More recent contributions have been with regard to soil relationships (Aitchison *et al* 1954; Ward 1966; Taylor *et al* 1974), to engineering problems (Selby & Lindsay 1982; Sheard & Bowman 1987a; 1987b) or to a general stratigraphic understanding (Firman 1966; 1967; Lindsay 1969; Stuart 1969; Daily *et al* 1976). In the Noarlunga and Willunga Embayments, Ward (1966) subdivided the Quaternary sediments into the Seaford and Ochre Cove Formations which he considered to be of alluvial origin and the Ngaltinga Clay of aeolian origin. Firman (1966) and later Sheard & Bowman (1987a; 1987b) divided Quaternary sediments from the Adelaide Plains Sub-Basin and Adelaide/Golden Grove Embayment into the Hindmarsh and Keswick Clays which they thought to have an alluvial origin. Thus there is some conflict in the interpretation of the origin of these sediments and their relationships, particularly between studies from the Adelaide Plains Sub-Basin and the Noarlunga and Willunga Embayments. These problems are discussed in this section using the results of detailed work undertaken in the Noarlunga and Willunga Embayments as a basis.

8.1 Sedimentary Features

8.1.1 Origins of the Sediments

Ward (1966) suggested an alluvial origin for the oldest Quaternary sediments in his area of study and an aeolian origin for upper clay-rich sediments. In the Adelaide area, fluvial, alluvial or colluvial origins have been suggested for similar sediments (Tate 1890; Howchin 1935; 1936; Glaessner & Wade 1958; Firman 1966; 1969a; Sheard & Bowman 1987a;

1987b). The present study indicates that Quaternary sediments from the Noarlunga and Willunga Embayments are of alluvial origin. Clay-rich units within the sequence, which are more common in upper parts are considered to result from overbank deposition while channel-fill deposits with cyclic sequences of gravel, sand, silt and clay are common in basal parts. Similar sedimentary features have been recognised by Sheard & Bowman (1987b) from the Hindmarsh and Keswick Clays in the Adelaide region and areas further north.

Ward's (1966) interpretation of the Ngaltinga Clay (renamed Ngaltinga Formation in this thesis) as aeolian in origin was based on the interbedding of carbonate beds through the unit. The carbonate was considered to be derived as wind-blown dust with the host clay-rich material assumed to have a similar source. The lack of sedimentary structure, the presence of silt-sized quartz grains scattered randomly through the deposit and the distribution through the area were all thought to indicate an aeolian deposit.

As part of this interpretation, Ward (1966; Appendix 3) reassessed data for heavy minerals collected by Aitchison *et al* (1954) from soils and rocks in the Adelaide area. These workers suggested that minerals which occurred in soils but not in rocks may have been introduced as wind-blown dust. Ward's interpretation of this data involved separating samples into groups according to the source of the sample. He concluded that groups B to F, comprising samples from Tertiary and Quaternary sediments and recent soils, had higher proportions of zircon, rutile, tourmaline, sillimanite and amphibole when compared with samples from basement rocks. These minerals had therefore been introduced to the area together with the Ngaltinga Clay during the Late Pleistocene.

There are several problems with the data as presented by Ward (1966). Firstly, summarised results for groups C to E covering the Ngaltinga Clay and soils developed from this material, total much greater than 100% heavy minerals (Table 14, p112; Group C=170%, D=140%, E=180%). The resultant data is therefore misleading. Secondly, with the exception of amphibole, those minerals considered by Ward to be more abundant in younger sediments and soils also occur in elevated amounts in basement rocks when compared with all other

heavy minerals which have been identified. Great quantities of iron oxides (termed ore minerals by Ward) and chlorite in basement rock samples ensure that absolute amounts of other heavy minerals are low, however if iron oxides and chlorite are ignored in the calculations, the relative abundance of the remaining minerals is little changed in any of Ward's groups. Heavy minerals, in general, tend to be more resistant than other minerals present in rocks and hence it would be expected that these minerals may be concentrated in sediments derived by erosion of older rocks. A change in the proportion of the minerals present may be evidence of an additional source, however the data presented by Ward does not show such a change. Chlorite, which is common in samples from basement rocks (10 to 30% of heavy minerals), is rarely identified in younger samples (Groups B to F) as it alters readily in soils and weathered sediments. Norrish & Pickering (1983) indicate that chlorite is an uncommon clay mineral of soils in the Adelaide area due to it's instability. An understanding of the resistivity of the heavy minerals identified in the study of Aitchison *et al* (1954) is therefore necessary to interpret their data.

Ward (1966) placed considerable importance on the interpretation that some heavy minerals had been introduced by aeolian means as this supported his contention that the Ngaltinga Formation was of aeolian origin. It is argued above that the heavy mineral abundances used by Ward to support this theory do not require a source other than the basement rocks in the region to produce such a suite of heavy minerals. Recent studies presented in this thesis of heavy minerals separated from samples collected at the Onkaparinga Trig and Maslin Bay sites indicate that there is little difference in the range of minerals present in the Robinson Point and Ngaltinga Formations. If an aeolian source was dominant during deposition of the Ngaltinga Formation then underlying alluvial sediments should have a significantly different heavy mineral assemblage. Such a difference is not observed and hence a similar source is postulated for both stratigraphic units.

An alluvial origin with both channel and overbank deposition recognised for sediments of the Robinson Point and Ngaltinga Formations is in agreement with suggested origins for the Hindmarsh and Keswick Clays. Sheard & Bowman (1987a; 1987b) indicate that the

Keswick Clay was deposited in alluvial fans or as overbank sediments. Some areas located in depressions on basement highs (eg Para and Eden Blocks) were formed through *in situ* weathering of Precambrian bedrock and Sheard & Bowman (1987a) indicate that the Ngaltinga Clay which Ward (1966) mapped on the Noarlunga Block also formed in this manner. The Hindmarsh Clay is also considered to be of alluvial origin with Sheard & Bowman (1987b) recognising the presence of cyclic sand, silt and clay layers, shoestring sand, gravel and boulder deposits and rapid lateral and vertical facies changes. Similar features occur frequently in the Robinson Point Formation and occasionally in the Ngaltinga Formation. Lindsay (1969) reported minor marine and estuarine facies within basal parts of the Hindmarsh Clay from drillholes in the Adelaide Plains Sub-Basin and a similar marine facies, which has been named the Burnham Limestone, is recognised in the Robinson Point Formation from the Noarlunga and Willunga Embayments.

8.1.2 Mineralogy of the Sediments

The mineralogy of Quaternary sediments from the Noarlunga and Willunga Embayments, in particular clay and diagenetic minerals, has been used in the present study to help distinguish environments of deposition and to understand changes which have taken place in this region following deposition. Minimal information regarding the mineralogy of sediments in this and nearby regions has been provided in previous studies and hence interpretations of the origins and diagenetic history of the sediments have been based solely on field observations of sedimentary structures and the distribution of various units through the region.

Ward (1966) attempted to use heavy mineral data from sediments and soils in the Adelaide region to help interpret a source for the Ngaltinga Clay. The interpretation of this data can be shown to be misleading (Section 8.1.1) and hence the postulated aeolian origin is unlikely to be correct. The identification of a similar heavy mineral assemblage throughout the Quaternary sequence and also identical detrital clay mineral assemblages indicates that a similar origin existed for both the Robinson Point and Ngaltinga Formations. In the Adelaide Plains Sub-Basin, Sheard & Bowman (1987a) report that smectite with lesser

amounts of illite and randomly interstratified clays are present within the Keswick Clay, however no conclusions were drawn from this observation. A slightly different clay mineralogy has been reported in the present study for sediments from the Robinson Point and Ngaltinga Formations with illite, randomly interstratified illite-smectite and kaolinite being the major clay minerals identified. Variations in the proportions of these clay minerals are useful in distinguishing between sediments of these two formations while the presence of smectite and halloysite indicate specific environmental conditions leading to diagenetic alteration. The lack of mineralogical information from previous studies precludes such detailed conclusions.

8.2 Diagenetic Features

Several features thought to be of diagenetic origin have been identified within the Quaternary sequence during the present study through field observations of the sediments and also detailed mineralogical investigations. These features include the presence of ferruginous mottles, the identification of palaeosols and the development of alunite and halloysite.

8.2.1 Ferruginous Mottling

The presence of ferruginous mottling within Quaternary sediments from the St Vincent Basin has been frequently noted. Early researchers recognised the mottled nature of the sediments as indicated by the terminology they used which included "alluvial mottled clays" (Howchin 1923; 1935; 1936; Reynolds 1953), "terrestrial mottled clays" (Aitchison *et al* 1954) and "varigated clays" (Glaessner & Wade 1958). Sheard & Bowman (1987a; 1987b) commented that small-scale mottling in both yellow and red colours was common, particularly in fine-grained units. In contrast, Daily *et al* (1976) and Firman (1981) emphasised a distinctive iron-mottled interval within the sequence and referred to it as the Ardrossan Soil or Palaeosol. Ward (1966) described mottled intervals within the Seaford and Ochre Cove Formations but did not discuss their origins.

Data from this study indicate that ferruginous mottling is extensive throughout the Quaternary sequence. Large, vertical and indurated mottles occur within sandy intervals surrounded by fine-grained sediments from both the Robinson Point and Ngaltinga Formations. They are not confined to a single stratigraphic interval as suggested by Daily *et al* (1976) and Firman (1981) but occur within confined sandy lenses. Such a distribution suggests that this prominent mottling is related to groundwater movement within confined aquifers rather than to soil forming events and hence cannot be used as a reliable stratigraphic marker unit. There are no other features within these mottled intervals similar to those described in Section 8.2.2 which suggest that they may be palaeosols.

Sheard & Bowman (1987a; 1987b) described small-scale mottling within fine-grained sediments of the Keswick and Hindmarsh Clays and similar mottling has been identified in clays from the Noarlunga and Willunga Embayments. The mottles often occur along fractures within the clays or on ped surfaces and represent sites of localised oxidation and deposition of iron. Mobilisation of iron takes place periodically within the sediments in response to fluctuating moisture conditions. Mottles of this sort are particularly obvious in silty and clayey beds which have undergone pedogenesis (Section 8.2.2). Thus mottling in fine-grained sediments occurs in response to a fluctuating moisture regime, which in some cases is related to near-surface alteration during pedogenesis.

8.2.2 Palaeosols

Carbonate palaeosols have been described from the Adelaide area within Late Pleistocene alluvial sediments of the Pooraka Formation and also from older calcretes which mantle a wide range of sediments in the area (Daily *et al* 1976). Strongly mottled sediments within older Quaternary clay and sand sequences have been interpreted as ferruginous palaeosols representing old laterite profiles (Daily *et al* 1976; Firman 1981). Such an interpretation for these ferruginous mottled zones has been shown to be incorrect based on the detailed investigations of mottled sediments undertaken in the current study (Section 8.2.1). They are now interpreted to result from water table fluctuation within confined aquifers.

Small-scale mottling patterns associated with columnar structure, upward fining cycles, bioturbation and mineralogical changes such as formation of smectite are commonly observed from parts of the Robinson Point Formation. These features are thought to represent pedogenic alteration of the alluvial sediments following periodic exposure on floodplains. Similar features have been recognised by Sheard & Bowman (1987a; 1987b) in parts of the Hindmarsh and Keswick Clays. In upper parts of the Hindmarsh Clay, Sheard & Bowman (1987b) describe palaeosols comprising remnant 'B' horizons which include carbonate segregations. Similar carbonate zones are recognised from parts of the Neva Clay and Snapper Point Sand Members with the frequency and extent of these zones increasing in the youngest sediments. Phillips & Milnes (1988) and Phillips (1988) discuss the carbonate interval overlying Quaternary sediments in the Noarlunga and Willunga Embayments and conclude that this represents the coalescence of a number of palaeosols. Isolated carbonate beds within upper parts of the Quaternary sequence are thought to have a similar origin and reflect a gradual change in climatic conditions which favoured the formation and preservation of carbonate palaeosols.

The present study concludes that pedogenic modification of the Quaternary sequence is more common than previously thought. Initial modification involved the bioturbation and mineralogic transformation of poorly drained alluvial sediments which were periodically exposed on floodplains. Later pedogenic events, which include preservation of carbonate-rich 'B' horizons, reflect increasing aridity and a decreasing importance of alluvial sedimentation.

8.3 Stratigraphy

The stratigraphy of Quaternary sediments from the Noarlunga and Willunga Embayments is modified in the present study from that defined by Ward (1966). The proposed stratigraphy is discussed in detail in Chapter 3. The Robinson Point Formation is equivalent to the Seaford and Ochre Cove Formations of Ward (1966) and has been proposed due to the

difficulty in distinguishing between Ward's units in the field. Ward (1966) considered that thick gravels marked the base of the Ochre Cove Formation with the Seaford Formation comprising interbedded sands and clays. Recent field studies have shown that a marker gravel horizon is not always present and can also occur at a variety of stratigraphic positions within the basal Quaternary sediments. In addition, sandy clay sediments which occur in upper parts of the Ochre Cove Formation are similar in terms of texture and mineralogy to parts of the Seaford Formation. For these reasons, it is considered that amalgamation of the two units into the Robinson Point Formation is more practical and reflects the similarities in origin, mineralogy and post depositional alteration of the basal Quaternary sediments.

The Ngaltinga Formation is equivalent to the Ngaltinga Clay of Ward (1966) with the exception that the overlying carbonate blanket has been separated from this stratigraphic unit. This material is vastly different to the alluvial sediments which form the Ngaltinga Formation and also overlies a wide variety of sediments in the area ranging in age from Precambrian to Quaternary. Twidale *et al* (1967) and Phillips & Milnes (1988) have also argued that this overlying carbonate blanket should be considered a separate stratigraphic unit from the underlying clay-rich sediment.

While there are distinct differences in clay mineralogy and texture between much of the Ngaltinga and Robinson Point Formations, parts of the Snapper Point Sand Member do not show these differences. These observations suggest the repetition of depositional environments and sedimentary sources throughout the Quaternary period. Lateral changes are also noted, with sediments of the Ngaltinga Formation more common in central parts of the embayments and, in particular, within the Willunga Embayment. Thus, it is concluded that the stratigraphic units proposed in this study represent different facies within an alluvial sequence and that there have been significant lateral and vertical facies changes during the Quaternary.

Sedimentological and mineralogical data for the Hindmarsh and Keswick Clays is limited and hence only general comparisons can be made with Quaternary sediments from the Noarlunga

and Willunga Embayments. Sheard & Bowman (1987a; 1987b) provide most information and suggest that the Keswick Clay is equivalent to the Ngaltinga Clay of Ward (1966). Sedimentological features described from parts of the Hindmarsh Clay (Lindsay 1969; Sheard & Bowman 1987b) are similar to features identified within the Robinson Point Formation and hence these two units may be equivalent.

8.4 Summary

Previous studies of Quaternary sediments from the St Vincent Basin have generally lacked sufficient sedimentological and mineralogical information to enable detailed conclusions to be drawn on the origin of these sediments and diagenetic changes which have subsequently taken place. A detailed study of these sediments along the coastline in the Noarlunga and Willunga Embayments where they are well exposed indicates that they represent a complex alluvial sequence which is coarser at the base and fines in an upward direction. Pulses of coarse sediment are recognised in upper parts of the sequence and are referred to the Snapper Point Sand Member. The decreasing importance of an alluvial source in younger sediments is reflected by the increased prevalence of carbonate palaeosols in upper parts of the sequence. In contrast, palaeosols from basal units developed in poorly drained alluvial sediments, possibly on floodplains, and are characterised by ferruginous mottling, bioturbation, soil-like structures and mineralogical transformations. Comparison with limited data for Quaternary sediments from the Adelaide Plains Sub-Basin and the Adelaide/Golden Grove Embayment suggests that similar processes were operating in these regions. The Hindmarsh Clay is likely to be equivalent to the Robinson Point Formation and the Keswick Clay equivalent to the Ngaltinga Formation.

CHAPTER 9
SUMMARY AND CONCLUSIONS

The Quaternary sequence exposed in coastal cliff sections within the Noarlunga and Willunga Embayments south of Adelaide has been studied in this thesis. Sedimentology, mineralogy, in particular clay mineralogy, stratigraphy and diagenetic features of the sediments have been considered and an integration of these aspects forms the basis of an understanding of the landscape history of the region. Previous investigations of Quaternary sediments in this area have been based on limited data, particularly with regard to mineralogical and diagenetic features and thus some previous conclusions regarding the origins of this sequence differ from those outlined in this thesis.

9.1 Sedimentary History

Underlying and interfingering with basal non-marine Quaternary sediments in the Noarlunga and Willunga Embayments is the Early Pleistocene Burnham Limestone which provides a convenient marker unit. While the Burnham Limestone is generally considered to be of estuarine origin (Ludbrook 1983), the identification of the marine gastropod *Hartungia dennanti chavani* in southern parts of the study area (May & Bourman 1984) suggests more exposed conditions in these areas. Thin beds of mottled dolomite associated with smectitic clays overlie the Burnham Limestone and have not previously been reported. The mottled dolomite may be of pedogenic origin although the absence of other pedogenic features makes this origin less likely. Comparison with studies of dolomite in the Coorong region of South Australia (von der Borch 1965; 1976; von der Borch *et al* 1975; von der Borch & Lock 1979) and summaries of dolomite occurrences in Quaternary sediments around the world by Last (1990) suggest that the dolomite above the Burnham Limestone results from an interaction between continental Mg-rich groundwater and highly saline waters of marine origin. They therefore reflect transitional environments from marine to non-marine sediments and suggest relatively high water tables at this time.

Non-marine sediments which overlie the Burnham Limestone have been divided into two stratigraphic units, the Robinson Point and Ngaltinga Formations. The Robinson Point Formation comprises an interbedded sequence of gravels, sands, silts and clays while the Ngaltinga Formation is dominantly massive clays with rare fine sandy interbeds. Isolated lens-shaped and thin tabular sand bodies occur in upper parts. Both units are interpreted to be of fluvial origin, representing deposition from anastomosed and meandering streams on alluvial plains by comparison with previous studies of fluvial sediments (Allen 1965; Williams 1973; Smith & Purtnam 1980, Friend 1983; Smith 1983; Galloway & Hobday 1983; Bridge 1985; Atkinson 1986; Fielding 1986; Besly & Fielding 1989; Smith 1990). Cross-bedded gravels and sands deposited in distributory channels are common within the Robinson Point Formation with interbedded finer sands and clays representing overbank sediments deposited in adjacent areas. Upward fining sedimentary cycles grading from gravel or sand to silt or clay are commonly observed. Fine-grained sediments from upper parts of these sedimentary cycles display thin vertical tubular structures, characteristic yellow-orange reticulate mottling patterns and columnar structures indicative of pedogenic modification of the sediments. Episodic deposition was evidently a feature of the alluvial plains allowing development of soils within exposed sediments. Palaeosols are described in numerous studies of alluvial sediments (for example Allen 1974; Retallack 1976; 1977; 1983; 1986; Bown & Kraus 1981; 1987; Nickel 1985; Fielding 1986; Kraus 1987; Besly & Fielding 1989; Smith 1990) and have been frequently used to help reconstruct the palaeogeomorphology, palaeoclimate and palaeoecology.

Fine-grained sediments of the Ngaltinga Formation represent suspended load deposition in more distal parts of the alluvial plain as overbank sedimentation. Rare lens-shaped and tabular sand bodies (shoe-string bodies; Fielding 1986) indicate deposition from minor distributory channels and crevasse splays. Carbonate mottles within clays at some localities were formed during pedogenesis and represent B_{Ca} horizons. Calcareous palaeosols are commonly observed in alluvial sequences (Williams 1973; Bown & Kraus 1981; 1987; Wright 1982; Atkinson 1986; Retallack 1986; Kraus 1987) and are generally considered to characterise soils of semi-arid climates where leaching is limited (Bown & Kraus 1981). The

increasing incidence of calcareous palaeosols in upper parts of the Ngaltinga Formation and the presence of a thick blanket of calcareous material overlying the alluvial sequence suggests a gradual change to drier climates during the Quaternary.

9.2 Mineralogy

The clay mineralogy of the Quaternary sequence has been investigated in detail following work by Callen (1976; 1977) which showed that clay mineralogy could be used to aid the interpretation of origins of Tertiary sediments from northern South Australia. Many studies have been made of the palaeoclimatic significance of clay minerals identified in marine sediments (for example, Jacobs & Hays 1972; Ataman & Gokcen 1975; Chamley 1979; 1989; Singer 1984; Pearson 1990; Robert & Chamley 1990) and in palaeosols and palaeo-weathering horizons (for example, Birkland 1969; Singer 1975; Abbot *et al* 1976; Meyer 1976; Singer 1980). In marine sediments, problems arise in these interpretations due to diagenetic changes to clays (Hower *et al* 1976; Nadeau *et al* 1985), effects of additional secondary sources of clays such as smectite from volcanic activity (Jeans *et al* 1982) and effects of differential transport of clays where finer particles such as smectite and illite are transported further distances before sedimentation (Millot 1964; Porrenga 1966; Gibbs 1977). Similar problems of interpretation exist with palaeosols (Singer 1980).

Fewer studies have been undertaken where clay minerals were used to help study the origins and history of the sedimentary sequence, rather than just the palaeoclimate. Macleod & Vita-Finzi (1982) for example, used clay minerals of alluvial valley-fills from Greece to determine the relative importance of diagenesis and parent materials in determining the local character of the sediments. They concluded that clay mineralogy reflected local provenance except where seasonal water-logging and desiccation promoted development of pseudo-gley features and increased smectite. Meyer & Pena Dos Reis (1985) attempted to classify environments where silicification and alunite formation took place in alluvial sequences from Portugal and utilised clay mineral distribution in their study. They found that smectite was formed from illite and kaolinite in upward-fining sequences with associated production of opaline silica.

Such transformations took place in soils from swampy environments. Sulphides formed in this organic-rich environment were later oxidised and the sulphuric acid which was produced reacted with clay minerals forming alunite and amorphous silica. Similar diagenetic reactions have been noted in Quaternary sediments studied in this thesis.

While broad studies of the palaeoclimatic significance of clay minerals in sedimentary sequences have sometimes proved difficult, it would appear that clay minerals are sensitive indicators of environmental change (Singer 1980; 1984). Local factors such as leaching and groundwater movement, topography, vegetation and associated geology are important modifiers of local environment and thus clay minerals will reflect these variables (Grim 1968; Allen & Hajek 1989). Thus, provided the clay mineralogy of the sequence is not considered in isolation, clay minerals can provide useful information on provenance and specific local environments both at the time of sedimentation and during subsequent diagenesis.

The clay minerals identified in Quaternary sediments from the Noarlunga and Willunga Embayments are dominantly kaolinite, illite and randomly interstratified illite-smectite. Lesser amounts of hydroxy interlayered smectite, smectite and halloysite are also identified. Most of these clays are considered to be of detrital origin and derived from the Mt Lofty Ranges to the east where they form the dominant clay mineral component of present-day soils and sediments.

The proportions of kaolinite, illite and randomly interstratified illite-smectite vary considerably through the Quaternary sequence with the Robinson Point Formation and coarser sediments containing more kaolinite than illite or randomly interstratified illite-smectite. Finer sediments, particularly those from the Ngaltinga Formation, contain higher proportions of illite and randomly interstratified illite-smectite compared with kaolinite. A study of the clay mineralogy of four size fractions <20μm from eight samples indicates that illite and expandable clays such as smectite and randomly interstratified illite-smectite are concentrated in finest fractions <0.2μm, while kaolinite occurs mostly in fractions >0.2μm.

Thus the concentration of kaolinite in coarser sediments, and in particular the Robinson Point Formation, appears to reflect primary sedimentation.

In fine-grained units of the sequence the smectitic proportion of randomly interstratified illite-smectite increases together with broadening of diffraction peaks for illite. Transformation reactions involving hydrated cations entering layer lattices of interstratified clay and illite with resultant loss of interlayer K^+ is postulated to account for these observations. Restricted drainage within clay-rich intervals would allow less leaching of hydrated cations and in such an environment, transformation of randomly interstratified clays and illite to more smectitic species could take place.

Preliminary investigations of the heavy mineral suite present in the Quaternary sequence have been undertaken and while greater numbers of heavy minerals are present in coarser-grained sediments, a similar suite of minerals can be found in both the Robinson Point and Ngaltinga Formations. Thus there appears to have been no change in the dominant source for the sediments throughout the Quaternary.

Smectite and halloysite are confined to specific intervals within the sequence, mostly near the base of the Robinson Point Formation. This limited occurrence, together with associated sedimentological features such as evidence of pedogenesis and minerals such as alunite, suggests that smectite and halloysite are products of diagenesis. This is discussed below.

9.3 Diagenetic History

Smectite is the dominant clay mineral of fine-grained sediments in basal parts of the Robinson Point Formation which have been subject to pedogenesis. Small vertical tubes which represent burrowing by organisms, columnar structures developed as a result of illuviation of clays and distinctive yellow-orange reticulate mottling suggest that these intervals represent palaeosols. Kaolinite, illite and randomly interstratified illite-smectite clays occur in much lower proportions in these intervals compared with surrounding

sediments while smectite is generally absent from adjacent sediments. This suggests that smectite has formed by transformation of other clays, particularly randomly interstratified illite-smectite and illite which show the greatest decreases in this interval. Smectite is considered to form most readily in an environment with restricted drainage (Crawford *et al* 1983; Borchardt 1989) and such transformation to smectite is reported from swampy, poorly drained soils in many areas (for example McArthur & Bettenay 1974; Meyer & Pena Dos Reis 1985). Repeated cycles of wetting and drying also favour formation of smectite (Buol *et al* 1973). Thus soils in lower parts of the Robinson Point Formation characterised by smectite formed on alluvial plains where high water tables existed, possibly due to a relatively moist climate. Repeated cycles of wetting and drying, reflecting a fluctuating groundwater table, are also likely and would enable development of yellowish goethitic mottles. Schwertmann & Taylor (1989) indicate that goethite forms preferentially in conditions of high water activity and low temperature and this supports the suggestion that pedogenesis took place in a poorly leached environment.

In other parts of the Robinson Point Formation, features suggesting pedogenesis such as yellow-red reticulate mottling, development of columnar structures, presence of thin tubules and thin bleached intervals possibly analogous to A_2 horizons are not accompanied by smectitic clay minerals. These local environments were evidently better drained, although periodic wetting and drying continued as indicated by development of ferruginous mottling. The presence of A_2 horizons suggests limited erosion took place and that the alluvial plain was one of continual aggradation.

In the Ngaltinga Formation, intervals of clay mottled with small red blotches of hematitic iron oxides occur and may represent palaeosols. Bown & Kraus (1981; 1987) interpret similar features from Tertiary sediments in Wyoming, USA as palaeosols. The absence of other features indicative of pedogenic modification associated with these mottled intervals in the Ngaltinga Formation makes it difficult to positively determine the origin of these features. The most obvious palaeosol features in the Ngaltinga Formation are intervals of mottled carbonate which occur with occasional tubular structures thought to be of biogenic origin.

Calcareous palaeosols suggest a drier climate than that which existed during formation of palaeosols in the Robinson Point Formation.

Alunite occurs in basal parts of the Robinson Point Formation as elongate pods and thin seams associated with halloysite-indurated sandy sediments. Based on field and thin section observations these minerals are interpreted to be of diagenetic origin. Alunite and halloysite commonly show evidence of stress and precipitation in cracks and such features are thought to represent formation during exposure and desiccation of the sediments. Support for this is given by Bird *et al* (1989) who studied hydrogen isotopes from the alunite and suggested that alunite precipitated in equilibrium with evaporated meteoric waters. Compared with surrounding sediments, randomly interstratified illite-smectite and illite are depleted in intervals where halloysite is identified and this suggests that halloysite has formed through diagenesis from these clays.

Diagenetic alunite has been reported in a number of studies (King 1953; Ross *et al* 1968; Goldbery 1978; 1980; Hall 1978; Rouchy & Pierre 1987; Khalaf 1990) and in all cases is attributed to acid weathering of clays. Several sources of sulphur have been suggested including hydrogen sulphide from oil fields (Khalaf 1990), bacterial reduction in reducing environments (Goldbery 1978; 1980), bacterial reduction of sulphate evaporites (Rouchy & Pierre 1987) and pyrite from lignitic sediments (King 1953). Intervals where alunite occurs in the Noarlunga and Willunga Embayments are closely associated with palaeosols rich in smectite which have developed as a result of high water tables on alluvial plains. In such a setting, reducing conditions are likely, possibly in a swampy environment, where H_2S could be generated through reduction of sulphate in groundwaters. Bird *et al* (1989) have studied the stable-isotope composition of three alunite samples from the Noarlunga Embayment and concluded that salt spray from the ocean is the likely source of sulphur for the alunite. Thus regional groundwaters have been enriched in sulphate by oceanic spray blown inland. Alunite ultimately formed during acid weathering initiated by oxidation of the sediments and H_2S. Sulphuric acid produced at this time reacted with clays, particularly illite and randomly interstratified illite-smectite which provided a source of K. Various cations and amorphous

silica are products of this reaction (Goldbery 1978; Thiry & Milnes 1991). Oxidation of the sediments was probably initiated by a lowering of the water table and improved groundwater flow through the sediments. Petrographic evidence of formation of alunite and halloysite under conditions of desiccation supports such an origin. Rouchy & Pierre (1987) suggested a similar lowering of the water table due to local diapiric uplift to account for alunite formation in their study from Egypt. Climatic change, tectonic uplift or sea level lowering are all possible causes of lower water tables in the study area, however the present data does not enable a definite conclusion to be made regarding which of these is most likely. Si and Al released from 2:1 clay minerals during formation of alunite subsequently formed halloysite rather than kaolinite due to Si substituted Al tetrahedra being inherited from the 2:1 clay minerals (Bailey 1989).

Pink hematitic mottling is often noted in association with alunite in Quaternary sediments of the Noarlunga and Willunga Embayments. Khalaf (1990) noted similar pink colours related to alunite development in Kuwait and considered this due to abundant opaque clusters of iron oxides, usually <5μm in size, which had formed in an oxidising environment following alunite formation. Iron occurs in clay minerals, particularly illite, in significant amounts (Rengasamy *et al* 1975; Norrish & Pickering 1983) and hence following acid weathering of the clays, iron is released to groundwaters. The formation of alunite and not jarosite indicates that iron remained in a reduced state while alunite developed, as Fe^{3+} is more likely to be incorporated in the crystal structure than Al^{3+} under the prevailing temperatures and pressures (Brophy *et al* 1962). Precipitation of iron as small clusters and mottles must therefore post-date alunite formation and relate to less acidic conditions where Fe^{2+} would be readily oxidised to Fe^{3+}.

The diagenetic reactions associated with basal parts of the Robinson Point Formation to produce alunite and halloysite are related to the local environmental conditions of high water tables which enabled reducing conditions to take place. Smectite formed in poorly drained soils immediately above the water table, together with development of goethitic mottles where the level of the water table fluctuated. Following oxidation of the sediments initiated

by lower water tables, alunite and halloysite formed under acidic weathering conditions. Iron released during weathering of clays was then available to form mottles and iron-impregnated zones once the conditions became less acidic.

Ferruginous mottling is present throughout much of the alluvial sequence with small yellow-orange accumulations in fine-grained sediments and larger red mottles in porous sandy sediments. Based on petrographic evidence, iron appears to precipitate at sites of localised oxidation either along cracks in finer-grained sediments or in pores of coarser sediments. Iron mottling is generally considered to develop in soils and sediments where fluctuations of pH and Eh allow iron to be reduced and mobilised and then oxidised and precipitated (Bown & Kraus 1981; Schwertmann 1985; Schwertmann & Taylor 1989). In near-surface pedogenic environments such mottling may reflect a seasonal climate (Van Wallenburg 1973; Schwertmann & Taylor 1989), however mottling may also be produced by fluctuations in groundwater levels in deeper parts of the profile (Bown & Kraus 1981). Coventry & Williams (1984) found that mottling, and in particular gleying, usually associated with high water tables could develop under a semi-arid climate given relatively short periods of profile saturation. Perched water tables rather than high regional groundwater tables can also be responsible for mottling (Guthrie & Hajek 1979). Thus care must be taken in interpreting conditions leading to mottle formation. They are not necessarily representative of widespread climate-induced groundwater changes, but often determined by specific local groundwater fluctuations.

The most prominent mottles in the Quaternary sequences studied occur within sandy intervals which are confined by clay-rich intervals where perched water tables could exist. Local redistribution of iron from weathering of clays within these intervals under slightly acidic conditions is the most likely source of iron for the mottles. Tardy & Nahon (1985) show that iron oxides can form mottles through replacement of kaolinite in areas of small pore size and such reactions are likely precursors to mottle formation in the Noarlunga and Willunga Embayments. Many of these mottled zones are indurated and amorphous silica released following weathering of clays and replacement by iron oxides is the most likely cause of the

induration. Silica would precipitate from solution in response to groundwater variations. Thiry & Milnes (1991) have suggested a similar mechanism for the development of some silicified zones in inland South Australia. The fluctuating groundwaters may reflect a climate with some seasonality, although as discussed above, caution must be shown when interpreting the climatic implications of local groundwater fluctuations.

Iron mottling in sandy sediments developed as a result of groundwater fluctuations in confined aquifers. Replacement of clay minerals during weathering under acidic conditions by iron oxides occurred at sites of localised oxidation. Excess cations were removed by groundwaters with silica precipitating locally in response to variable groundwater levels and resulting in induration of these intervals. Silicification therefore post-dates the initiation of mottle formation and possibly relates to a drier local environment where flow of groundwater was reduced.

9.4 Landscape History

A review of the sedimentary and diagenetic history of the Quaternary sequences from the Noarlunga and Willunga Embayments suggests that for much of the Quaternary, the region comprised a series of alluvial fans eminating from the Mt Lofty Ranges. A minor marine incursion took place early in this period, represented by the Burnham Limestone, which is interbedded with alluvial sediments at many localities. This transgression was most pronounced in the Willunga Embayment and greater rates of sediment supply to the Noarlunga Embayment may have ensured that only isolated and marginal marine conditions prevailed in this region. Further north in the Adelaide Plains Sub-Basin, a marine transgression of similar age is recognised from borehole data (Lindsay 1969). Thus an Early Pleistocene marine transgression may have been a widespread event in the St Vincent Basin.

The dominance of coarser sediments in basal parts of the Quaternary sequence represented by the Robinson Point Formation indicates that sediment supply was probably greatest during this period due either to uplift of source areas, a wet climate or combination of the two.

Subsequent sedimentation represented by thick clay-rich sequences of the Ngaltinga Formation suggests less active erosion in source areas. Pulses of coarser sediment such as channel sands and crevasse splay deposits assigned to the Snapper Point Sand Member in uppermost parts of the sequence suggest renewed erosion in source areas at this time or alternatively higher rainfalls. A migration of distributory channels across the alluvial plain could account for isolated sandy deposits within the Ngaltinga Formation, however the fact that the influx of coarser sediment is widespread throughout the area at a similar stratigraphic position argues for a regional change such as climate or tectonism.

Further confirmation of the changing nature of the sediment supply is provided by carbonate palaeosols which are preserved in the sequence and represent the introduction of material from a second sedimentary source. Phillips (1988) and Phillips & Milnes (1988) suggest that this calcareous material was derived by aeolian processes. Erosion of coastal calcareous dunes developed during lower stands of the sea is one possible source of this carbonate. It is argued elsewhere that a probable sulphur source for alunite was oceanic spray which contributed sulphate to regional groundwaters. Thus the prevailing winds have contributed first sulphate and later carbonate to the sediments through the Quaternary period where they have been important components in the diagenesis of the sequence. A more arid climate which limited leaching of carbonate from soil profiles must also have contributed to the preservation of the calcareous palaeosols.

Thus in a broad sense, a consideration of the amount and nature of sediment contributed to the embayments together with the nature of diagenetic changes to these sediments suggests a gradual change in climate during the Quaternary. High water tables leading to reducing conditions and development of smectites in palaeosols at the base of the sequence suggest relatively moist climates. A lowering of the water table when alunite formed may have resulted from a drier climate. The development of ferruginous mottling in much of the Robinson Point Formation suggests a seasonal climate with fluctuating groundwater tables. Calcareous palaeosols and reduced sediment contributions whilst the Ngaltinga Formation was deposited indicate less erosion and runoff from source areas and limited leaching of soils

in the area. The development of a thick blanket of calcareous sediment overlying the alluvial sediments reflects minimal fluvial input from inland areas and continued low leaching of soils. Thus the climate must have gradually become more arid. Zhisheng *et al* (1986) have interpreted aridity in the Murray Basin of southeastern Australia from a study of fluvio-lacustrine sediments of ancient Lake Bungunnia. They conclude that for the Quaternary period up until about 700,000 years BP the climate was relatively wet, but with some drier periods. Aridity and development of arid-zone landforms such as dunes and salt lakes became dominant after this time and in particular during the last 500,000 years. These observations support conclusions from the present study which suggest that the climate was relatively wetter during early Quaternary deposition in the Noarlunga and Willunga Embayments and that aridity increased during deposition of later sediments. Quaternary sediments in the study area have not been dated and hence no direct correlations can be made with the timescale proposed by Zhisheng *et al* (1986).

Sediments of the Robinson Point and Ngaltinga Formations are considered to have been deposited in an alluvial/fluvial environment. Comparison with previous work suggests that sedimentological features of the Quaternary sediments from the Noarlunga and Willunga Embayments are similar to those described from alluvial fan depositional systems (Allen 1965; Williams 1973; Collinson 1978; Galloway & Hobday 1983; Bridge 1984; 1985; Nickel 1985; Smith 1990). These studies show that close to the source areas, generally uplifted areas, debris flows and braided streams deposit coarse material. With increasing distance from the ranges, the amount of channel deposition and coarse sedimentation decreases with fine-grained suspended load deposits on floodplains being common. Exposure of sediments on the alluvial fans and frequent changes of stream course enable palaeosols to develop. Therefore a complex stratigraphic sequence where there is frequent lateral and vertical sediment variation results from sedimentation on alluvial fans.

In the Noarlunga and Willunga Embayments, the Robinson Point Formation represents coarser-grained facies closer to the ranges with deposition from braided and anastomosed streams. Limited erosion of sediments is indicated by widespread preservation of palaeosols

and hence a continual supply of sediment in an aggradational environment is assumed. Short periods of stasis allowed pedogenic modification of these sediments. High water tables and limited leaching, particularly in areas adjacent to the main channels, enabled diagenetic development of smectitic and halloysitic clays together with alunite. The Robinson Point Formation is widespread in the Noarlunga Embayment but occurs less frequently in present-day coastal sections of the Willunga Embayment where deposition took place on more distal parts of the fans. Sediments of the Neva Clay Member represent deposition on these more distal parts of the alluvial fans dominated by overbank and floodplain facies. Isolated channel sedimentation characterised by infrequent sandy channel and crevasse splay deposits of the Snapper Point Sand Member persisted in these parts of the fans. The dominance of this style of sedimentation throughout the region in later periods of the Quaternary suggests that supply of sediment to the embayments gradually decreased, possibly due to drier climatic conditions. Thus, while sediments of the Robinson Point Formation dominated deposition in early parts of the Quaternary, in distal portions of the alluvial fans, sediments of the Ngaltinga Formation were being deposited concurrently with coarser sediments of the Robinson Point Formation. The stratigraphy is therefore not a simple system but one in which interfingering and gradation between facies takes place.

The landscape of the region today is still one of alluvial fans draining the Mt Lofty Ranges. There is little evidence of significant deposition of sediments from streams draining across these fans and in fact stream incision and gullying is commonly observed. Bourman (1975) discusses the present-day river systems around the Fleurieu Peninsula south of Adelaide and concludes that gullying in upper reaches and minor aggradation in lower reaches of streams is widespread. This implies very limited sediment inputs from catchment areas. In earlier periods of the Quaternary, erosion in the Mt Lofty Ranges must have supplied considerably more sediment to form alluvial fans in the Noarlunga and Willunga Embayments than is presently the case. A wetter climate than the semi-arid one experienced today and/or significant uplift in the ranges brought about by tectonic activity are likely during formation of the alluvial fans during early parts of the Quaternary period.

9.5 Advances on Previous Work

An understanding of the sedimentological and diagenetic history of the Quaternary sediments from the Noarlunga and Willunga Embayments through detailed field and mineralogical observations indicates that the sediments form complex alluvial fan deposits. Previous work by Ward (1966) based on more limited information, had indicated that finer-grained sediments from this sequence were of aeolian origin. No evidence can be found to support such a contention. In addition, similar sediments from nearby areas have been considered to be fluvial in origin (Firman 1966; 1969; Sheard & Bowman 1987a; 1987b). The interpretations of Ward regarding the origins of the Quaternary sediments led to inconsistencies regarding the stratigraphy he proposed for the area. In the light of interpretations made in this thesis, modifications have been made to the stratigraphy for the region which reflect the differing facies identified in the Quaternary sequences.

Detailed mineralogical analyses have not been made in any previous study of Quaternary sediments from the Noarlunga and Willunga Embayments or nearby areas. Identification of detrital and diagenetic clay mineral suites from the study area as well as diagenetic minerals such as alunite have enabled the nature of the sedimentary environment to be better understood. The frequency of palaeosols and their changing nature through the sequence have also enabled conclusions to be drawn regarding the nature of sedimentation, potential sediment sources and possible climatic changes. Previous work has interpreted large, conspicuous, ferruginous mottles as palaeosols (Daily *et al* 1976; Firman 1981). The present study suggests that these mottles are produced by fluctuating groundwaters within confined aquifers and hence are a reflection of variation in local groundwater conditions. Mottling may not necessarily be associated with pedogenesis and therefore should not be used to define ancient land surfaces without consideration of other sedimentary and mineralogical features.

9.6 Suggestions for Future Research

In understanding the landscape history of Quaternary sediments from the Noarlunga and Willunga Embayments, one of the difficulties encountered is the lack of age control on the various sedimentary units. Thus methods for dating the sediments should be investigated to enable the timing of diagenetic events, periods of climatic change and increased tectonic activity to be more accurately identified. Such information would be useful when making comparisons between areas where similar sediments or events are identified. For example, Zhisheng *et al* (1986) have used palaeomagnetic dating techniques for Late Cainozoic sediments from the Murray Basin. Bird *et al* (1990) in their study of surficial alunite in Australia have used K/Ar techniques to date alunite. Three samples from the current study gave ages ranging from 0.7 to 1.7 Ma and it would be useful to date a wider range of alunites from the Noarlunga and Willunga Embayments selected to represent the varying stratigraphic and geographic locations in which alunite occurs. The possibility exists that there may be several phases of alunite formation related to the continuous fluctuations of groundwater tables which appear to have taken place during the Quaternary period.

Bird *et al* (1989) have also studied the hydrogen and sulphur isotopic composition of alunites in Australia including three from the present study area. These studies suggest that sulphur for the alunite was derived from sulphate salts of oceanic origin and that alunite precipitated in equilibrium with evaporated meteoric waters. A more detailed study of a wider range of alunites from the study area would determine whether all alunite had similar origins despite the variation in stratigraphic and geographic location. The model proposed in this study for formation of alunite and halloysite could then be modified based on more comprehensive data.

The study of mineralogical components of the Quaternary sediments in this thesis has been undertaken using various techniques including X-ray diffraction, optical petrology and scanning electron microscopy. On the basis of data collected using these techniques a number of mineral transformations, particularly involving clay minerals have been proposed.

More detailed mineral chemistry using the electron microprobe and transmission and analytical electron microscopes would be necessary to fully understand these alterations. Such additional detailed studies are beyond the scope of this thesis which was intended as a cross-disciplinary study of the Quaternary sequence to provide a different focus for interpretation of the origins of these sediments in comparison with the narrower studies which had been previously undertaken. Several studies (Norrish & Pickering 1983; Porrenga 1968) have suggested that diagenetic illite may form in poorly drained floodplain sediments similar to those of the Neva Clay Member. Detailed mineral chemistry could help determine whether any illite of this origin is present within the Quaternary sequence and hence enable a modification to the present conclusion that most illite is likely to be of detrital origin. For example, recent detailed work by Robertson & Eggleton (1991) has shown that halloysite tubes can form directly from kaolinite and do not necessarily require Al-substituted tetrahedra derived from 2:1 layer silicates as precursors. The present study has concluded that development of iron mottles associated with alunite and halloysite formation takes place at a later stage. Similarly, silicification of indurated and iron mottled intervals requires earlier replacement of clay minerals by iron oxides with silicification being a later diagenetic event. Detailed studies of mineral chemistry would provide a better understanding of these diagenetic transformations and confirm the order in which they take place.

REFERENCES

Abbott, P. L., Minch, J. A. & Peterson, G. L. (1976) Pre-Eocene paleosol south of Tijuana, Baja California, Mexico. *J. Sedim. Petrol.* 46, 355-361.

Aitchison, M. E., Sprigg, R. C. & Cochrane, G. W. (1954) The soils and geology of Adelaide and suburbs. *Bull., geol. Surv. S. Aust.* 32.

Allen, B. L. & Hajek, B. F. (1989) Mineral occurrences in soil environments. *In*: Dixon, J. B. & Weed, S. E. (Eds.) *Minerals in Soil Environments* (2nd Ed.), SSSA, Madison, WI, 199-278.

Allen, J. R. L. (1965) A review of the origin and characteristics of Recent alluvial sediments. *Sedimentology* 5, 89-191.

Allen, J. R. L. (1974) Studies in fluviatile sedimentation: implications of pedogenic carbonate units, Lower Old Red Sandstone, Anglo-Welsh outcrop. *Geol. J.* 9, 181-208.

Anand, R. R. & Gilkes, R. J. (1984) Weathering of hornblende, plagioclase and chlorite in meta-dolerite, Australia. *Geoderma* 34, 261-280.

Anand, R. R., Gilkes, R. J., Armitage, T. M. & Hillyer, J. W. (1985) Feldspar weathering in lateritic saprolite. *Clays Clay Miner.* 33, 31-43.

Ataman, G. & Gokcen, S. L. (1975) Determination of source and paleoclimate from the comparison of grain and clay fractions in sandstones: a case study. *Sediment. Geol.* 13, 81-107.

Atkinson, C. D. (1986) Tectonic control on alluvial sedimentation as revealed by an ancient catena in the Capella Formation (Eocene) of northern Spain. *In*: Wright, V. P. (Ed.) *Paleosols, their recognition and interpretation.* Blackwell Scientific Publications, Oxford, 139-179.

Avery, B. W. & Bullock, P. (1977) Mineralogy of clayey soils in relation to soil classification. *Soil Survey Tech. Monograph* 10, Soil Survey of England and Wales.

Bailey, S. W. (1980) Structures of layer silicates. *In*: Brindley, G. W. & Brown, G. (Eds.) *Crystal structures of clay minerals and their X-ray identification.* Mineralogical Society Monograph 5, London, 1-123.

Bailey, S. W. (1989) Halloysite: A critical assessment. *In: 9th International Clay Program and Abstracts, Int. Clay Conf., Strasbourg, 1989.*

Barnhisel, R. I. & Bertsch, P. M. (1989) Chlorites and hydroxy-interlayered vermiculite and smectite. *In*: Dixon, J. B. & Weed, S. E. (Eds.) *Minerals in Soil Environments* (2nd Ed.), SSSA, Madison, WI, 729-788.

Bear, F. E. (1964) *Chemistry of the Soil.* Reinhold Publ. Corp., New York.

Belperio, A. P., Smith, B. W., Polach, H. A., Nittrouer, C. A., DeMaster, D. J., Hails, J. R. & Gostin, V. A. (1984) Chronological studies of the Quaternary marine sediments of northern Spencer Gulf, South Australia. *Marine Geol.* 61, 265-296.

Besly, B. M. & Fielding, C. R. (1989) Paleosols in Westphalian coal-bearing and red-bed sequences, central and northern England. *Palaeogeogr. Palaeoclimatol. Palaeoecol.* 70, 303-330.

Bird, M. I., Andrew, A. S., Chivas, A. R. & Lock, D. E. (1989) An isotopic study of surficial alunite in Australia. 1. Hydrogen and sulphur isotopes. *Geochim. Cosmochim. Acta.* 53, 3223-3237.

Bird, M. I., Chivas, A. R. & McDougall, I. (1990) An isotopic study of surficial alunite in Australia. 2. Potassium-argon geochronology. *Chem. Geol. (Isotope Geoscience Section)* 80, 133-145.

Birkeland, P. W. (1969) Quaternary paleoclimatic implications of soil-clay mineral distribution in a Sierra Nevada-Great Basin transect. *J. Geol.* 77, 289-302.

Blodgett, R. H. (1988) Calcareous paleosols in the Triassic Dolores Formation, southwestern Colorado. *In*: Reinhardt, J. & Sigleo, W. R. (Eds.) *Paleosols and weathering through geologic time: principles and applications.* Geol. Soc. Am. Sp. Paper 216, 103-121.

Borchardt, G. (1989) Smectites. *In*: Dixon, J. B. & Weed, S. E. (Eds.) *Minerals in Soil Environments* (2nd Ed.), SSSA, Madison, WI, 675-727.

Borchardt, G., Jackson, M. L. & Hole, F. D. (1966) Expansible layer silicate genesis in soils depicted in mica pseudomorphs. *In*: Heller, L. & Weiss, A. (Eds.) *Proc. Int. Clay Conf. 1966*, Vol. 1, Isr. Prog. Sci. Trans., Jerusalem, 175-185.

Bourman, R. P. (1972) Geomorphic aspects of the Onkaparinga drainage system, South Australia. *Taminga* 9, 117-143.

Bourman, R. P. (1975) Environmental geomorphology: Examples from the area south of Adelaide. *Proc. R. Geog. Soc. Aust. (SA Branch)* 76, 1-23.

Bourman, R. P. (1989) Investigation of ferricretes and weathered zones in parts of southern and southeastern Australia - a reassessment of the 'laterite' concept. Unpubl. PhD Thesis, Univ. of Adelaide.

Bowler, J. M. (1982) Aridity in the late Tertiary and Quaternary of Australia. *In*: Barker, W. R. & Greenslade, P. J. M. (Eds.) *Evolution of the Flora and Fauna of Arid Australia.* Peacock, Adelaide, 35-44.

Bowler, J. M., Hope, G. S., Singh, G. & Walker, D. (1976) Late Quaternary climates of Australia and New Guinea. *Quat. Res.* 6, 359-394.

Bown, T. M. & Kraus, M. J. (1981) Lower Eocene alluvial paleosols (Willwood Formation, northwest Wyoming, USA) and their significance for paleoecology, paleoclimatology and basin analysis. *Palaeogeogr. Palaeoclimatol. Palaeoecol.* 34, 1-30.

Bown, T. M. & Kraus, M. J. (1987) Integration of channel and floodplain suites. I. Developmental sequence and lateral relations of alluvial paleosols. *J. Sedim. Petrol.* 57, 587-601.

Bridge, J. S. (1984) Large scale facies sequences in alluvial overbank environments. *J. Sedim. Petrol.* 54, 583-588.

Bridge, J. S. (1985) Paleochannel patterns inferred from alluvial deposits: a critical evaluation. *J. Sedim. Petrol.* 55, 579-589.

Brill, B. A. (1988) Illite crystallinity, b_o and Si content of K-white mica as indicators of metamorphic conditions in low-grade metamorphic rocks at Cobar, NSW. *Aust. J. Earth Sci.* 35, 295-302.

Brindley, G. W. & Brown, G. (1980) *Crystal structures of clay minerals and their X-ray identification.* Mineralogical Society Monograph 5, London.

Brophy, G. P., Scott, E. S. & Snellgrove, R. A. (1962) Sulphate studies II: Solid solution between alunite and jarosite. *Am. Mineral.* 47, 112-126.

Brothers, R. N. (1954) The relative Pleistocene chronology of the South Kaipara district, New Zealand. *Trans. R. Soc. N. Z.*, 82, 677-694.

Buol, S. W., Hole, F. D. & McCracken, R. J. (1973) *Soil Genesis and Classification.* Ames, Iowa State Univ. Press.

Buurman, P. (1975) Possibilities of paleopedology. *Sedimentology* 22, 289-298.

Buurman, P. (1980) Paleosols in the Reading Beds (Paleocene) of Alum Bay, Isle of Wight, UK. *Sedimentology* 27, 593-606.

Callen, R. A. (1976) The stratigraphy, sedimentology and uranium deposits of Tertiary rocks: Lake Frome area, South Australia. Unpubl. M.Sc. Thesis, Univ. of Adelaide.

Callen, R. A. (1977) Late Cainozoic environments of parts of northeastern South Australia. *J. geol. Soc. Aust.* 24, 151-169.

Callen, R. A. & Tedford, R. H. (1976) New Late Cainozoic rock units and depositional environments, Lake Frome area, South Australia. *Trans. R. Soc. S. Aust.* 100, 125-168.

Campana, B. & Wilson, R. B. (1953) The geology of the Jervis and Yankalilla Military sheets. *Rep. Invest., geol. Surv. S. Aust.* 3.

Cent, J. & Brewer, R. (1971) Preparation of thin sections of soil materials using synthetic resins. *CSIRO Div. Soils, Tech. Pap.* 7.

Chamley, H. (1979) North Atlantic clay sedimentation and paleoenvironment since the Late Jurassic. *In*: Talwani, M., Hay, W. & Ryan, W. B. F. (Eds) *Deep drilling results in the Atlantic Ocean: Continental margins and paleoenvironments.* Am. Geophys. Union, Washington, DC, 342-360.

Chamley, H. (1989) *Clay Sedimentology.* Springer, Heidelberg.

Churchman, G. J., Whitton, J. S., Claridge, G. G. C. & Theng, B. K. G. (1984) Intercalation method using formamide for differentiating halloysite from kaolinite. *Clays Clay Miner.* 32, 241-248.

Churchman, G. J. & Gilkes, R. J. (1989) Recognition of intermediates in the possible transformation of halloysite to kaolinite in weathering profiles. *Clay Minerals* 24, 579-590.

Collinson, J. D. (1978) Alluvial sediments. *In*: Reading, H. G. (Ed.) *Sedimentary Environments and Facies.* Blackwell Scientific Publications, Oxford, 15-60.

Cooper, B. J. (1979) Eocene to Miocene stratigraphy of the Willunga Embayment. *Rep. Invest., geol. Surv. S. Aust.* 50.

Cooper, B. J. (1985) The Cainozoic St Vincent Basin - tectonics, structure, stratigraphy. *Spec. Publ., S. Aust. Dept. Mines and Energy* 5, 35-49.

Cornelius, H. S. (1927) The Onkaparinga Coal Mining Syndicate. *Min. Rev. Adelaide* 45, 102-103.

Coventry, R. J. & Williams, J. (1984) Quantitative relationships between morphology and current soil hydrology in some alfisols in semi-arid tropical Australia. *Geoderma* 33, 191-218.

Crawford, A. R. (1965) The geology of Yorke Peninsula. *Bull., geol. Surv. S. Aust.* 39.

Crawford, T. W. Jr., Whittig, L. D., Begg, E. L. & Huntington, G. L. (1983) Eolian influence on development and weathering of some soils of Point Reyes Peninsula, California. *Soil Sci. Soc. Am.* J. 47, 1179-1185.

Crespin, I. (1954) Stratigraphy and micropalaeontology of the marine Tertiary rocks between Adelaide and Aldinga, South Australia. *Rep. Bur. Miner. Resour. Geol. Geophys. Aust.* 12.

Crocker, R. L. (1946) Post-Miocene climatic and geologic history and its significance in relation to the genesis of the major soil types of South Australia. *CSIR Aust. Bull.* 193.

Daily, B., Firman, J. B., Forbes, B. G. & Lindsay, J. M. (1976) Geology. *In*: Twidale, C. R., Tyler, M. J. & Webb, B. P. (Eds.) *Natural History of the Adelaide Region.* R. Soc. S. Aust., Adelaide, 5-42.

Daily, B., Milnes, A. R., Twidale, C. R. & Bourne, J. A. (1979) Geology and Geomorphology. *In*: Tyler, M. J., Twidale, C. R. & Ling, J. K. (Eds.) *Natural History of Kangaroo Island.* R. Soc. S. Aust., Adelaide, 1-38.

Day, R. P. (1965) Particle fractionation and particle size analysis. *In*: Black, C. A. *et al* (Eds.) *Methods of Soil Analysis, Part 1.* Am. Soc. Agron., Madison, Wisc., 545-567.

Deer, W. A., Howie, R. A. & Zussman, J. (1962) *Rock forming minerals, Vol. 3, Sheet silicates*. Longmans, Green & Co. Ltd., London.

Dickinson, S. B. (1943) Alunite deposits near Angepena Station, North Flinders Range. *Min. Rev.* 79, 108.

Dixon, J. B. (1989) Kaolin and serpentine group minerals. *In*: Dixon, J. B. & Weed, S. E. (Eds.) *Minerals in Soil Environments* (2nd Ed.), SSSA, Madison, WI, 467-525.

Dixon, J. B. & McKee, T. R. (1974) Spherical halloysite formation in a volcanic soil of Mexico. *Trans., Int. Congr. Soil Sci., 10th, 1974 (Moscow)*, 7, 115-124.

Dudas, M. J. & Harward, M. E. (1975) Weathering and authigenic halloysite in soil developed in Mazama ash. *Soil Sci. Soc. Am. Proc.* 39, 561-566.

Eberl, D. D. (1984) Clay mineral formation and transformation in rocks and soils. *Phil. Trans. R. Soc. Lond.* A311, 241-257.

Fairbridge, R. W. (1961) Eustatic changes in sea level. *In*: Ahrens, L. H. *et al* (Eds.) *Physics of the Earth*, v.4, Pergamon, London.

Falvey, D. A. & Mutter, J. C. (1981) Regional plate tectonics and the evolution of Australia's passive continental margins. *BMR J. Aust. Geol. Geophys.* 6, 1-29.

Fanning, D. S. & Jackson, M. L. (1965) Clay mineral weathering in southern Wisconsin soils developed in loess and in shale-derived till. *Clays Clay Miner.* 13, 175-191.

Fanning, D. S., Keramidas, V. Z. & El-Desoky, M. A. (1989) Micas. *In*: Dixon, J. B. & Weed, S. E. (Eds.) *Minerals in Soil Environments* (2nd Ed.), SSSA, Madison, WI, 551-634.

Fielding, C. R. (1986) Fluvial channel and overbank deposits from the Westphalian of the Durham coalfield, northeast England. *Sedimentology* 33, 119-140.

Firman, J. B. (1963) Quaternary geological events near Port Adelaide. *Quart. geol. Notes, geol. Surv. S. Aust.* 7.

Firman, J. B. (1965) Late Cainozoic lacustrine deposits in the Murray Basin, South Australia. *Quart. geol. Notes, geol. Surv. S. Aust.* 16, 1-2.

Firman, J. B. (1966) Stratigraphic units of Late Cainozoic age in St Vincent Basin, South Australia. *Quart. geol. Notes, geol. Surv. S. Aust.* 17, 6-9.

Firman, J. B. (1967) Stratigraphy of Late Cainozoic deposits in South Australia. *Trans. R. Soc. S. Aust.* 91, 165-178.

Firman, J. B. (1969) Stratigraphy and landscape relations of soil materials near Adelaide, South Australia. *Trans. R. Soc. S. Aust.* 93, 39-54.

Firman, J. B. (1976) Limestone at the base of the Pleistocene sequence in South Australia. *Quart. geol. Notes, geol. Surv. S. Aust.* 58, 2-5.

Firman, J. B. (1981) Regional stratigraphy of the regolith on the southwestern margin of the Great Australian Basin province, South Australia. *Dept. Mines & Energy S. Aust. Rep.* Bk. 81/40.

Forbes, B. G. (Compiler), (1983) *Noarlunga* map sheet, *Geological Atlas of South Australia*, 1:50 000 series. Geol. Surv. S. Aust.

Foscolos, A. E. & Kodama, H. (1974) Diagenesis of clay minerals from Lower Cretaceous shales of northeastern British Columbia. *Clays Clay Miner.* 22, 319-335.

Friend, P. F. (1978) Distinctive features of some ancient river systems. *In*: Miall, A. D. (Ed.) *Fluvial Sedimentology*. Mem. Can. Soc. Petrol. Geol., Calgary 5, 531-543.

Friend, P. F. (1983) Towards the field classification of alluvial architecture or sequence. *Spec. Publ. Int. Ass. Sediment.* 6, 345-354.

Friend, P. F. & Moody-Stuart, M. (1972) Sedimentation of the Wood Bay Formation (Devonian) of Spitsbergen: regional analysis of a late orogenic basin. *Norsk Polarinstitutt skrifter* 157, 1-77.

Galloway, W. E. & Hobday, D. K. (1983) Terriginous clastic depositional systems. *Applications to petroleum, coal and uranium exploration.* Springer-Verlag, New York.

Garrels, R. M. & Christ, C. L. (1965) *Solutions, minerals and equilibria.* Harper & Row, New York.

Geological Survey of South Australia (1982) Geological map of South Australia, 1:2 000 000 scale.

Gibbs, R. J. (1967) Clay mineral mounting techniques for X-ray diffraction analysis: a discussion. *J. Sedim. Petrol.* 38, 242-243.

Gibbs, R. J. (1977) Clay mineral segregation in the marine environment. *J. Sedim. Petrol.* 47, 237-243.

Glaessner, M. F. (1951) Three foraminiferal zones in the Tertiary of Australia. *Geol. Mag.* 88, 273-283.

Glaessner, M. F. (1953) Conditions of Tertiary sedimentation in southern Australia. *Trans. R. Soc. S. Aust.* 76, 141-146.

Glaessner, M. F. & Wade, M. (1958) The St Vincent Basin. *J. geol. Soc. Aust.* 5, 115-126.

Goldbery, R. (1978) Early diagenetic, non-hydrothermal Na-alunite in Jurassic flint-clays, Makhtesh Ramon, Israel. *Bull., geol. Soc. Am.* 89, 687-698.

Goldbery, R. (1980) Early diagenetic Na-alunites in Miocene algal mat intertidal facies, Ras Sudar, Sinai. *Sedimentology* 27, 189-198.

Grim, R. E. (1968) *Clay Mineralogy.* McGraw-Hill, New York.

Guthrie, R. L. & Hajek, B. F. (1979) Morphology and water regime of a Dothan soil. *Soil Sci. Soc. Am. Proc.* 43, 142-144.

Hall, R. B. (1978) World non-bauxite aluminium resources: alunite. *U. S. geol. Surv., Prof. Pap.* 1076-A.

Harris, W. K. (1985) Middle to Late Eocene depositional cycles and dinoflagellate zones in southern Australia. *Spec. Publ., S. Aust. Dept. Mines and Energy* 5, 133-144.

Hemley, J. J., Hostetler, P. B., Gude, A. J. & Mountjoy, W. T. (1969) Some stability relationships of alunite. *Econ. Geol.* 64, 599-610.

Howchin, W. (1923) A geological sketch-section of the sea cliffs on the eastern side of Gulf St Vincent, from Brighton to Sellicks Hill with descriptions. *Trans. R. Soc. S. Aust.* 47, 279-315.

Howchin, W. (1935) Notes on the geological sections obtained by several borings situated on the plain between Adelaide and Gulf St Vincent, Part I. *Trans. R. Soc. S. Aust.* 59, 68-102.

Howchin, W. (1936) Notes on the geological sections obtained by several borings situated on the plain between Adelaide and Gulf St Vincent, Part II - Cowandilla (Government) Bore. *Trans. R. Soc. S. Aust.* 60, 1-34.

Hower, J., Eslinger, E. V., Hower, M. E. & Perry, E. A. (1976) Mechanisms of burial metamorphism of argillaceous sediment. 1. Mineralogical and chemical evidence. *Bull., geol. Soc. Am.* 87, 725-737.

Huang, P. M. (1966) Mechanism of neutral fluoride interaction with soil clay minerals and silica solubility scale for silicates common in soils. Unpubl. PhD Thesis, Univ. of Wisconsin-Madison. (cited in Borchardt, G., 1989).

Hutton, J. T. & Dixon, J. C. (1981) The chemistry and mineralogy of some South Australian calcretes and associated soft carbonates and their dolomitisation. *J. geol. Soc. Aust.* 28, 71-79.

Ismail, F. T. (1970) Biotite weathering and clay formation in arid and humid regions, California. *Soil Sci.* 109, 257-261.

Jack, R. L. (1914) Alunite in South Australia. Locality - Mt Lofty Ranges. *Rev. Min. Ops.* 19, 39-43.

Jack, R. L. (1915) Alunite discovery on Section 310, Hundred of Napperby. *Rev. Min. Ops.* 21, 25-27.

Jack, R. L. (1918) Alunite deposits, Section A, Hundred of Ramsey. *Min. Rev.* 28, 51-53.

Jackson, M. L. (1965) Clay transformations in soil genesis during the Quaternary. *Soil Sci.* 99, 15-22.

Jackson, M. L. (1968) Weathering of primary and secondary minerals in soils. *Trans. Int. Congr. Soil Sci., 9th* (Adelaide, Aust.) 4, 281-292.

Jackson, R. G. (1976) Depositional model of point bars in the Lower Wabash River. *J. Sedim. Petrol.* 46, 579-594.

Jacobs, M. B. & Hays, J. D. (1972) Paleoclimatic events indicated by changes in deep-sea sediments. *J. Sedim. Petrol.* 42, 889-989.

Jeans, C. V., Merriman, R. J., Mitchell, J. G. & Bland, D. J. (1982) Volcanic clays in the Cretaceous of southern England and Northern Ireland. *Clay Miner.* 17, 105-156.

Jones, J. B. & Segnit, E. R. (1971) The nature of opal. I. Nomenclature and constituent phases. *J. geol. Soc. Aust.* 18, 57-68.

Keller, W. D. (1964) The origin of high-alumina clay minerals - A review. *Clays Clay Miner.* 16, 129-151.

Keller, W. D., Gentile, R. J. & Reesman, A. L. (1967) Allophane and Na-rich alunite from kaolinitic nodules in shale. *J. Sedim. Petrol.* 37, 215-220.

Kerr-Grant, C. (1956) The Adelaide earthquake of 1st March, 1954. *Trans. R. Soc. S. Aust.* 79, 177-185.

Khalaf, F. I. (1990) Diagenetic alunite in clastic sequences, Kuwait, Arabian Gulf. *Sedimentology* 37, 155-164.

King, D. (1953) Origin of alunite deposits at Pidinga, South Australia. *Econ. Geol.* 48, 689-703.

Kisch, H. J. (1980) Illite crystallinity and coal rank associated with lowest grade metamorphism of the Taveyanne greywacke in the Helvetic zone of the Swiss Alps. *Eclogae Geologicae Helveticae* 73, 753-777.

Kisch, H. J. (1983) Mineralogy and petrology of burial diagenesis and incipient metamorphism in clastic rocks. *In*: Larson, G. & Chillingar, G. V. (Eds.) *Developments in Sedimentology, Vol. 25B*, Elsevier, Amsterdam, 289-493.

Komarneni, S., Jackson, M. L. & Cole, D. R. (1985) Oxygen isotope changes during mica alteration. *Clays Clay Miner.* 33, 214-218.

Kraus, M. J. (1987) Integration of channel and floodplain suites. II. Vertical relations of alluvial paleosols. *J. Sedim. Petrol.* 57, 602-612.

Kubler, B. (1967) La cristallinite d'illite et les zones tout a fait superieur du metamorphisme. *In: Colloque sur les Etages Tectoniques a la Baconniere*, 105-122, Neuchatel, Paris.

Last, W. M. (1990) Lacustrine dolomite - an overview of modern, Holocene and Pleistocene occurrences. *Earth Sci. Rev.* 27, 221-263.

Lawrence, C. R. (1966) Cainozoic stratigraphy and structure of the Mallee region, Victoria. *Trans. R. Soc. Vic.* 79, 517-535.

Lawrence, C. R. (1976) Murray Basin. *In*: Douglas, J. G. & Ferguson, J. A. (Eds.) Geology of Victoria, Chap. 9, Quaternary. *Spec. Publ., geol. Soc. Aust.* 5, 275-327.

Leeder, M. R. (1976) Palaeogeographic significance of pedogenic carbonates in the topmost Old Red Sandstone of the Scottish Border Basin. *Geol. J.* 11, 21-28.

Lindsay, J. M. (1969a) Foraminifera and stratigraphy of the type section of Port Willunga Beds, Aldinga Bay, South Australia. *Trans. R. Soc. S. Aust.* 91, 93-110.

Lindsay, J. M. (1969b) Cainozoic foraminifera and stratigraphy of the Adelaide Plains Sub-Basin, South Australia. *Bull., geol. Surv. S. Aust.* 42.

Lindsay, J. M. (1970) Melton Limestone: Multiple Mid-Tertiary transgressions, south eastern Gawler Platform. *Quart. geol. Notes, geol. Surv. S. Aust.* 33, 2-10.

Lindsay, J. M. & Williams, A. J. (1977) Oligocene marine transgression at Hartley and Monarto, southwestern margin of the Murray Basin. *Quart. geol. Notes, geol. Surv. S. Aust.* 64, 9-16.

Ludbrook, N. H. (1963) Correlation of the Tertiary rocks of South Australia. *Trans. R. Soc. S. Aust.* 87, 5-15.

Ludbrook, N. H. (1980) *A guide to the geology and mineral resources of South Australia.* Geol. Surv. S. Aust., Govt. Printer, Adelaide.

Ludbrook, N. H. (1983) Molluscan faunas of the Early Pleistocene Point Ellen Formation and Burnham Limestone, South Australia. *Trans. R. Soc. S. Aust.* 107, 37-50.

McArthur, W. M. & Bettenay, E. (1974) The development and distribution of the soils of the Swan Coastal Plain, Western Australia. *Soil Publ., CSIRO, Aust.* 16.

McKeague, J. A. & Day, J. H. (1966) Dithionite and oxalate-extractable Fe and Al as aids in differentiating various classes of soils. *Can. J. Soil Sci.* 46, 13-22.

Macleod, D. A. & Vita-Finzi, C. (1982) Environment and provenance in the development of recent alluvial deposits in Epirus, northwest Greece. *Earth Surf. Proc. Landforms* 7, 29-43.

Mawson, D. (1907) Mineralogical notes: Barytes sand crystals at Hallett's Cove. *Trans. R. Soc. S. Aust.* 31, 119-120.

May, R. I. & Bourman, R. P. (1984) Coastal landslumping in Pleistocene sediments at Sellicks Beach, South Australia. *Trans. R. Soc. S. Aust.* 108, 85-94.

Meyer, R. (1976) Continental sedimentation, soil genesis and marine transgression in the basal beds of the Cretaceous in the east of the Paris Basin. *Sedimentology* 23, 235-253.

Meyer, R. & Pena Dos Reis, R. B. (1985) Paleosols and alunite silcretes in continental Cenozoic of western Portugal. *J. Sedim. Petrol.* 55, 76-85.

Miles, K. R. (1952) Geology and underground water resources of the Adelaide Plains area. *Bull., geol. Surv. S. Aust.* 27.

Millott, G. (1964) Translated by Farrant, W. R. & Paquet, H. (1970) *Geology of Clays.* Springer-Verlag, New York.

Milnes, A. R., Compston, W. & Daily, B. (1977) Pre to syn-tectonic emplacement of Early Palaeozoic granites in southeastern South Australia. *J. geol. Soc. Aust.* 24, 87-106.

Milnes, A. R. & Hutton, J. T. (1983) Calcretes in Australia. *In: Soils: An Australian Viewpoint*, CSIRO, Melbourne, 119-162.

Milnes, A. R., Ludbrook, N. H., Lindsay, J. M. & Cooper, B. J. (1983) The succession of Cainozoic marine sediments on Kangaroo Island, South Australia. *Trans. R. Soc. S. Aust.* 107, 1-35.

Milnes, A. R., Bourman, R. P. & Fitzpatrick, R. W. (1985a) Petrology and mineralogy of 'laterites' in southern and eastern Australia and South Africa. *Proc. Int. Seminar on Laterite*, Oct. 14-17, 1985, Tokyo, Japan.

Milnes, A. R., Bourman, R. P. & Northcote, K. H. (1985b) Field relationships of ferricretes and weathered zones in southern South Australia: A contribution to 'laterite' studies in Australia. *Aust. J. Soil Res.* 23, 441-465.

Milnes, A. R. & Ludbrook, N. H. (1986) Provenance of microfossils in aeolian calcarenites and calcretes in southern South Australia. *Aust. J. Earth Sci.* 33, 145-159.

Mitchell, B. D., Farmer, V. C. & McHardy, W. J. (1964) Amorphous inorganic materials in soils. *Adv. Agron.* 16, 327-383.

Nadeau, P. H., Wilson, M. J., McHardy, W. J. & Tait, J. M. (1985) The conversion of smectite to illite during diagenesis: Evidence from some illitic clays from bentonites and sandstones. *Mineral. Mag.* 49, 393-400.

Nemecz, E. & Vardju, G. (1967) Relationships between 'flintclay' and bauxite formation in the Pilis Mountains. *Acad. Sci. Hungaricae Acta Geol.* 11, 453-473.

Nickel, E. (1985) Carbonates in alluvial fan systems, an approach to physiography, sedimentology and diagenesis. *Sediment. Geol.* 42, 83-104.

Norrish, K. (1973) Factors in the weathering of mica to vermiculite. *In*: Serratosa, J. M. (Ed.) *1972 Proc. Int. Clay Conf., Div. de Ciencias, Madrid*, 417-432.

Norrish, K. & Taylor, R. M. (1961) The isomorphous replacement of iron by aluminium in soil goethites. *J. Soil Sci.* 12, 294-306.

Norrish, K. & Hutton, J. T. (1969) An accurate X-ray spectrographic method for the analysis of a wide range of geological samples. *Geochim. Cosmochim. Acta.* 33, 431-453.

Norrish, K. & Pickering, J. G. (1977) Clay mineralogic properties. *In*: Russell, J. S. & Greacen, E. L. (Eds.) *Soil Factors in Crop Production in a Semi-arid Environment.* Uni. of Queensland Press.

Norrish, K. & Pickering, J. G. (1983) Clay minerals. *In*: *Soils: An Australian Viewpoint*, CSIRO, Melbourne, 281-308.

Northcote, K. H. (1976) Soils. *In*: Twidale, C. R., Tyler, M. J. & Webb, B. P. (Eds.) *Natural History of the Adelaide Region*, R. Soc. S. Aust., Adelaide, 61-74.

Norton, L. D., Bigham, J. M., Hall, G. F. & Smeck, N. E. (1983) Etched thin sections for coupled optical and electron microscopy and micro-analysis. *Geoderma* 30, 55-64.

Offler, R. & Fleming, P. D. (1968) A synthesis of folding and metamorphism in the Mt Lofty Ranges, South Australia. *J. geol. Soc. Aust.* 15, 245-266.

Parker, A. J., Fanning, C. M. & Flint, R. B. (1985) Geology. *In*: Twidale, C. R., Tyler, M. J. & Davies, M. (Eds.) *Natural History of Eyre Peninsula*, R. Soc. S. Aust., Adelaide, 21-45.

Patterson, S. H. & Murray, H. H. (1984) Kaolin, refractory clay, ball clay and halloysite in North America, Hawaii and the Caribbean region. *U. S. geol. Surv., Prof. Pap.* 1306.

Pearson, M. J. (1990) Clay mineral distribution and provenance in Mesozoic and Tertiary mudrocks of the Moray Firth and northern North Sea. *Clay Miner.* 25, 519-541.

Phillips, S. E. (1988) The interaction of geological, geomorphic and pedogenic processes in the genesis of calcrete. Unpubl. PhD Thesis, Univ. of Adelaide.

Phillips, S. E. & Milnes, A. R. (1988) The Pleistocene terrestrial carbonate mantle on the southeastern margin of the St Vincent Basin, South Australia. *Aust. J. Earth Sci.* 35, 463-481.

Picard, M. D. & High, L. R. (1972) Criteria for recognising lacustrine rocks. *In*: Rigby, J. K. & Hamblin, W. K. (Eds.) *Recognition of ancient sedimentary environments.* Soc. Econ. Paleon. Miner., Spec. Pub. 16, 108-145.

Picard, M. D. & High, L. R. (1981) Physical stratigraphy of ancient lacustrine deposits. *In*: Ethridge, F. G. & Flores, R. M. (Eds.) *Recent and ancient non-marine depositional environments: Models for exploration.* Soc. Econ. Paleon. Miner., Spec. Pub. 31, 233-259.

Porrenga, D. A. (1968) Non-marine glauconitic illite in the Lower Oligocene of Aardedrug, Belgium. *Clay Miner.* 7, 421-430.

Preiss, W. V. (Compiler) (1987) The Adelaide Geosyncline - late Proterozoic stratigraphy, sedimentation, palaeontology and tectonics. *Bull., geol. Surv. S. Aust.* 53.

Raven, M. D. (1990) XPLOT Version 3.2, User Manual. Manipulation of X-ray powder diffraction data. *CSIRO Div. Soils, Tech. Mem.* 24/1990.

Rengasamy, P., Krishna Murti, G. S. R. & Sarma, V. A. K. (1975) Isomorphous substitution of iron for aluminum in some soil kaolinites. *Clays Clay Miner.* 23, 211-214.

Retallack, G. J. (1976) Triassic palaeosols in the upper Narrabeen Group of NSW. Part I: Features of the palaeosols. *J. geol. Soc. Aust.* 23, 383-399.

Retallack, G. J. (1977) Triassic palaeosols in the upper Narrabeen Group of NSW. Part II: Classification and reconstruction. *J. geol. Soc. Aust.* 24, 19-36.

Retallack, G. J. (1983) A paleopedological approach to the interpretation of terrestrial sedimentary rocks. The mid-Tertiary fossil soils of Badlands National Park, South Dakota. *Bull., geol. Soc. Am.* 94, 823-840.

Retallack, G. J. (1986) Fossil soils as grounds for interpreting long-term controls on ancient rivers. *J. Sedim. Petrol.* 56, 1-18.

Retallack, G. J. (1988) Field recognition of paleosols. *In*: Reinhardt, J. & Sigleo, W. R. (Eds.) *Paleosols and weathering through geologic time: principles and applications.* Geol. Soc. Am., Spec. Paper 216, 1-20.

Reynolds, M. A. (1953) The Cainozoic succession of Maslin and Aldinga Bays, South Australia. *Trans. R. Soc. S. Aust.* 76, 114-140.

Reynolds, R. C. (1980) Interstratified clay minerals. *In*: Brindley, G. W. & Brown, G. (Eds.) *Crystal structures of clay minerals and their X-ray identification.* Mineralogical Society Monograph 5, London, 249-303.

Reynolds, R. C. & Hower, J. (1970) The nature of interlayering in mixed-layer illite-montmorillonites. *Clays Clay Miner.* 18, 25-36.

Rich, C. I. (1968) Hydroxy interlayers in expansible layer silicates. *Clays Clay Miner.* 16, 15-30.

Riley, G. (1973) The use of Scotchcast No. 3 as an impregnating medium for soils. *CSIRO Div. Soils, Tech. Mem.* 53/1973.

Robert, C. & Chamley, H. (1990) Paleoenvironmental significance of clay mineral associations at the Cretaceous - Tertiary passage. *Palaeogeogr. Palaeoclimatol. Palaeoecol.* 79, 205-219.

Robertson, I. D. M. & Eggleton, R. A. (1991) Weathering of granitic muscovite to kaolinite and halloysite and of plagioclase-derived kaolinite to halloysite. *Clays Clay Miner.* 39, 113-126.

Ross, C. S. & Kerr, P. F. (1934) Halloysite and allophane. *U. S. geol. Surv., Prof. Pap.* 185-G.

Ross, C. S., Bergquist, H. R., Monroe, W. H., Fahey, J. J. & Ross, M. (1968) Natroalunite in upper Cretaceous sedimentary rocks of north-central Texas. *J. Sedim. Petrol.* 38, 1155-1165.

Rouchy, J. M. & Pierre, C. (1987) Authigenic natroalunite in middle Miocene evaporites from the Gulf of Suez (Gemsa, Egypt). *Sedimentology* 34, 807-812.

Sawhney, B. L. (1989) Interstratification in layer silicates. *In*: Dixon, J. B. & Weed, S. E. (Eds.) *Minerals in Soil Environments* (2nd Ed.), SSSA, Madison, WI, 790-828.

Schulze, D. G. (1989) An introduction to soil mineralogy. *In*: Dixon, J. B. & Weed, S. E. (Eds.) *Minerals in Soil Environments* (2nd Ed.), SSSA, Madison, WI, 1-34.

Schwertmann, U. (1964) The differentiation of iron oxide in soils by a photochemical extraction with acid ammonium oxalate. *Z. Pflanzenerahr. Dung. Bodenkunde* 105, 194-201.

Schwertmann, U. (1985) The effect of pedogenic environments on iron oxide minerals. *In*: *Advances in Soil Science*, Vol. 1, 172-196, Springer-Verlag, New York.

Schwertmann, U. & Taylor, R. M. (1989) Iron Oxides. *In*: Dixon, J. B. & Weed, S. E. (Eds.) *Minerals in Soil Environments* (2nd Ed.), SSSA, Madison, WI, 379-438.

Segnit, R. W. (1939) The Precambrian-Cambrian successions. *Bull., geol. Surv. S. Aust.* 18.

Selby, J. & Lindsay, J. M. (1982) Engineering geology of the Adelaide city area. *Bull., geol. Surv. S. Aust.* 51.

Self, P. G. (1989) PC-PW1800 User Manual. PC-based system for the control of a Philips PW1800 X-ray diffraction system. *CSIRO Div. Soils Tech. Mem.* 1/1989.

Sheard, M. J. & Bowman, G. M. (1987a) Definition of the Keswick Clay, Adelaide/Golden Grove Embayment, Para and Eden Blocks, South Australia. *Quart. geol. Notes, geol. Surv. S. Aust.* 103, 4-9.

Sheard, M. J. & Bowman, G. M. (1987b) Redefinition of the upper boundary of the Hindmarsh Clay, Adelaide Plains Sub-Basin and Adelaide/Golden Grove Embayment. *Quart. geol. Notes, geol. Surv. S. Aust.* 103, 9-16.

Singer, A. (1975) A Cretaceous laterite in the Negev Desert, southern Israel. *Geol. Mag.* 112, 151-162.

Singer, A. (1980) The paleoclimatic interpretation of clay minerals in soils and weathering profiles. *Earth Sci. Rev.* 15, 303-327.

Singer, A. (1984) The paleoclimatic interpretation of clay minerals in sediments - a review. *Earth Sci. Rev.* 21, 251-293.

Slansky, E. (1983) Halloysite in a weathered profile at Port Macquarie, New South Wales. *Trans. R. Soc. S. Aust.* 107, 177-185.

Smith, D. G. (1983) Anastomosed fluvial deposits: modern examples from western Canada. *Spec. Publ. Int. Ass. Sediment.* 6, 155-168.

Smith, D. G. & Putnam, P. E. (1980) Anastomosed river deposits: modern and ancient examples in Alberta, Canada. *Can. J. Earth Sci.* 17, 1396-1406.

Smith, R. M. H. (1990) Alluvial paleosols and pedofacies sequences in the Permian Lower Beaufort of the southwestern Karoo Basin, South Africa. *J. Sedim. Petrol.* 60, 258-276.

Sprigg, R. C. (1942) The geology of the Eden-Moana fault block. *Trans. R. Soc. S. Aust.* 66, 185-214.

Sprigg, R. C. (1946) Reconnaissance geological survey of portion of the western escarpment of the Mount Lofty Ranges. *Trans. R. Soc. S. Aust.* 70, 313-347.

Srodon, J. (1984) X-ray powder diffraction identification of illitic materials. *Clays Clay Miner.* 32, 337-349.

Srodon, J. & Eberl, D. D. (1984) Illite. *In*: Bailey, S. W. (Ed.) *Micas, Reviews in Mineralogy*, Vol. 13. Mineral. Soc. Am., Washington, DC., 495-544.

Stephenson, A. E. (1986) Lake Bungunnia: a Plio-Pleistocene megalake in southern Australia. *Palaeogeogr. Palaeoclimatol. Palaeoecol.* 57, 137-156.

Stephenson, A. E. & Brown, C. M. (1989) The ancient Murray River system. *BMR J. Aust. Geol. Geophys.* 11, 387-395.

Stuart, W. J. (1969) Stratigraphic and structural development of the St Vincent Tertiary Basin, South Australia. Unpubl. PhD Thesis, Univ. of Adelaide.

Stuart, W. J. (1970) The Cainozoic stratigraphy of the eastern coastal area of Yorke Peninsula, South Australia. *Trans. R. Soc. S. Aust.* 94, 151-178.

Sutton, D. J. & White, R. E. (1968) The seismicity of South Australia. *J. geol. Soc. Aust.* 15. 25-32.

Tardy, Y. & Nahon, D. (1985) Geochemistry of laterites, stability of Al-goethite, Al-hematite, and Fe^{3+}-kaolinite in bauxites and ferricretes: an approach to the mechanism of concretion formation. *Am. J. Sci.* 285, 865-903.

Tate, R. (1878) Notes on the correlation of the coral-bearing strata of South Australia, with a list of fossils occurring in the colony. *Trans. Proc. Phil. Soc. Adelaide*, 1877-78, 120-123.

Tate, R. (1882) Notes on the Tertiary strata beneath Adelaide. *Trans. R. Soc. S. Aust.* 5, 40-43.

Tate, R. (1890) The stratigraphical relations of the Tertiary formations about Adelaide, with especial reference to the Croydon Bore. *Trans. R. Soc. S. Aust.* 13, 180-184.

Taylor, J. K., Thompson, B. P. & Shepherd, R. G. (1974) The soils and geology of the Adelaide area. *Bull., geol. Surv. S. Aust.* 46.

Theng, B. K. G., Churchman, G. J., Whitton, J. S. & Claridge, G. G. C. (1984) Comparison of intercalation methods for differentiating halloysite from kaolinite. *Clays Clay Miner.* 32, 249-258.

Thiry, M. & Milnes, A. R. (1991) Pedogenic and groundwater silcretes at Stuart Creek opal field, South Australia. *J. Sedim. Petrol.* 61, 111-127.

Tomita, K., Takahashi, H. & Watanabe, T. (1988) Quantitative curves for mica/smectite interstratification by X-ray powder diffraction. *Clays Clay Miner.* 36, 258-262.

Torrent, J., Guzmann, R. & Parra, M. A. (1982) Influence of relative humidity on the crystallisation of Fe(III) oxides from ferrihydrite. *Clays Clay Miner.* 30, 337-340.

Twidale, C. R. (1976) Geomorphological evolution. *In*: Twidale, C. R., Tyler, M. J. & Webb, B. P. (Eds.) *Natural History of the Adelaide Region.* R. Soc. S. Aust., Adelaide, 43-60.

Twidale, C. R., Daily, B. & Firman, J. B. (1967) Eustatic and climatic history of the Adelaide area, South Australia - a discussion. *J. Geol.* 75, 237-242.

Van Wallenburg, C. (1973) Hydromorphic soil characteristics in alluvial soils in connection with soil drainage. *In*: Schlichting, E. & Schwertmann, U. (Eds.) *Pseudogley and gley-genesis and use of hydromorphic soils*. Trans. Comm. V & VI, Int. Soc. Soil Sci. Verlag Chemie, Weinheim, 393-403.

von der Borch, C. C. (1965) The distribution and preliminary geochemistry of modern carbonate sediments of the Coorong area, South Australia. *Geochim. Cosmochim. Acta* 29, 781-799.

von der Borch, C. C. (1976) Stratigraphy and formation of Holocene dolomitic carbonate deposits of the Coorong area, South Australia. *J. Sedim. Petrol.* 46, 952-966.

von der Borch, C. C. & Lock, D. (1979) Geological significance of Coorong dolomites. *Sedimentology* 26, 813-824.

von der Borch, C. C., Lock, D. & Schwebel, D. (1975) Groundwater formation of dolomite in the Coorong region of South Australia. *Geology* 3, 283-285.

Ward, L. K. (1917) The Stuart's Range opal field. *Min. Rev.* 25.

Ward, W. T. (1965) Eustatic and climatic history of the Adelaide area, South Australia. *J. Geol.* 73, 592-602.

Ward, W. T. (1966) Geology, geomorphology and soils of the south-western part of County Adelaide, South Australia. *Soil Publ., CSIRO Aust.* 23.

Ward, W. T. (1967) The Adelaide area: A reply. *J. Geol.* 75, 352-357.

Weaver, C. E. (1956) The distribution and identification of mixed-layer clays in sedimentary rocks. *Am. Mineral.* 41, 202-221.

Weaver, C. E. (1960) Possible uses of clay minerals in search for oil. *Bull., Am. Assoc. Petrol. Geol.* 44, 1505-1518.

Webber, H. M. & Wilson, A. L. (1964) The absorptiometric determination of silicon in water. IV: Method for determining 'reactive' silicon in power station waters containing phosphate. *Analyst* 89, 632-641.

Williams, G. E. (1969) Glacial age of piedmont alluvial deposits in the Adelaide area, South Australia. *Aust. J. Sci.* 32, 257.

Williams, G. E. (1973) Late Quaternary piedmont sedimentation, soil formation and paleoclimates in arid South Australia. *Z. Geomorph.* 17, 102-125.

Wilson, A. M. (1981) Calcrete profiles near Bakara and Bow Hill in western Murray Basin, South Australia. Unpubl. BA (Hons) Thesis, Dept. Soil Sci., Univ. of Adelaide.

Wilson, M. J. & Nadeau, P. H. (1985) Interstratified clay minerals and weathering processes. *In*: Drever, J. I. (Ed.) *The Chemistry of Weathering*. D. Reidel, Dordrecht, Netherlands, 97-118.

Wopfner, H. (1972) Depositional history and tectonics of South Australian sedimentary basins. *Min. Resour. Rev. S. Aust.* 133, 32-50.

Wright, V. P. (1982) Calcrete paleosols from the Lower Carboniferous, Llanelly Formation, South Wales. *Sediment. Geol.* 33, 1-33.

Wright, V. P. (1986) *Paleosols their recognition and interpretation.* Blackwell Scientific Pub., Oxford.

Zalba, P. E. (1982) Scan electron micrographs of clay deposits of Buenos Aires Province, Argentina. *In*: Van Olphen, H. & Veniale, F. (Eds.) *Developments in Sedimentology* 35, 7th Int. Clay Conf., Bologna and Pavia, Italy, Sept. 6-12, 1981, 513-528.

Zeuner, F. E. (1959) *The Pleistocene Period.* Hutchinson, London.

Zhisheng, A., Bowler, J. M., Opdyke, N. D., Macumber, P. G. & Firman, J. B. (1986) Palaeomagnetic stratigraphy of Lake Bungunnia; Plio-Pleistocene precursor of aridity in the Murray Basin, southeastern Australia. *Palaeogeogr. Palaeoclimatol. Palaeoecol.* 54, 219-239.

FIGURES

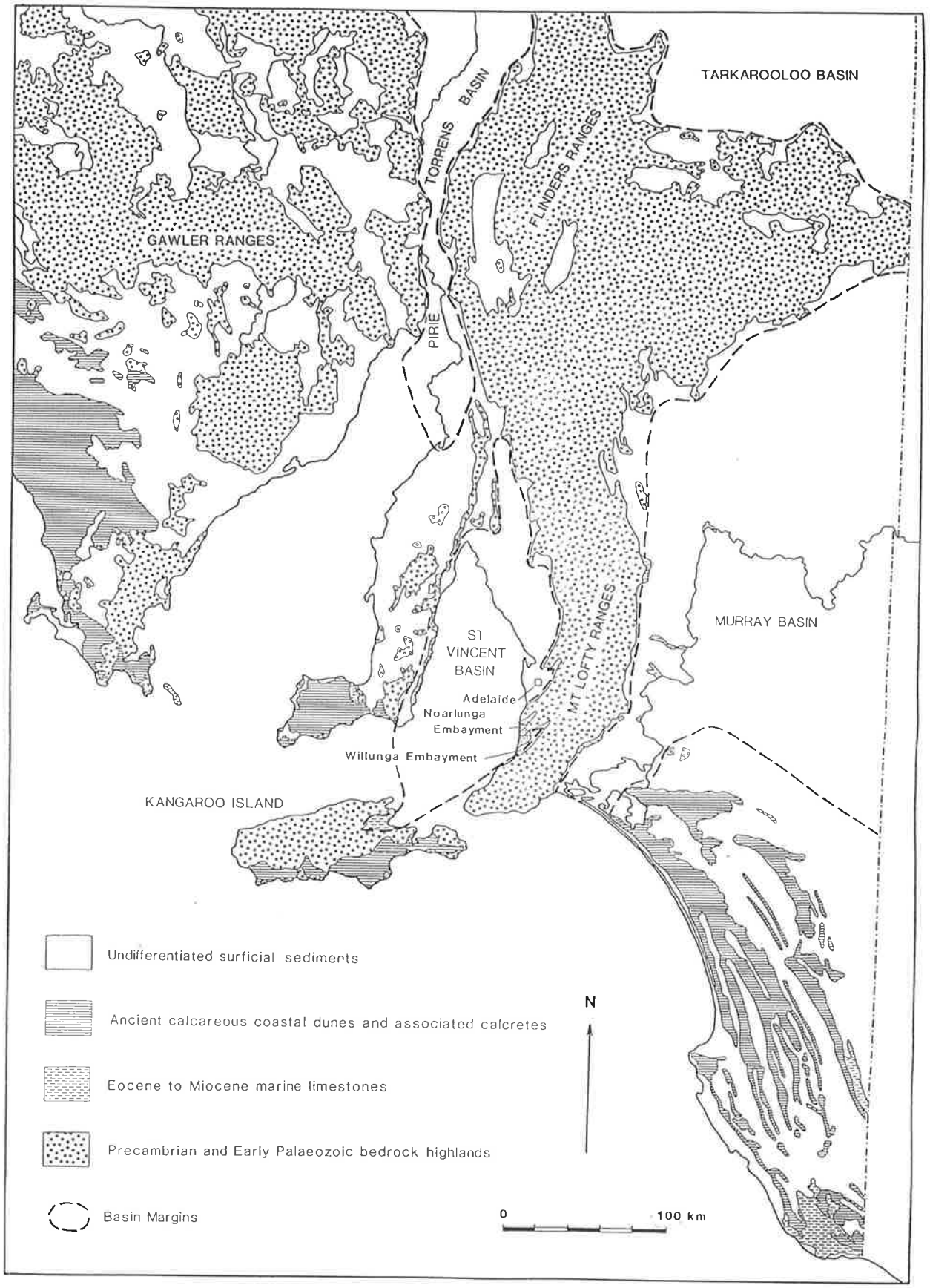

Figure 1.1 Map of southern South Australia showing generalised geology. (Source: Geological Survey of South Australia, 1982)

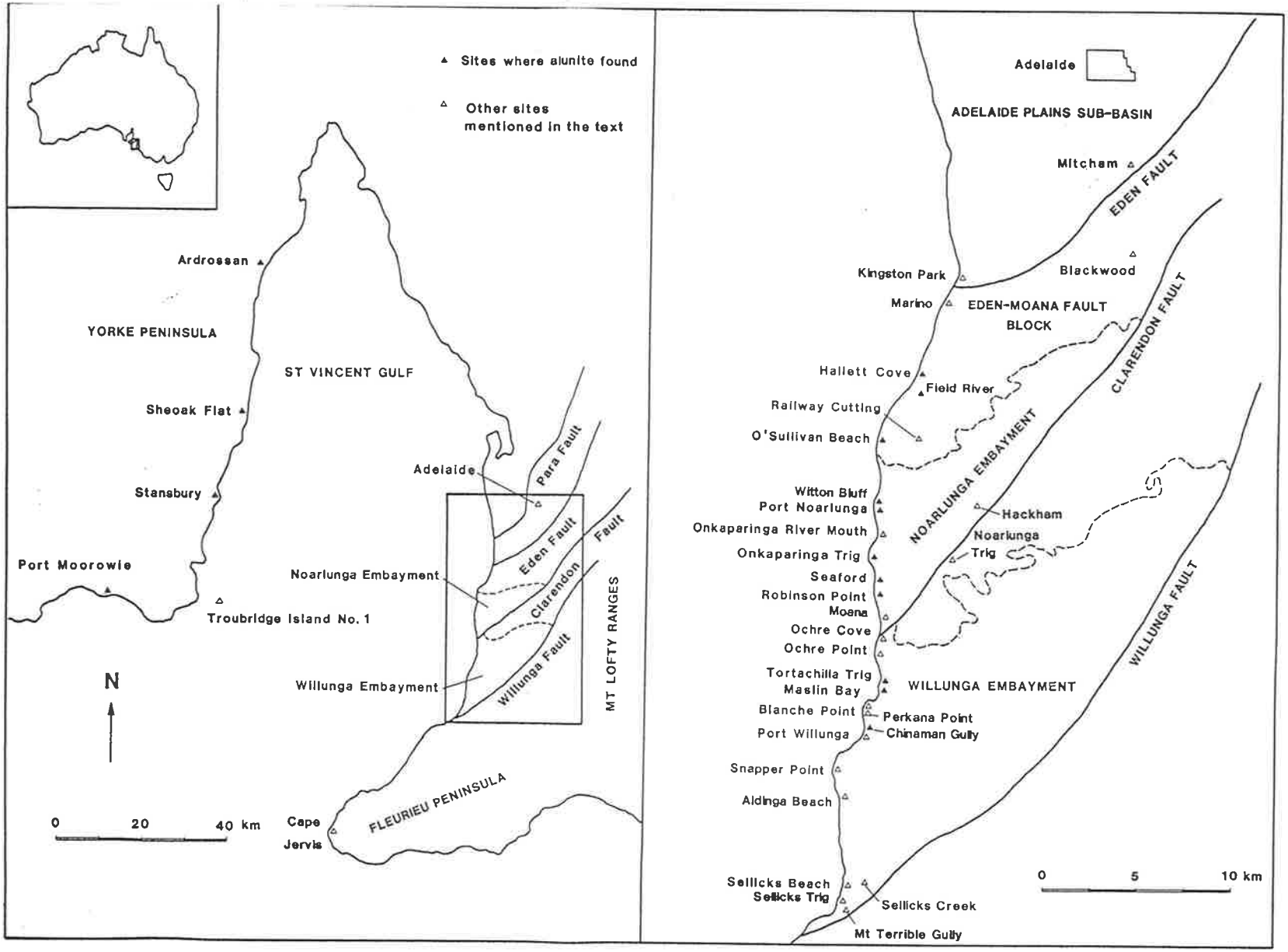

Figure 1.2 Map of the St Vincent Basin area of southern South Australia showing localities mentioned in the text. Sites where alunite has been observed are shown by the filled triangles, while open triangles indicate other sites mentioned in the text.

Figure 3.1 Burnham Limestone at Sellicks Beach. Upper surface of the Tertiary Port Willunga Formation (T) is overlain by sandy and clayey sediments in which three gravel bands are present (G). Hammer (28 cm long) rests on the Burnham Limestone. A sketch section of this interval is provided in Figure 3.2.

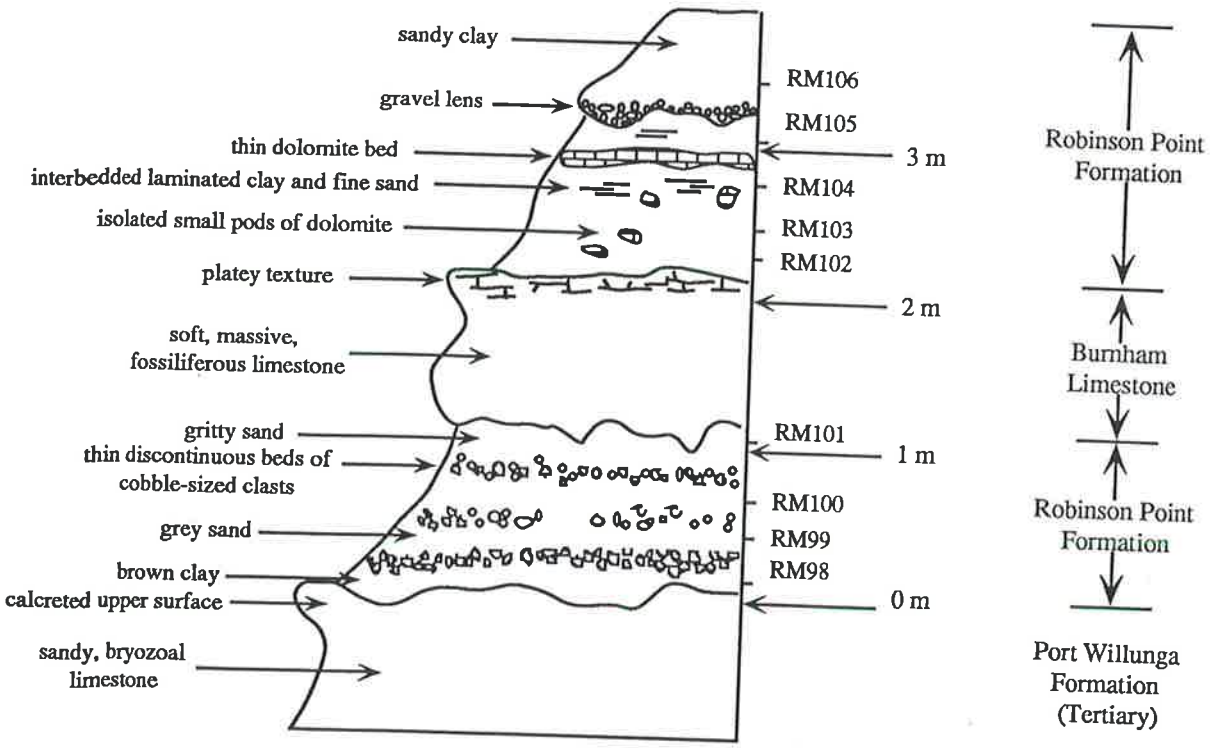

Figure 3.2 Sketch section of the interval containing the Burnham Limestone at Sellicks Beach. Sample locations (see Appendix 1 for details) and interpreted stratigraphy are shown.

Figure 3.3 Coastal cliffs at Sellicks Beach which are up to 50 m in height and comprise coarse-grained alluvial sediments assigned to the Robinson Point Formation. Numerous gravel layers are interbedded with coarse sands and sandy clays. Ferruginous mottling is common throughout the sequence but most pronounced near the top of the cliffs (F). Alluvial sediments overlie marine sediments of the Tertiary Port Willunga Formation (T) and Early Pleistocene Burnham Limestone (B).

Figure 3.4 Coastal cliffs immediately south of Snapper Point. Rubbly limestone of the Burnham Limestone (B) occurs at the base of the cliff and is overlain by greenish clays of the Neva Clay Member of the Ngaltinga Formation. A thin discontinuous interval of soft, mottled carbonate (C) occurs in upper parts of the Neva Clay Member. Sands and sandy clays (S), which are mottled by iron oxides near the base, comprise the upper half to third of the cliffs and are assigned to the Snapper Point Sand Member of the Ngaltinga Formation. Calcrete layers occur at the top of the cliffs. This section is designated as the type section for the Ngaltinga Formation (see Section 3.3.2).

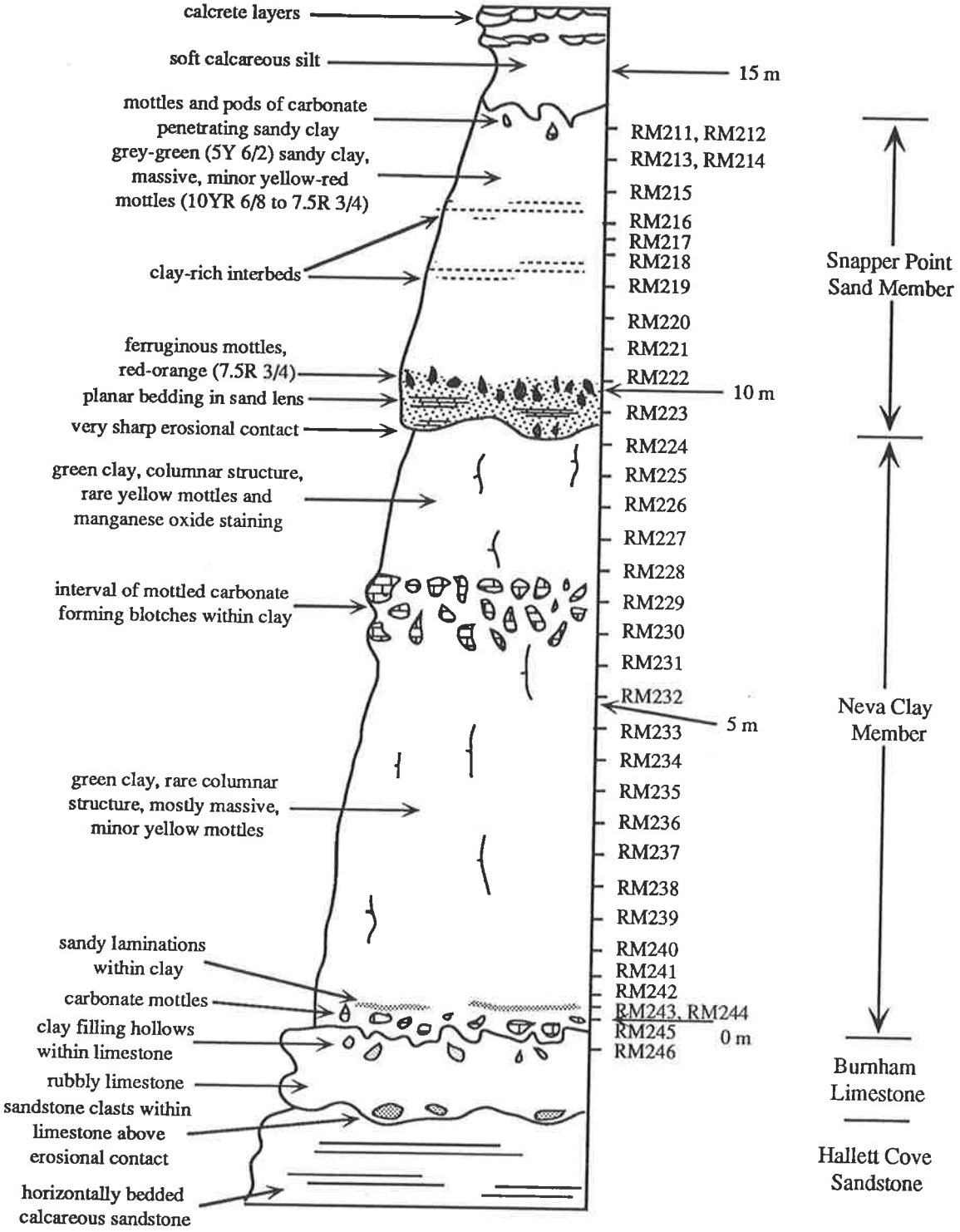

Figure 3.5: Sketch section of coastal cliffs near Snapper Point (see Figure 3.4). Sample locations (see Appendix 1 for details) and interpreted stratigraphy are shown.

Figure 3.6 Root structures which are preserved on the upper surface of the Hallett Cove Sandstone on a shore platform adjacent to the section depicted in Figure 3.4 (hammer is 28 cm long).

Figure 3.7 Coastal cliffs just north of Snapper Point where sands of the Snapper Point Sand Member (S) fill an erosional channel cut into the Neva Clay Member. The carbonate interval (C) within the upper part of the Neva Clay Member has also been eroded during formation of the channel.

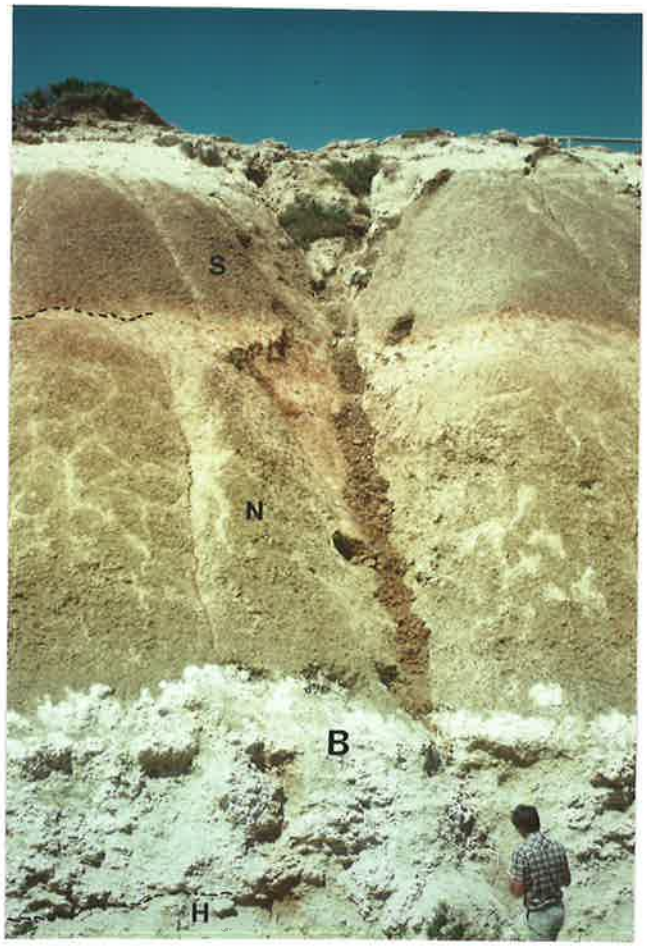

Figure 3.8 Quaternary sediments exposed in the upper part of coastal cliffs immediately south of Port Willunga kiosk. Rubbly marine sediments of the Hallett Cove Sandstone (H) and Burnham Limestone (B) are overlain by yellow-green clays assigned to the Neva Clay Member (N). These grade up to lenses of mottled sand which occur at the base of the Snapper Point Sand Member (S) which, at this locality, comprises reddish clays and sandy clays. A calcrete occurs at the top of the section.

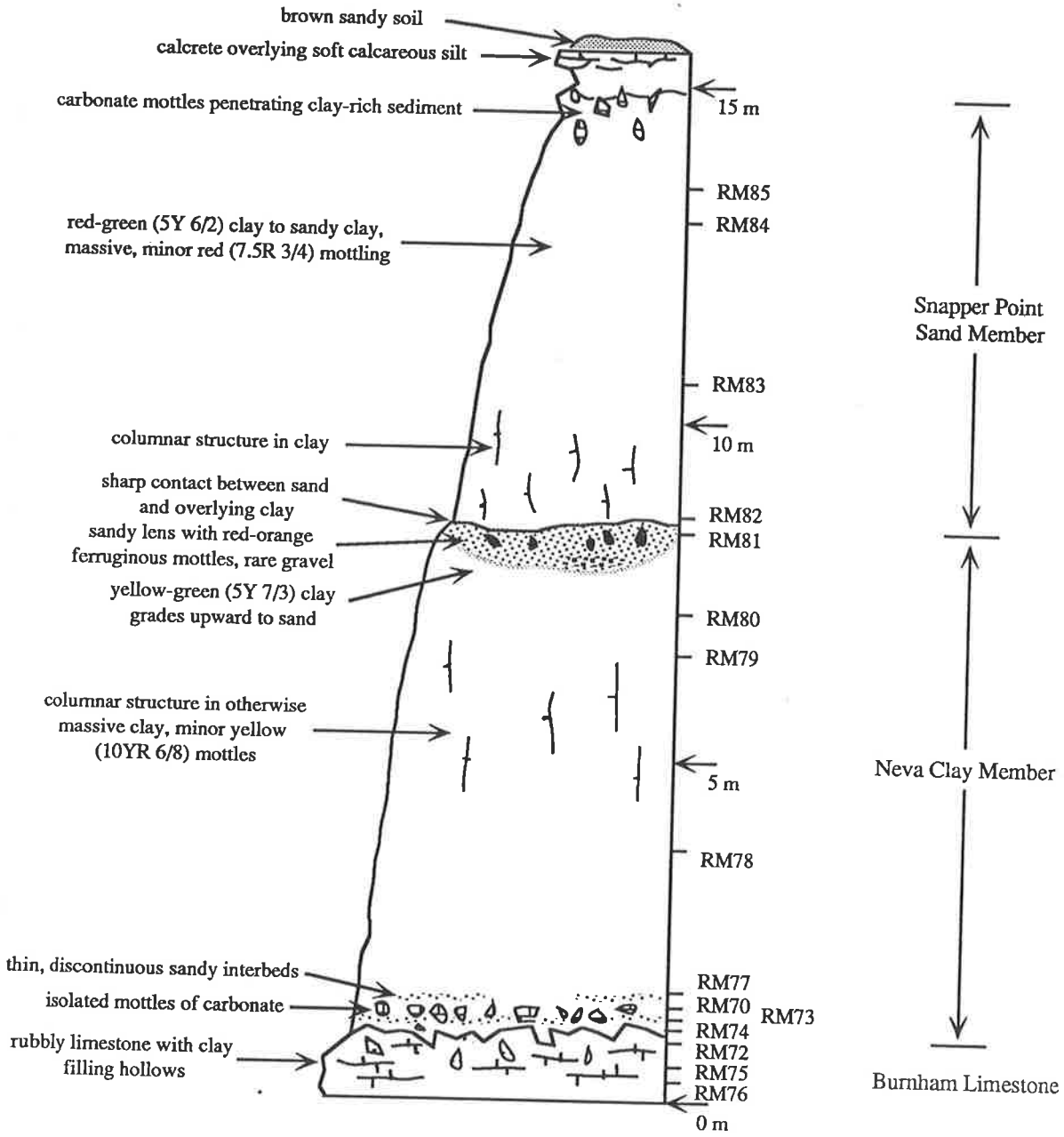

Figure 3.9: Sketch section of Quaternary sediments exposed in upper parts of the coastal cliffs in the Port Willunga area. Sample locations (see Appendix 1 for details) and interpreted stratigraphy are shown.

Figure 3.10 Coastal cliffs adjacent to Chinaman Gully. Tertiary sediments forming the base of the cliffs are mostly obscured by surface wash and slumped sediment. A strongly mottled sandy interval (F) marks the base of the Snapper Point Sand Member and overlies a thin sequence of greenish clays assigned to the Neva Clay Member (N). Calcrete occurs at the top of the cliffs.

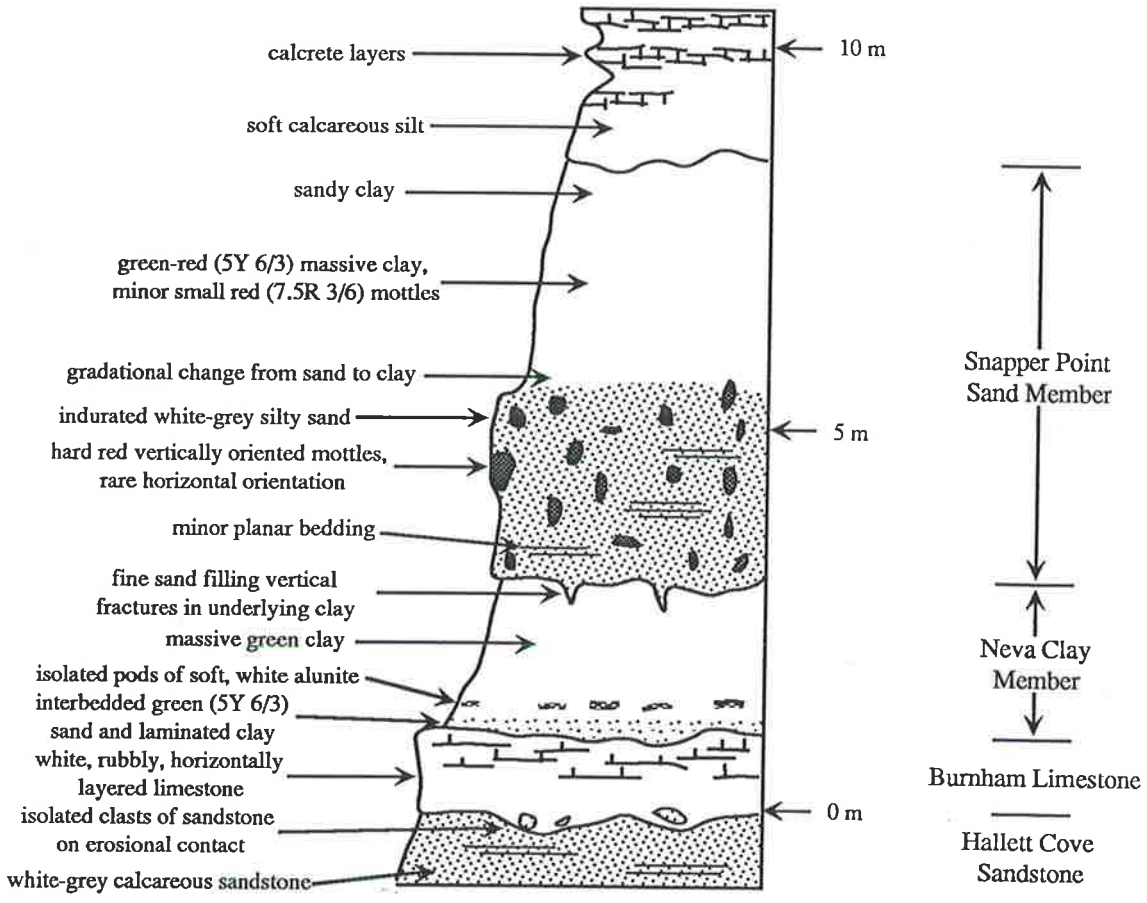

Figure 3.11: Sketch section of the upper part of coastal cliffs in the Chinaman Gully area showing the interpreted stratigraphy

Figure 3.12 Aerial view of coastal cliffs at Blanche Point. Marine sediments of Tertiary age (T) are overlain by the Hallett Cove Sandstone (H) and the Burnham Limestone (B). Non-marine sediments of the Robinson Point (R) and Ngaltinga (N) Formations are visible in the upper half of the cliffs. The Robinson Point Formation comprises a red, mottled sandy unit overlying unmottled yellowish clays and sands. The red, mottled unit appears to occur discontinuously as it is not present in central parts of the photo.

Figure 3.13 Undulating contact between sandy sediments of the Robinson Point Formation (R) and Ngaltinga Formation (N) exposed in coastal cliffs just south of Blanche Point. The base of the Robinson Point Formation is obscured by surface wash.

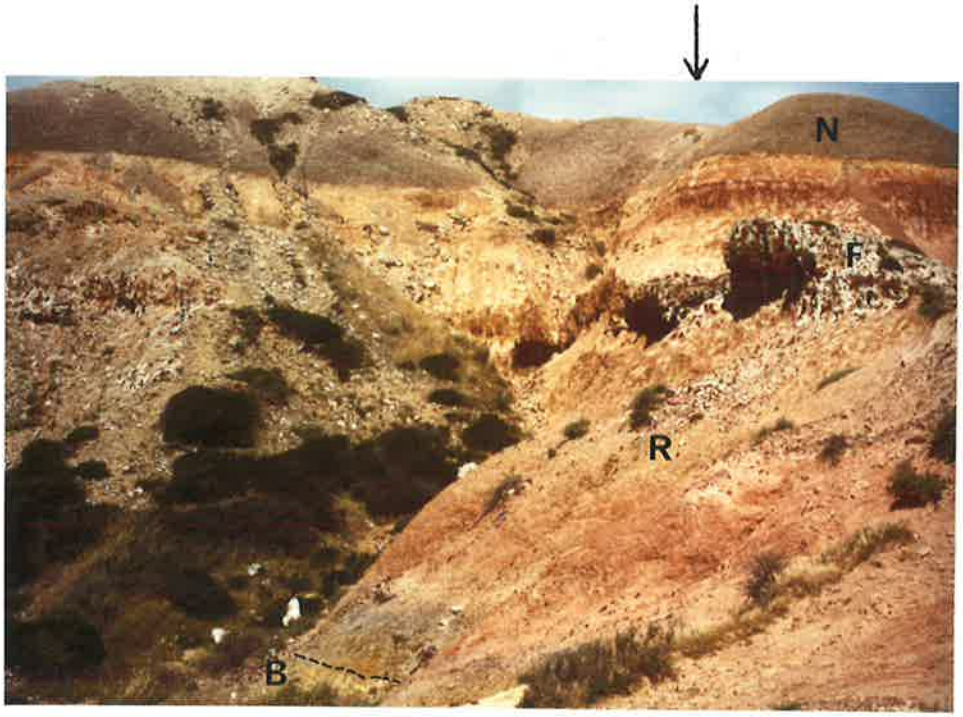

Figure 3.14 Quaternary sediments exposed in coastal cliffs at Maslin Bay, just north of the beach access track. Mottled carbonate (B) equivalent to the Burnham Limestone occurs at the base of the sequence and is overlain by sands and sandy clays of the Robinson Point Formation (R). A distinctive iron mottled unit (F) occurs within the Robinson Point Formation. Red-green clays of the Ngaltinga Formation (N) are exposed in upper parts of the sequence. The location of the sampled section depicted in Figure 3.15 is shown by the arrow.

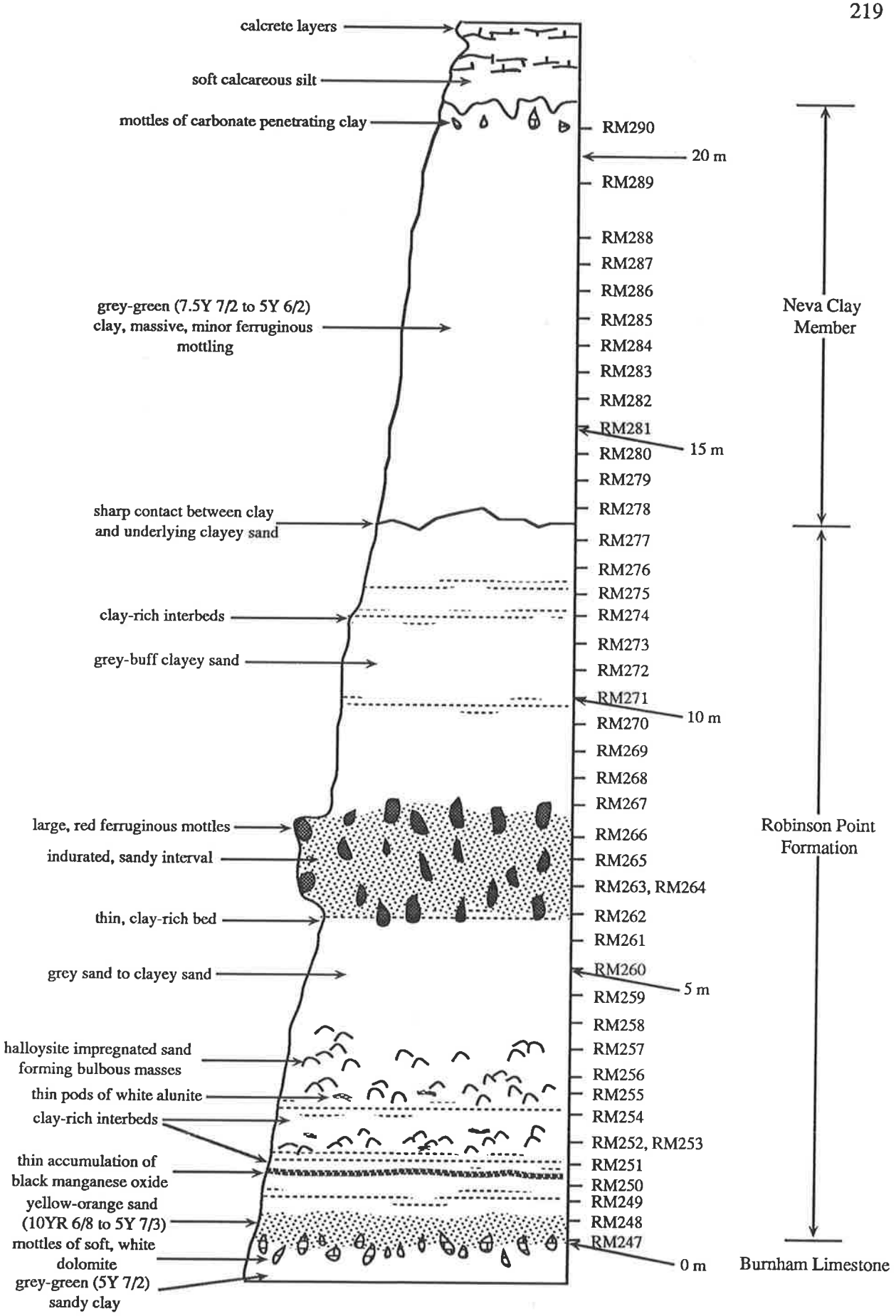

Figure 3.15: Sketch section of the Quaternary sequence exposed in coastal cliffs at Maslin Bay. Sample locations (see Appendix 1 for details) and interpreted stratigraphy are shown.

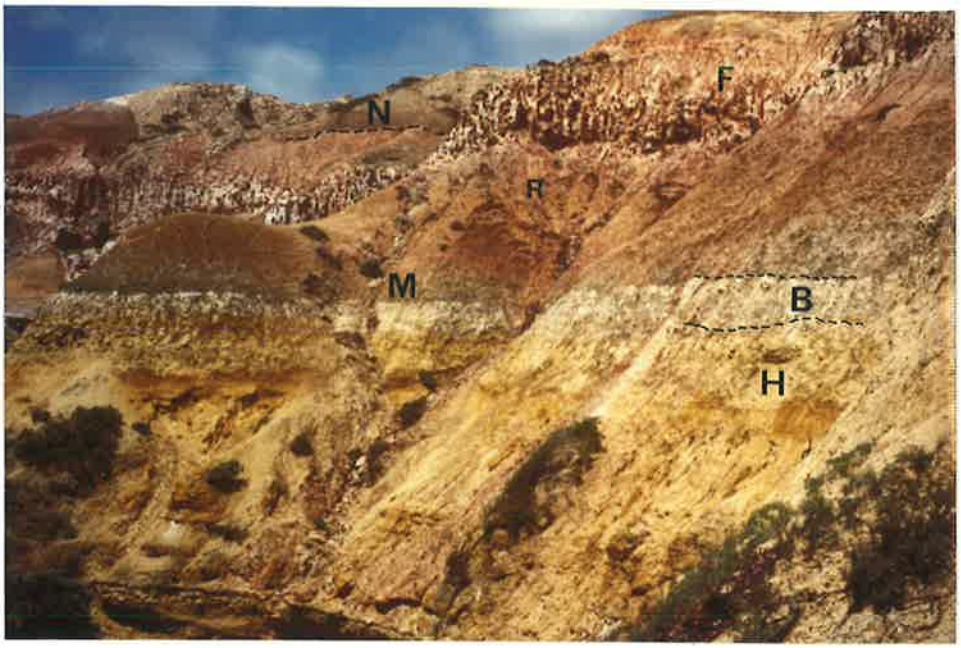

Figure 3.16 Quaternary sediments exposed in coastal cliffs adjacent to Tortachilla Trig in the Maslin Bay area. Yellowish fossiliferous sands equivalent to the Hallett Cove Sandstone (H) are overlain by mottled white dolomite equivalent to the Burnham Limestone (B). Sands and sandy clays of the Robinson Point Formation (R) include an interval rich in manganese (M) at the base and a conspicuously iron mottled unit in central parts (F). Red-green clays of the Ngaltinga Formation (N) are exposed in upper parts of the cliffs.

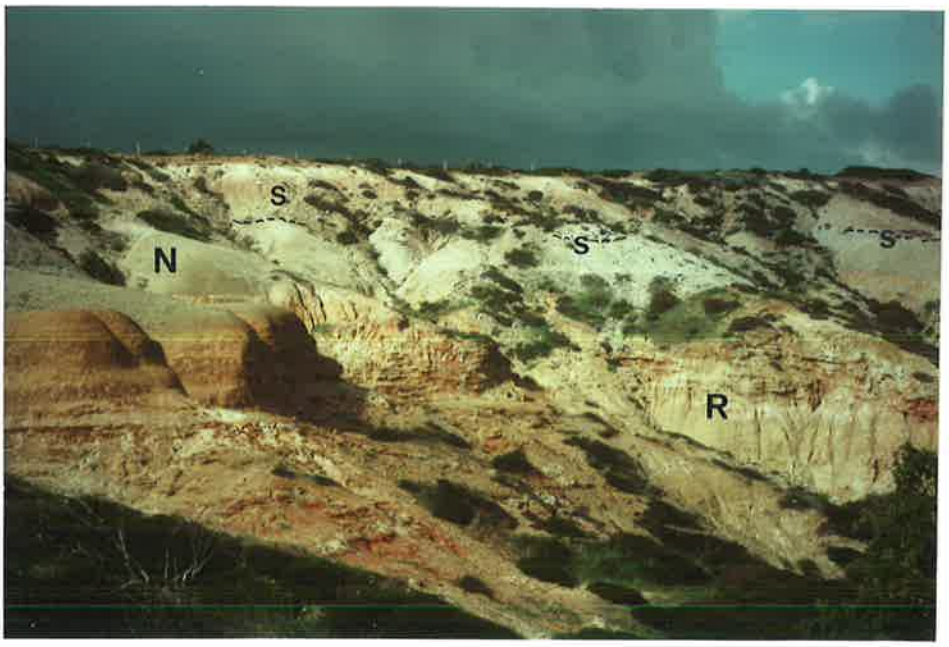

Figure 3.17 Quaternary sediments exposed in coastal cliffs near Ochre Point. Sands, gravels and sandy clays of the Robinson Point Formation (R) occupy the lower half of the section with central parts of this formation being coarser and displaying cross-bedding. Greenish clays of the Neva Clay Member (N) overlie the Robinson Point Formation with sands and brownish sandy clays of the Snapper Point Sand Member (S) occurring in upper parts of the sequence. Basal parts of the Snapper Point Sand Member are frequently indurated and mottled with iron oxides (for example on the right hand edge of photo). Calcareous sediment which includes a calcrete layer caps the sequence.

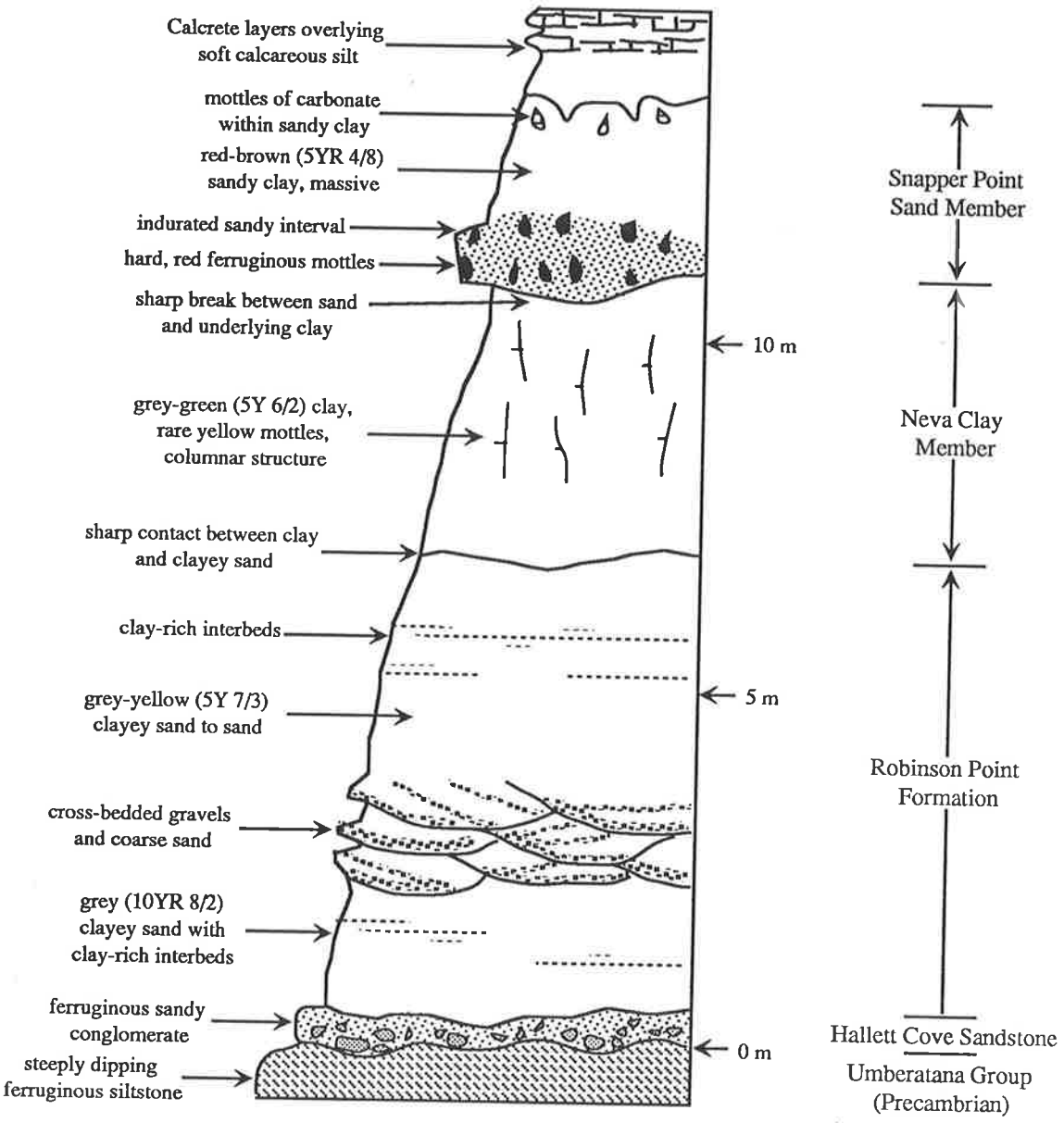

Figure 3.18: Sketch section of Quaternary sediments exposed in coastal cliffs near Ochre Point. The interpreted stratigraphy of the sequence is shown.

Figure 3.19 Indurated reddish sandy sediments from the Robinson Point Formation exposed in coastal cliffs between Ochre Point and Ochre Cove. Vertical columnar structure, vertical and horizontal bleaching trends and more widespread bleaching in upper parts are suggestive of pedogenic alteration. No primary bedding structures are observed and there are isolated gravel-sized clasts scattered randomly through the sandy sediments. (Hammer is 28 cm long)

Figure 3.20 Quaternary sediments exposed in coastal cliffs near Seaford. The bottom half of the sequence comprises gravels, sands and sandy clays of the Robinson Point Formation (R). Central parts of this formation are coarser grained and show some cross-bedding. The Robinson Point Formation is overlain by greenish clays of the Neva Clay Member (N) and white to brown sands and sandy clays of the Snapper Point Sand Member (S). A calcrete caps the sequence.

Figure 3.21 Quaternary sediments exposed in coastal cliffs 600 metres south of Robinson Point. The basal part of the sequence comprises an interbedded sequence of gravels, sands and clays which is assigned to the Robinson Point Formation. Individual sedimentary units fine upward from gravel or sand to silt or clay. Green-grey clays of the Neva Clay Member (N) overlie the Robinson Point Formation. Sandy sediments of the Snapper Point Sand Member (S) fill a small channel eroded into the Neva Clay Member and grade up to brownish sandy clays. The channel-fill sediments show some ferruginous mottling. Cliffs are approximately 15 m high. A sketch of this locality is given in Figure 3.22.

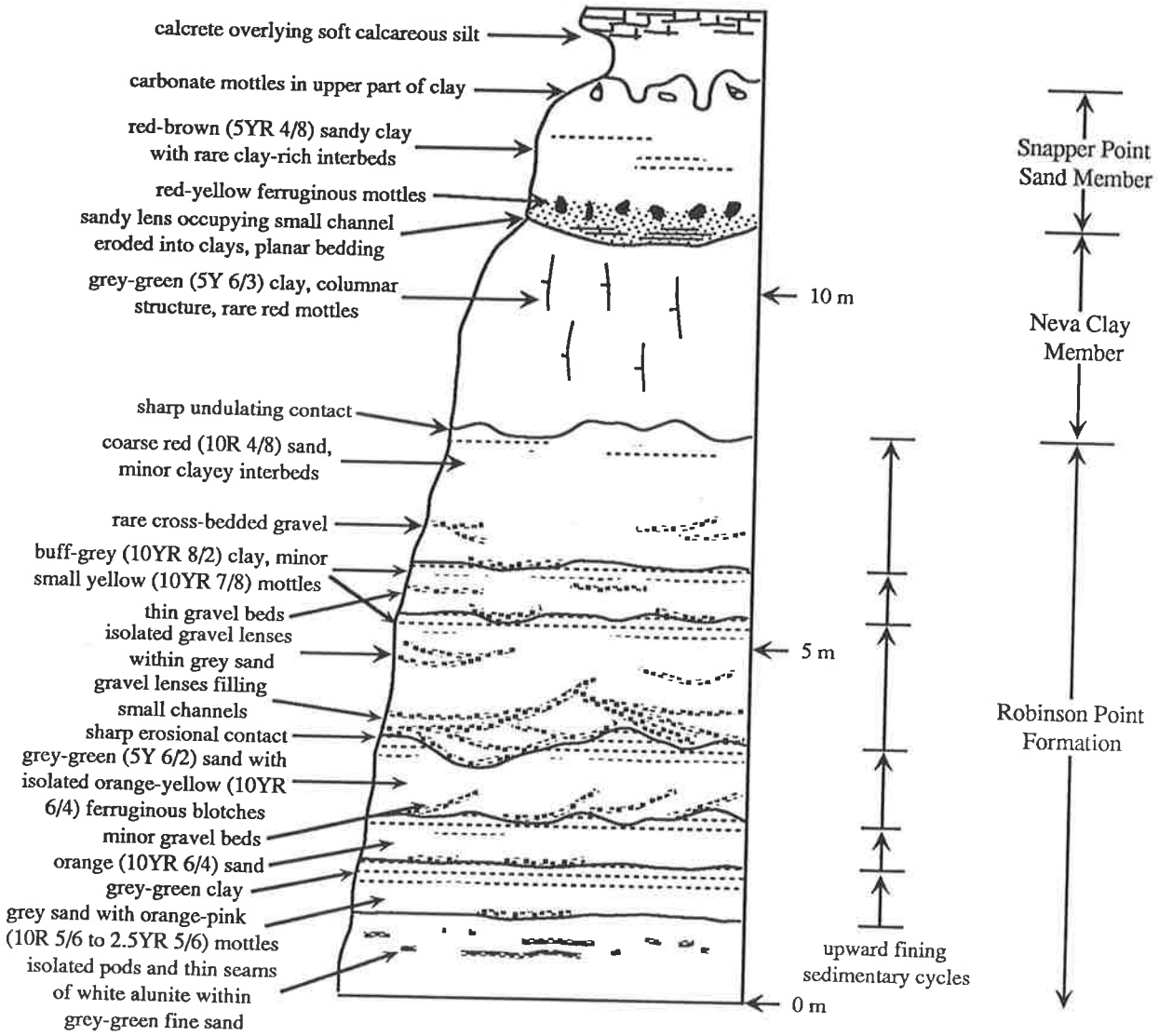

Figure 3.22: Sketch section of Quaternary sediments exposed in coastal cliffs south of Robinson Point. The position of upward fining cycles within the Robinson Point Formation is shown together with the interpreted stratigraphy.

Figure 3.23 Detail of sedimentary depositional cycles in lower parts of the Robinson Point Formation near Robinson Point. The contact between the lower mottled clay and overlying gritty sand is irregular. A further three upward fining sedimentary units can be distinguished above this irregular contact. Depositional units are shown by the dashed black lines. (Hammer is 28 cm long)

Figure 3.24 Unusual red-pink and yellow-brown colours associated with thin seams of white alunite in sandy sediments from the base of the Robinson Point Formation near Seaford. (Pencil is 13 cm in length)

Figure 3.25 Aerial view of coastal cliffs just south of Onkaparinga Trig. Tertiary sediments of the Port Willunga Formation (T) form a bench at the base of the cliffs and are overlain by yellowish sands and silts of the Robinson Point Formation (R). The majority of the cliffs are formed by red to green clays of the Neva Clay Member (N). Isolated patches of soft, white dolomite occur in upper parts of this member. White silts and sands with occasional ferruginous mottles which grade up to brown sandy clays in upper parts are assigned to the Snapper Point Sand Member (S). A calcrete layer caps the sequence. The cliffs in this area are approximately 20 m high.

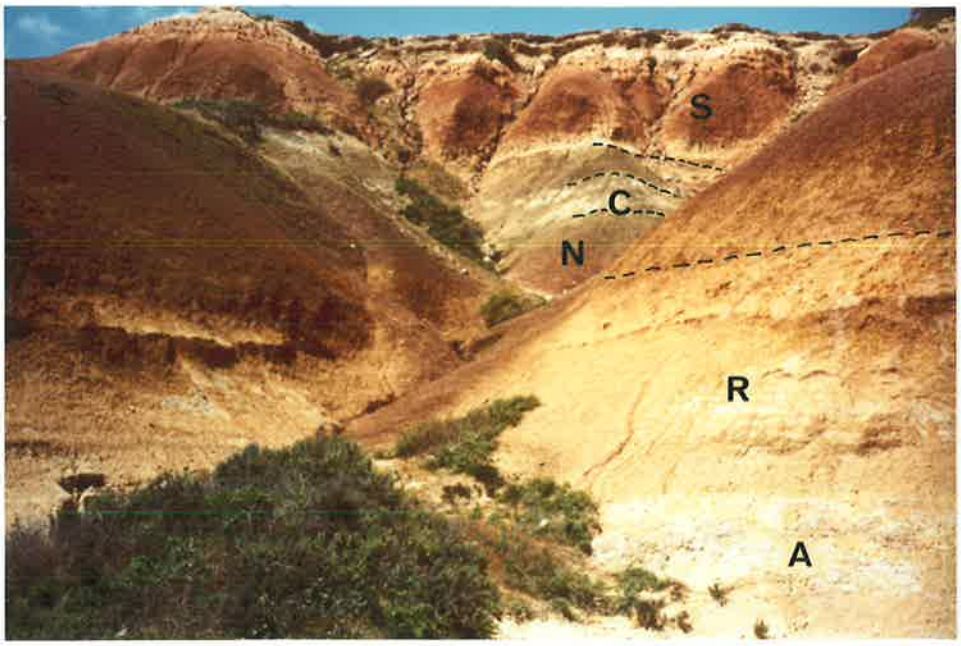

Figure 3.26 More detailed view of Quaternary sediments exposed in coastal cliffs just south of Onkaparinga Trig and the locality of the sampled section shown in Figure 3.27. Alunite (A) occurs near the base of the Robinson Point Formation (R). Mottled white carbonate (C) is clearly seen in upper parts of the clay-rich Neva Clay Member (N). A white sandy interval occurs at the base of the Snapper Point Sand Member (S) and grades up to brown sandy clay.

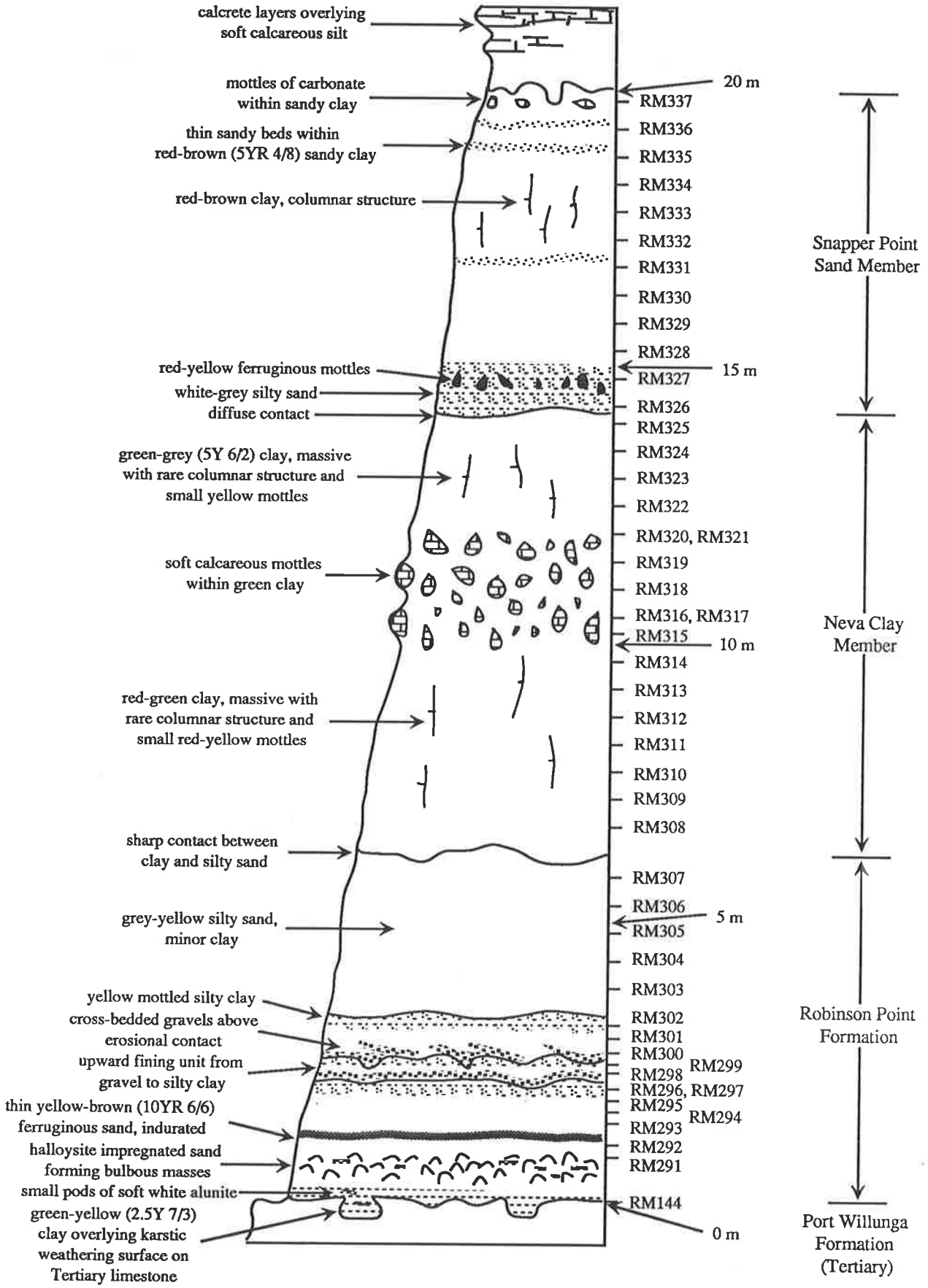

Figure 3.27: Sketch section of coastal cliffs near Onkaparinga Trig showing sample sites (see Appendix 1 for details) and interpreted Quaternary stratigraphy.

Figure 3.28 The Robinson Point Formation exposed in coastal cliffs south of Robinson Point. This is a more detailed photo of the right hand side of Figure 3.21. Clay-rich beds (C) mark the top of upward fining sedimentary units. Cross-bedded gravels (G) in the centre of the photo fill a broad channel eroded into underlying sandy clays of a previous depositional unit. (Hammer is 28 cm long)

Figure 3.29 Quaternary sediments exposed in a gully eroded by outflow from a storm-water drain, just east of the Onkaparinga River mouth. Clays of the Neva Clay Member (N) occur at the base of the exposed section and include a 1 m thick interval of mottled carbonate (C). Sands and sandy clays of the Snapper Point Sand Member (S) overlie the clays with the section being capped by thick calcareous sediment which is mottled near the base and indurated at the top. Section exposed is approximately 7 m thick.

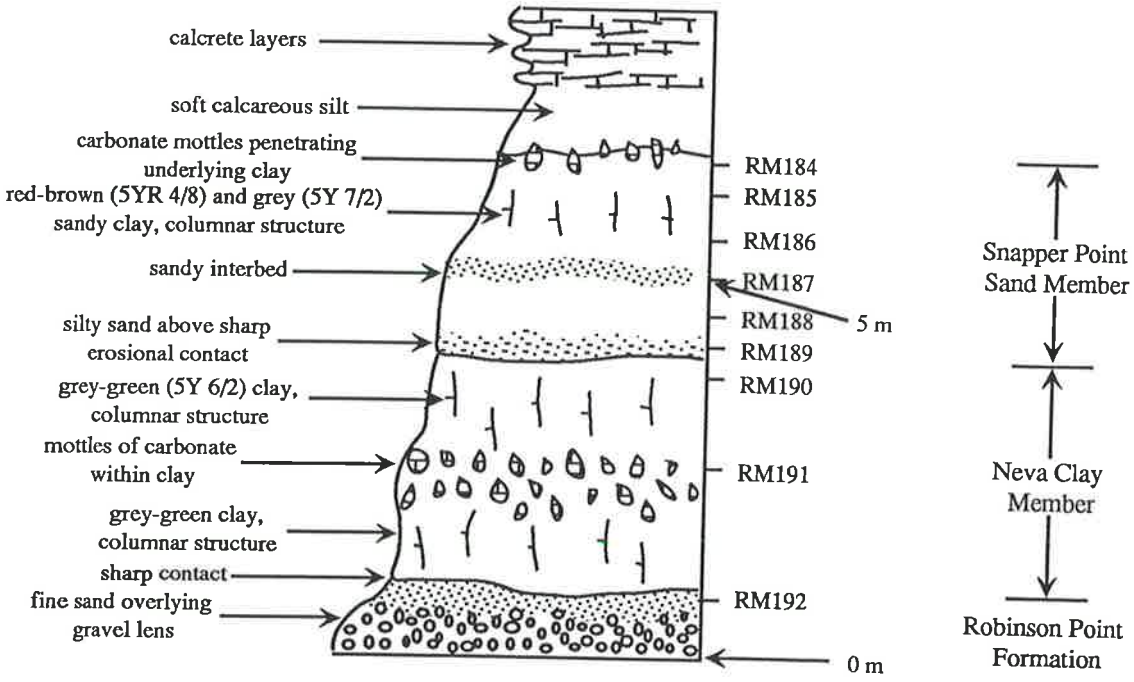

Figure 3.30 Sketch section showing the Quaternary sequence exposed in the storm-water outflow gully near the mouth of the Onkaparinga River. Sample locations (see Appendix 1 for details) and interpreted stratigraphy are also shown.

Figure 3.31 Aerial view of Tertiary and Quaternary sediments exposed in coastal cliffs between Port Noarlunga and Witton Bluff. White sediments forming the lower half of the cliffs are limestones of Tertiary age. These are overlain by orange-coloured sandy and gravelly sediments of the Robinson Point Formation. An interval of green to red clays assigned to the Ngaltinga Formation occurs in upper parts of the sequence. Cliffs are approximately 20 m high at this locality.

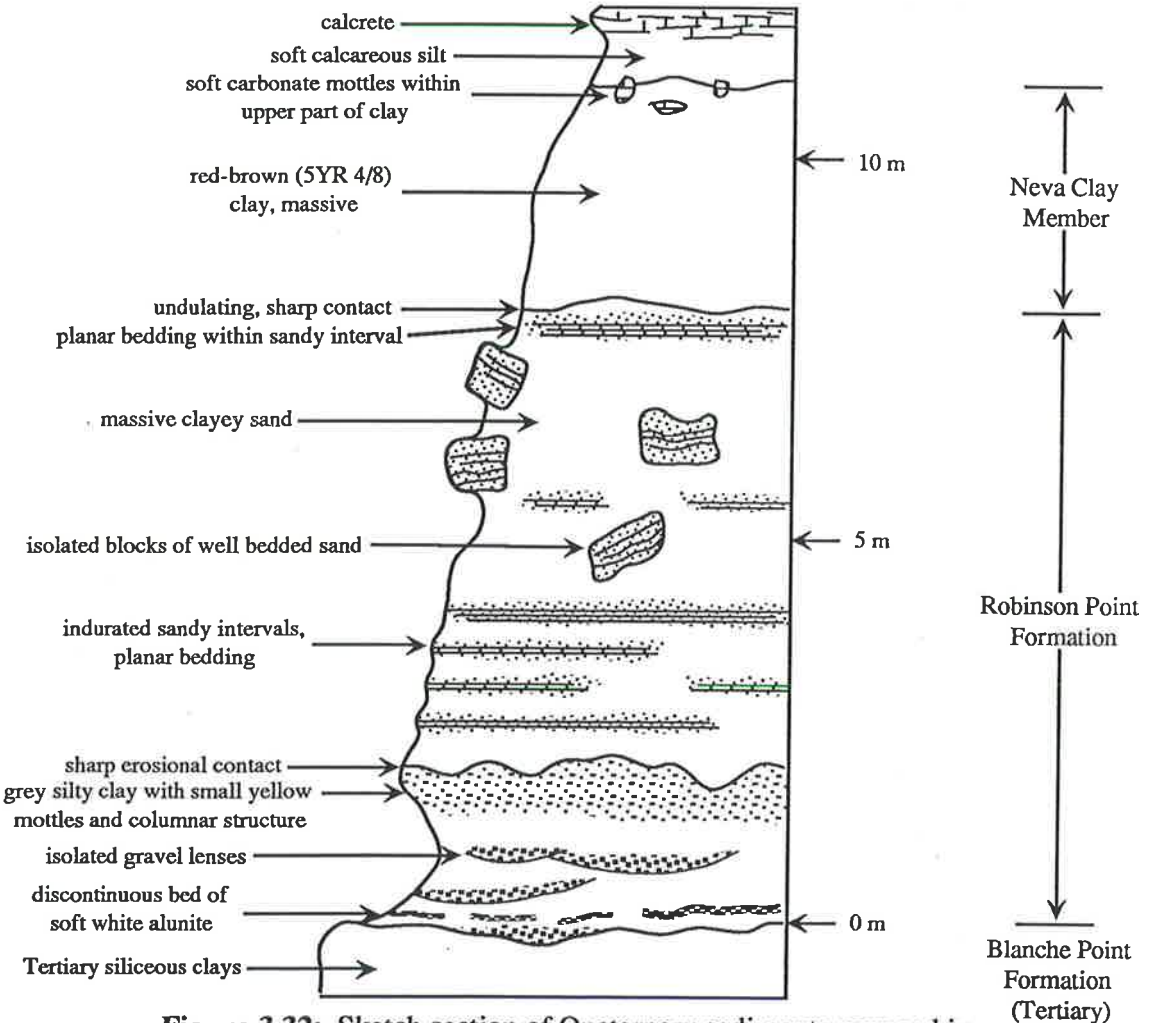

Figure 3.32: Sketch section of Quaternary sediments exposed in coastal cliffs between Port Noarlunga and Witton Bluff showing more detail than the aerial view of Figure 3.31.

Figure 3.33 Near horizontal bands of white alunite which occur in basal sandy and gritty sediments of the Robinson Point Formation just north of Port Noarlunga. The alunite tends to have sharp lower boundaries with surrounding sandy sediments but more diffuse upper contacts. (Lens cap is 50 mm in diameter.)

Figure 3.34 An unusually thick bed of white alunite which occurs at the base of the Robinson Point Formation in coastal cliffs between Port Noarlunga and Witton Bluff. The lower boundary of the alunite is sharp but irregular and includes several rounded masses which protrude into the underlying sediments. (Hammer is 28 cm in length.)

Figure 3.35 A sequence of interbedded sands and sandy clays forming the Robinson Point Formation just south of Witton Bluff. Sediments in lower and upper parts of the Robinson Point Formation are horizontally bedded. Sediments in central parts of this unit display no coherent bedding with large blocks of indurated sand occurring randomly throughout the otherwise soft, structureless sediments. Clays of the Ngaltinga Formation (N) can be seen in the upper left portion of the photo. The section shown is approximately 7 m thick.

Figure 3.36 Quaternary sediments exposed in The Amphitheatre at Hallett Cove. White sands of Permian age occur at the base of the sequence (P) and are overlain by yellow to red sandy clays and sands of the Robinson Point Formation (R). Sediments in upper parts of this unit are often mottled and a conspicuous indurated zone (F) occurs within the mottled sediments. Reddish clays assigned to the Ngaltinga Formation (N) overlie the Robinson Point Formation and the sequence is capped by calcareous sediments. The sequence exposed is approximately 20 m thick. The location of the sketched section depicted in Figure 3.37 is shown by the arrow.

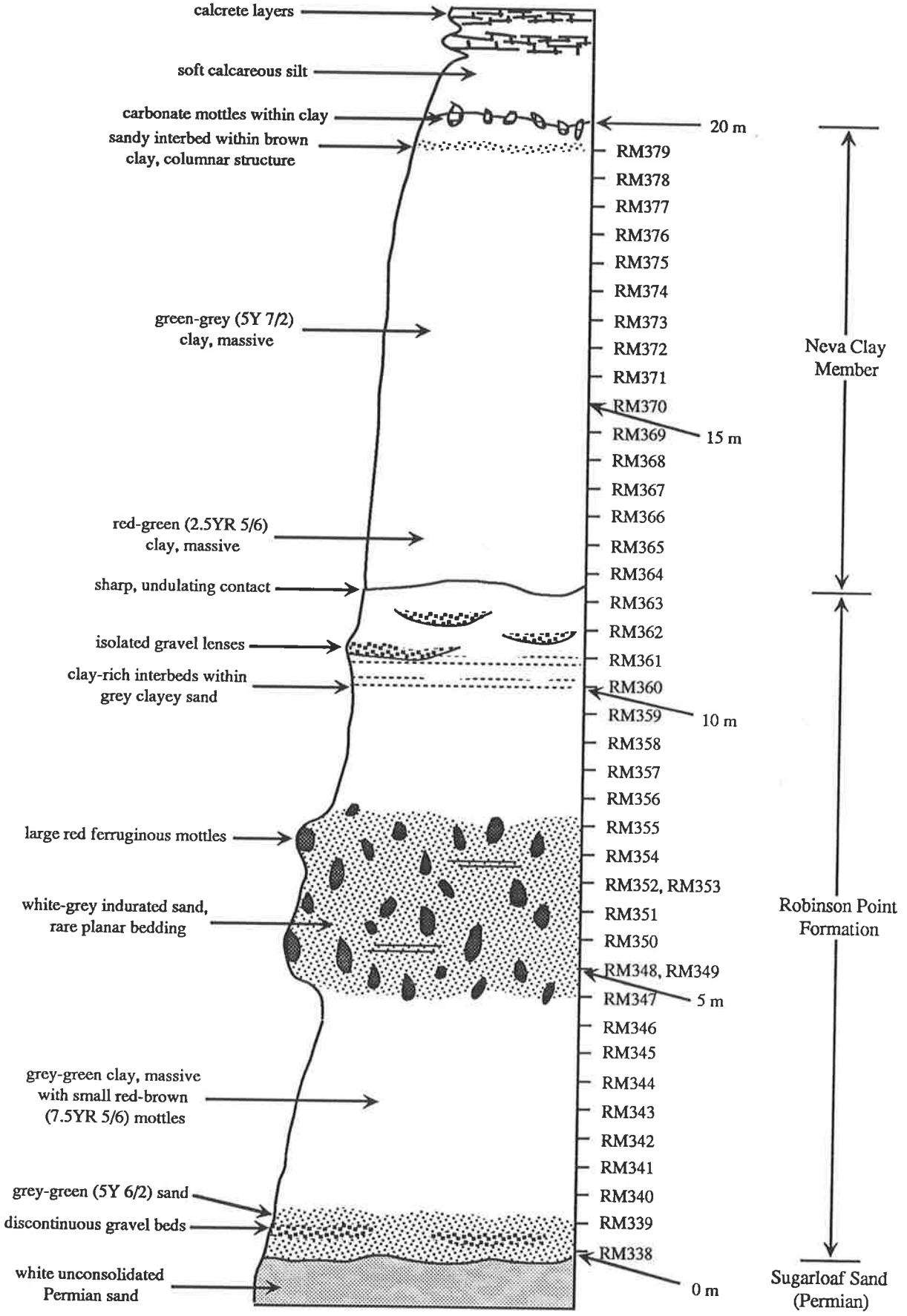

Figure 3.37: Sketch section of Quaternary sediments exposed in The Amphitheatre at Hallett Cove. Sample locations (see Appendix 1 for details) and interpreted stratigraphy are shown.

Figure 3.38 Aerial view of The Amphitheatre at Hallett Cove. The Hallett Cove Sandstone (H) forms a bench in central parts of the photo with redder coloured sediments representing the Robinson Point Formation (R) and lighter coloured sediments the Ngaltinga Formation (N).

Figure 3.39 Quaternary sediments exposed in a railway cutting just south of O'Sullivan Beach Road. The Quaternary sediments fill a channel eroded into Precambrian sediments (P) with sands at the base assigned to the Robinson Point Formation (R) and reddish clays near the top of the sequence assigned to the Ngaltinga Formation (N). Basal sands are often mottled with iron oxides and bedding, which is highlighted by thin indurated intervals, is trough-like and generally follows the outline of the channel. The section exposed is approximately 6 m thick.

FIGURE 3.40: DISTRIBUTION OF STRATIGRAPHIC UNITS ALONG THE COASTLINE IN THE NOARLUNGA (HALLETT COVE TO ROBINSON POINT) AND WILLUNGA EMBAYMENTS (OCHRE POINT TO SELLICKS BEACH)

NOTE: Vertical scale 1 cm represents 2 m except for Sellicks Beach where 1 cm represents 4 m.
See Figure 1.2 for locational information
For further details regarding individual sites see Figures 3.2, 3.5, 3.9, 3.11, 3.15, 3.18, 3.22, 3.27, 3.30, 3.32, and 3.37.

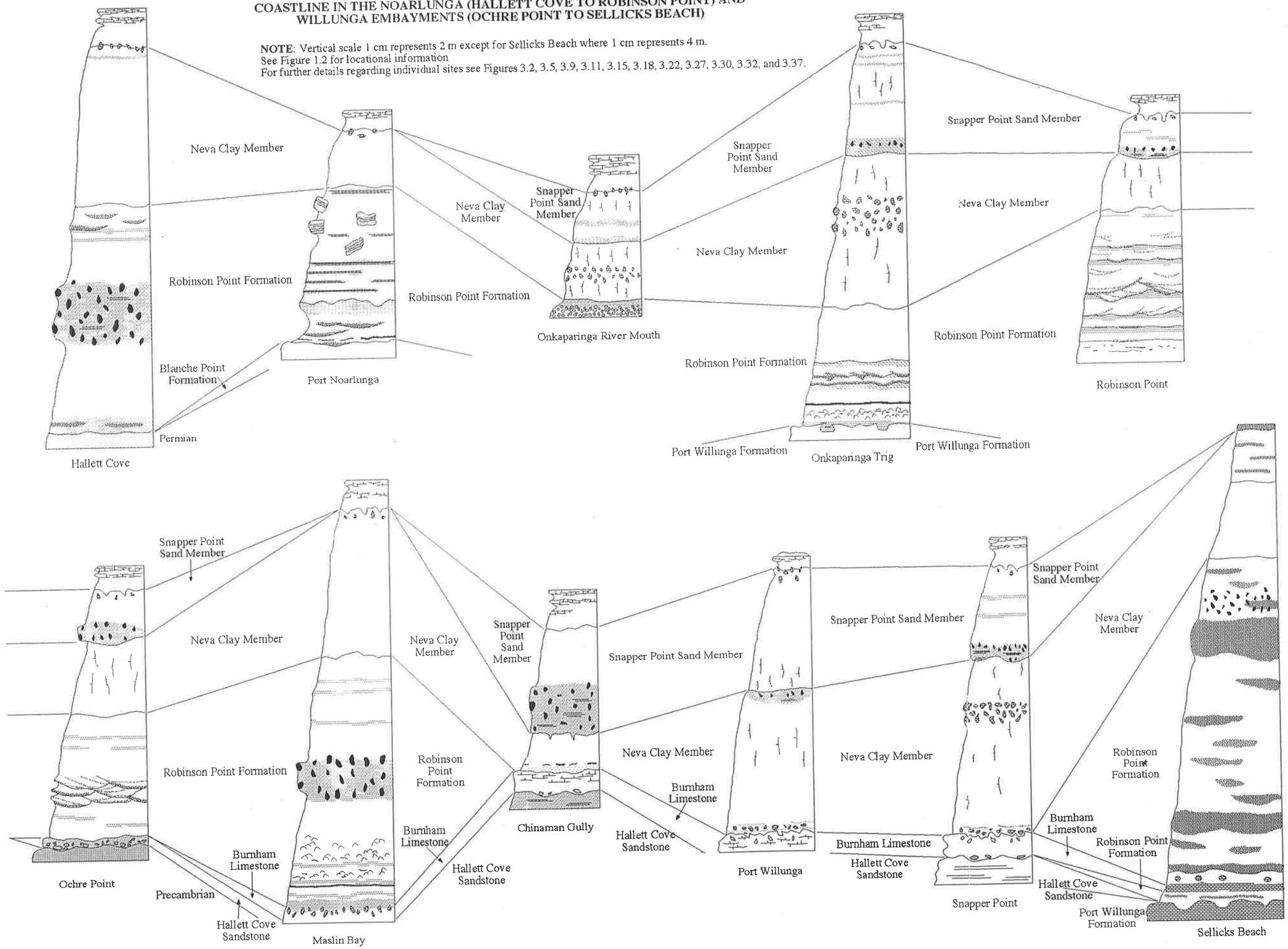

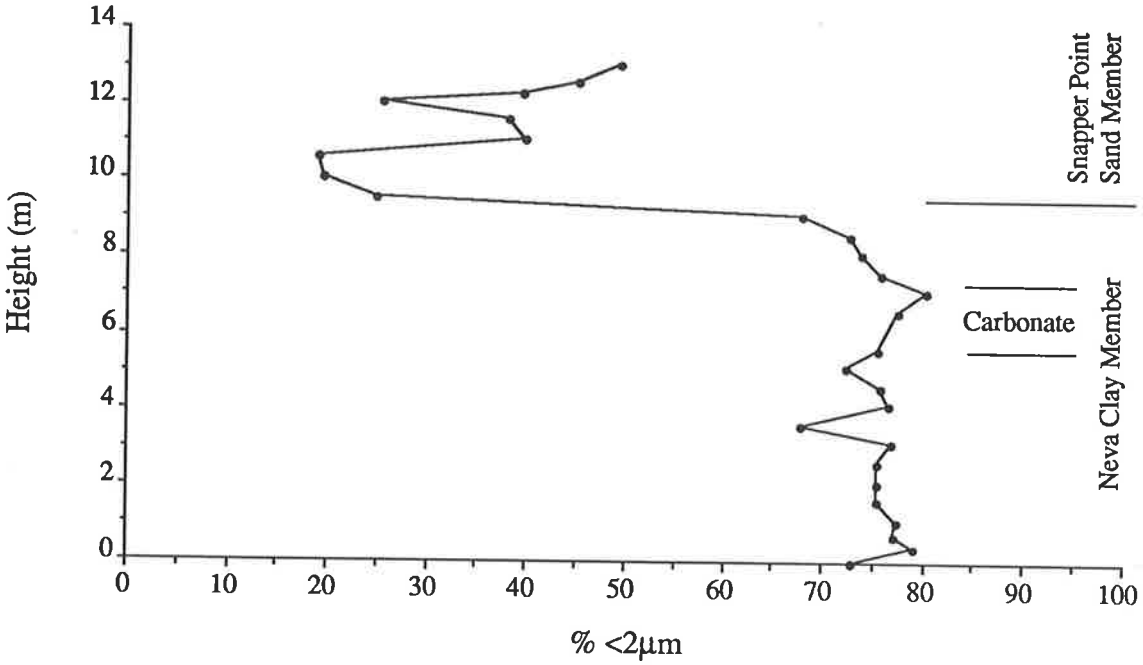

Figure 4.1 % <2μm for samples from the Snapper Point site. For sample numbers and locations refer to the sketch section in Figure 3.5.

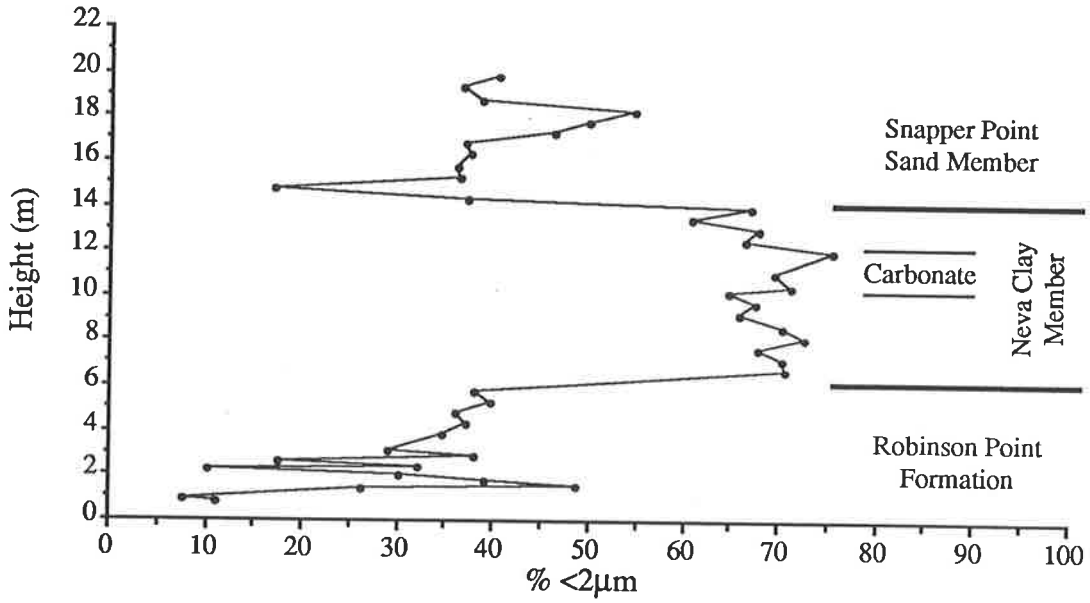

Figure 4.2 % <2μm for samples from the Onkaparinga Trig site. For sample numbers and locations refer to the sketch section in Figure 3.27.

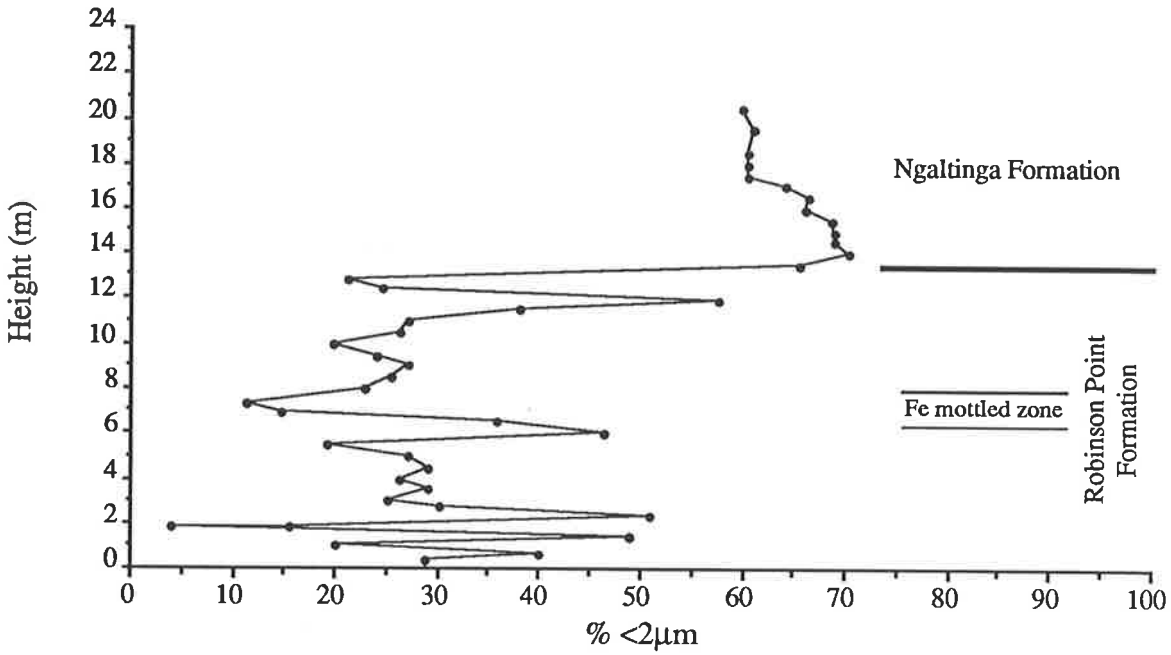

Figure 4.3 % <2μm for samples from the Maslin Bay site. For sample numbers and locations refer to the sketch section in Figure 3.15.

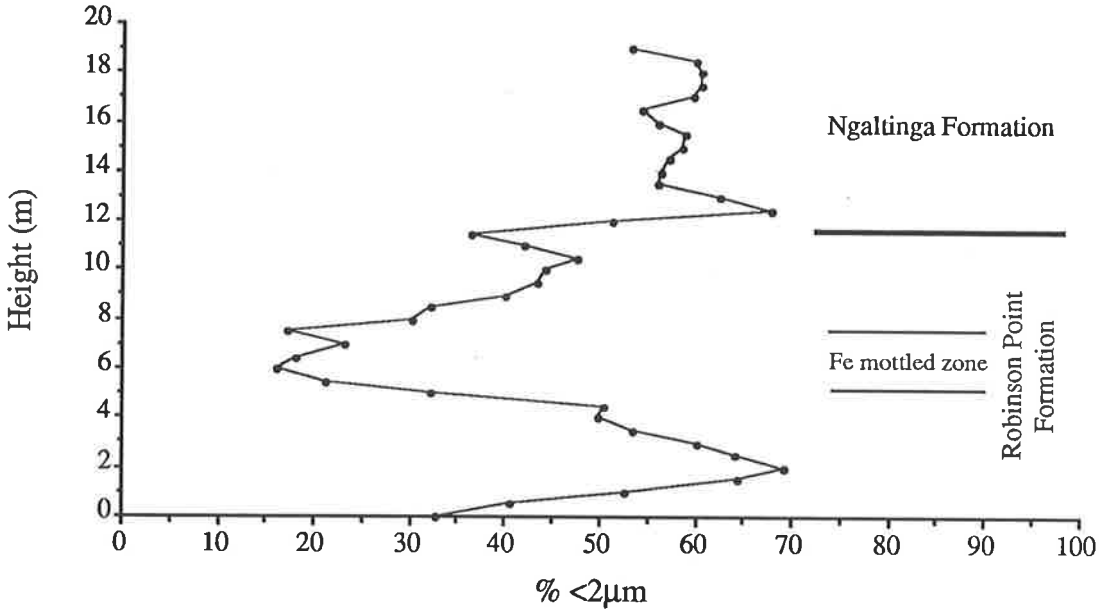

Figure 4.4 % <2μm for samples from the Hallett Cove site. For sample numbers and locations refer to the sketch section in Figure 3.37.

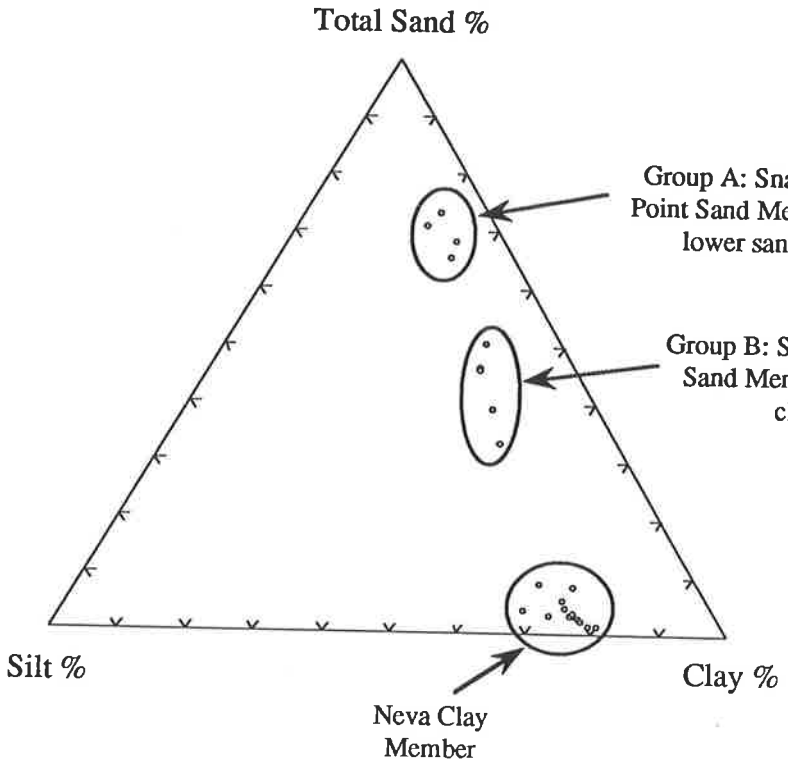

Figure 4.5 Particle size data for samples from the Snapper Point site summarised on a ternary diagram using sand, silt and clay as end-members.

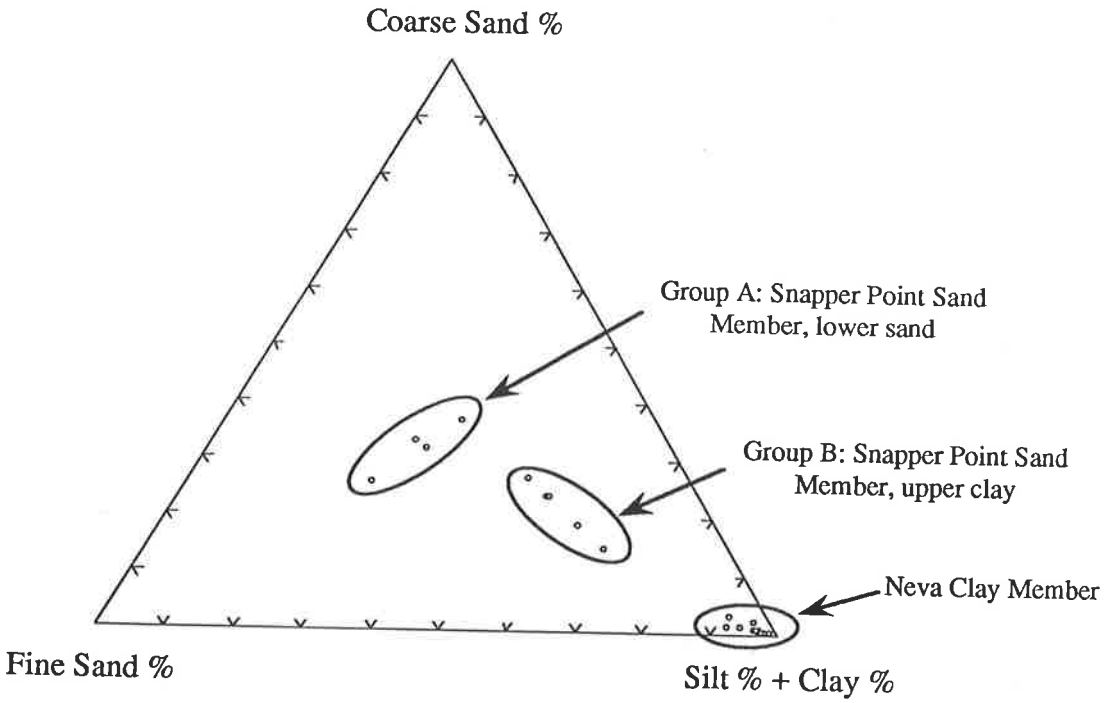

Figure 4.6 Particle size data for samples from the Snapper Point site summarised on a ternary diagram using coarse sand, fine sand and silt plus clay as end-members.

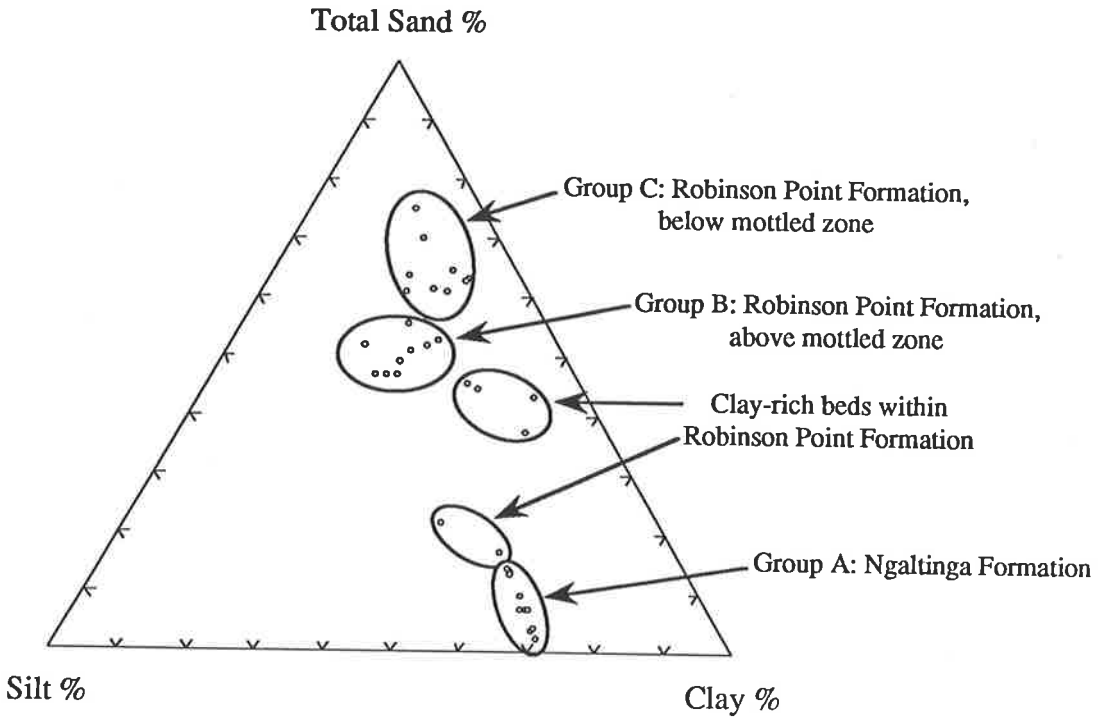

Figure 4.7 Particle size data for samples from the Maslin Bay site summarised on a ternary diagram using sand, silt and clay as end-members.

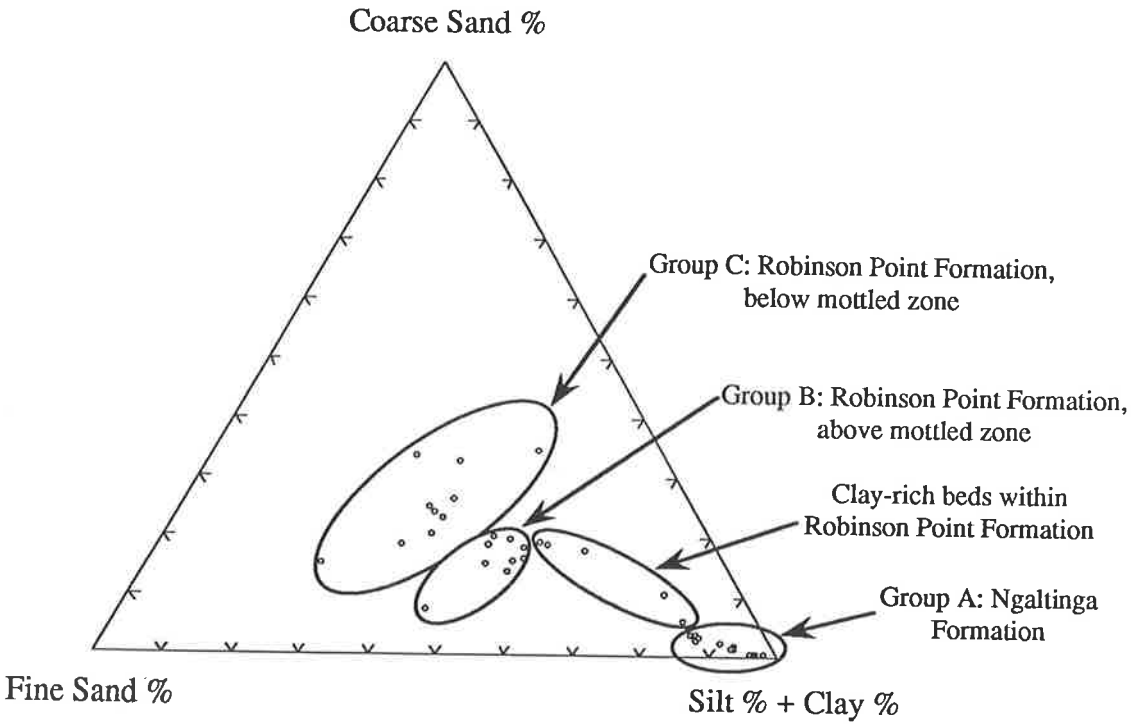

Figure 4.8 Particle size data for samples from the Maslin Bay site summarised on a ternary diagram using coarse sand, fine sand and silt plus clay as end-members.

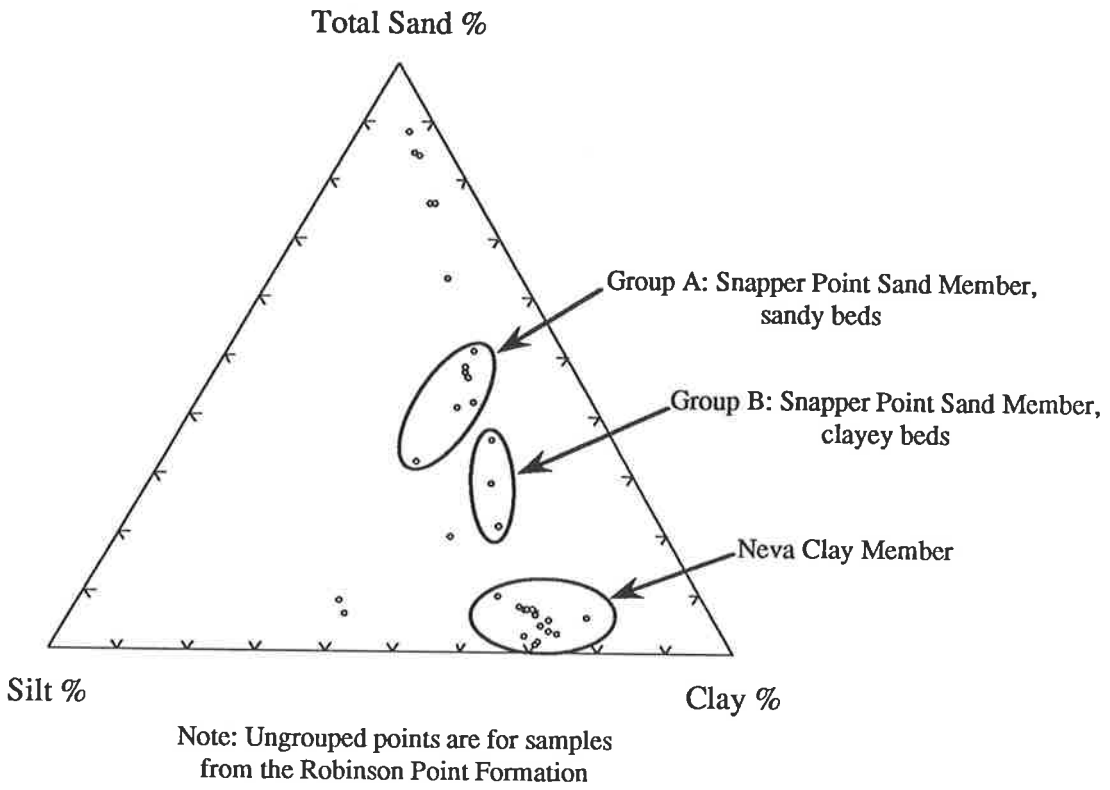

Note: Ungrouped points are for samples from the Robinson Point Formation

Figure 4.9 Particle size data for samples from the Onkaparinga Trig site summarised on a ternary diagram using sand, silt and clay as end-members.

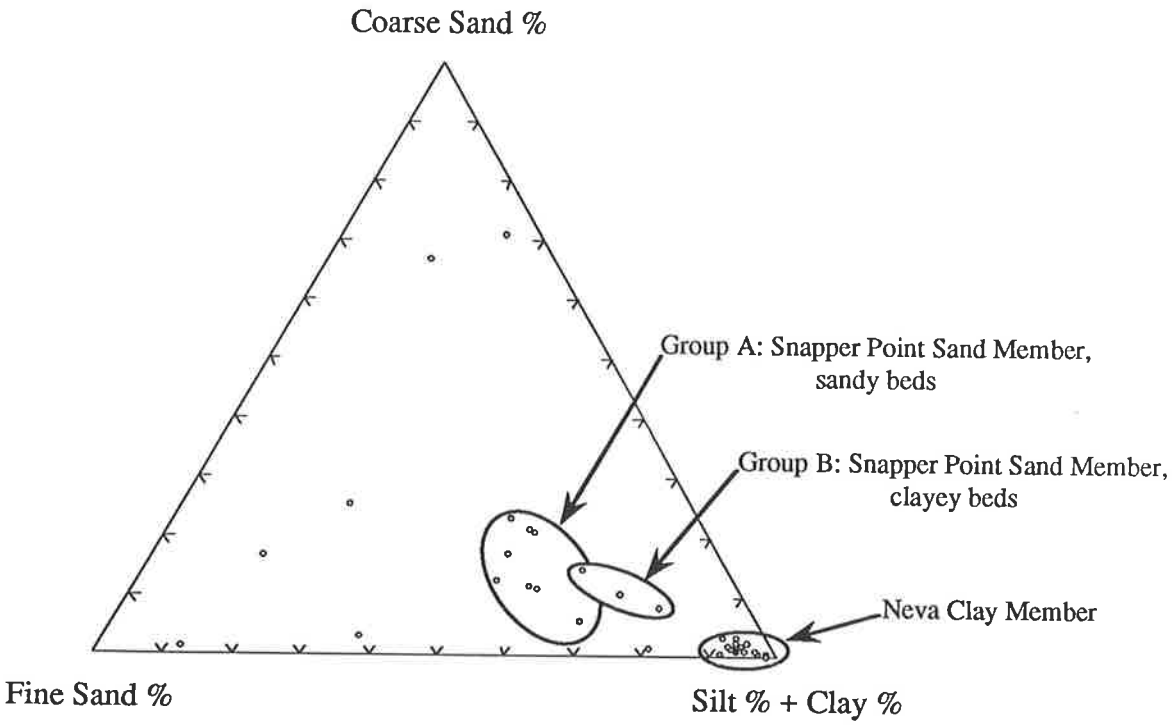

Note: Ungrouped points are for samples from the Robinson Point Formation

Figure 4.10 Particle size data for samples from the Onkaparinga Trig site summarised on a ternary diagram using coarse sand, fine sand and silt plus clay as end-members.

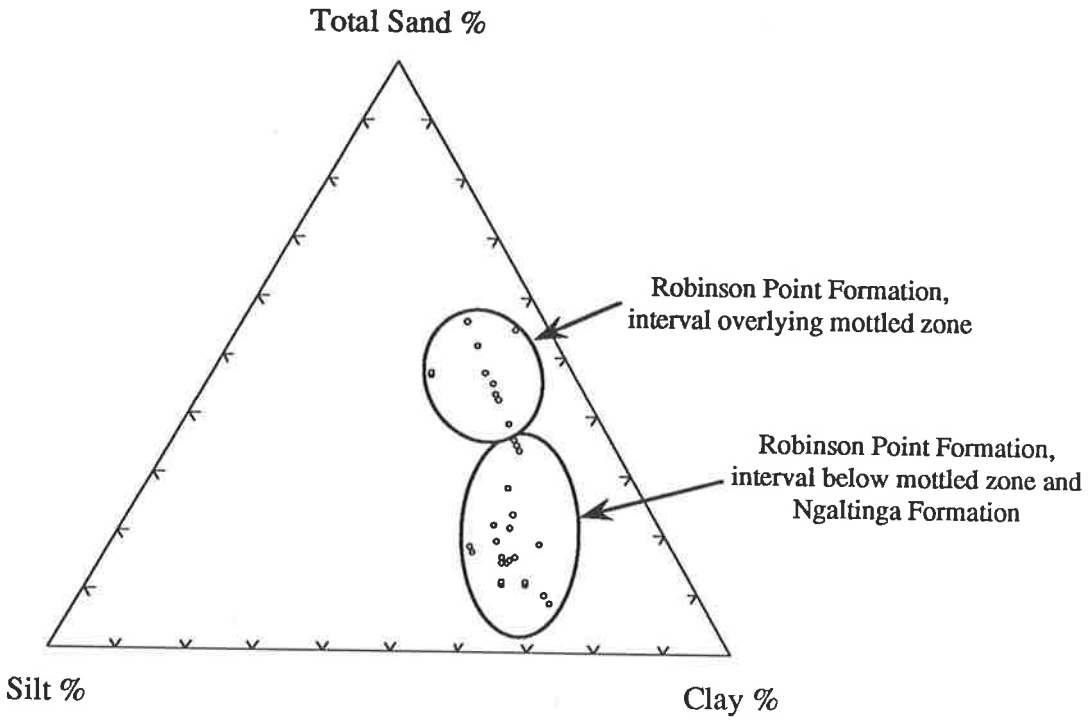

Figure 4.11 Particle size data for samples from the Hallett Cove site summarised on a ternary diagram using sand, silt and clay as end-members.

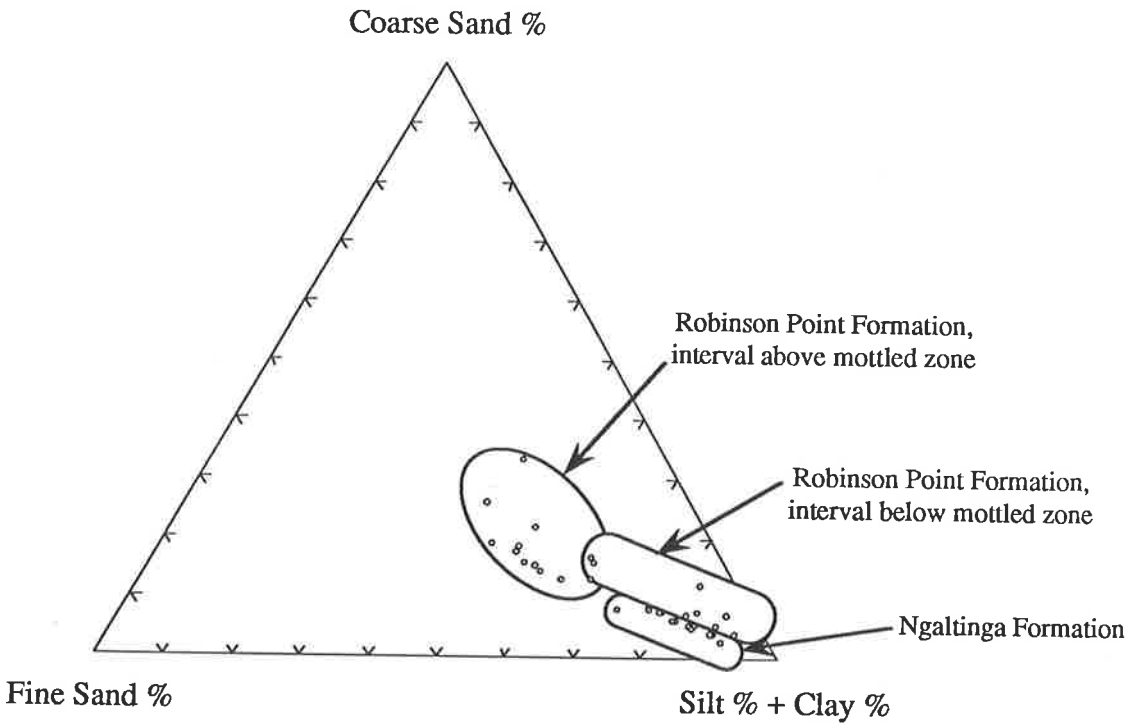

Figure 4.12 Particle size data for samples from the Hallett Cove site summarised on a ternary diagram using coarse sand, fine sand and silt plus clay as end-members.

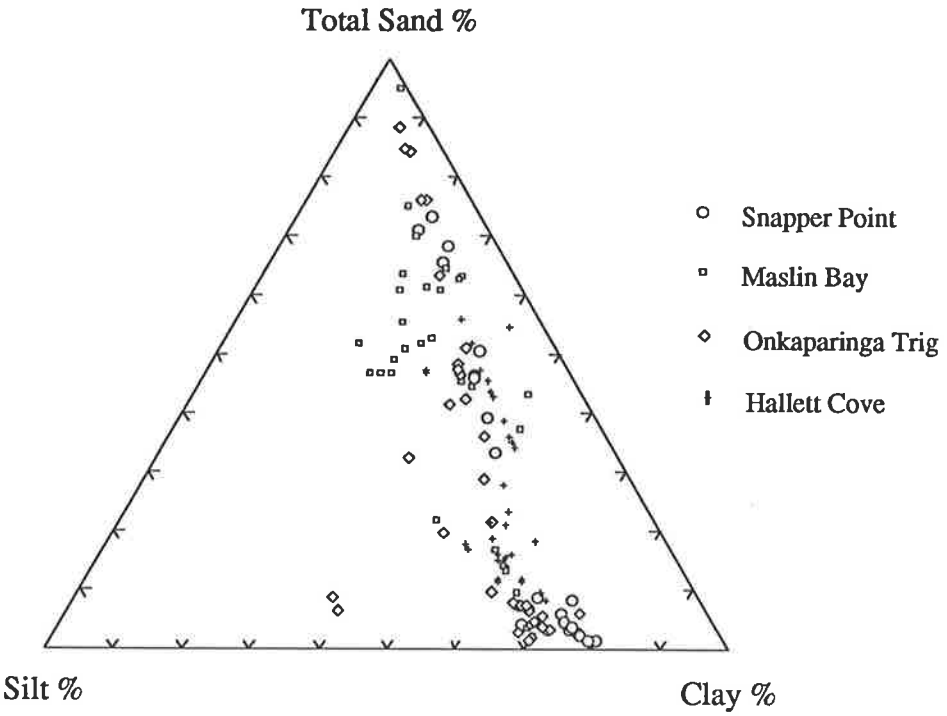

Figure 4.13 Particle size data for samples from all four sites summarised on a ternary diagram using sand, silt and clay as end-members.

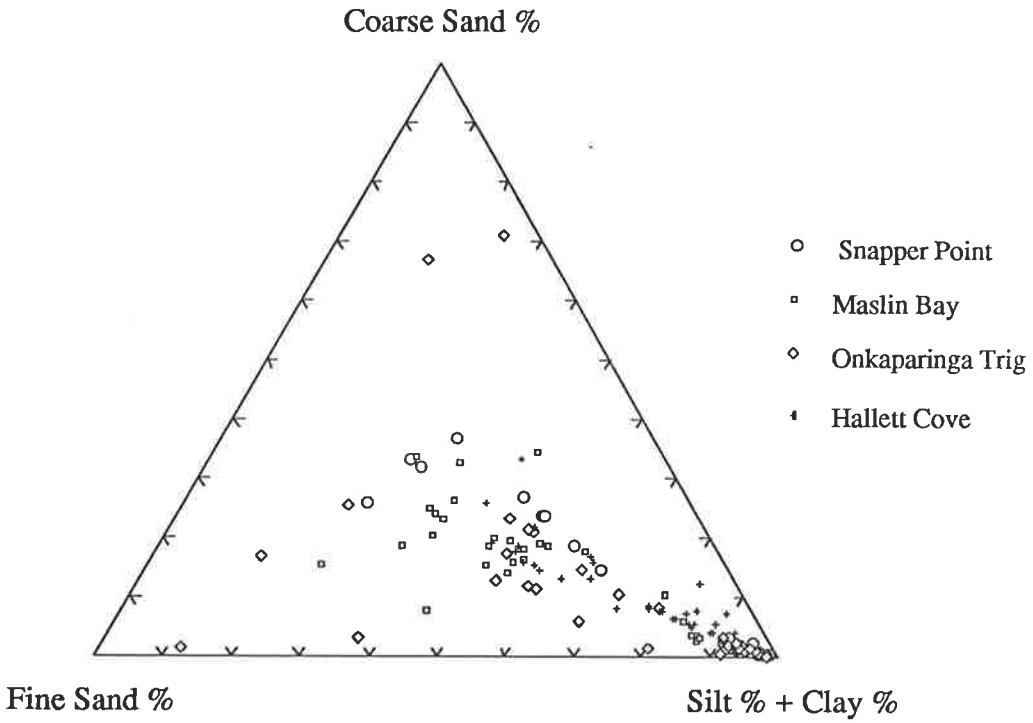

Figure 4.14 Particle size data for samples from all four sites summarised on a ternary diagram using coarse sand, fine sand and silt plus clay as end-members.

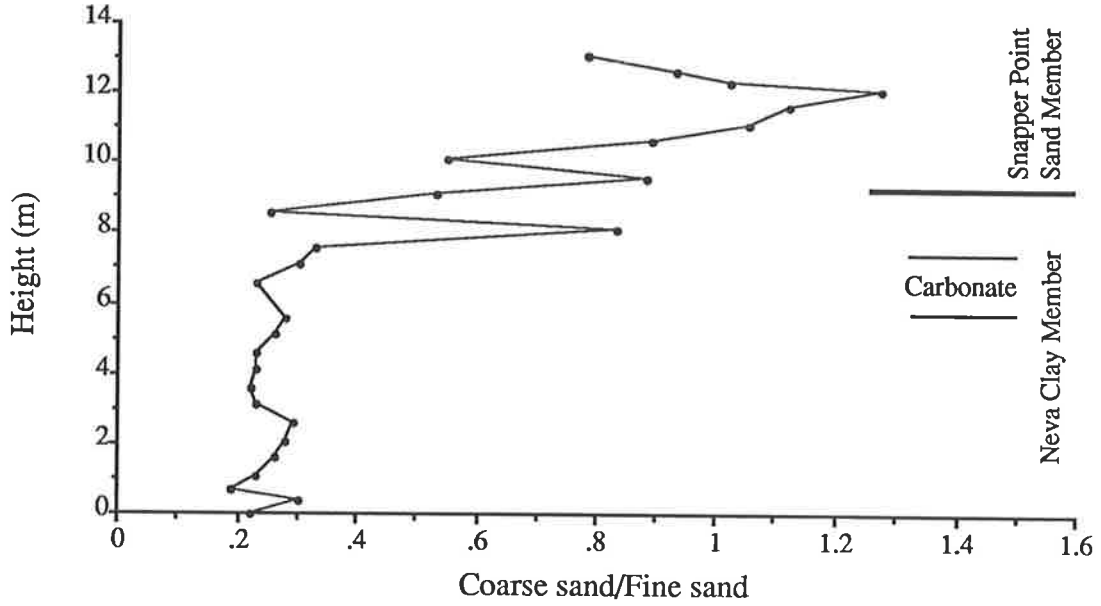

Figure 4.15 Coarse sand to fine sand ratios for samples collected from the Snapper Point site. For sample numbers and locations refer to the sketch section in Figure 3.5.

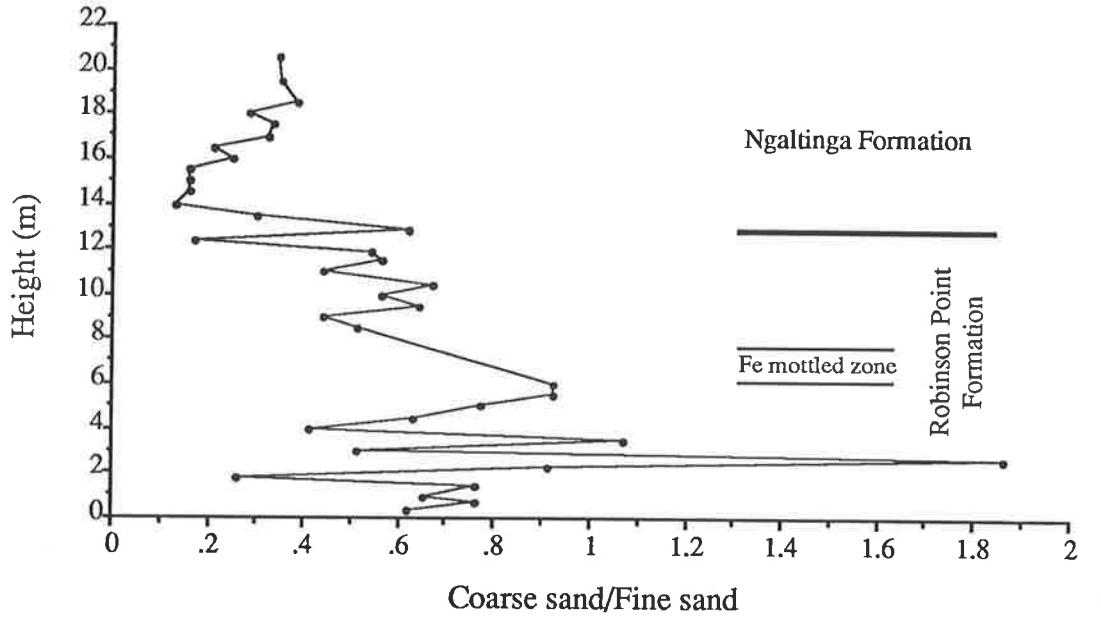

Figure 4.16 Coarse sand to fine sand ratios for samples collected from the Maslin Bay site. For sample numbers and locations refer to the sketch section in Figure 3.15.

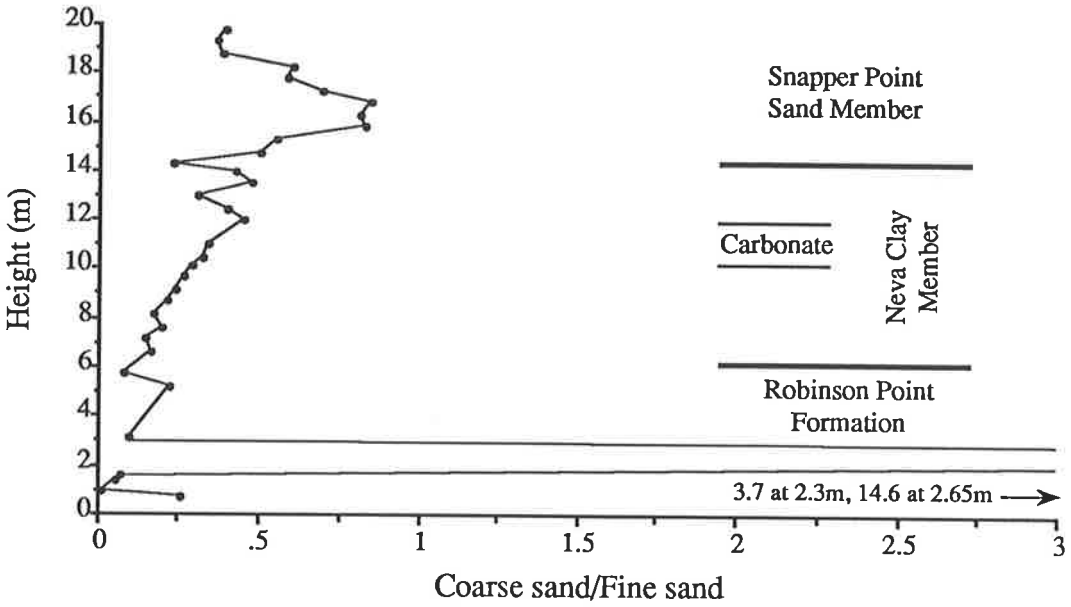

Figure 4.17 Coarse sand to fine sand ratios for samples collected from the Onkaparinga Trig site. For sample numbers and locations refer to the sketch section in Figure 3.27.

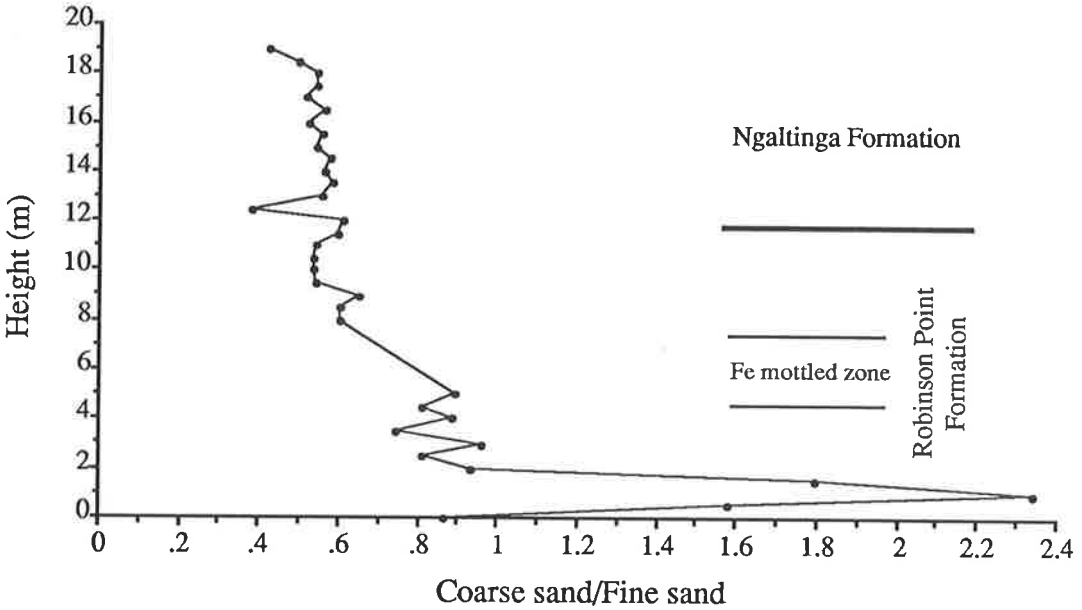

Figure 4.18 Coarse sand to fine sand ratios for samples collected from the Hallett Cove site. For sample numbers and locations refer to the sketch section in Figure 3.37.

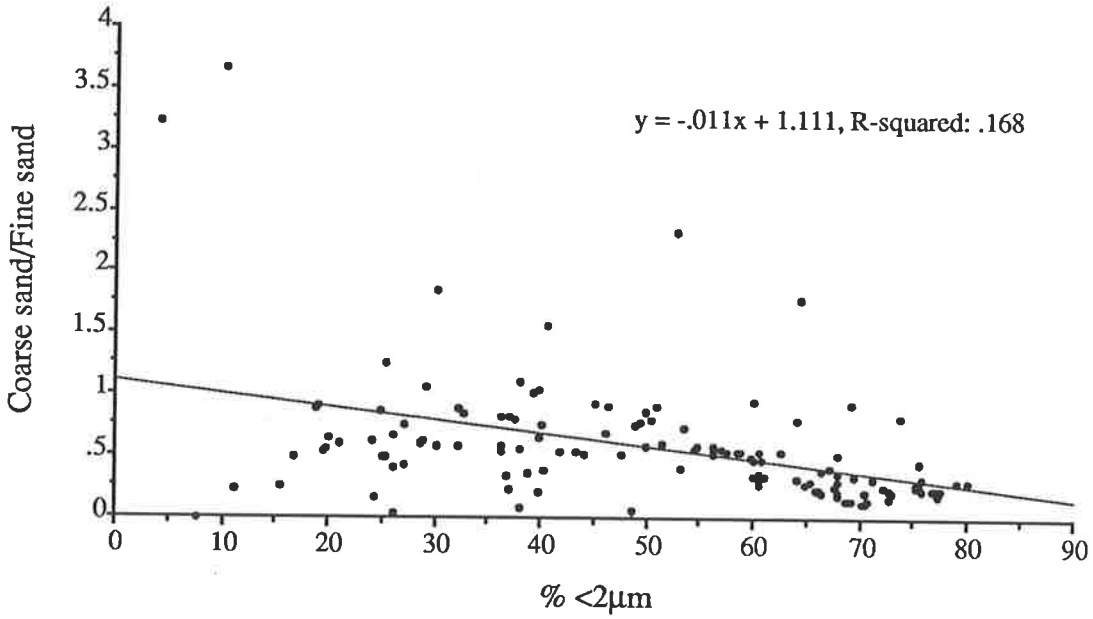

Figure 4.19 Graph plotting the coarse sand to fine sand ratio versus % <2μm for samples from all four sites. Regression analysis indicates that no correlation exists between the two parameters.

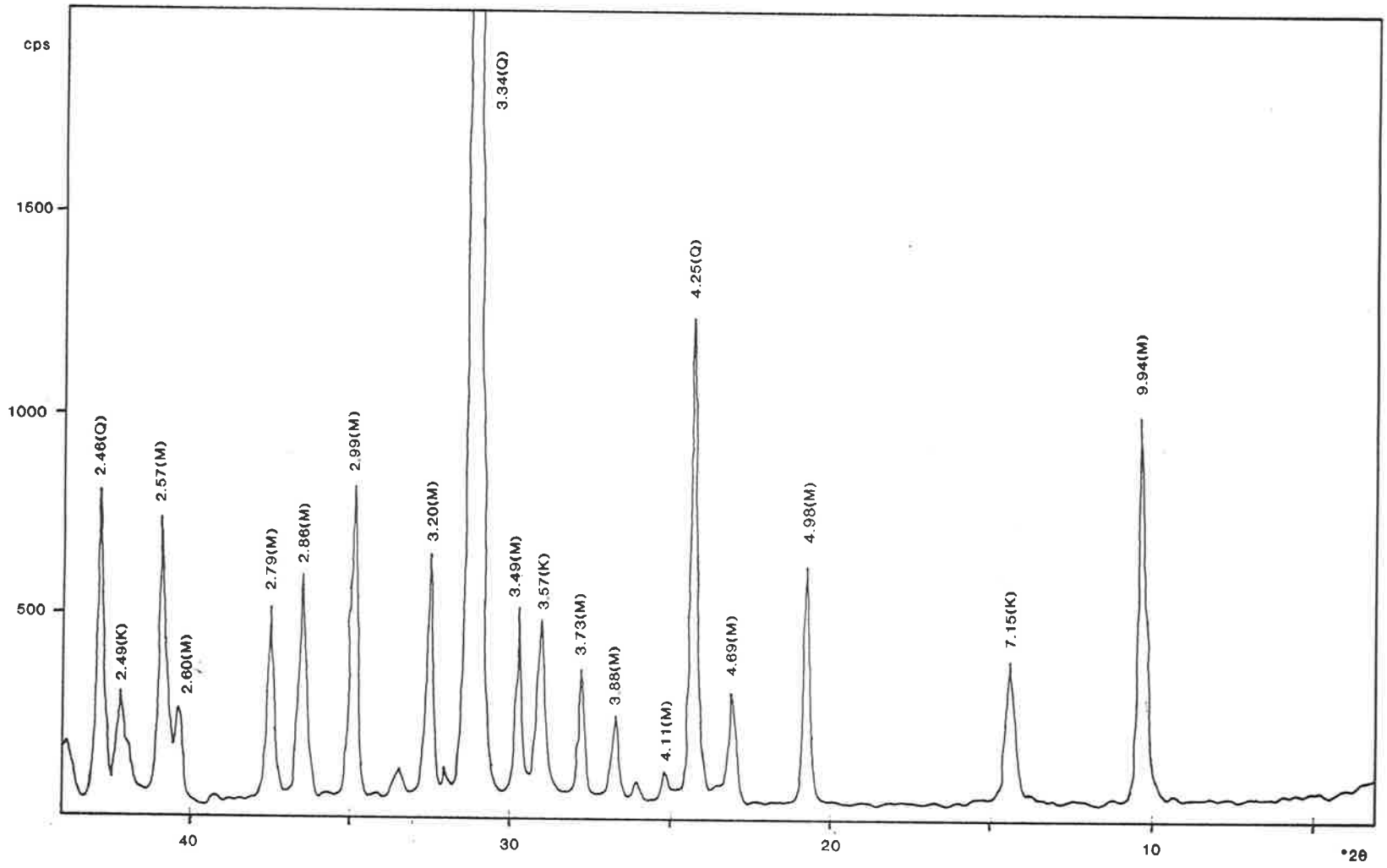

Figure 4.20 XRD trace of weathered Precambrian shale collected from a quarry near Bradbury. Relatively sharp peaks for mica (M) and kaolinite (K) are shown. Quartz (Q) is also present. Sample RM56, bulk material, finely ground, pressed powder mount.

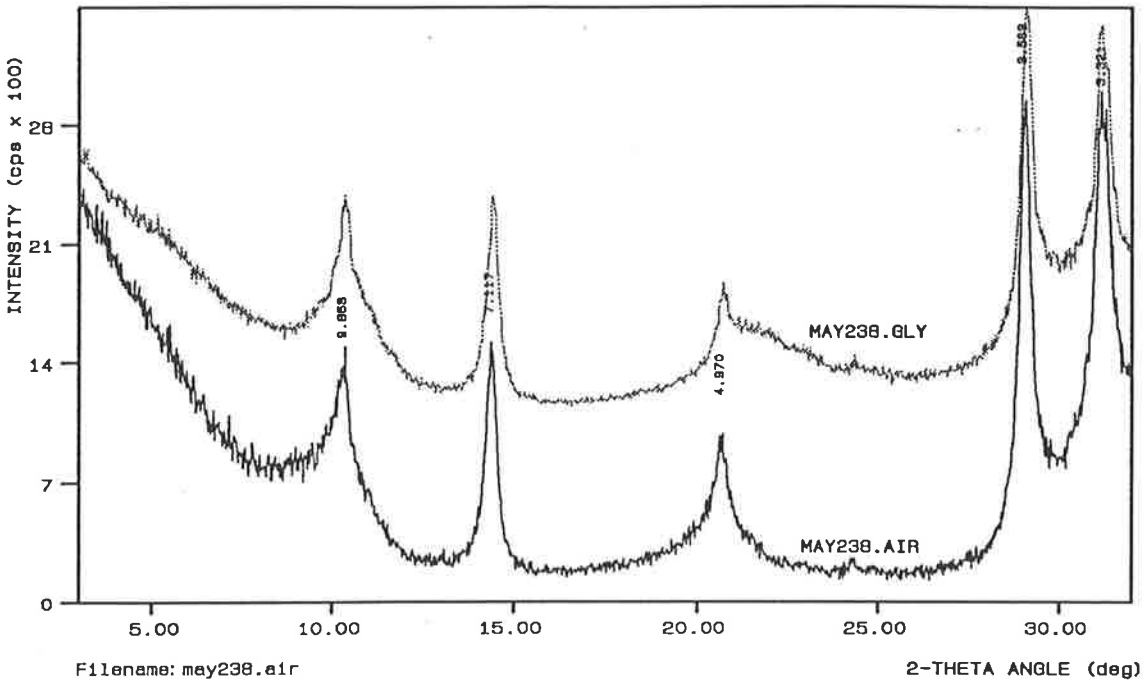

RM238

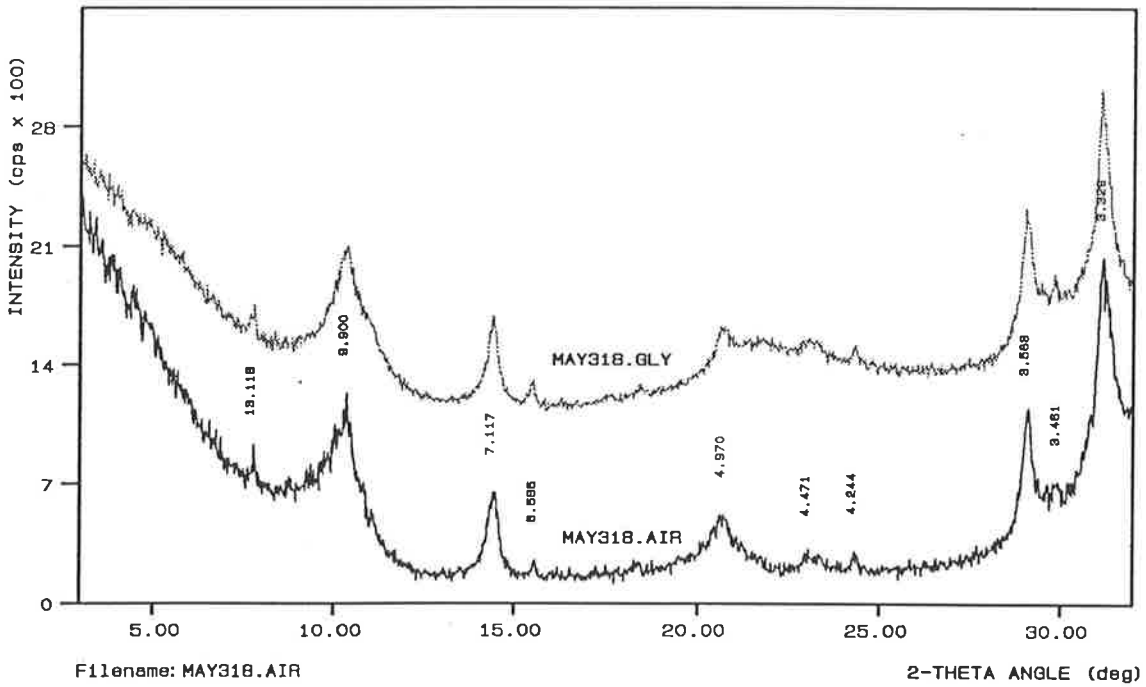

RM318

Figure 4.21 XRD traces of the <2μm fraction of samples which have been air-dried, Mg-saturated (AIR) and glycerol solvated after Mg-saturation (GLY). The traces show broad mica peaks at 9.9Å which are typical of those from soil illites. Examples of three samples are given which show variation in the width of the (001) illite peak at 9.9Å. RM238 (Snapper Point), peak width 0.9 °2θ; RM318 (Onkaparinga Trig), peak width 1.2 °2θ; RM341 (Hallett Cove), peak width 0.5 °2θ.

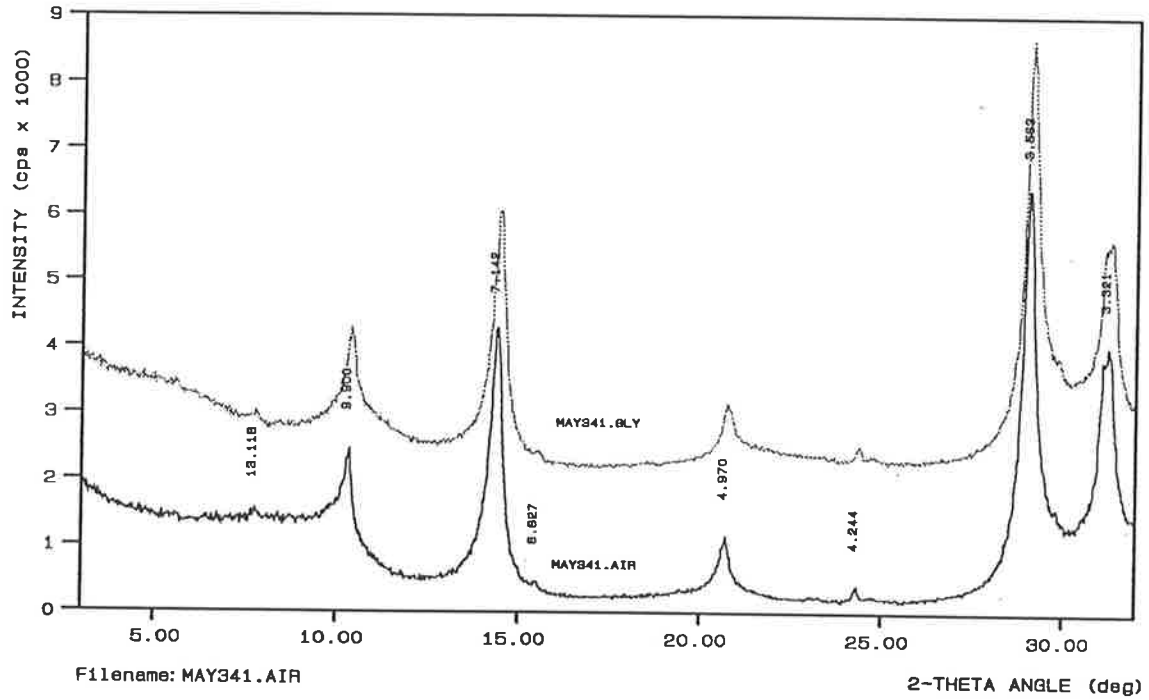
INTENSITY (cps x 1000)
9
8
7
6
5
4
3
2
1
0
5.00
10.00
15.00
20.00
25.00
30.00
2-THETA ANGLE (deg)
Filename: MAY341.AIR
MAY341.GLY
MAY341.AIR
13.118
9.900
7.142
6.827
4.970
4.244
3.582
3.321

RM341

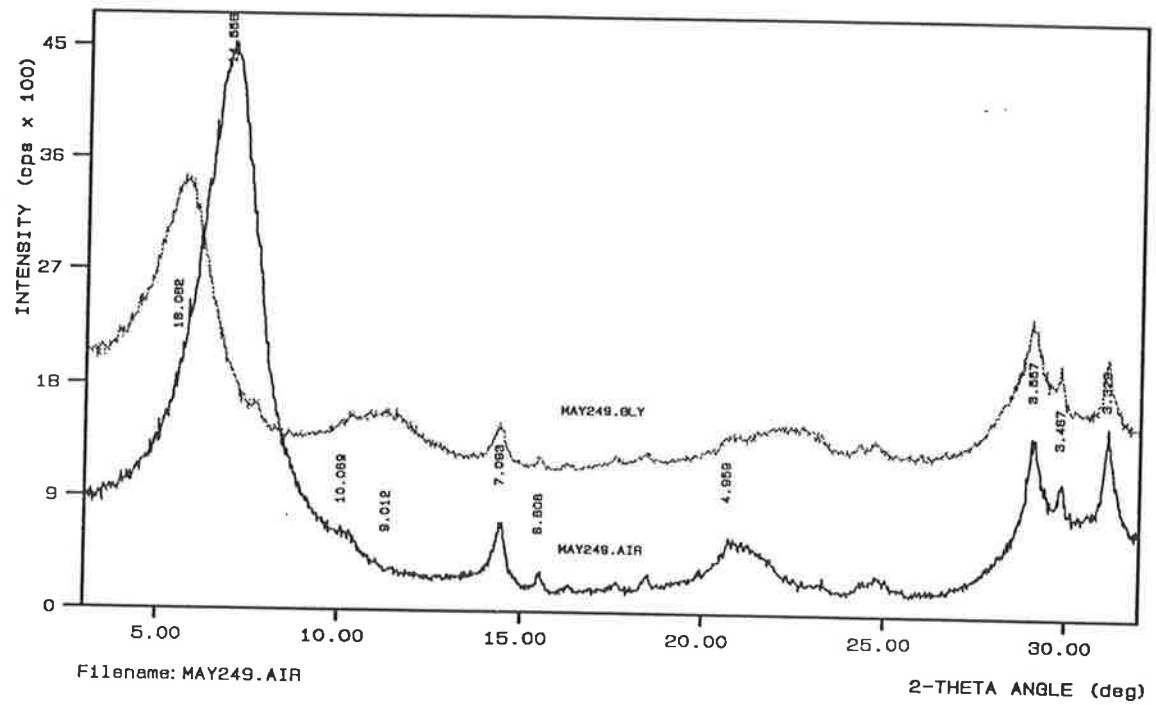

RM249

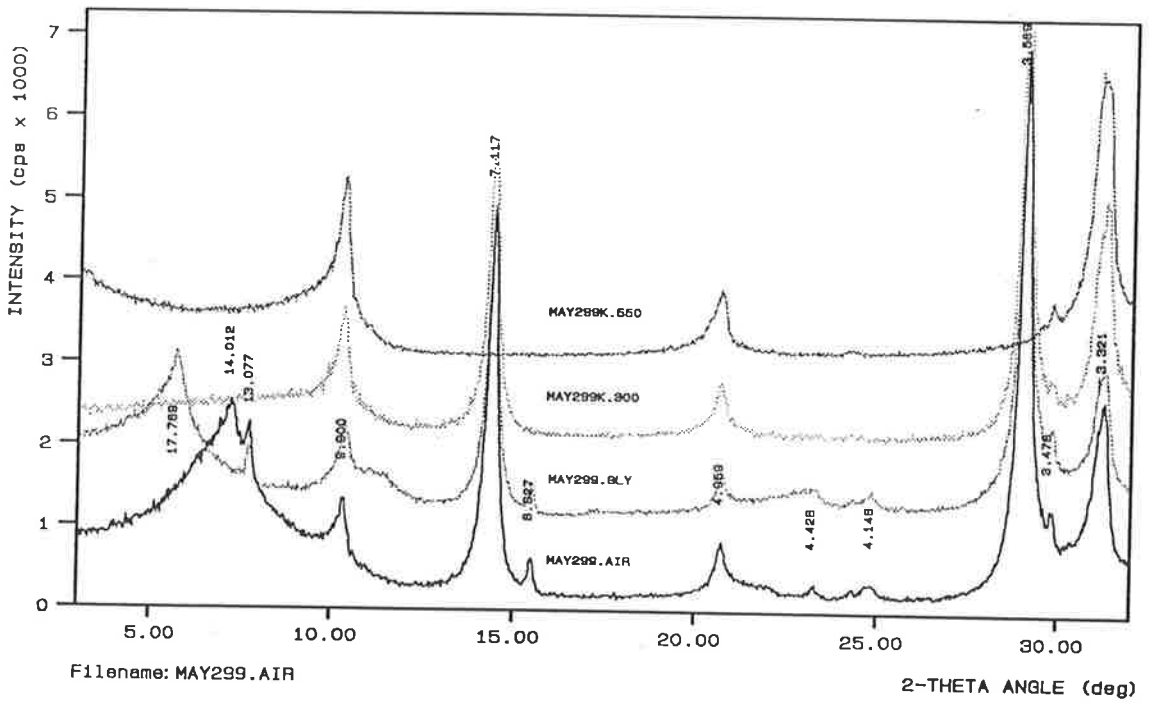

RM299

Figure 4.22 Typical XRD traces of the <2μm fraction of samples containing smectite. Mg-saturated, air-dried and Mg-saturated, glycerol solvated traces are shown for both RM249 (Maslin Bay) and RM304 (Onkaparinga Trig). Traces for material which had been K-saturated and then heated to 300°C and 550°C are additionally shown for sample RM299 (Onkaparinga Trig). Peaks which occur at about 13.1Å and 8.8Å in RM299 and RM304 are due to the Calgon dispersant which was used during sample preparation.

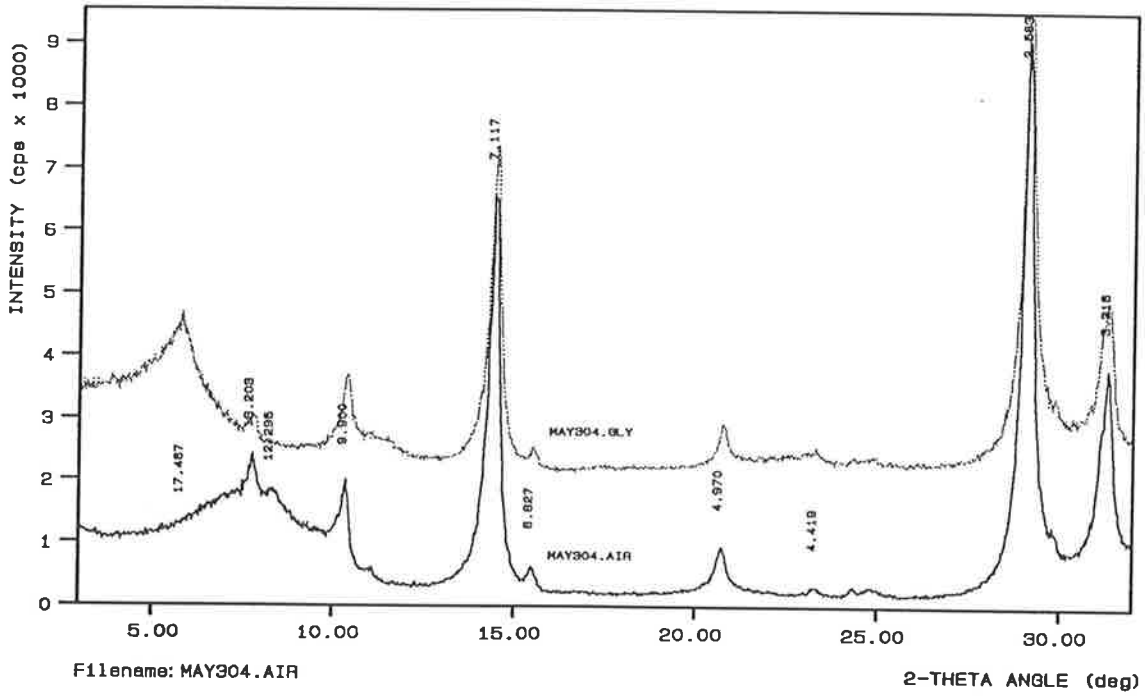
INTENSITY (cps x 1000)
9
8
7
6
5
4
3
2
1
0
5.00
10.00
15.00
20.00
25.00
30.00
Filename: MAY304.AIR
2-THETA ANGLE (deg)
MAY304.GLY
MAY304.AIR
17.487
12.295
9.960
7.117
6.627
4.970
4.419
3.215

RM304

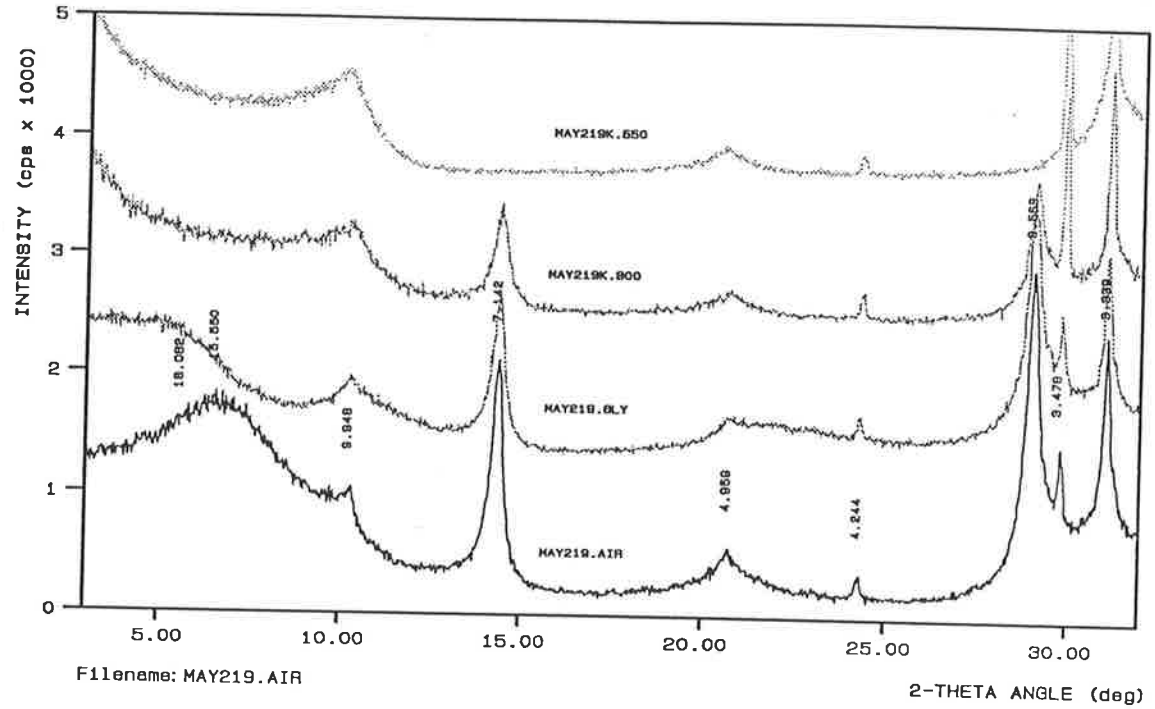

RM219

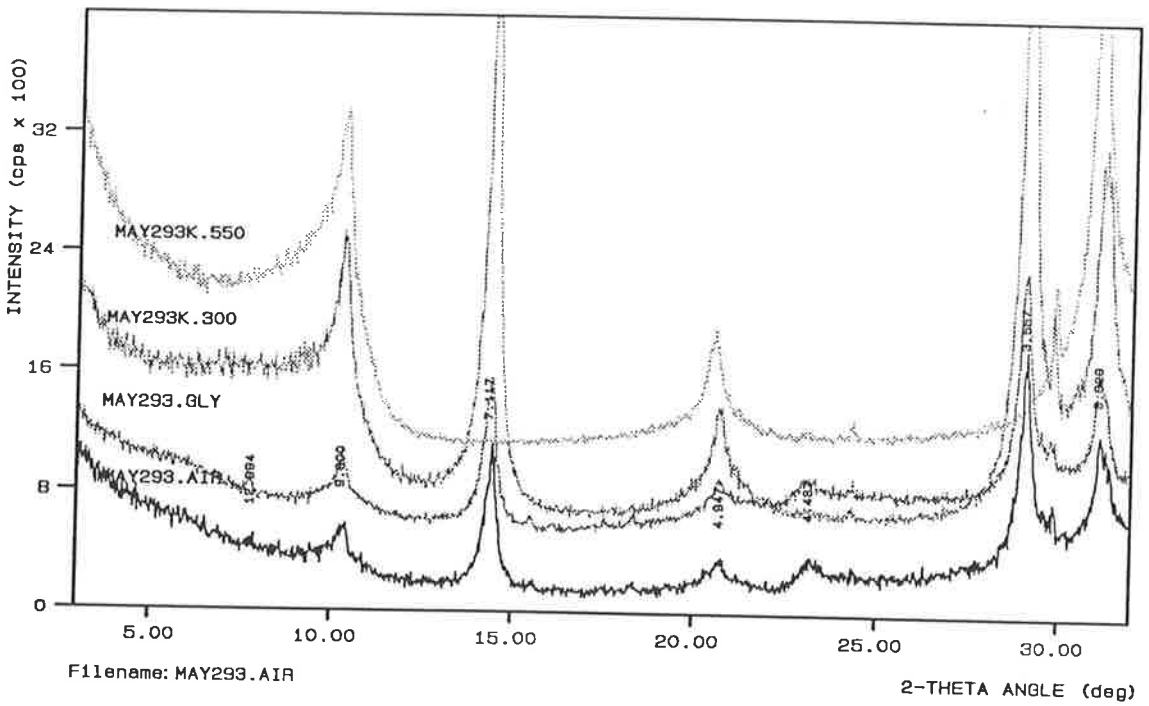

RM293

Figure 4.23 XRD traces of the <2μm fraction of samples containing randomly interstratified illite-smectite which is represented on the traces by elevated intensities at low angles of °2θ for air-dry and glycerol solvated samples. A variation in the proportion of smectitic interlayers is represented by the XRD traces selected. RM219 (Snapper Point) contains approximately 40% smectitic layers; RM293 (Onkaparinga Trig) contains <20% smectitic layers; RM312 (Onkaparinga Trig) contains approximately 20% smectitic layers; RM320 (Onkaparinga Trig) contains 20 to 30% smectitic interlayers; RM368 (Hallett Cove) contains 40 to 50% smectitic layers. Illite (9.9Å) and kaolinite (7.1Å) are also present in all samples. Peaks at 13.1Å and 8.8Å are due to Calgon used as a dispersant during sample preparation.

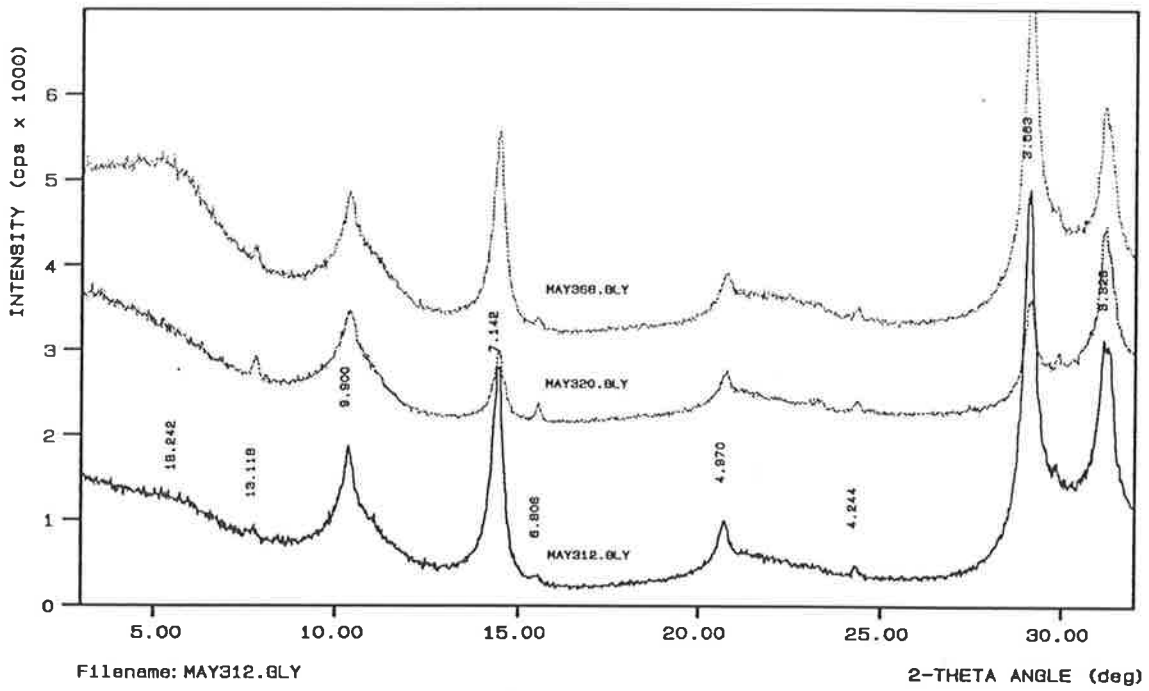

RM312, RM320, RM368

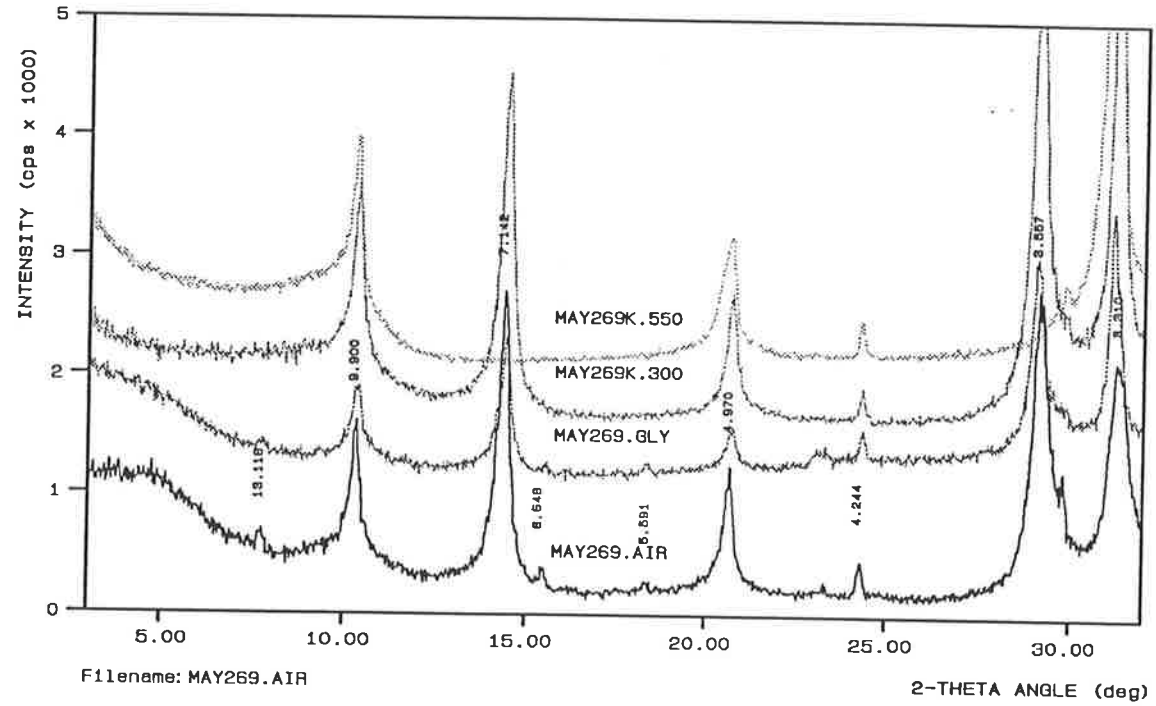

RM269

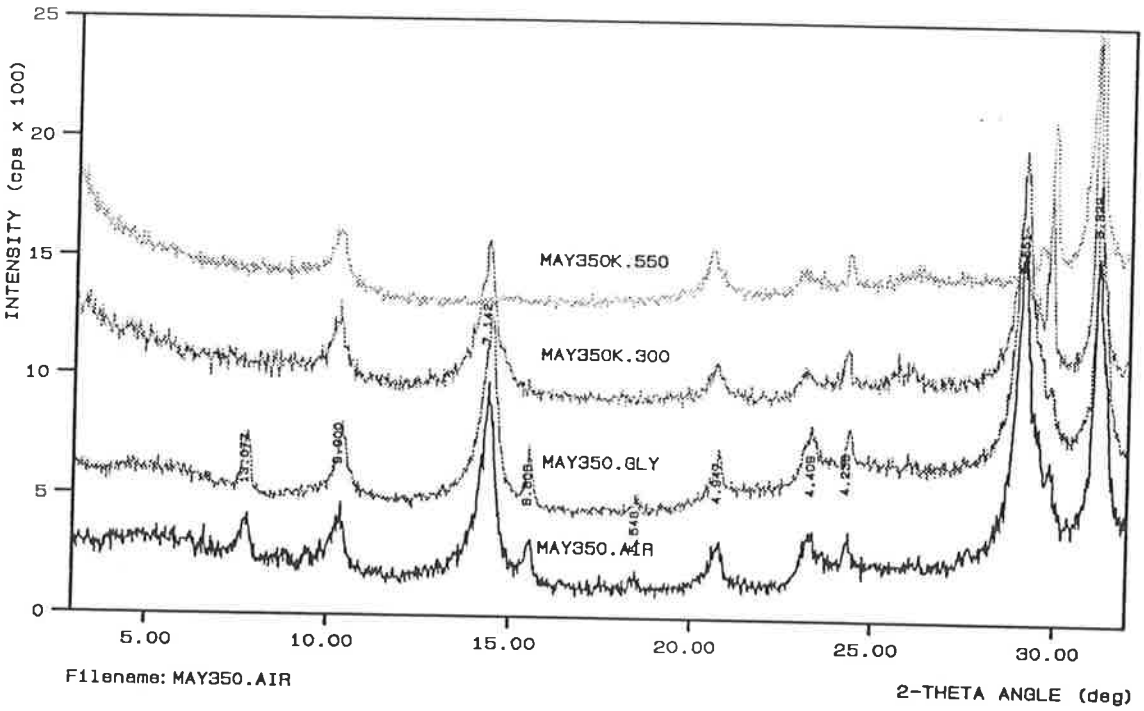

RM350

Figure 4.24 XRD traces of the <2μm fraction of samples showing variable collapse of smectitic layers to 10Å on heating the samples to 300°C and 550°C. Samples RM269 (Maslin Bay) and RM350 (Hallett Cove) show complete collapse on heating while samples RM282 (Maslin Bay) and RM332 (Onkaparinga Trig) show only partial collapse. XRD traces are shown for air-dry, glycerol solvated, heated to 300°C and heated to 550°C treatments for all samples. Illite (9.9Å) and kaolinite (7.1Å) are also present in all samples. Peaks at 13.1Å and 8.8Å which are present in some samples are due to Calgon which was used as a dispersant during sample preparation.

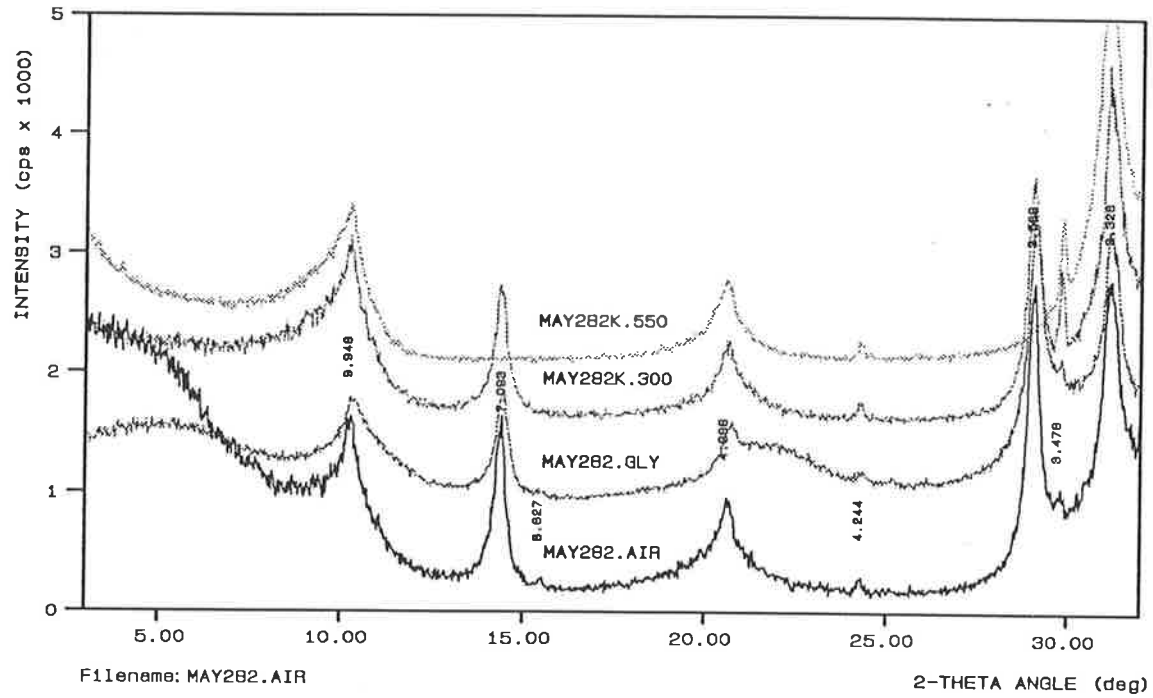
INTENSITY (cps x 1000)
MAY282K.550
MAY282K.300
MAY282.GLY
MAY282.AIR
8.948
7.083
8.827
4.244
8.478
Filename: MAY282.AIR
2-THETA ANGLE (deg)

RM282

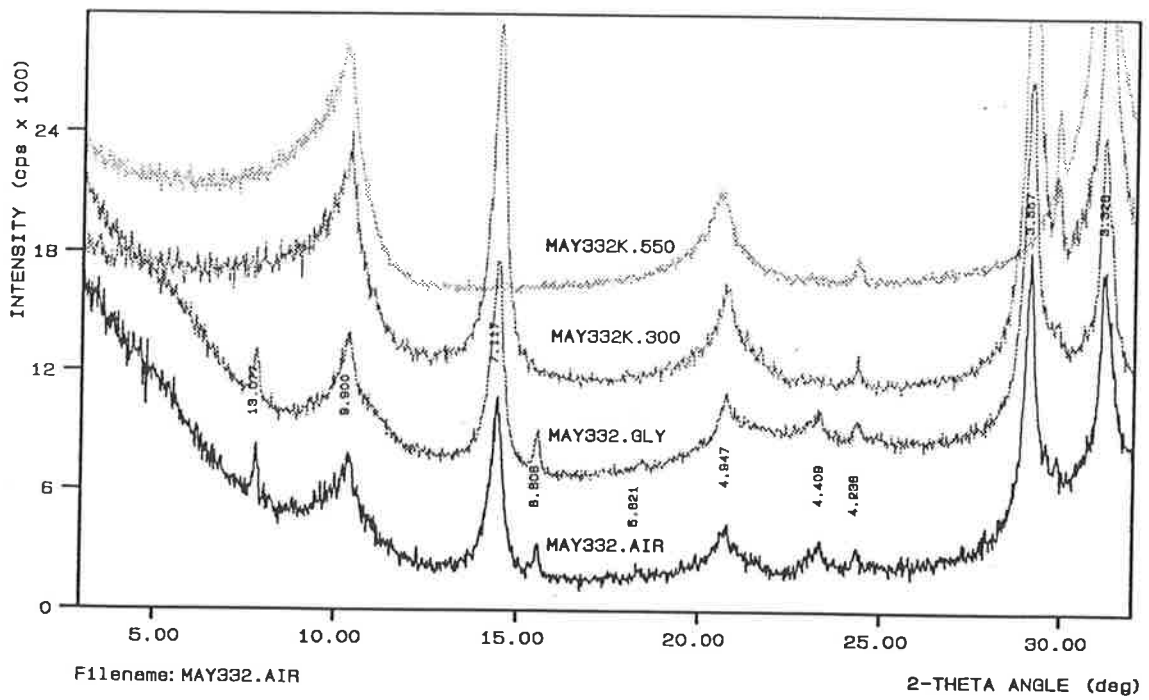
INTENSITY (cps x 100)
MAY332K.550
MAY332K.300
MAY332.GLY
MAY332.AIR
13.072
9.900
7.117
8.808
5.821
4.847
4.409
4.238
Filename: MAY332.AIR
2-THETA ANGLE (deg)

RM332

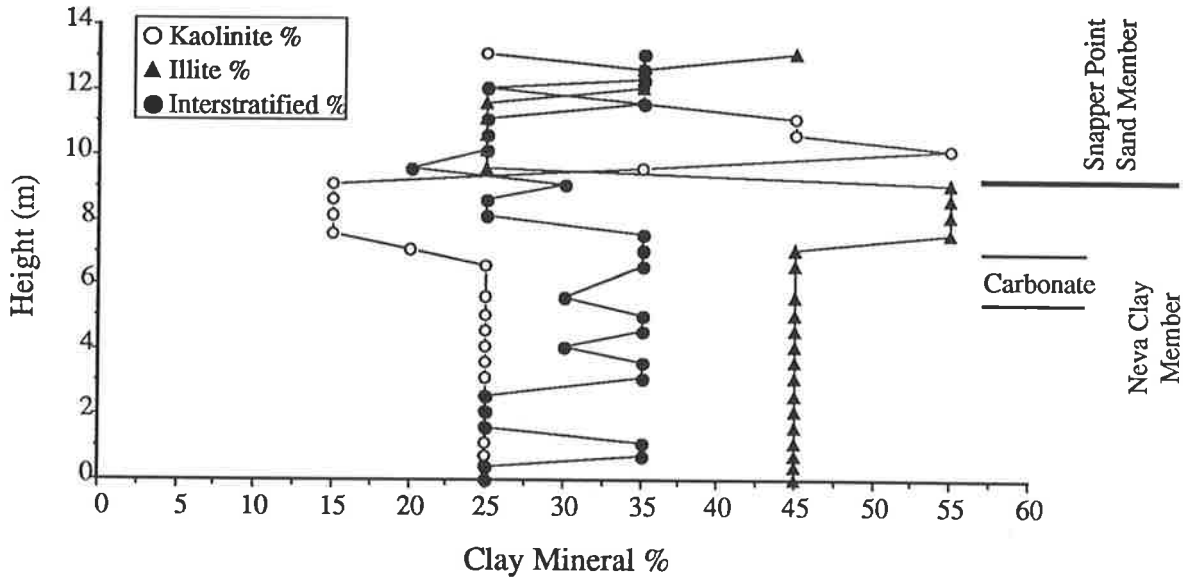

Figure 4.25 Clay mineral proportions in the <2μm fraction for samples from the Snapper Point site. For sample numbers and locations refer to the sketch section in Figure 3.5.

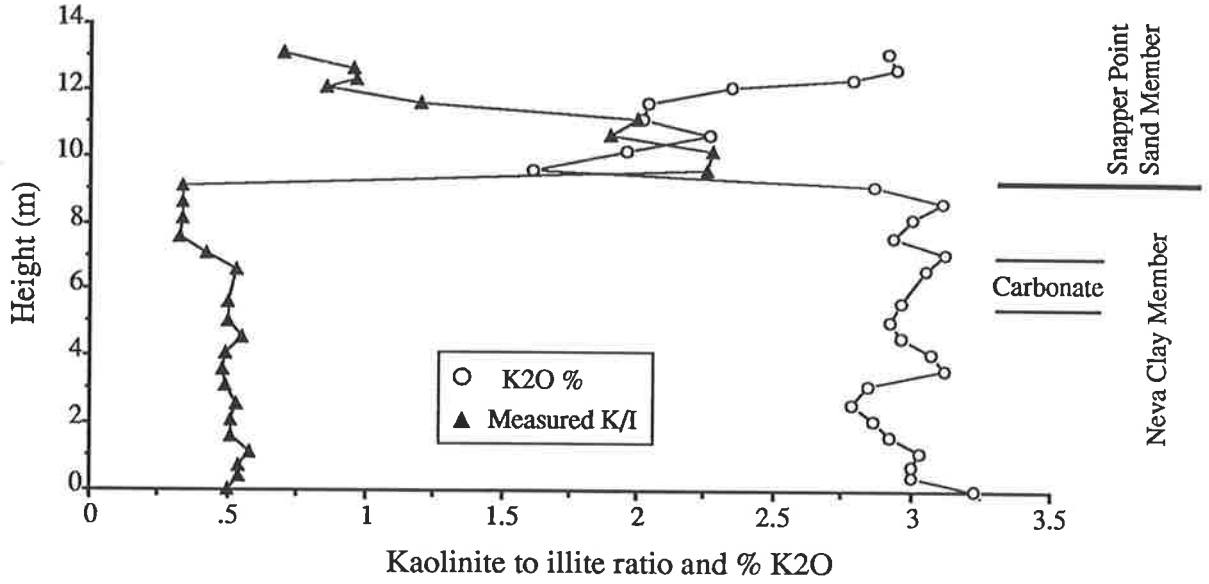

Figure 4.26 Kaolinite to illite ratios and % K2O for the <2μm fraction of samples from the Snapper Point site. For sample numbers and locations refer to the sketch section in Figure 3.5.

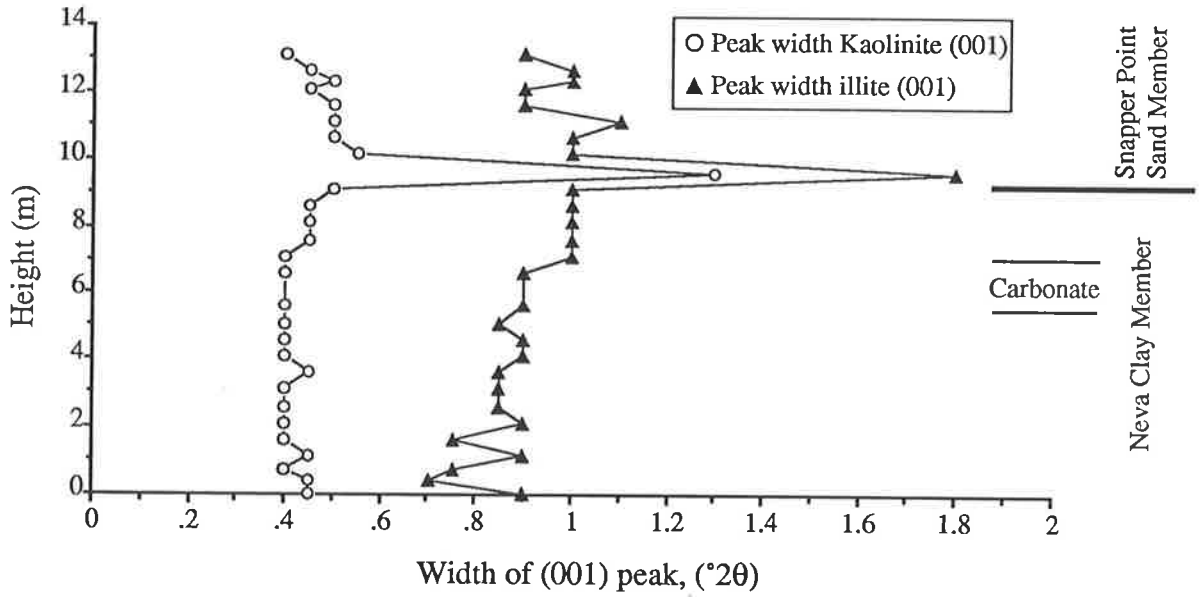

Figure 4.27 Widths in °2θ measured on the (001) peaks of kaolinite and illite from the <2μm fraction of samples from the Snapper Point site. The sharp increase in peak width at the base of the Snapper Point Sand Member for both kaolinite and illite is due to the presence of halloysite. For sample numbers and locations refer to the sketch section in Figure 3.5.

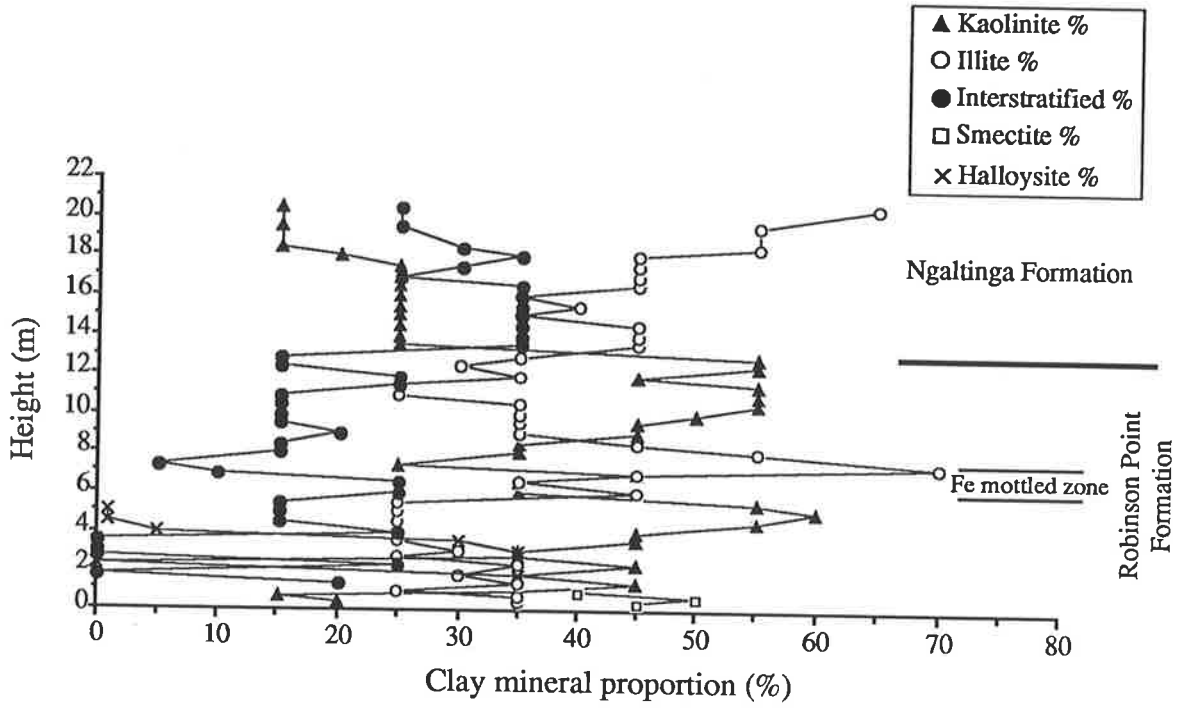

Figure 4.28 Clay mineral proportions in the <2μm fraction for samples from the Maslin Bay site. For sample numbers and locations refer to the sketch section in Figure 3.15.

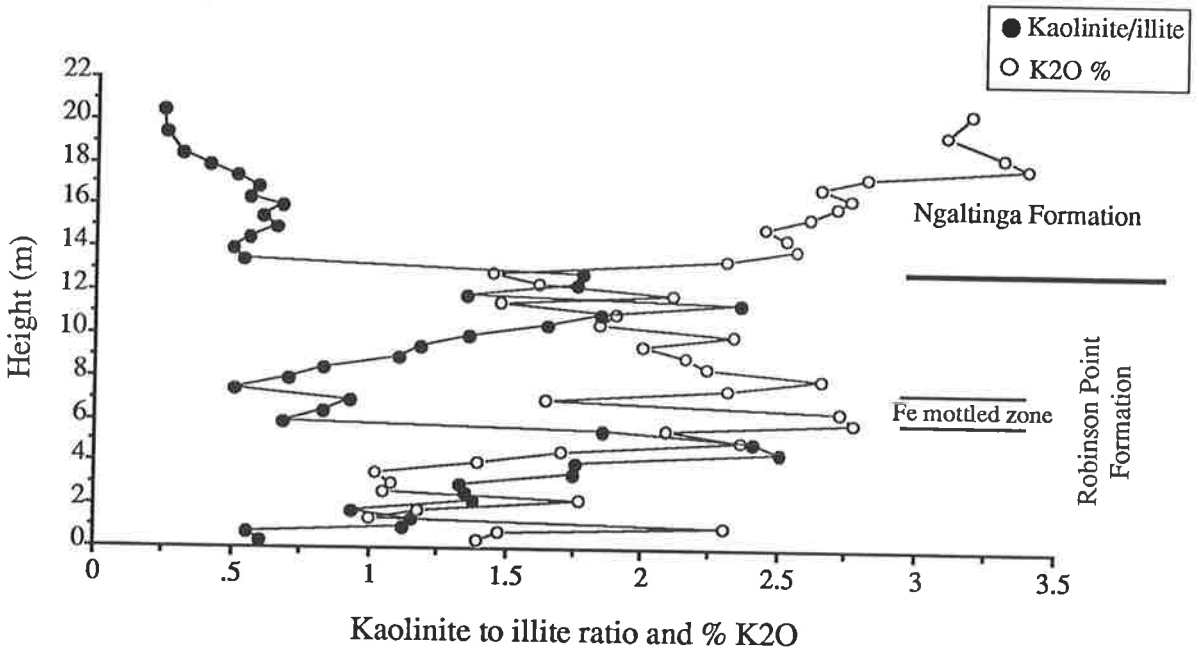

Figure 4.29 Kaolinite to illite ratios and % K2O for the <2μm fraction of samples from the Maslin Bay site. For sample numbers and locations refer to the sketch section in Figure 3.15.

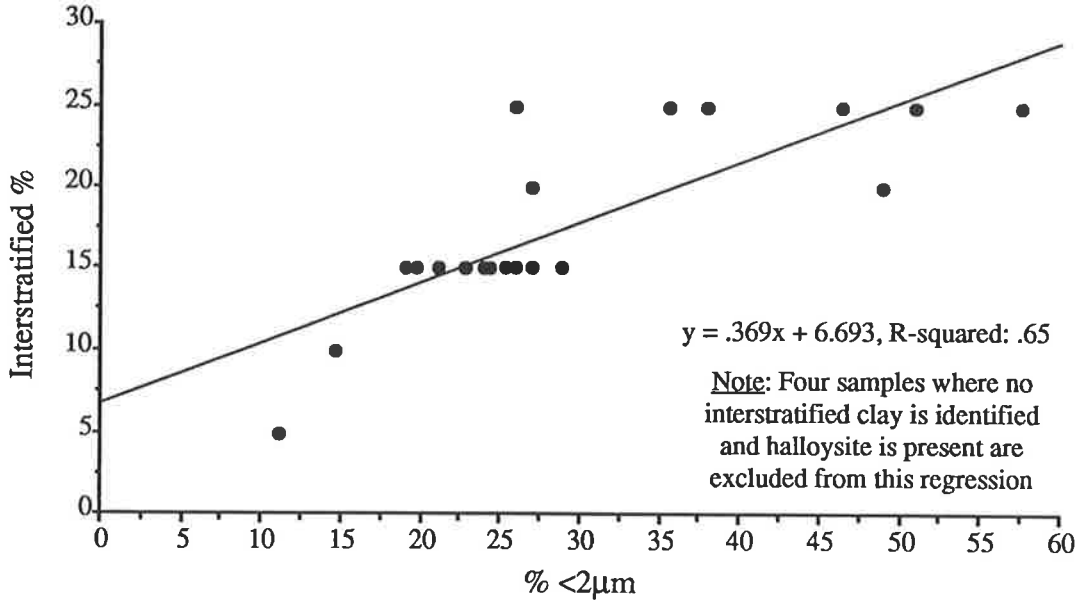

Figure 4.30 Graph showing the relationship between the proportion of randomly interstratified clays in the clay fraction and % <2μm for samples from the Maslin Bay site. While a general increase in the proportion of randomly interstatified clays with the % <2μm is suggested, regression analysis indicates that this is not statistically significant.

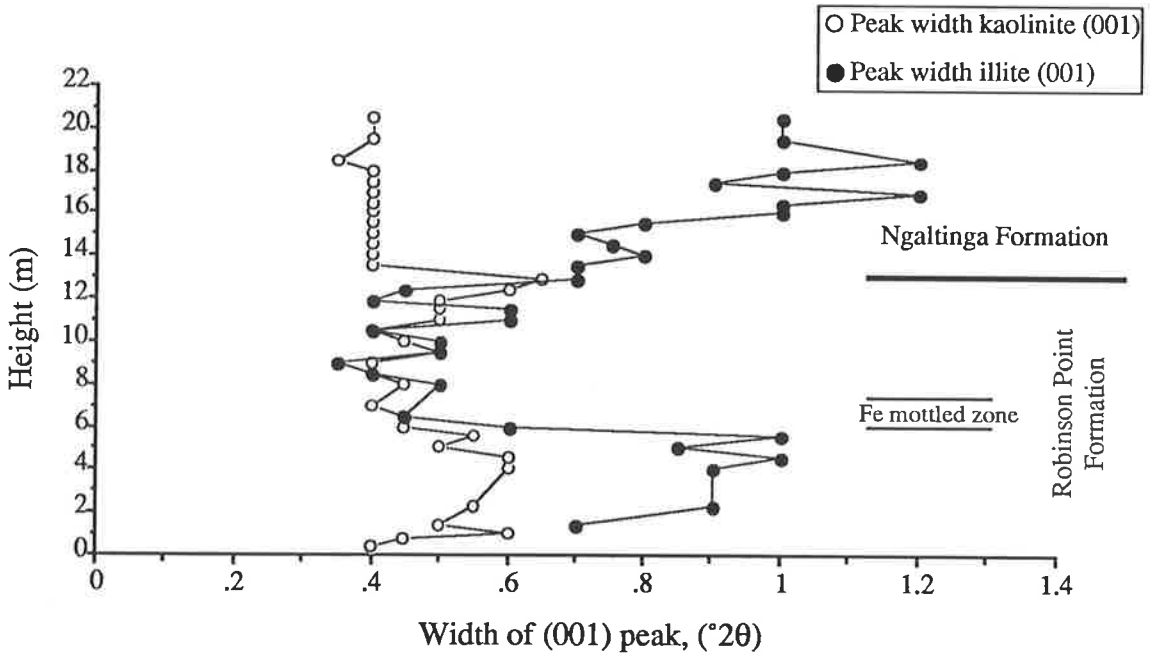

Figure 4.31 Widths in °2θ measured on the (001) peaks of kaolinite and illite from the <2μm fraction of samples from the Maslin Bay site. For sample numbers and locations refer to the sketch section in Figure 3.15.

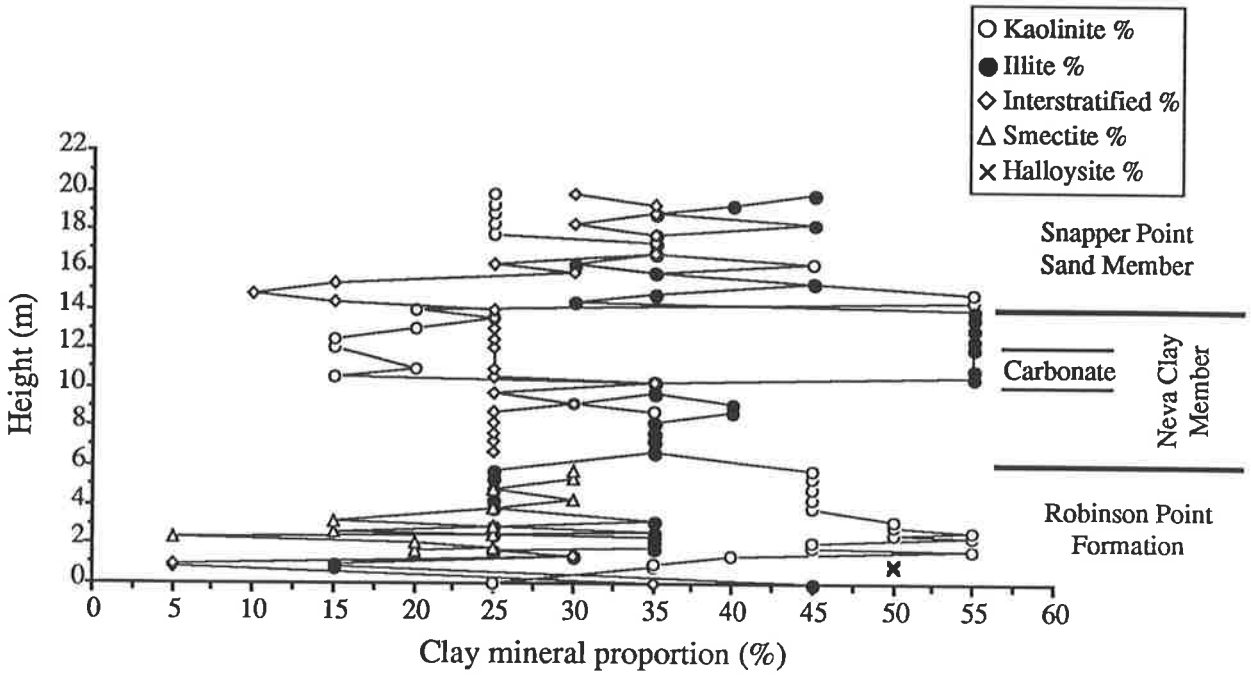

Figure 4.32 Clay mineral proportions in the <2μm fraction for samples from the Onkaparinga Trig site. For sample numbers and locations refer to the sketch section in Figure 3.27.

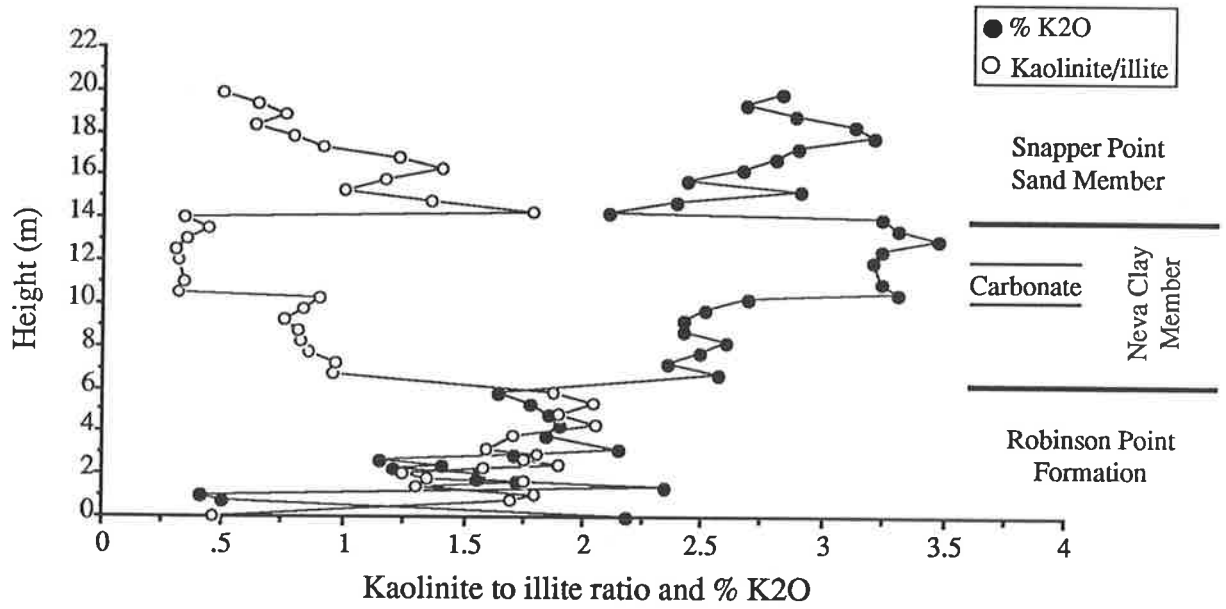

Figure 4.33 Kaolinite to illite ratios and % K2O for the <2μm fraction of samples from the Onkaparinga Trig site. For sample numbers and locations refer to the sketch section in Figure 3.27.

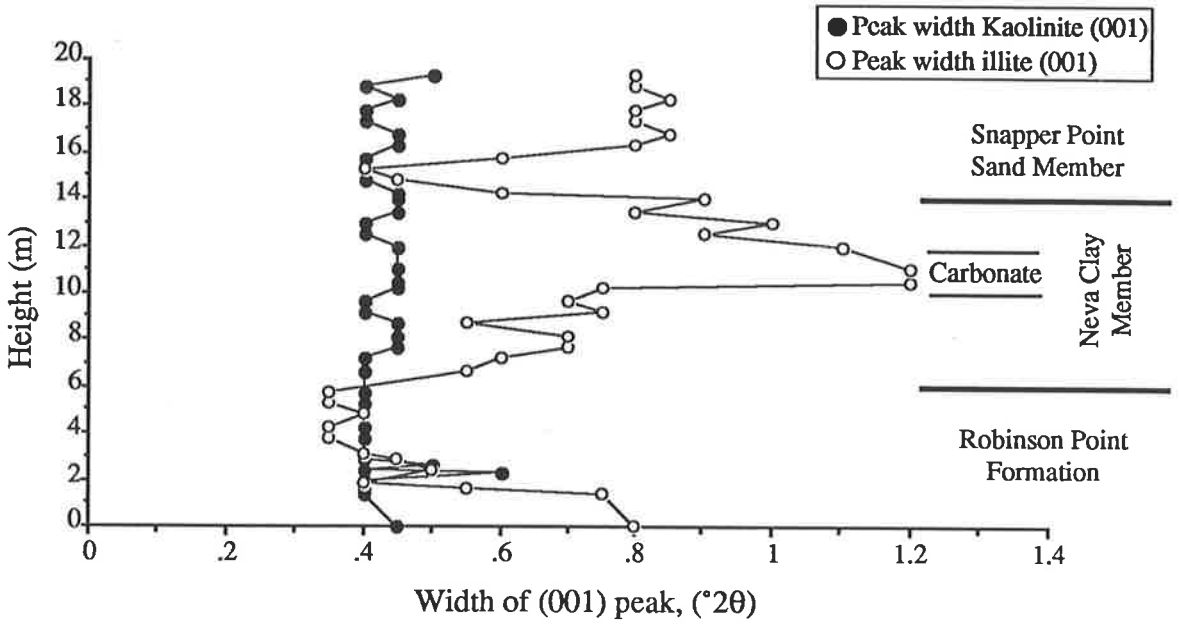

Figure 4.34 Widths in °2θ measured on the (001) peaks of kaolinite and illite from the <2μm fraction of samples from the Onkaparinga Trig site. For sample numbers and locations refer to the sketch section in Figure 3.27.

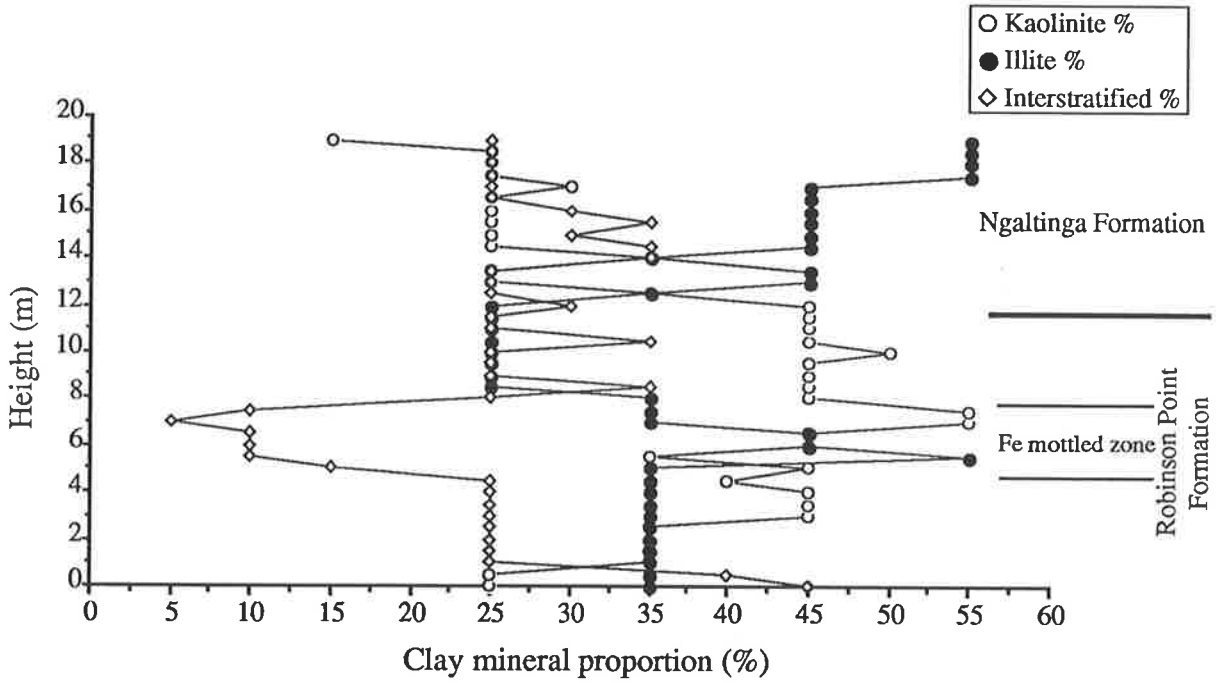

Figure 4.35 Clay mineral proportions in the <2μm fraction for samples from the Hallett Cove site. For sample numbers and locations refer to the sketch section in Figure 3.37.

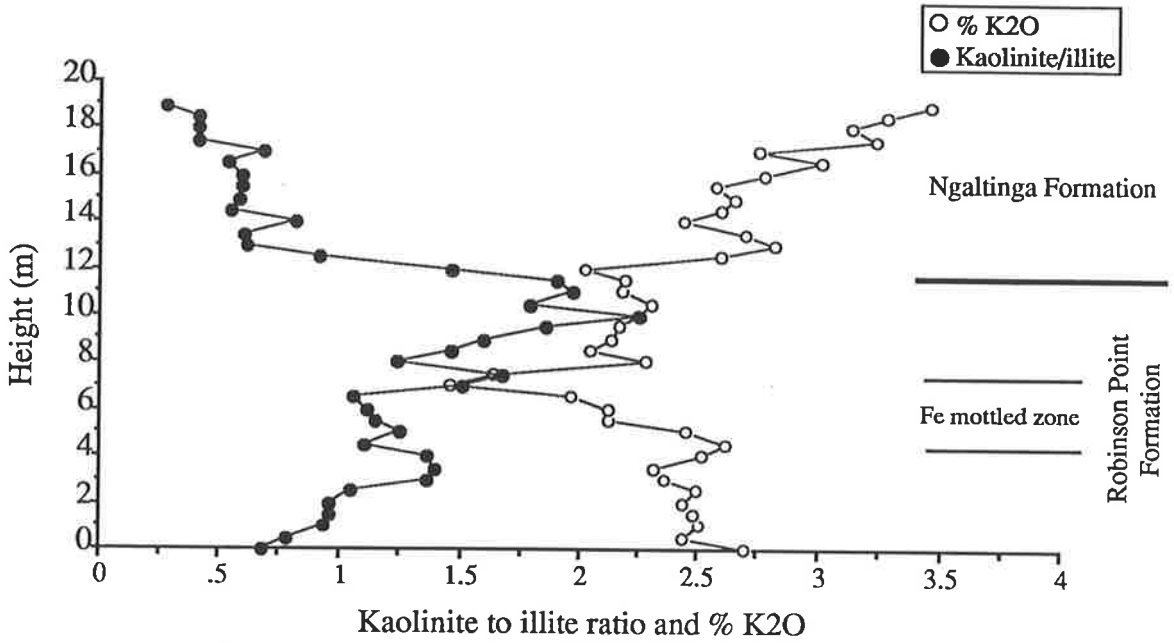

Figure 4.36 Kaolinite to illite ratios and % K2O for the <2μm fraction of samples from the Hallett Cove site. For sample numbers and locations refer to the sketch section in Figure 3.37.

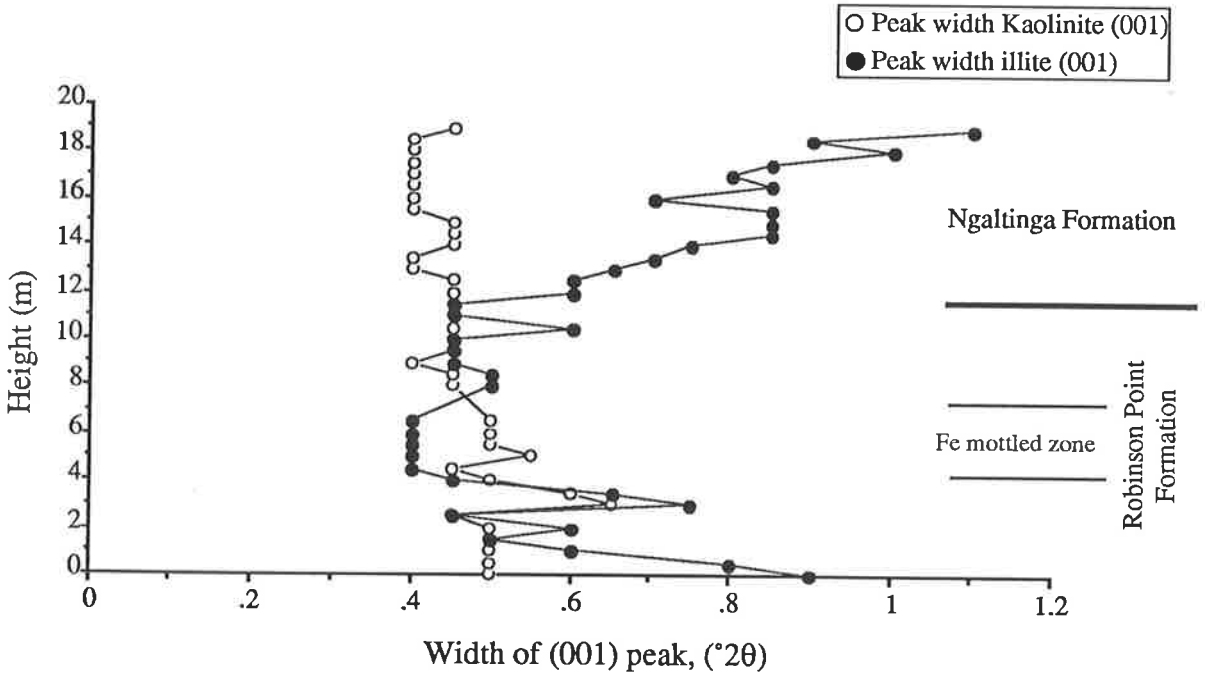

Figure 4.37 Widths in °2θ measured on the (001) peaks of kaolinite and illite from the <2μm fraction of samples from the Hallett Cove site. For sample numbers and locations refer to the sketch section in Figure 3.37.

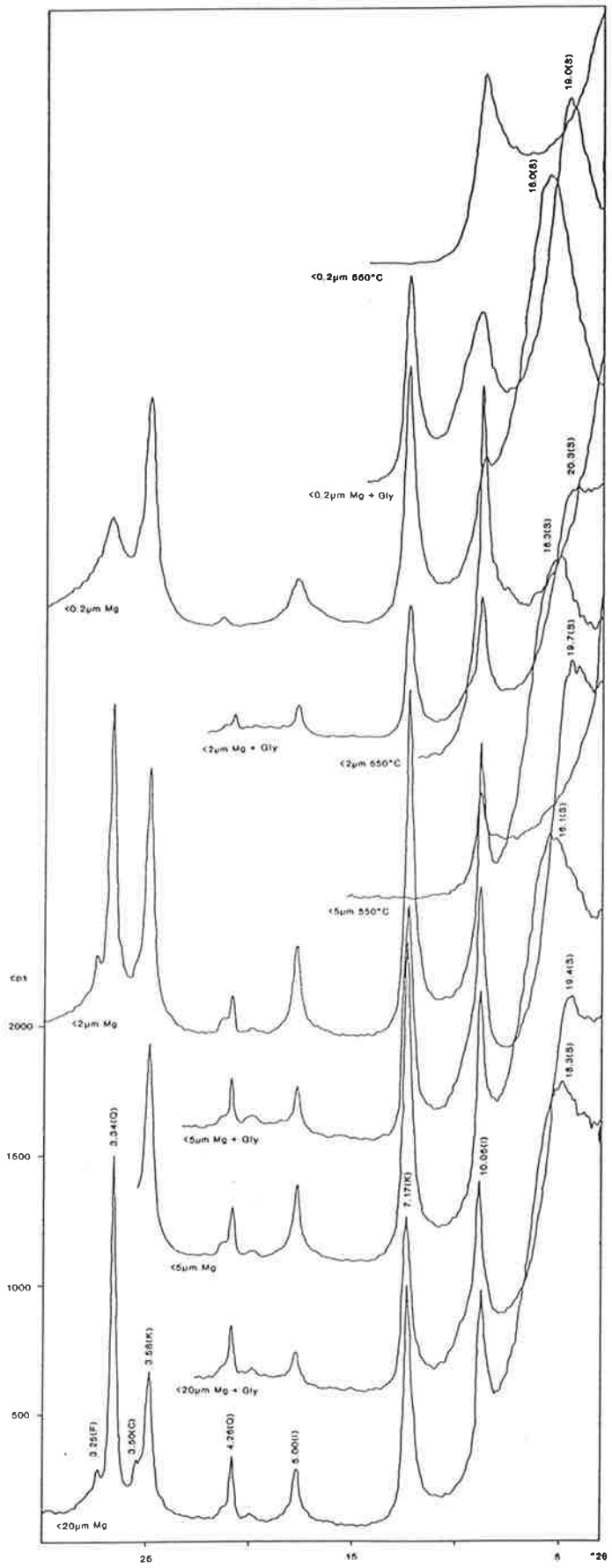

Figure 4.38 XRD traces of the <20µm, <5µm, <2µm and <0.2µm fractions separated from samples RM262 (Maslin Bay), RM304 (Onkaparinga Trig) and RM312 (Onkaparinga Trig). Traces are given for each fraction which show effects of various treatments which include Mg-saturation, Mg-saturation and glycerol solvation and K-saturated and heated to 550°C. Clay minerals identified include smectite (S), illite (I) and kaolinite (K) while other minerals present include quartz (Q), feldspar (F) and goethite (G). Corundum (C) present in the ceramic tile on which the clay fractions are sedimented is also recognised.

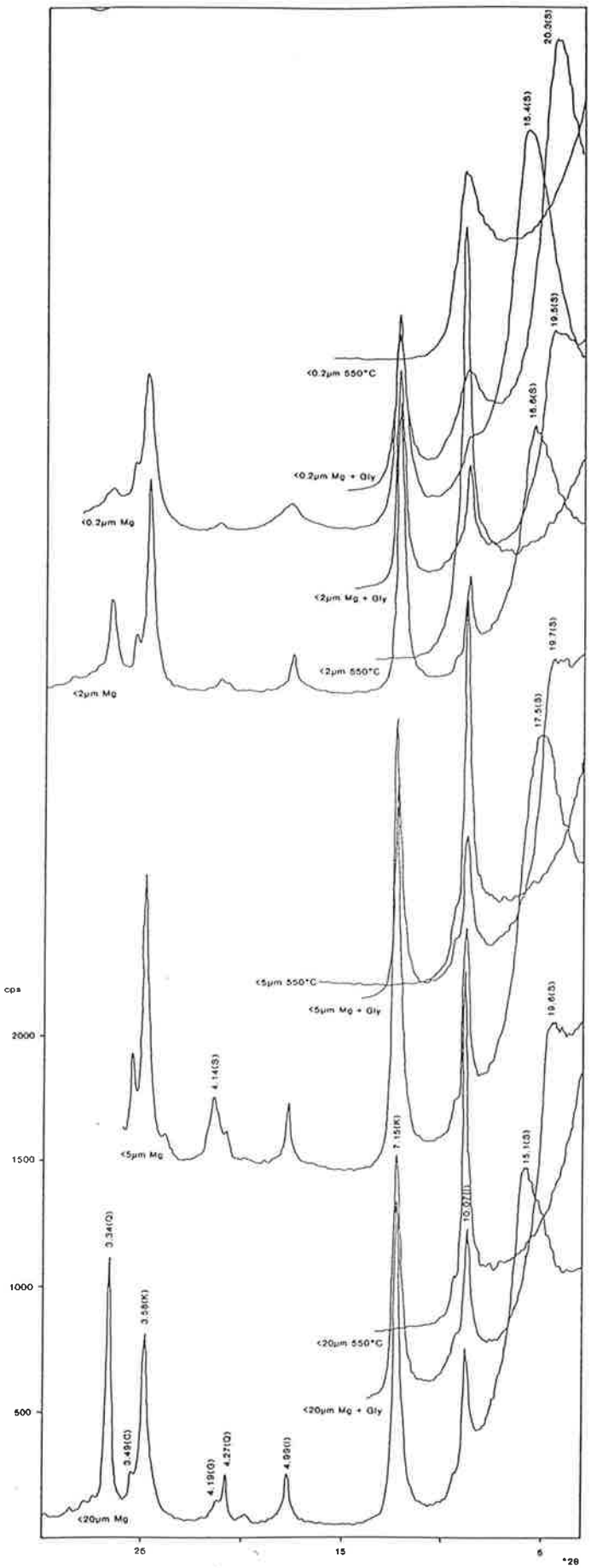
cps
2000
1500
1000
500
25
15
5
°2θ
<0.2µm 550°C
<0.2µm Mg + Gly
<0.2µm Mg
<2µm Mg + Gly
<2µm 550°C
<2µm Mg
<5µm 550°C
<5µm Mg + Gly
<5µm Mg
<20µm 550°C
<20µm Mg + Gly
<20µm Mg
20.3(S)
18.4(S)
19.5(S)
18.6(S)
19.7(S)
17.5(S)
19.6(S)
7.15(K)
15.1(S)
15.97(I)
3.34(Q)
3.58(K)
3.49(C)
4.19(O)
4.27(Q)
4.99(I)
4.14(S)

RM304

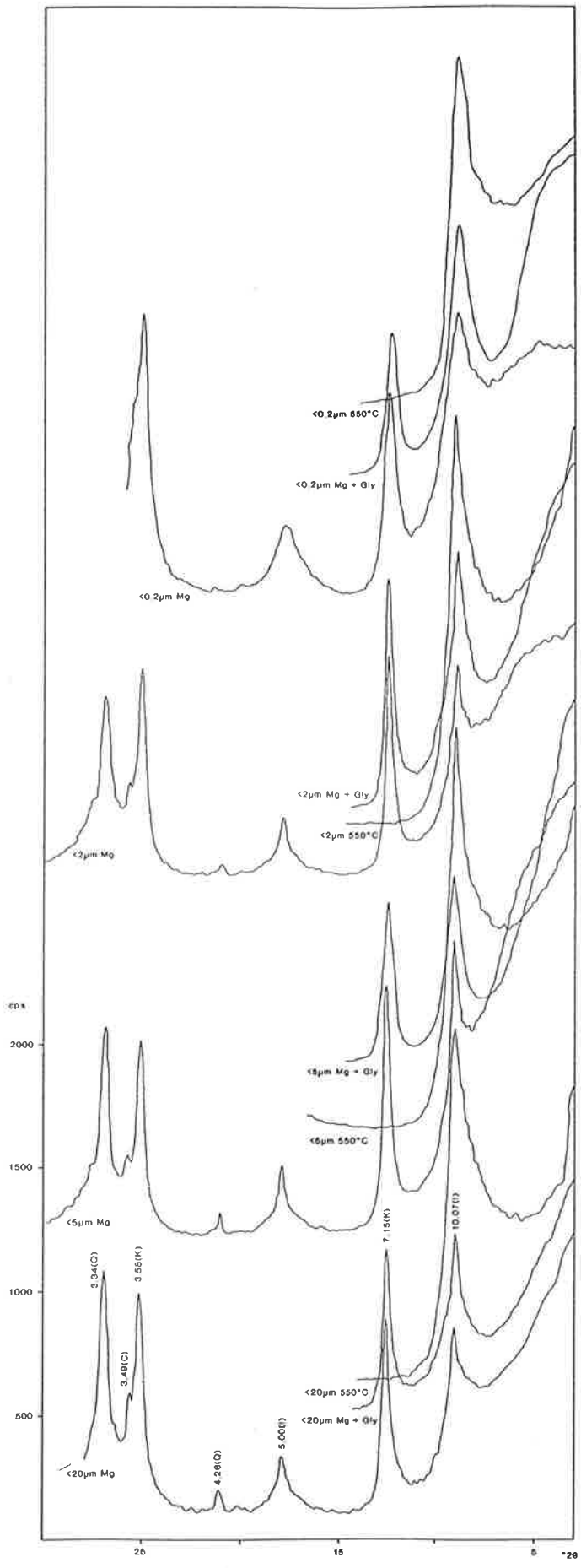
<0.2µm 550°C
<0.2µm Mg + Gly
<0.2µm Mg
<2µm Mg + Gly
<2µm 550°C
<2µm Mg
<5µm Mg + Gly
<5µm 550°C
<5µm Mg
<20µm 550°C
<20µm Mg + Gly
<20µm Mg
cps
2000
1500
1000
500
3.34(Q)
3.58(K)
3.49(C)
4.26(Q)
5.00(I)
7.15(K)
10.07(I)
26
15
5
°2θ

RM312

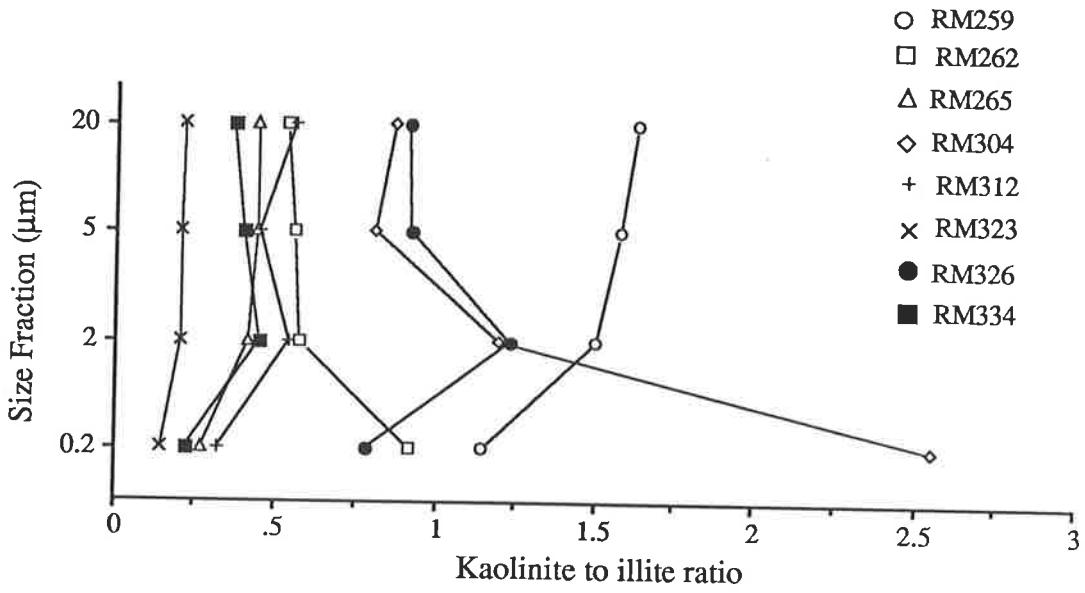

Figure 4.39 Graph showing kaolinite to illite ratios for the <20µm, <5µm, <2µm and <0.2µm size fractions separated from samples RM259, RM262, RM265 (Maslin Bay), RM304, RM312, RM323, RM326 and RM334 (Onkaparinga Trig). Apart from samples which contain smectite (RM262, RM304), all samples show a decrease in the proportion of kaolinite compared with illite in the finest fraction (<0.2µm). The presence of silt-sized muscovite in sample RM326 accounts for the relative decrease in kaolinite in coarsest fractions (>2µm) which is the opposite trend to that shown in all other samples.

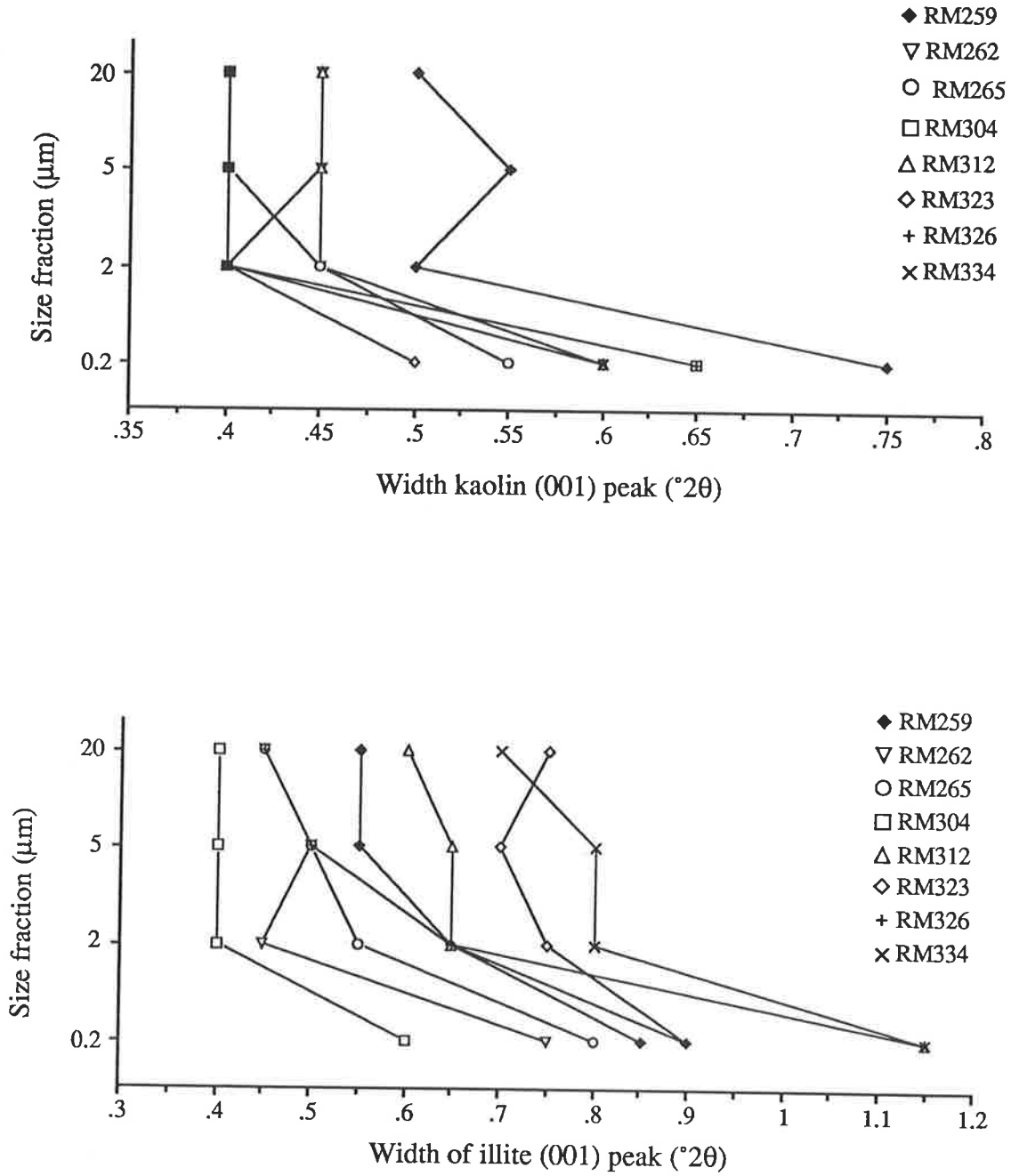

Figure 4.40 Graphs showing the relationship between the width of the (001) peak (°2θ) for both kaolinite and illite versus the four size fractions (<20µm, <5µm, <2µm and <0.2µm) separated from samples RM259, RM262, RM265, RM304, RM312, RM323, RM326 and RM334. Peak width increases in the smallest size fractions and is also generally greater for illite compared with kaolinite.

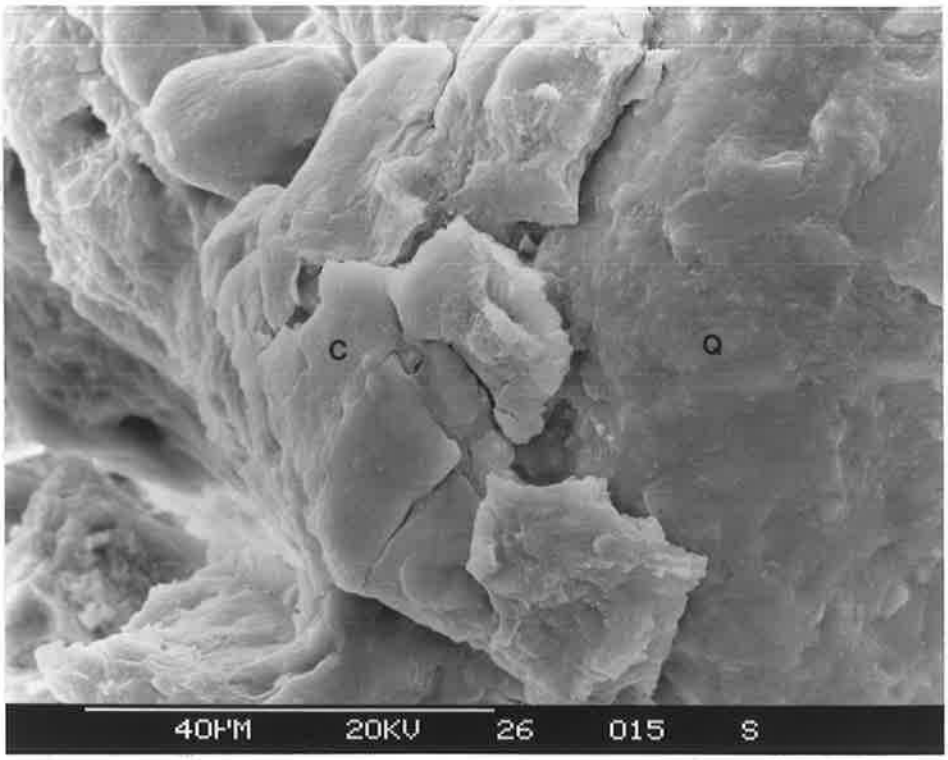

Figure 4.41 Scanning electron micrograph from sample RM326 (Onkaparinga Trig) showing clays (C) forming a thick skin around large detrital quartz grains (Q). (Bar scale represents 40µm.)

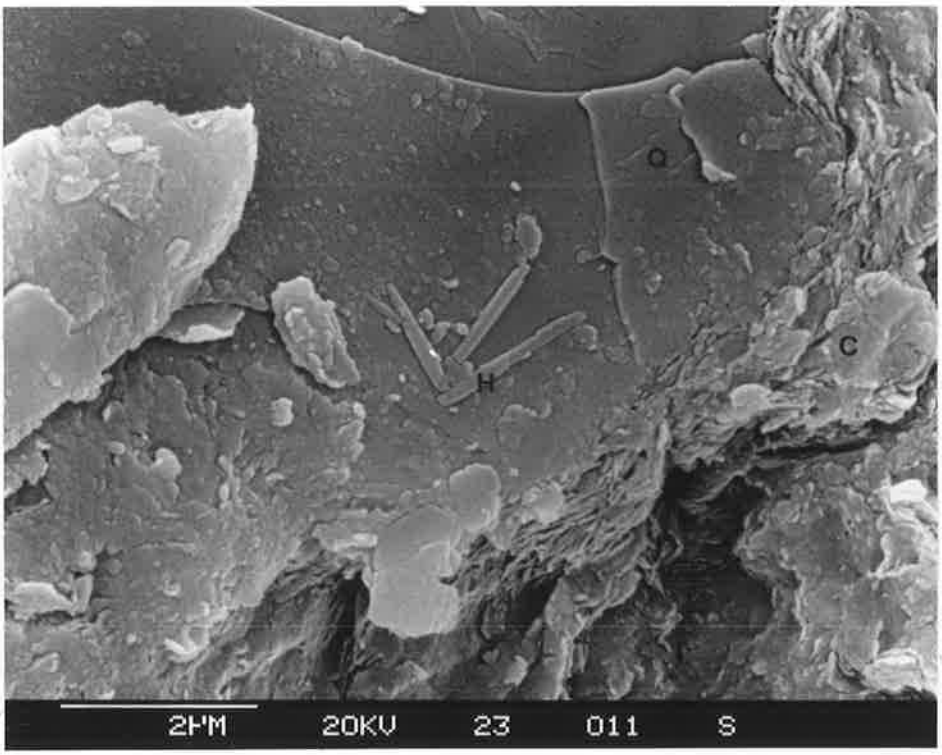

Figure 4.42 Scanning electron micrograph from sample RM323 (Onkaparinga Trig) showing oriented individual clay aggregates within the clay skin (C) surrounding a detrital quartz grain (Q). Rod-like material up to 2µm in length which occurs on the surface of the quartz grain is halloysite (H). (Bar scale represents 2µm.)

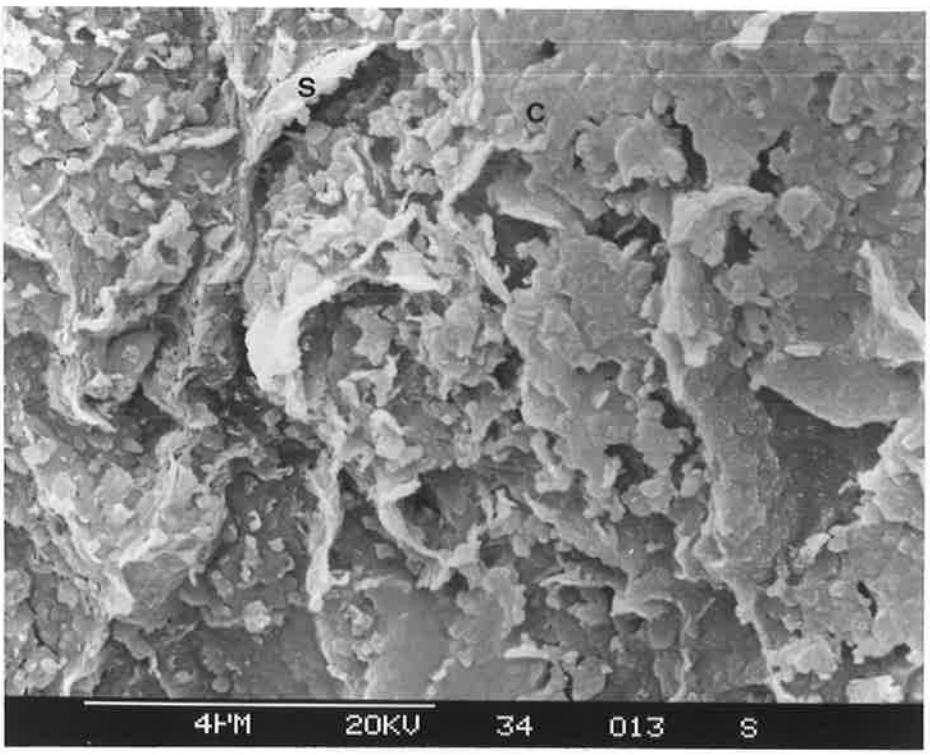

Figure 4.43 Scanning electron micrograph from sample RM334 (Onkaparinga Trig) showing flat platelets of clay (C) up to 0.4μm in diameter. Irregular and curled clays are noted on the margins of the more massive clay and may represent interstratified illite-smectite or smectitic phases (S). (Bar scale represents 4μm.)

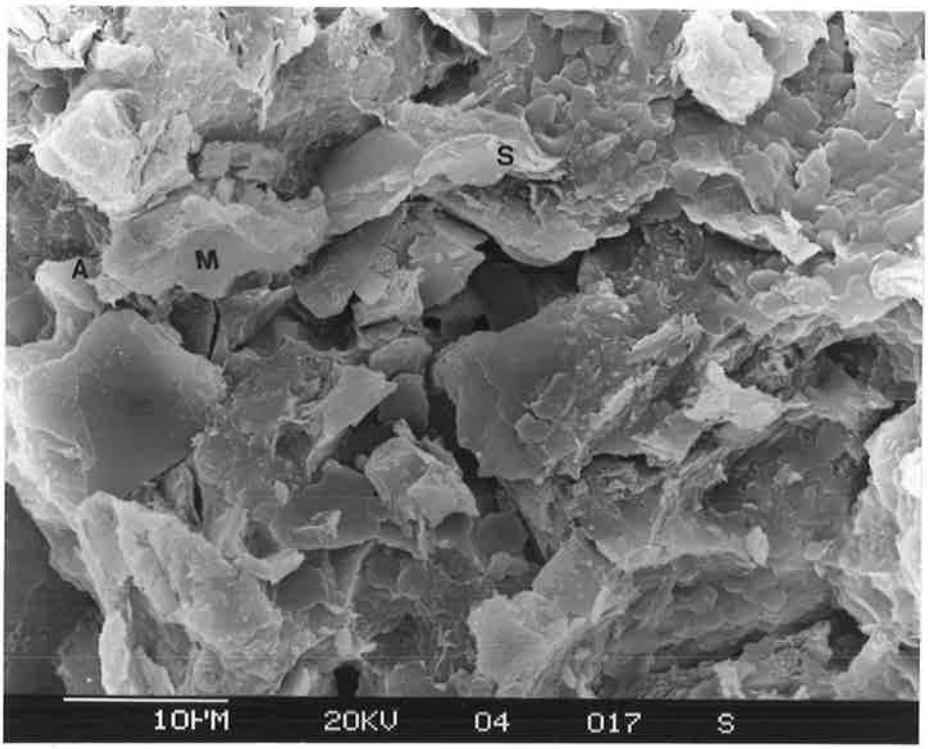

Figure 4.44 Scanning electron micrograph from sample RM304 (Onkaparinga Trig) showing silt-sized muscovite grains (M) forming the major component. Fine-grained clays coat the muscovite grains and often show curling on the edges which is thought to indicate the presence of smectitic phases (S). Very fine hair-like material protrudes from some muscovite grains and is interpreted as authigenic clay (A). (Bar scale represents 10μm.)

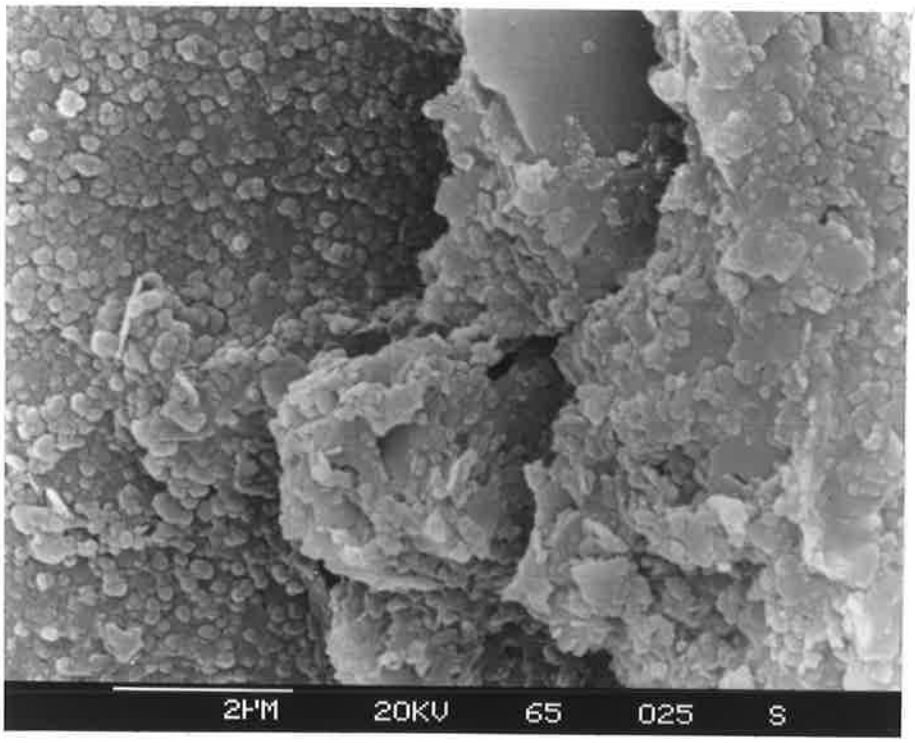

Figure 4.45 Scanning electron micrograph from sample RM265 (Maslin Bay) showing spherical particles of uniform size up to 0.25µm in diameter coating the surface of a quartz grain on the left hand half of the micrograph. X-ray spectra indicate that the spherules are composed of silica. (Bar scale represents 2µm.)

Figure 5.1 Alunite/halloysite interval near the base of the Robinson Point Formation just south of Onkaparinga Trig. White nodular material adjacent to the hammer is halloysite impregnated sandy sediment which occurs in a broad band. Thin seams of white material approximately 50 cm above the hammer are composed of alunite. Red to pink nodular material adjacent to the alunite bands comprises a mixture of hematite and halloysite while thin bands of yellow-brown sediment are dominated by goethite. (Hammer is 28 cm in length.)

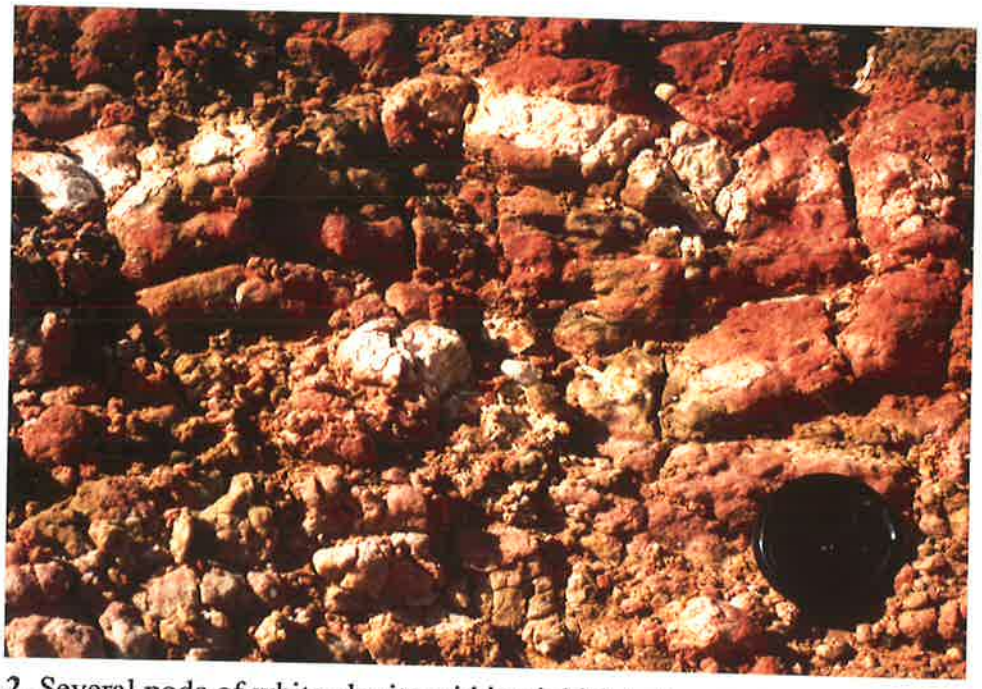

Figure 5.2 Several pods of white alunite within pinkish halloysite impregnated sands near the base of the Robinson Point Formation south of Onkaparinga Trig. The lower boundaries of the alunite pods are sharp while upper boundaries are more diffuse. (Lens cap is 50 mm in diameter.)

Figure 5.3 Several discontinuous bands of white alunite up to 10 cm thick which occur within a red to pink ferruginous zone at the base of the Robinson Point Formation near Robinson Point. (Hammer is 28 cm long.)

Figure 5.4 Large mass of white alunite which occurs in sandy sediments near the base of the Robinson Point Formation south of Robinson Point. The lower contact of the alunite with surrounding sediment is sharp while the upper contact is diffuse. (Five cent piece is 2 cm in diameter.)

Figure 5.5 White alunite (A) occurring as isolated pods and thin seams above and below a remnant of the Pliocene Hallett Cove Sandstone (H) immediately south of the Port Stanvac Oil Refinery. (Lens cap is 50 mm in diameter.)

Figure 5.6 Thin seams and isolated nodular masses of white alunite occurring within the Eocene South Maslin Sand adjacent to the Onkaparinga River several km upstream of the river mouth. (Hammer is 28 cm long.)

Figure 5.7 Thin, discontinuous seams and large pods of white alunite in ferruginous mottled grey clays of Pleistocene age at Port Moorowie on Yorke Peninsula. The hammer (28 cm long) rests on the contact between white mottled sands of Permian age and Pleistocene sediments while cream coloured carbonate impregnates sandy clays immediately above the alunite interval.

Figure 5.8 Large ferruginous mottles which occur within indurated sands of the Snapper Point Sand Member adjacent to Chinaman Gully. Yellow material coating some mottles is jarosite. (Lens cap is 50 mm in diameter.)

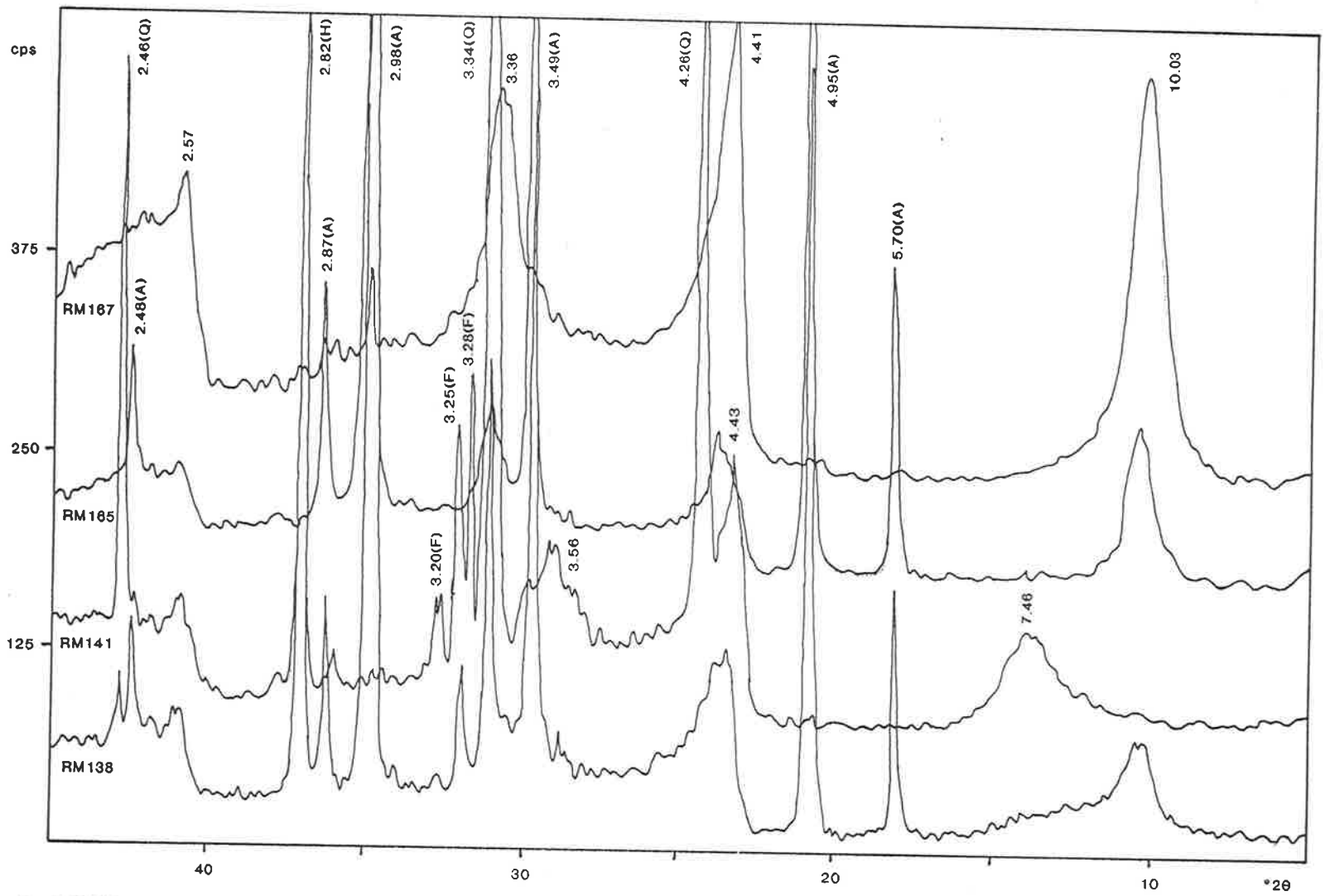

Figure 5.9 Typical XRD traces of samples containing alunite and halloysite. Traces represent sub-samples of the original material which have been finely ground and pressed into metal holders for analysis. RM138 (Robinson Point) is a mix of alunite (A) and 10Å halloysite, RM141 (Onkaparinga Trig) comprises mostly 7Å halloysite together with quartz (Q) and minor feldspar (F), RM165 (Port Moorowie) is a mix of 10Å halloysite and alunite (A), while RM167 (Port Moorowie) comprises 10Å halloysite. Halite (H) is also present in samples RM138 and RM141.

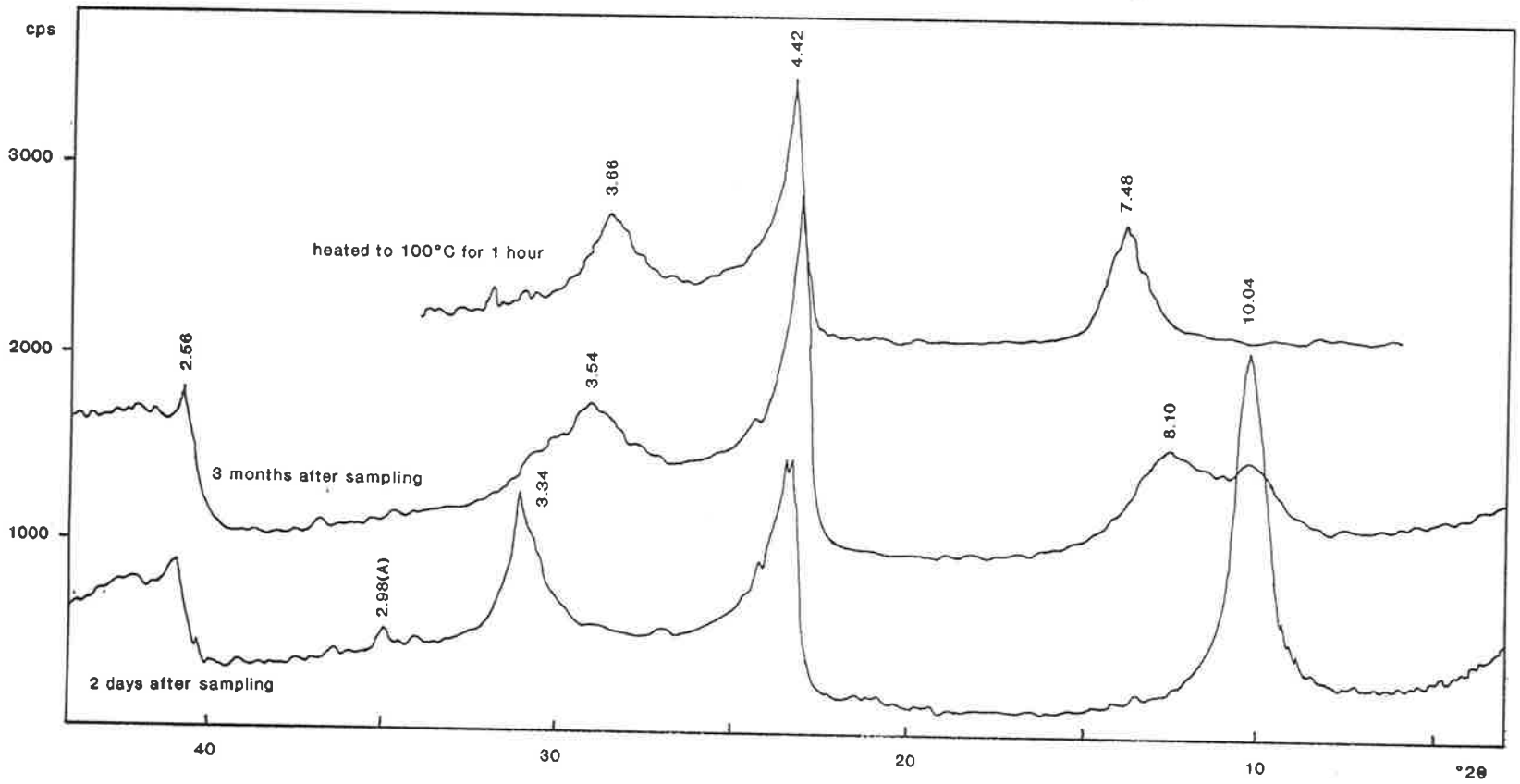

Figure 5.10 XRD traces of sample RM64 (Port Moorowie) which comprises mostly halloysite with minor alunite, showing the effects of dehydration of the sample in the laboratory following sampling. Two days after sampling halloysite is present in the hydrated 10Å form. After three months storage in the laboratory, both 10Å and 7Å halloysite are present. Heating the sample to 100°C for one hour completely dehydrates the sample leaving halloysite only in the 7Å form.

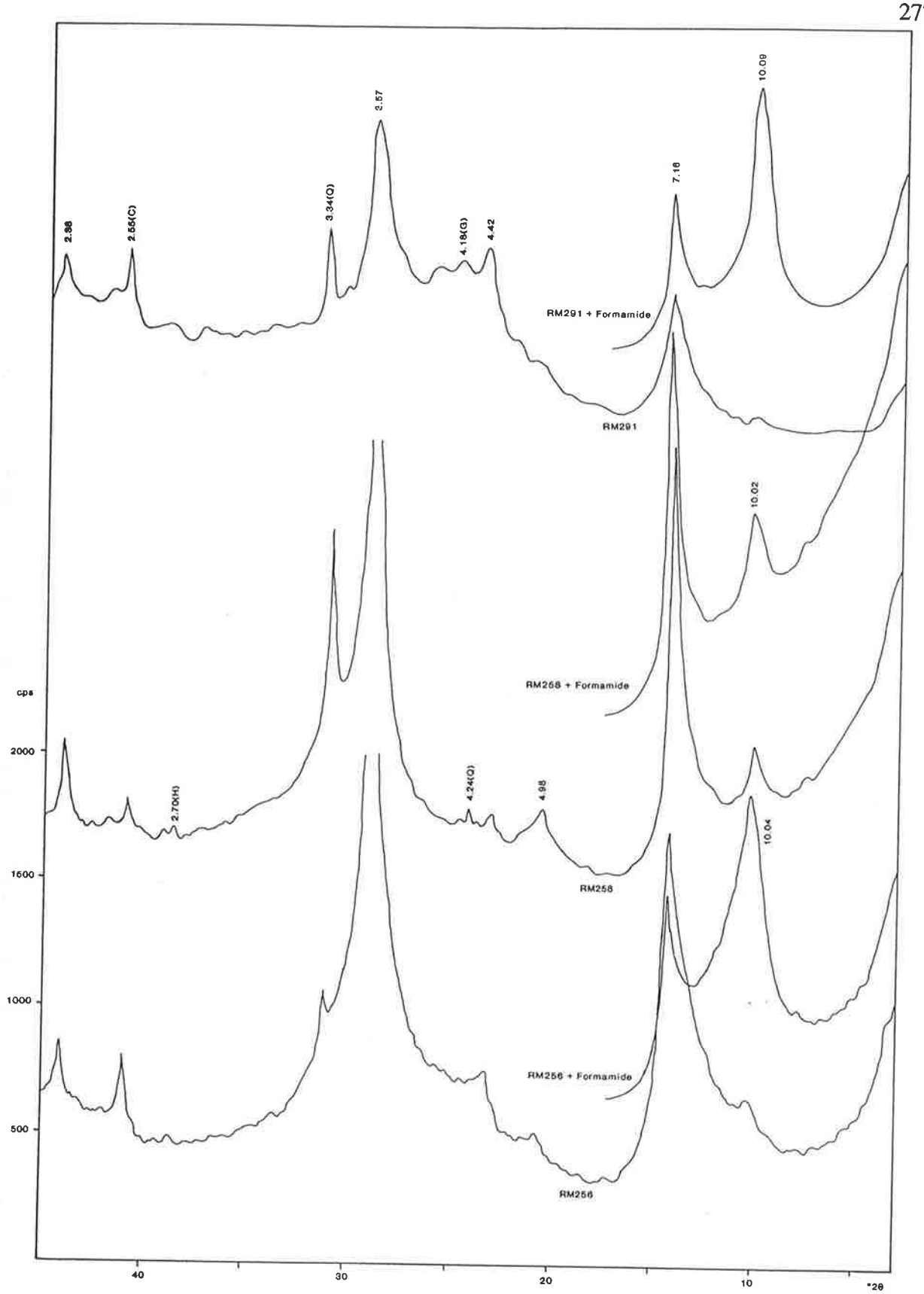

Figure 5.11 XRD traces of the <2μm fraction of three samples showing the effect of addition of formamide on the basal spacing of halloysite. 7Å halloysite expands to 10Å allowing the proportion of kaolinite (which remains at 7Å basal spacing) in the sample to be determined. RM256 (halloysite:kaolinite = 50:50) and RM258 (halloysite:kaolinite = 15:85) are from Maslin Bay with RM291 (halloysite:kaolinite = 60:40) being from Onkaparinga Trig.

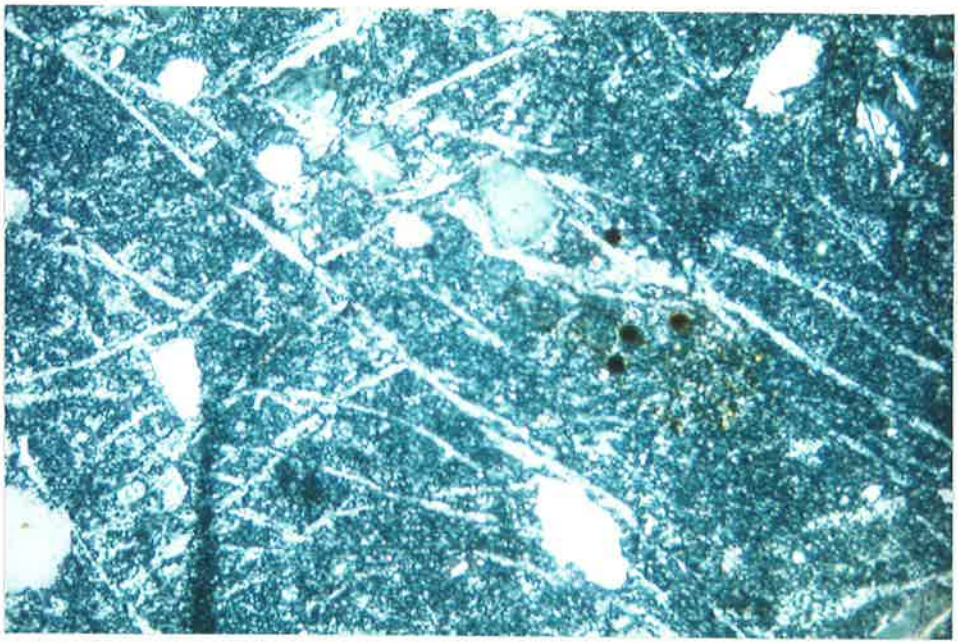

Figure 5.12 Photomicrograph of sample RM120 (Port Noarlunga) showing a series of fractures cutting across matrix material consisting of an intimate mixture of cryptocrystalline alunite and halloysite. Fractures have been infilled by secondary material which is alunite-rich. Framework grains consist of sub-angular to sub-rounded quartz which show some embaying of edges. Dark spots represent damage by the electron microprobe beam. Transmitted light, crossed polars, width of field 0.5 mm.

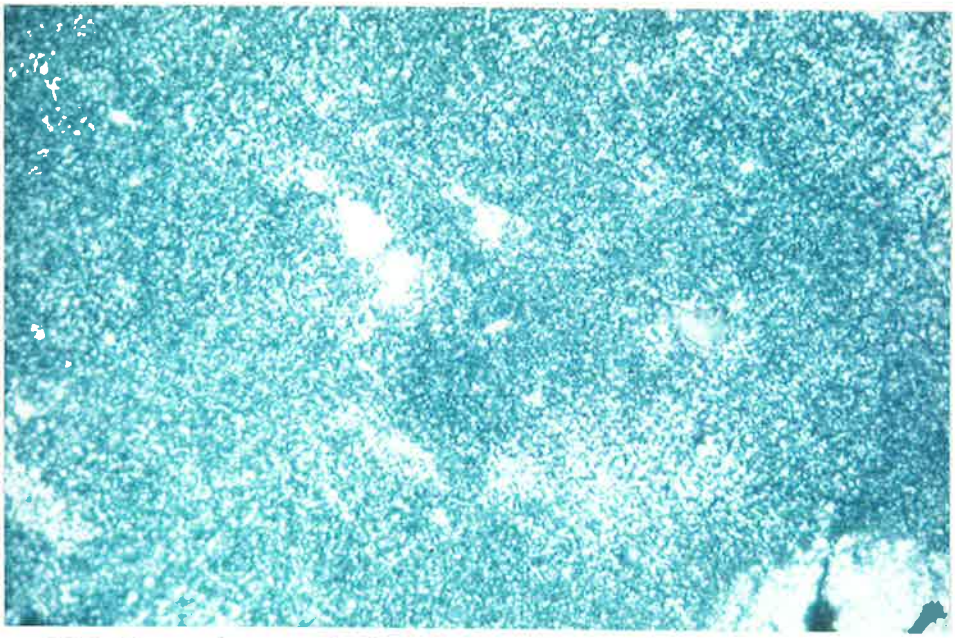

Figure 5.13 Photomicrograph of sample RM142 (Onkaparinga Trig) comprising microcrystalline alunite which exhibits a speckled birefringence pattern caused by small lozenge-shaped grains of alunite up to 1μm in size. Transmitted light, crossed polars, width of field 0.5 mm.

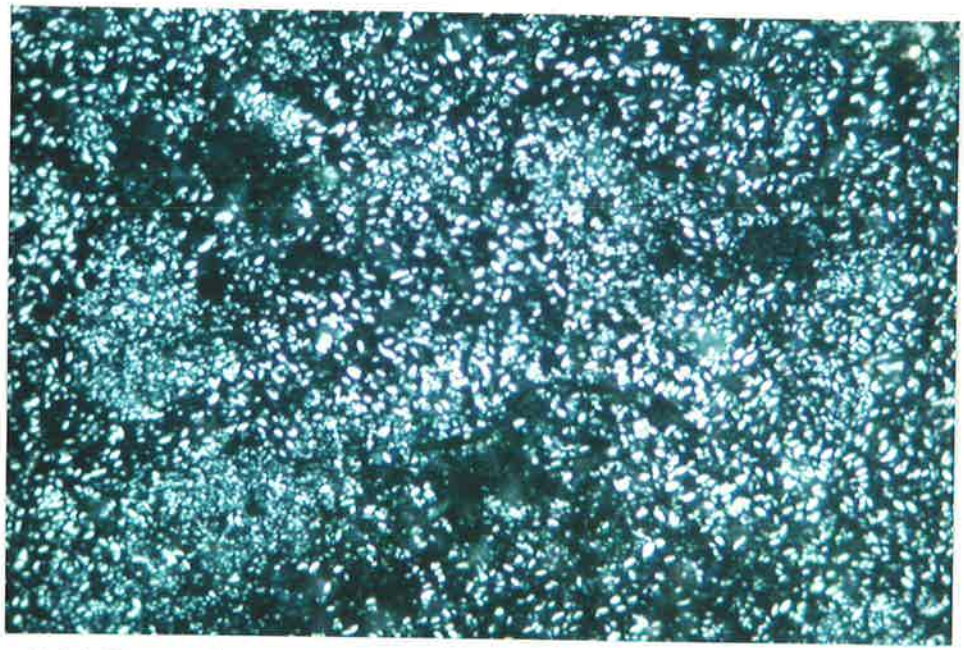

Figure 5.14 Photomicrograph of sample RM63 (Port Moorowie) showing alunite occurring as small lozenge-shaped grains up to 1μm in size and set in a dark-coloured, almost isotropic matrix of cryptocrystalline alunite and halloysite. Transmitted light, crossed polars, width of field 0.2 mm.

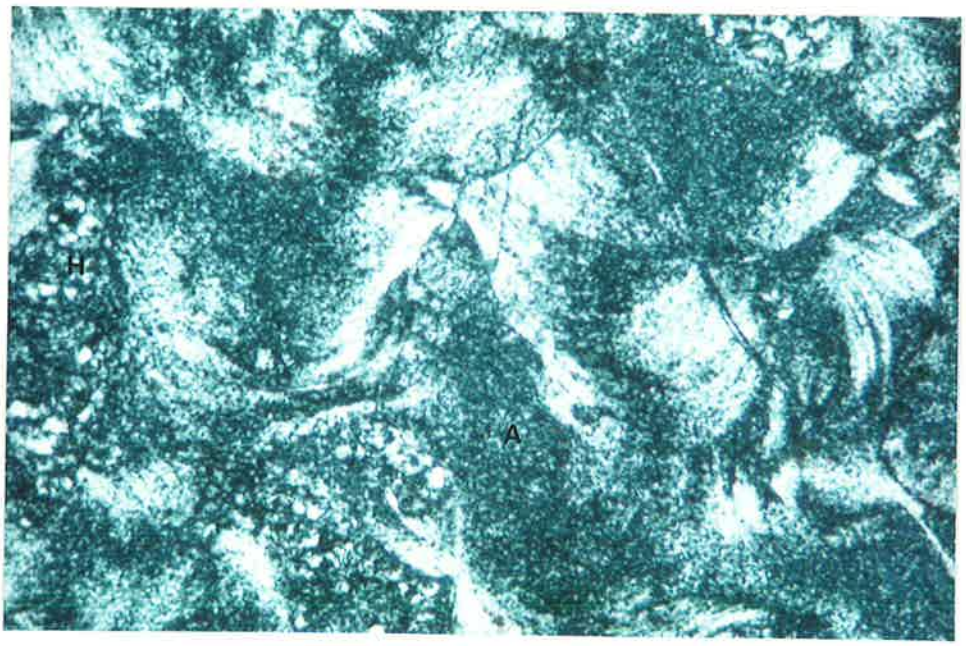

Figure 5.15 Photomicrograph of sample RM63 (Port Moorowie) showing speckled birefringence pattern characteristic of alunite (A) in central parts with a coarser, interlocking pattern on the left hand edge resembling halloysite-rich material (H). The undulose extinction pattern seen throughout the micrograph is thought to be related to stress during desiccation of the sediments. Transmitted light, crossed polars, width of field 0.5 mm.

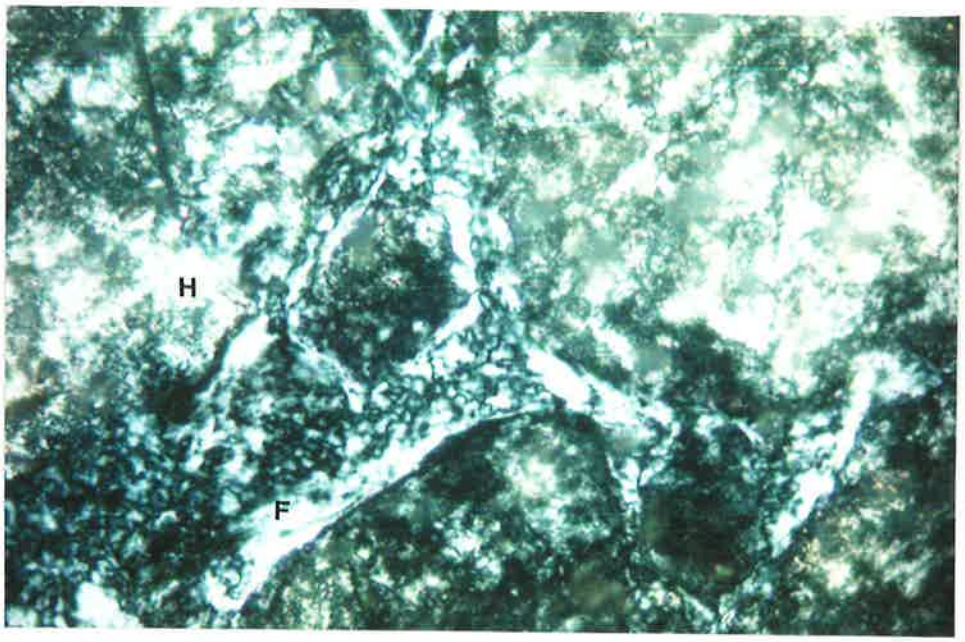

Figure 5.16 Photomicrograph of sample RM167 (Port Moorowie) comprising dominantly buff-coloured halloysite (H). Fractures developed through the sediment have been filled with secondary halloysite (F) exhibiting a different birefringence pattern. Transmitted light, crossed polars, width of field 0.5 mm.

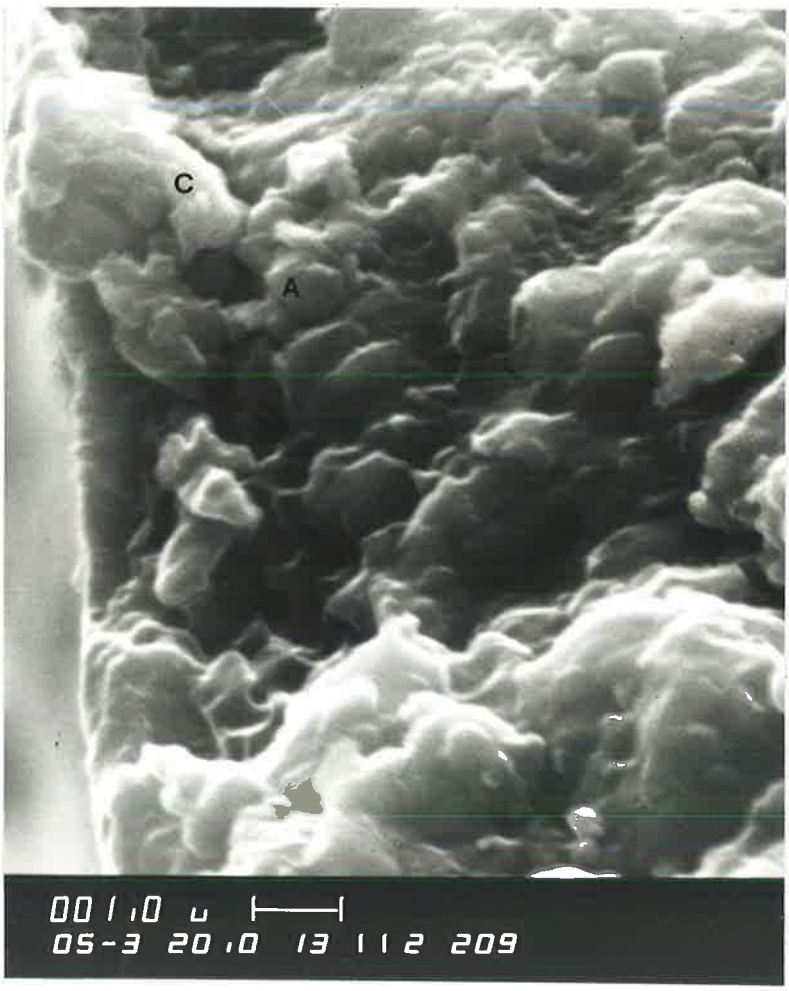

Figure 5.17 Scanning electron micrograph of sample RM63 (Port Moorowie) following fracturing of a thin section. The broken edge of a slide is shown with small rhombohedra being alunite (A) and small platelets representing clay minerals (C). (Bar scale represents 1 μm.)

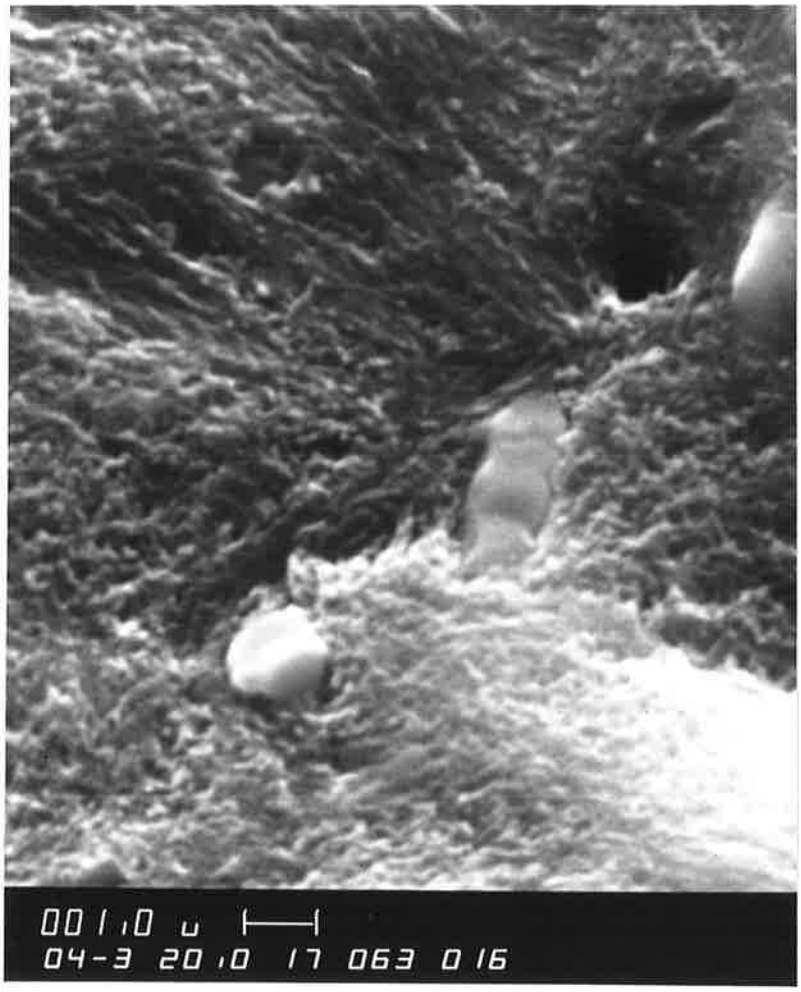

Figure 5.18 Scanning electron micrograph of sample RM63 (Port Moorowie) showing a thin section following etching with methylene chloride for 2 minutes. Alunite occurs as small rhombohedra up to 1 μm in size with halloysite occurring as masses of thin laths. (Bar scale represents 1 μm.)

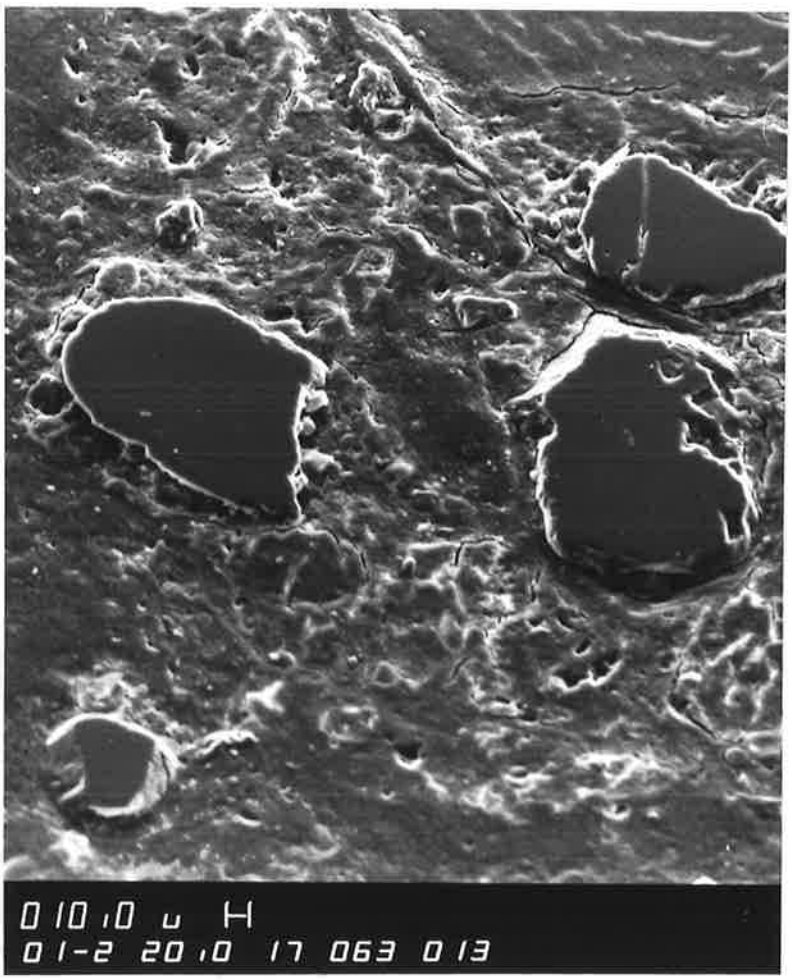

Figure 5.19 Scanning electron micrograph of sample RM63 (Port Moorowie) showing a thin section following etching with methylene chloride for 2 minutes. Quartz grains remain unaffected by the etching process and stand out as flat-topped mesas. (Bar scale represents 10 μm.)

Figure 5.20 Transmission electron micrograph of sample RM166 (Port Moorowie) showing short, stubby tubes of halloysite. (Width of field, 10 μm.)

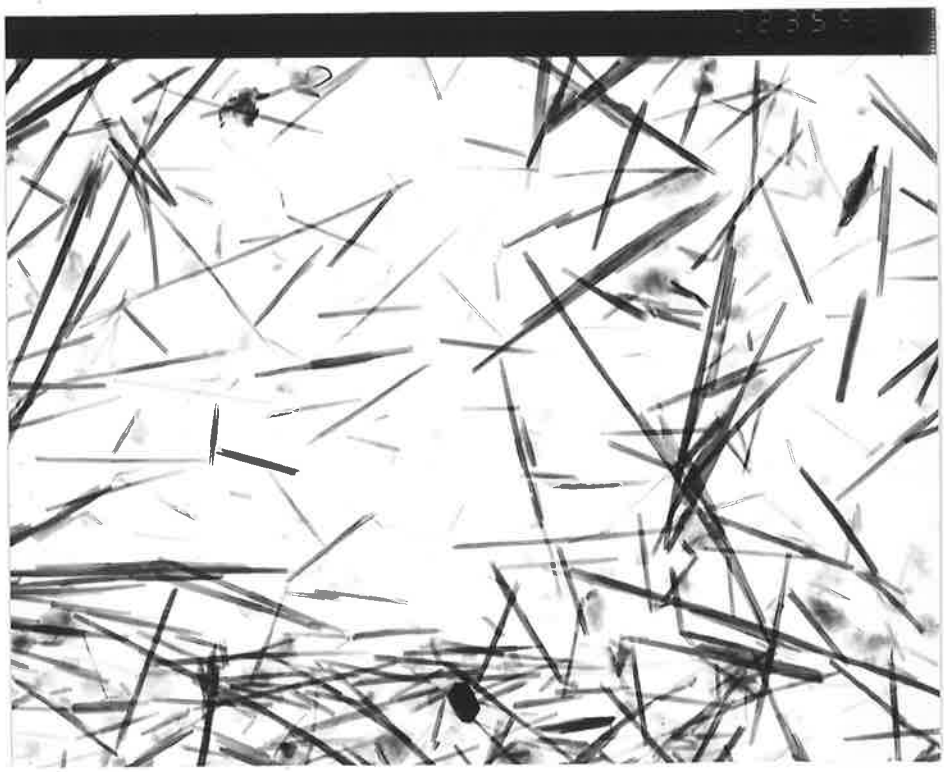

Figure 5.21 Transmission electron micrograph of sample RM141 (Port Noarlunga) showing long, slender tubes of halloysite. (Width of field, 10 μm.)

Figure 5.22 Transmission electron micrograph of sample RM138 (Robinson Point) showing a mix of halloysite tubes and small euhedral rhombs of alunite which vary from 0.5 to 1 μm in size. (Width of field, 10 μm.)

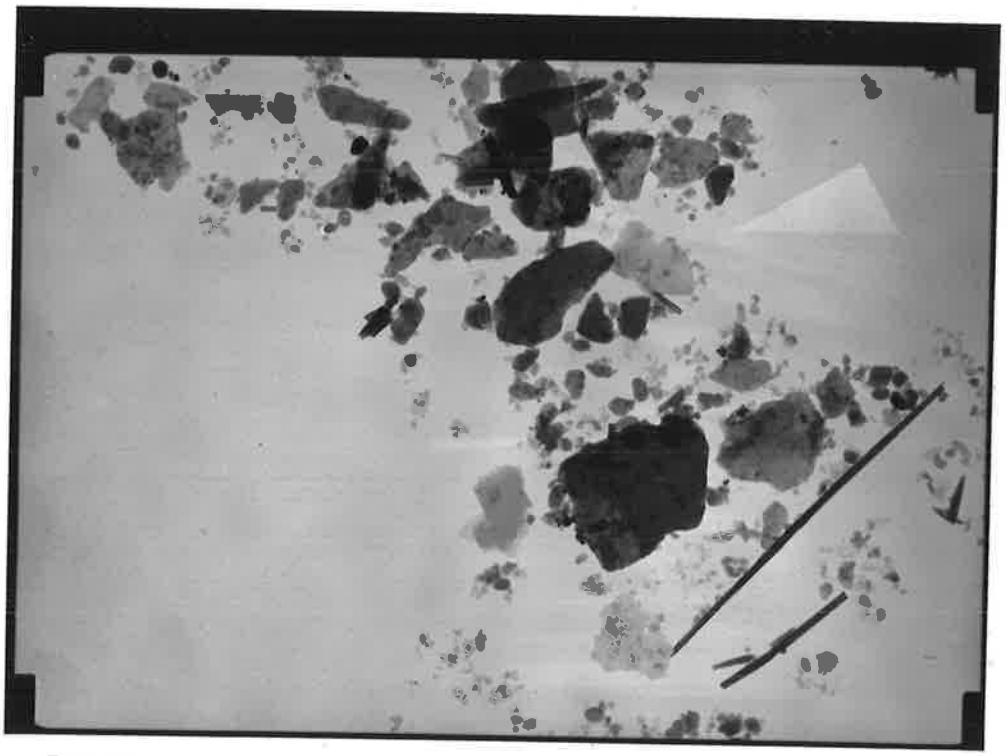

Figure 5.23 Transmission electron micrograph of sample RM167 (Port Moorowie) showing clay minerals which occur within the alunite/halloysite-rich sample. Large particles up to 2 μm in size are irregular to rounded in shape while smaller particles less than 0.2 μm in size tend to be of euhedral, almost hexagonal shape. (Width of field, 8 μm.)

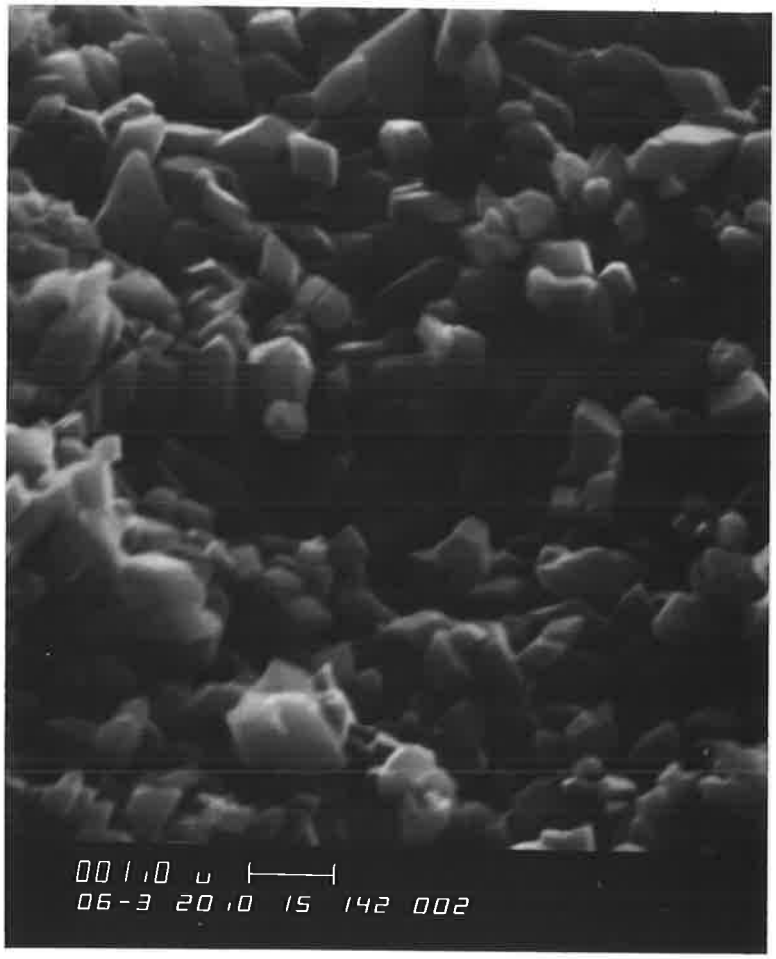

Figure 5.24 Scanning electron micrograph of sample RM142 (Onkaparinga Trig) showing a mass of blocky, diamond-shaped alunite crystals. (Bar scale represents 1 μm.)

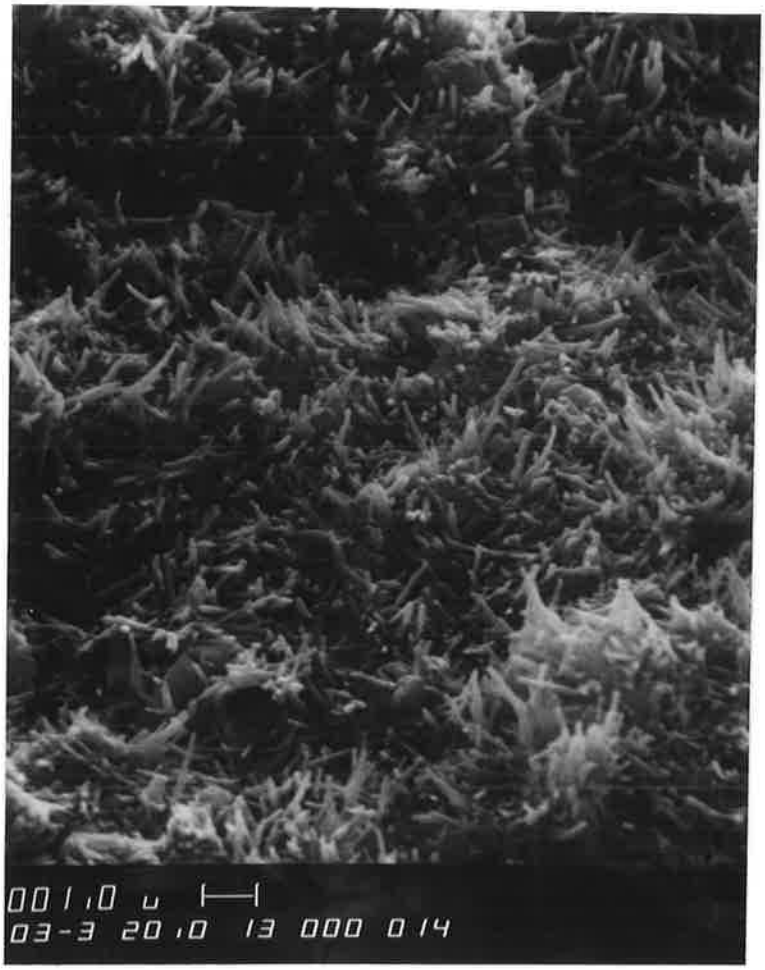

Figure 5.25 Scanning electron micrograph of sample RM69 (Seaford) showing halloysite which occurs as matted layers of thin tubes. Nested within the halloysite are rare rhombs of alunite. (Bar scale represents 1 μm.)

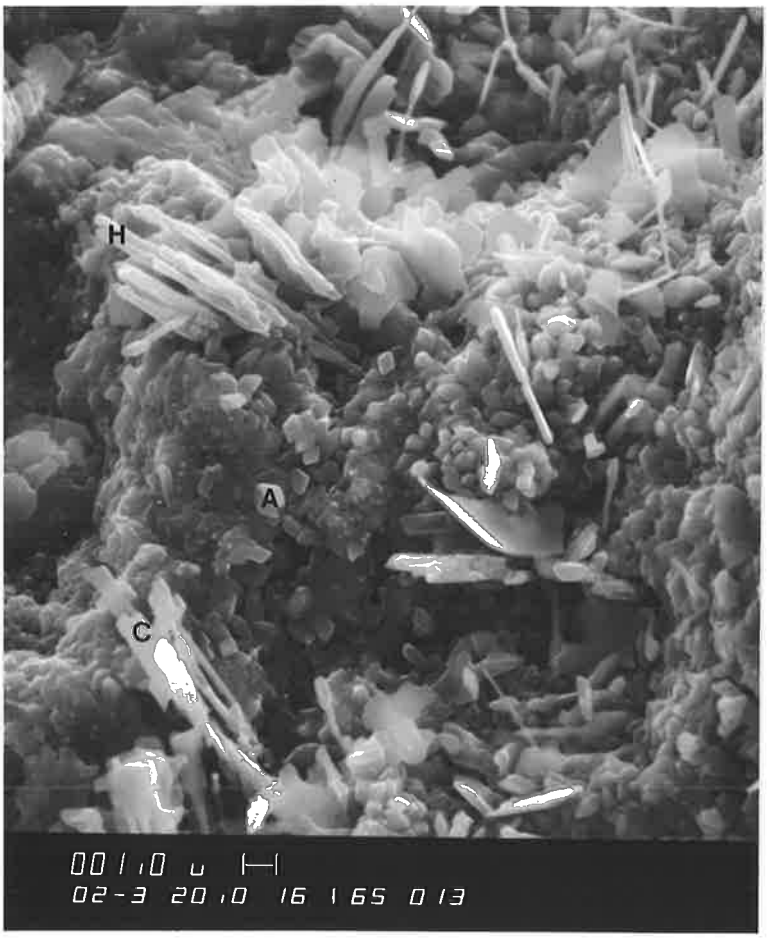

Figure 5.26 Scanning electron micrograph of sample RM165 (Port Moorowie) showing masses of alunite rhombs (A) together with some long halloysite tubes (H). Thin, etched, irregular shaped plates are thought to be aluminosilicate clays (C). Thin wispy material, particularly in the upper right hand corner of the micrograph is identified as halite. (Bar scale represents 1 μm.)

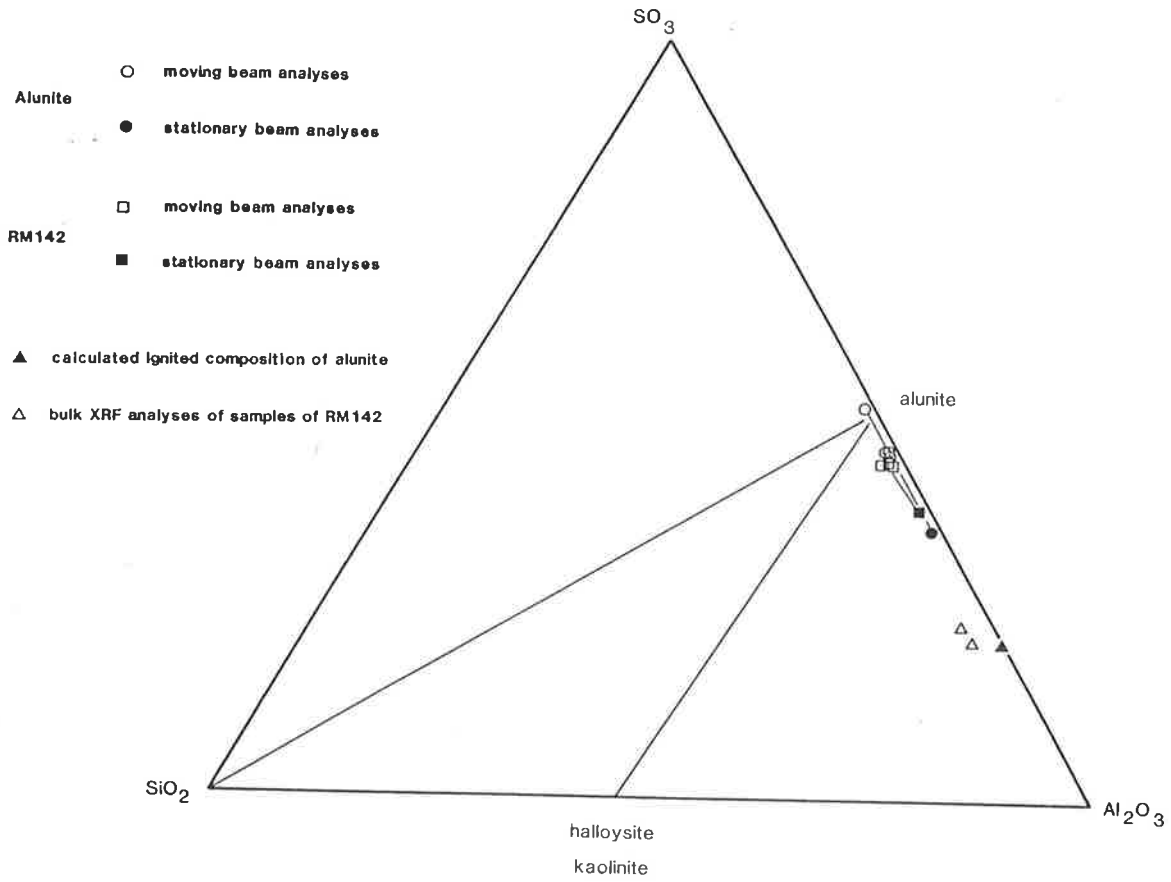

Figure 5.27 Ternary diagram showing results of experiments using the electron microprobe with moving and stationary beam analyses on alunitic samples. RM142 was collected from Onkaparinga Trig while the alunite sample is a standard from the collection at CSIRO, Division of Soils, Adelaide. Stationary analyses show far greater sulphur loss compared with moving beam analyses.

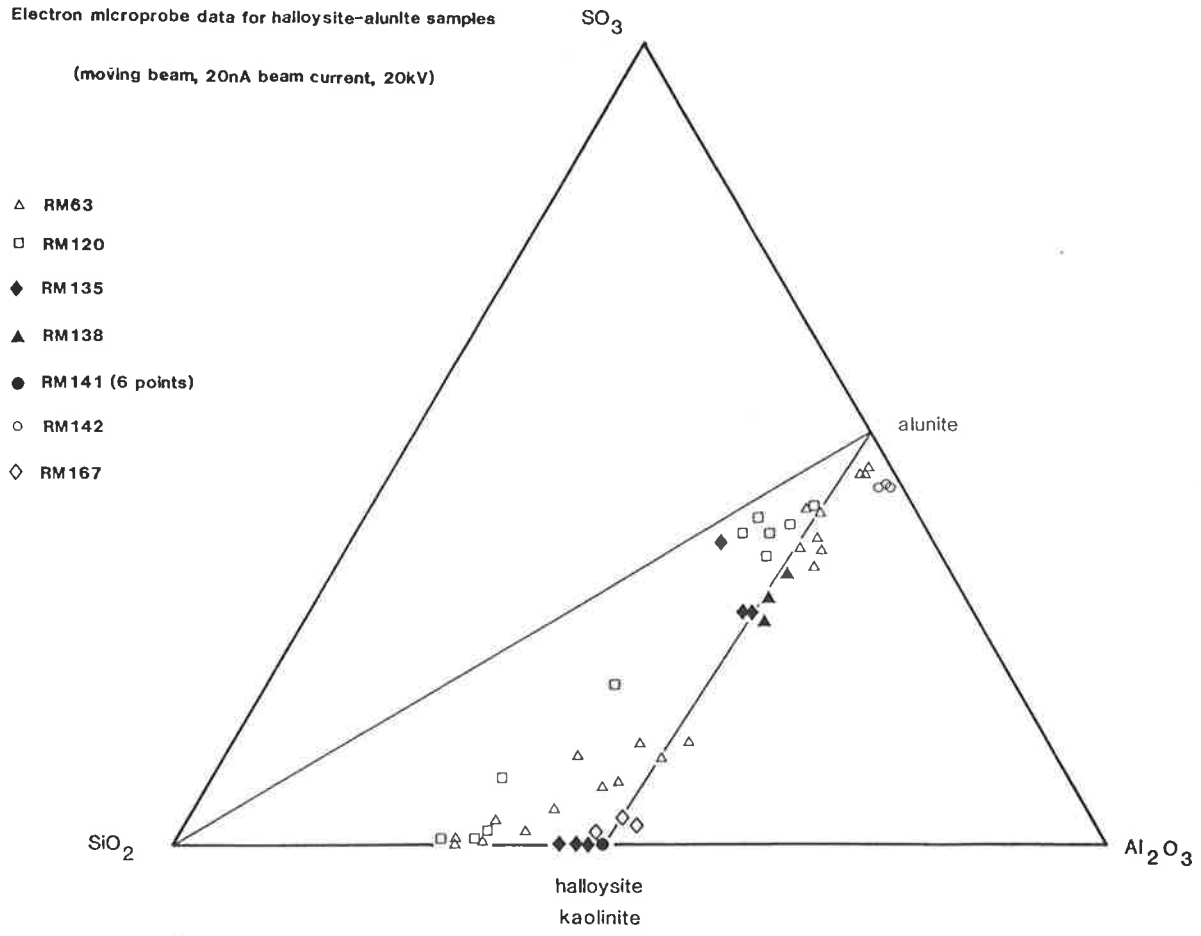

Figure 5.28 Ternary diagram showing electron microprobe data for 7 alunite and halloysite samples collected during the present study and analysed using a moving beam. Most samples plot close to the alunite-halloysite tie line and represent mixtures of these two components. A number of points plot toward the silica end-member and suggest the presence of a microcrystalline or amorphous silica phase.

Figure 5.29 Iron mottled interval within the Robinson Point Formation at Hallett Cove. The mottled zone is indurated and sandy while sediments above and below this zone are clay-rich. The white sediments at the base of the exposure are of Permian age. Mottled interval is approximately 2.5 m thick.

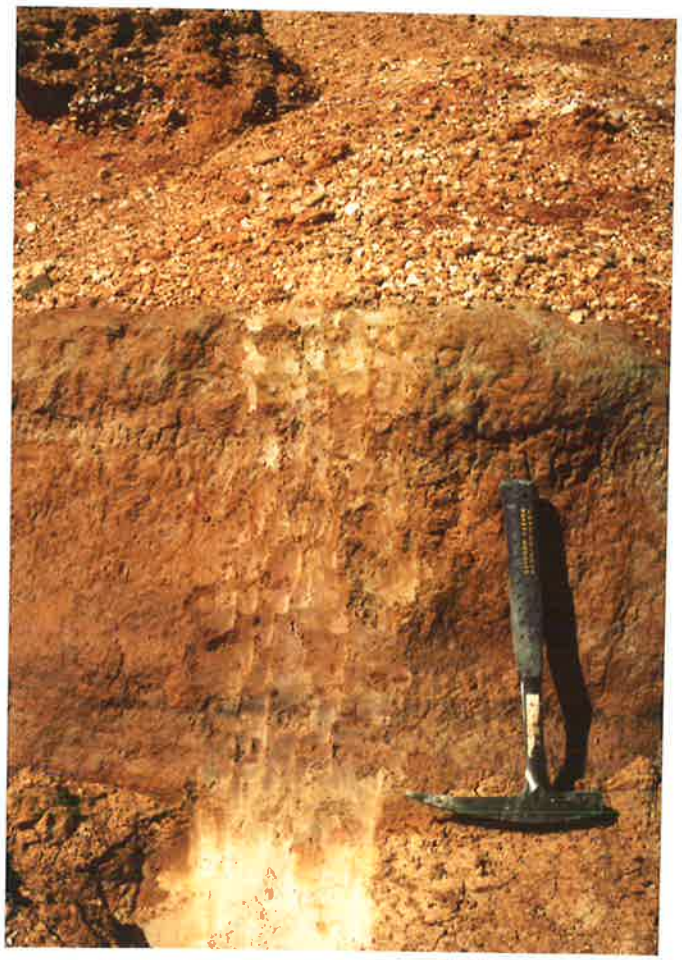

Figure 5.30 Fine-grained silty sediments near the base of the Robinson Point Formation at Onkaparinga Trig which are thought to represent a palaeosol. Ferruginous mottling in these grey-coloured sediments comprises irregular yellow-orange patches which impart an overall orange colour to this interval. (Hammer is 28 cm long.)

Figure 5.31 Ferruginous mottling within basal sediments of the Robinson Point Formation at Port Noarlunga. Fine grey silty clays (C) near the base display numerous small yellow-orange patches of iron which tend to be vertically oriented. Coarser sediments above this interval show much coarser mottling patterns which in places have a rectangular fabric. Mottled silty clays at the base of the sequence are approximately 2 m thick.

Figure 5.32 Ferruginous mottling (F) within the upper part of the Robinson Point Formation at Blanche Point. Mottled sediments are underlain by fine sandy clays and overlain by clays of the Ngaltinga Formation (N). Mottles on the right side of the photo occur within an indurated sandy interval while on the left side of the photo mottling occurs in soft sandy sediments. Section exposed is approximately 10 m thick.

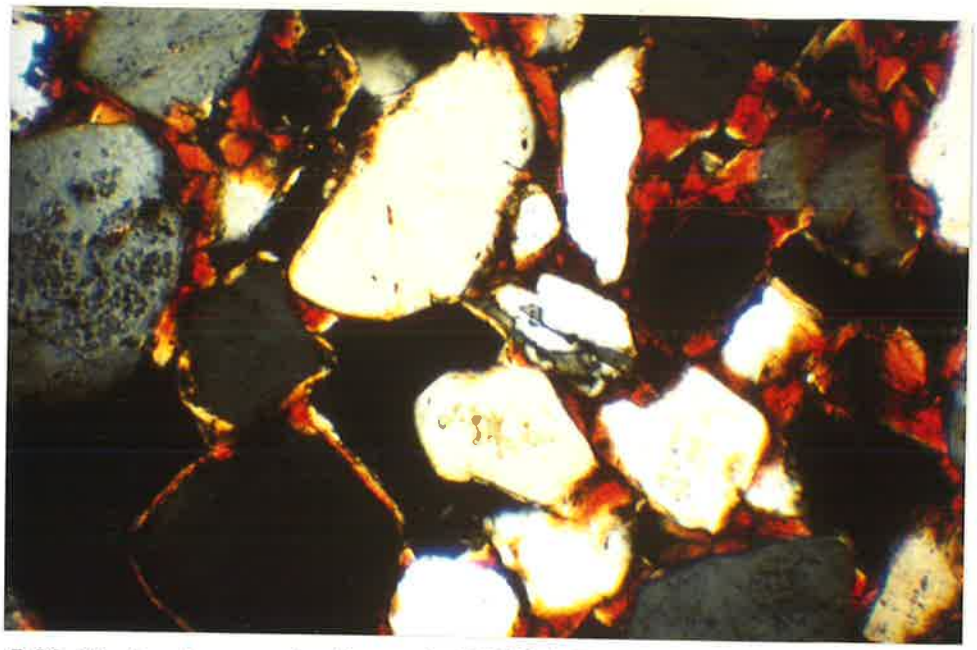

Figure 5.33 Photomicrograph of sample RM134 (Robinson Point Formation from near Robinson Point) which is a porous sandstone showing a mixture of iron oxides and clays partially filling some pore space and coating framework quartz grains. Transmitted light, crossed polars, width of field 1.2 mm.

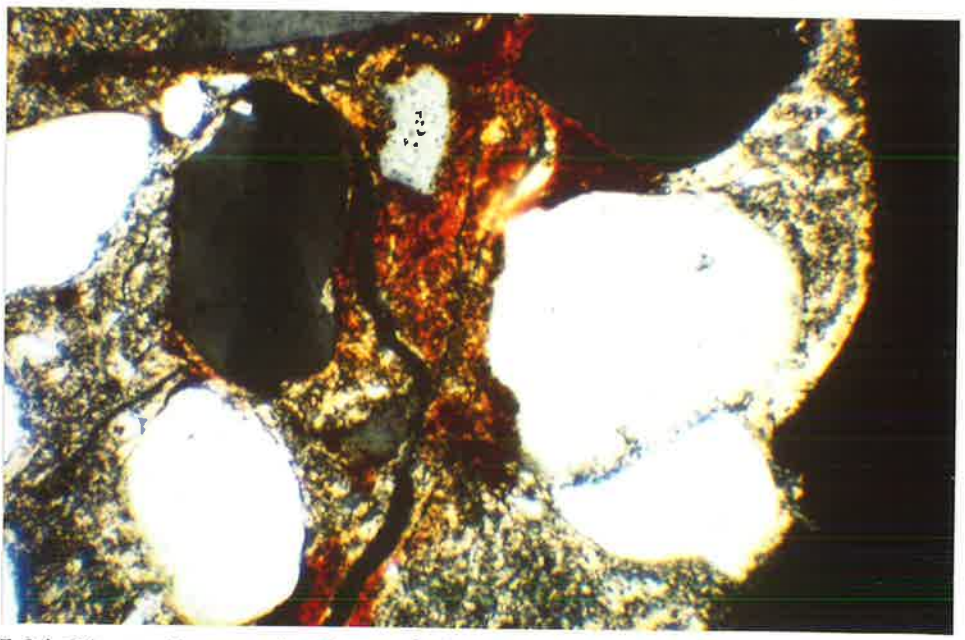

Figure 5.34 Photomicrograph of sample RM80 (Snapper Point Sand Member from Port Willunga) showing reddish iron oxides accumulating along an elongate zone which follows a fracture through the clay-rich matrix. Clay minerals fill all spaces between quartz grains and appear to be replaced by iron oxides in small patches and elongate zones. Transmitted light, crossed polars, width of field 1.2 mm.

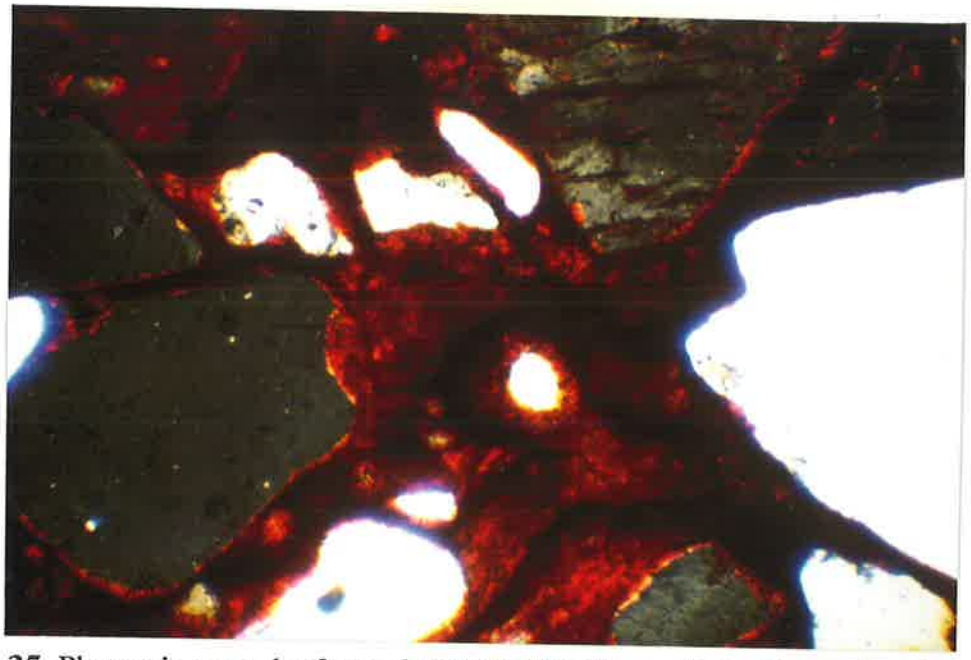

Figure 5.35 Photomicrograph of sample RM349 (Robinson Point Formation from Hallett Cove) which shows dark red iron oxides completely impregnating all intergranular space. Iron oxides have also partly replaced corroded quartz and feldspar grains. Transmitted light, crossed polars, width of field 1.2 mm.

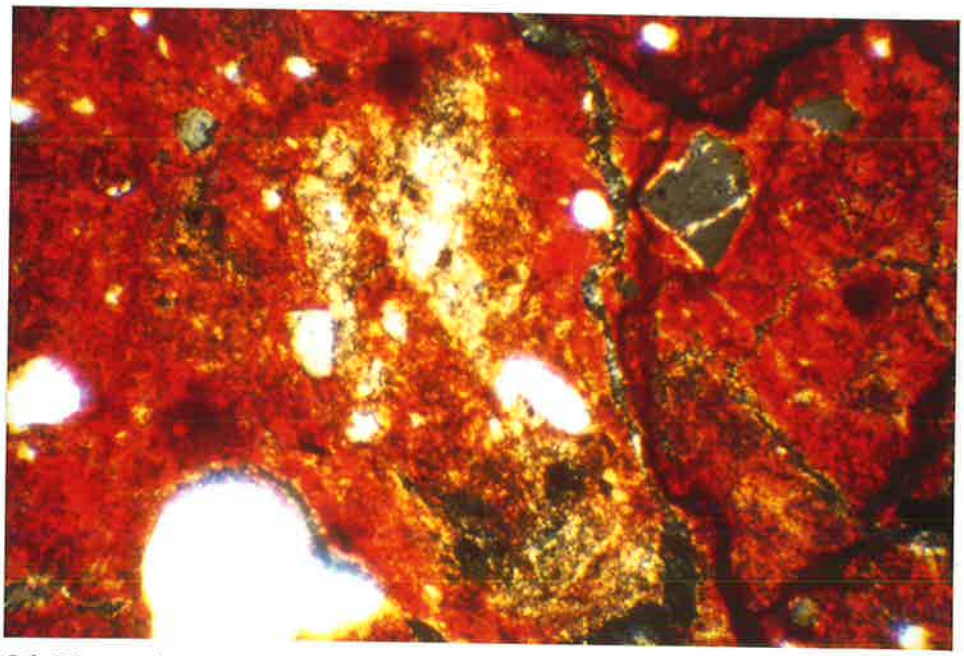

Figure 5.36 Photomicrograph of sample RM349 (Robinson Point Formation from Hallett Cove) showing a small remnant of yellowish clay minerals which is completely surrounded by red iron oxides. Iron oxides appear to replace clays in most intergranular spaces leaving these isolated pockets of clay. Transmitted light, crossed polars, width of field 1.2 mm.

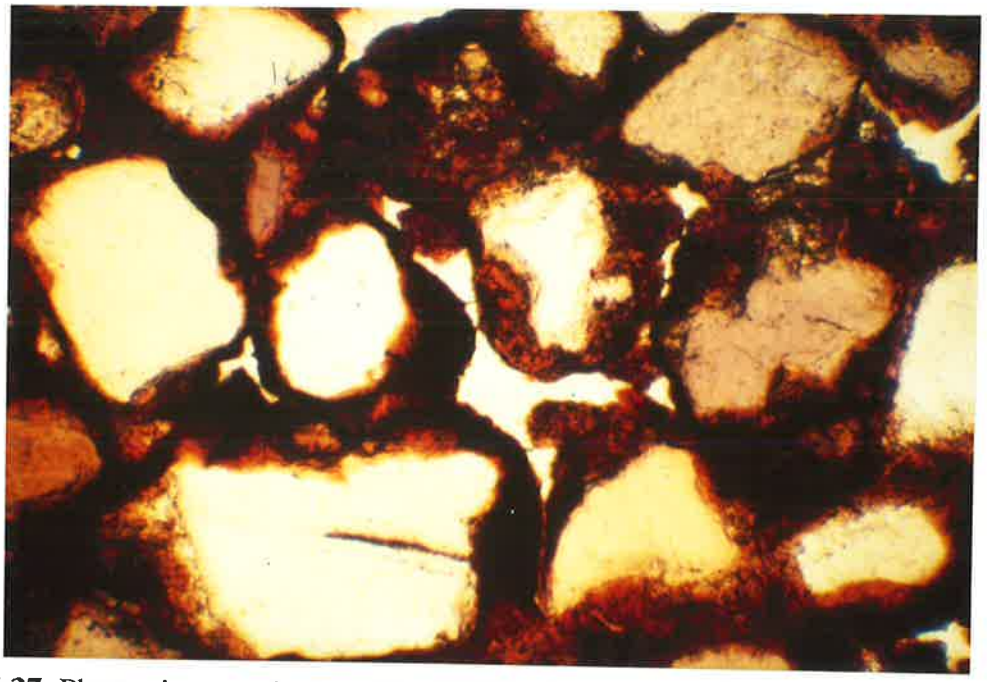

Figure 5.37 Photomicrograph of sample RM264 (Robinson Point Formation from Maslin Bay) showing partial replacement by iron oxides of clay minerals which coat most quartz grains in this sandy sample. Transmitted light, plane polarised, width of field 1.2 mm.

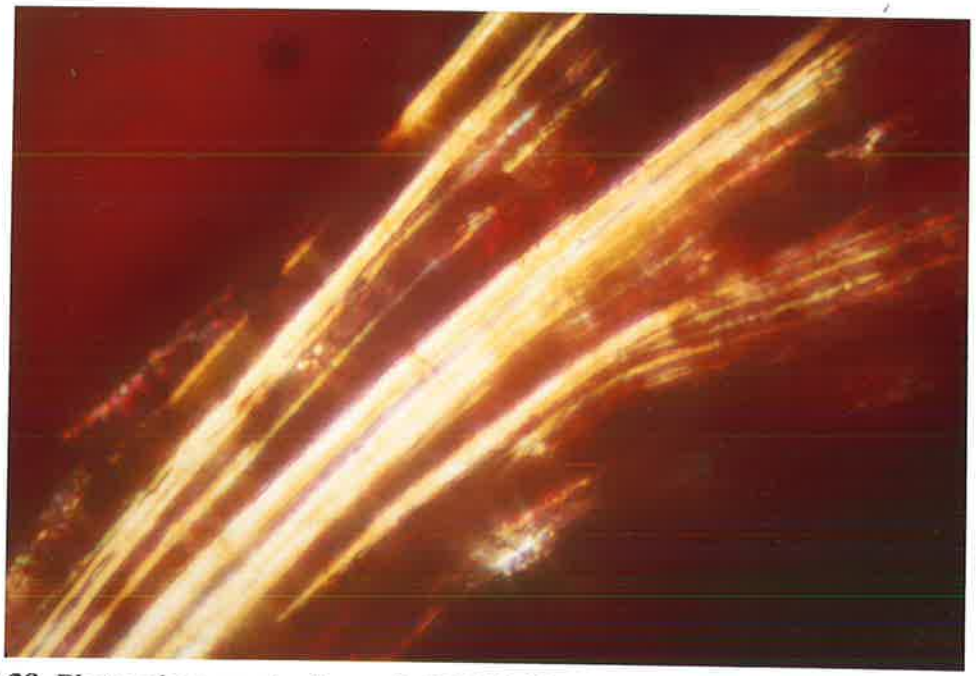

Figure 5.38 Photomicrograph of sample RM40 (Snapper Point Sand Member from Ochre Point) showing precipitation of iron oxides which have partially replaced a mica and forced apart individual sheets from the mica crystal. Transmitted light, crossed polars, width of field 0.2 mm.

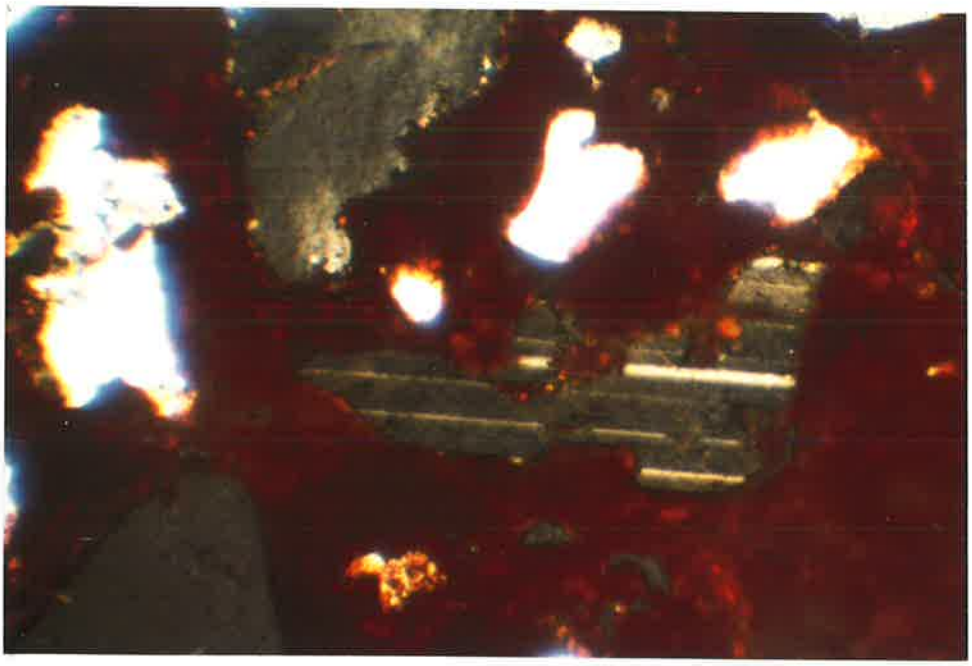

Figure 5.39 Photomicrograph of sample RM41 (Snapper Point Sand Member from Ochre Point) showing red iron oxides which have impregnated all intergranular space and also partially replaced feldspar and quartz grains. Transmitted light, crossed polars, width of field 1.2 mm.

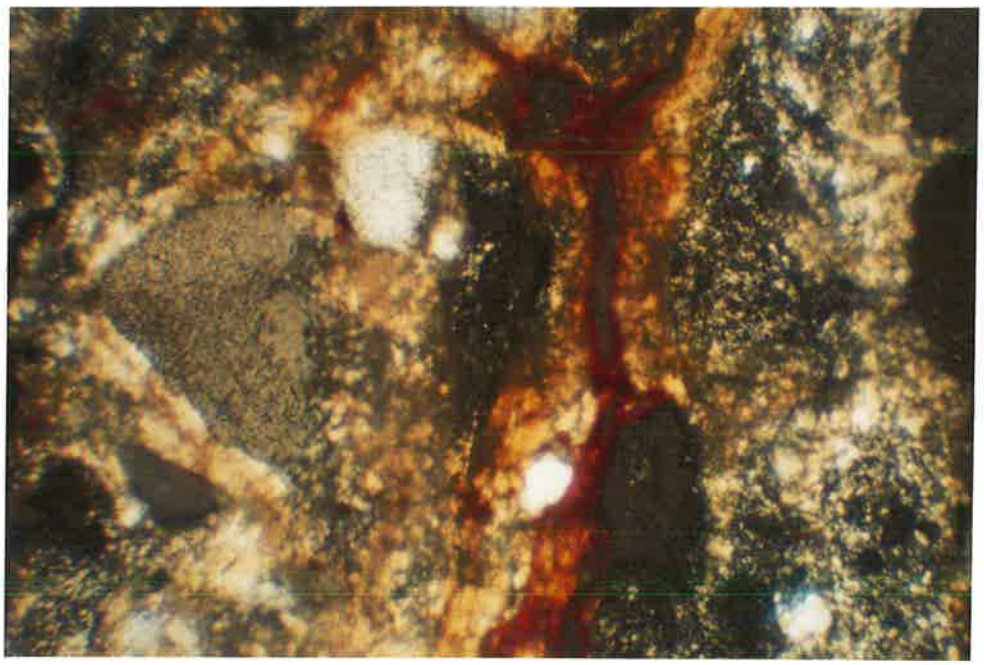

Figure 5.40 Photomicrograph of sample RM264 (Robinson Point Formation from Maslin Bay) showing iron oxides precipitated along a fracture zone within the clay-rich matrix immediately adjacent to an iron-rich mottle. Initial precipitation was of yellow goethite with a subsequent phase of red hematite. Transmitted light, crossed polars, width of field 1.2 mm.

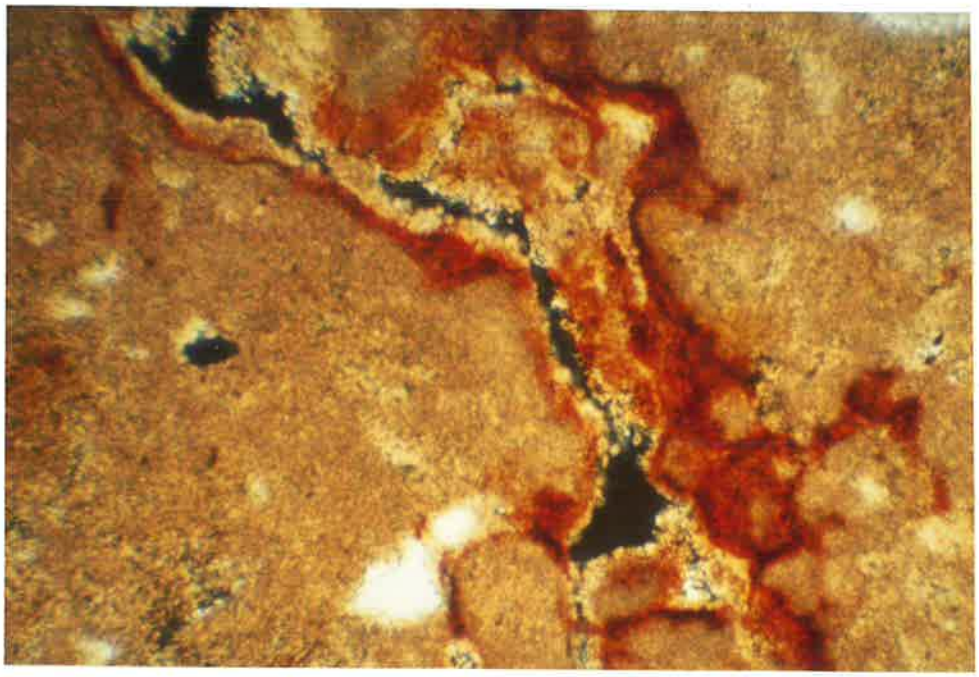

Figure 5.41 Photomicrograph of sample RM170 (Neva Clay Member from Snapper Point) showing precipitation of red hematitic iron oxides along margins of a fracture zone through the carbonate-rich sample. A second phase of carbonate has precipitated subsequent to the iron oxides and fills the fracture zone. Transmitted light, crossed polars, width of field 1.2 mm.

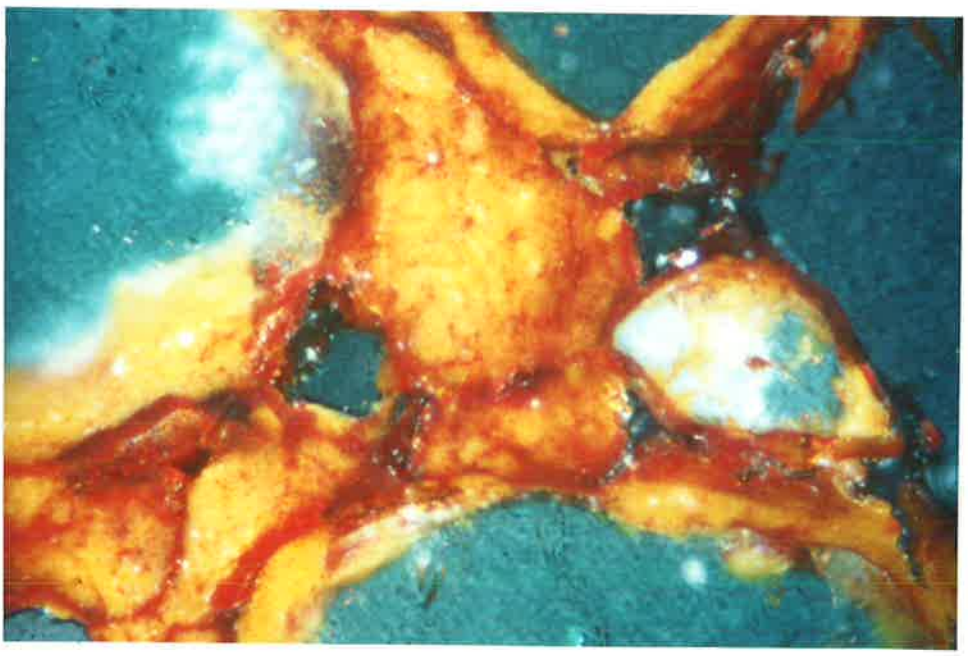

Figure 5.42 Photomicrograph of sample RM40 (Snapper Point Sand Member from Ochre Point) showing several phases of precipitation of red hematitic iron oxides as thin bands within the yellowish goethite-clay material which fills the intergranular space between quartz grains. Transmitted light, crossed polars, width of field 0.5 mm.

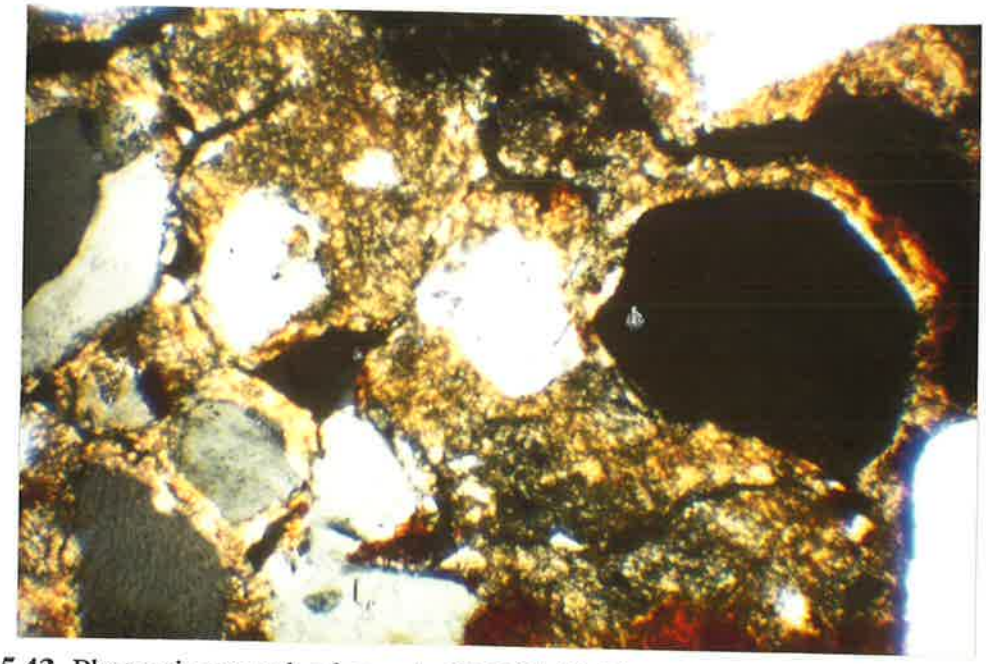

Figure 5.43 Photomicrograph of sample RM264 (Robinson Point Formation from Maslin Bay) showing a sandy sediment with clay filling intergranular space adjacent to a mottled zone. Clays are partially replaced by opaline silica (dark, almost isotropic area at top of micrograph) which is thought to account for the indurated nature of this interval. Transmitted light, crossed polars, width of field 1.2 mm.

Figure 5.44 Sediments of the Robinson Point Formation at Onkaparinga Trig showing a grey-white silty interval at the base of the photo which displays a vertical, columnar structure. This is characteristic of fine-grained sediments in the study area which are thought to have undergone pedogenic modification. Overlying sandy sediments contain some thin gravel bands, some of which show low angle cross beds. (Twenty cent piece is 3 cm in diameter.)

Figure 5.45 A carbonate interval within grey-green clays of the Neva Clay Member at Snapper Point which displays a blocky structure similar to that developed in the surrounding clays.

Figure 5.46 Bed of mottled carbonate up to 2 m thick which occurs within the Neva Clay Member at Onkaparinga Trig. Carbonate masses are variable in size and generally have sharp contacts with surrounding clays. (Pen is 13 cm long.)

Figure 5.47 A mass of carbonate occurring within the carbonate-rich interval of the Neva Clay Member at the Onkaparinga River Mouth site. The carbonate impregnates the clay and displays a vertical prismatic structure similar to the surrounding clays. The upper boundary of the carbonate mass is sharp with the lower boundary diffuse. (Pen is 14 cm long.)

Figure 5.48 A 1 m thick interval of carbonate (C) which occurs at the boundary between the Robinson Point and Ngaltinga Formations at Witton Bluff. The carbonate appears to have a platy structure at this locality.

Figure 5.49 Bed of mottled carbonate (M) up to 40 cm thick which occurs immediately above the Burnham Limestone (B) at Port Willunga in the basal part of the Neva Clay Member. This interval can be traced laterally for tens of metres. (Hammer is 28 cm long)

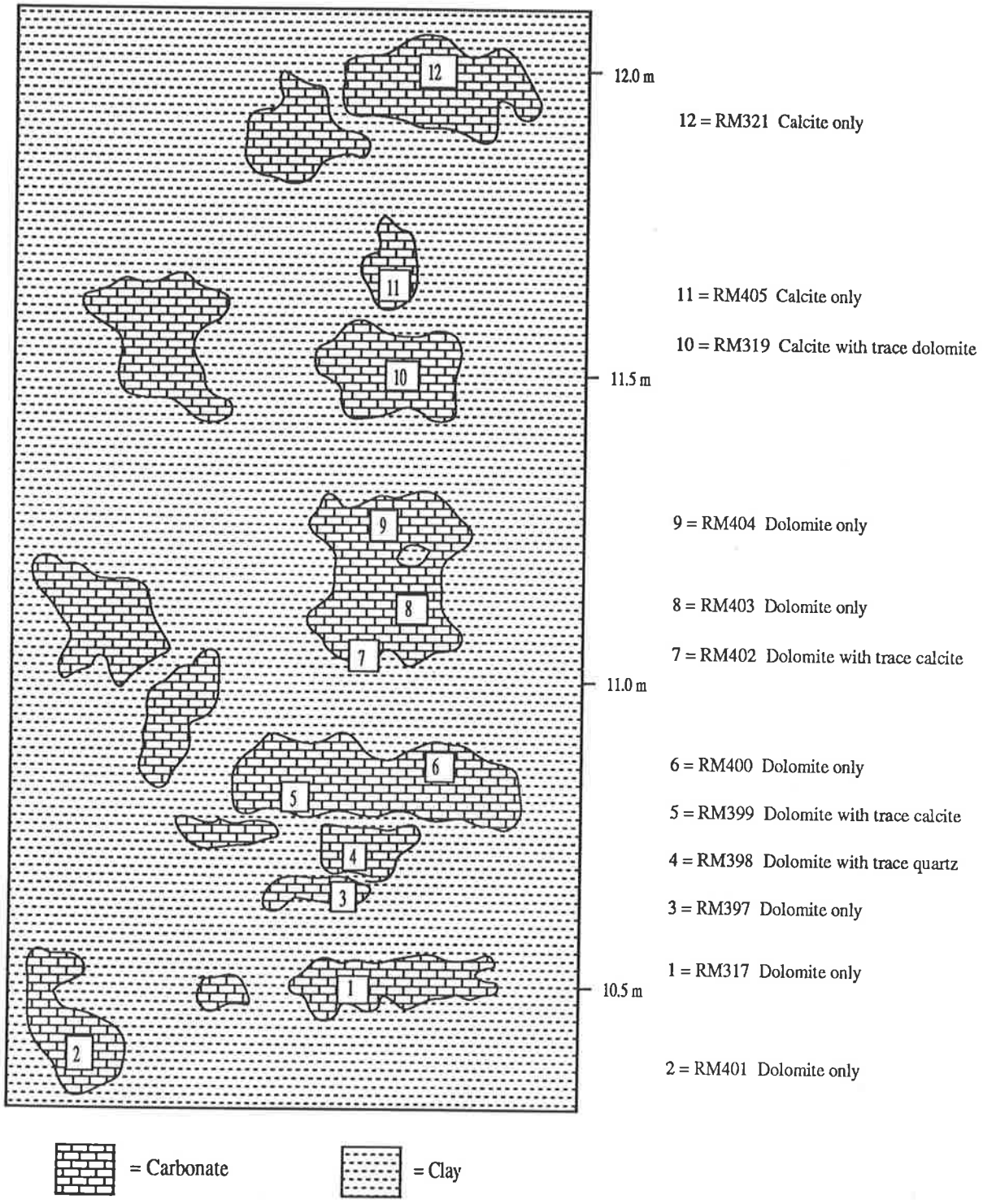

Figure 5.50: Sketch through carbonate interval within Neva Clay Member at Onkaparinga Trig showing sample locations and carbonate mineralogy. Refer to Figure 3.27 for relationship with other sediments at this site. Dolomite is the major carbonate mineral at the base of the interval with calcite dominant in upper parts.

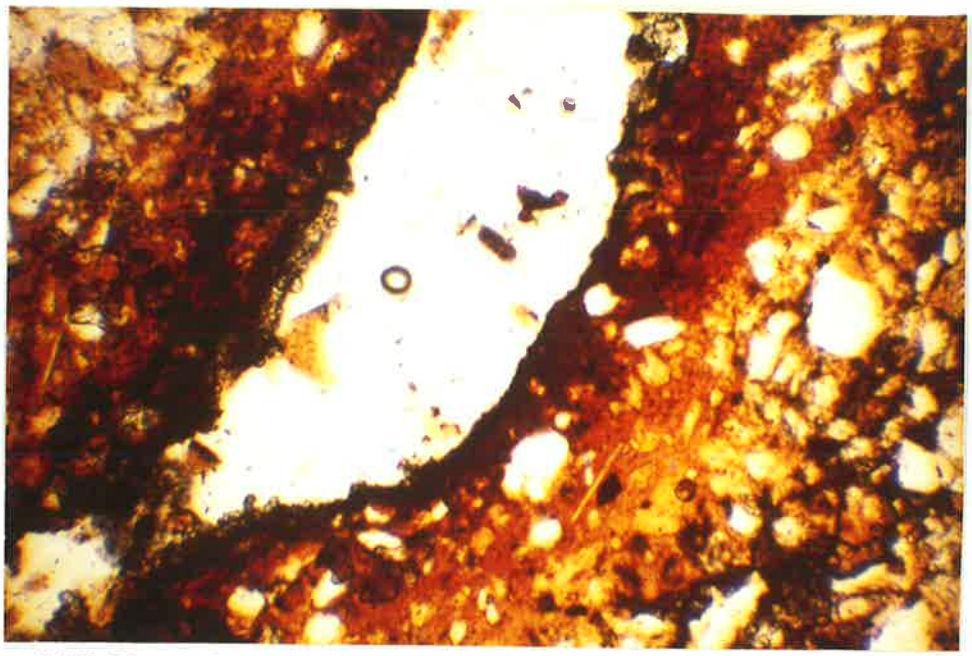

Figure 5.51 Photomicrograph of sample RM297 (Robinson Point Formation from Onkaparinga Trig) which comprises silt-sized quartz grains and mica laths in a clay matrix. The elongate void which has been sectioned and is coated by dark brown to black material is interpreted as a pore of biogenic origin. Transmitted light, plane polarised, width of field 1.2 mm.

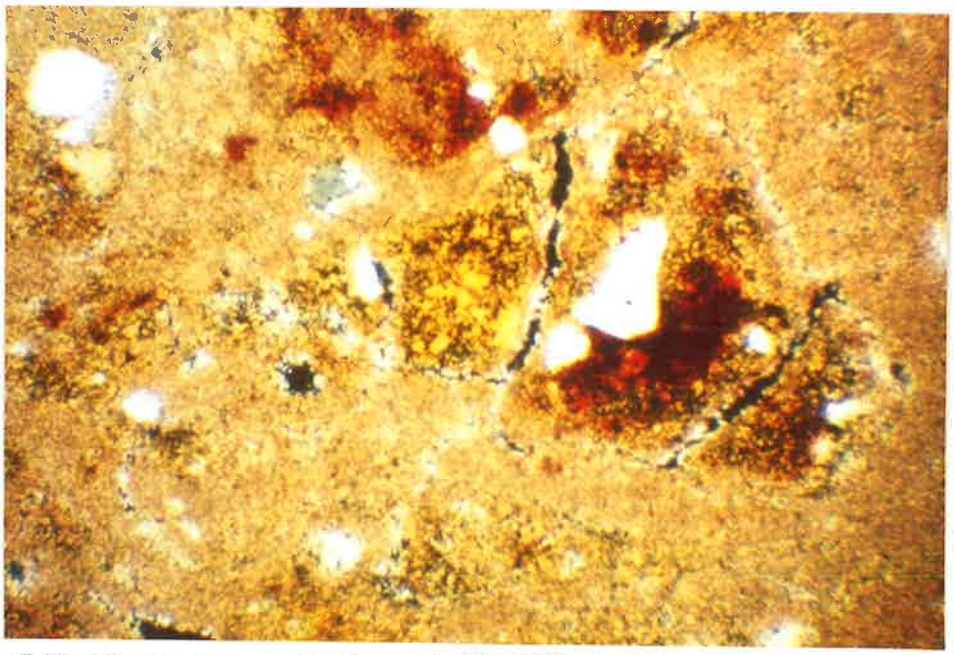

Figure 5.52 Photomicrograph of sample RM170 (Neva Clay Member from Snapper Point) showing the microcrystalline nature of carbonate which forms mottles within these intervals. Rare silt-sized quartz grains are present together with isolated patches of unaltered yellowish clay which is partly impregnated by red iron oxides. Transmitted light, crossed polars, width of field 1.2 mm.

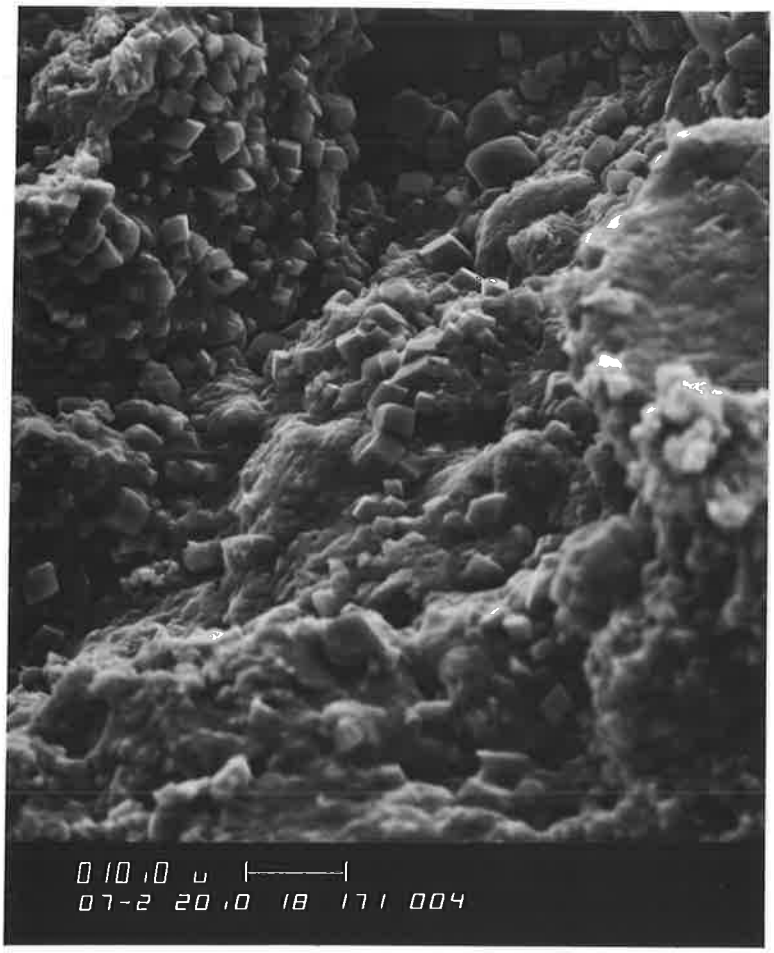

Figure 5.53 Scanning electron micrograph of a carbonate mottle from sample RM171 (Neva Clay Member from Snapper Point) showing the euhedral nature of carbonate crystals up to 4 μm in size occurring in voids. The carbonate rhombs appear to be embedded in a microcrystalline matrix. (Bar scale represents 10 μm.)

TABLES

Howchin (1923) General	Segnit (1939) Ochre Point	Campana & Wilson (1953) Sellicks Beach	Firman (1966) Adelaide Plains Sub-Basin	Ward (1966) Noarlunga & Willunga Embayments	Daily *et al* (1976) General	Forbes (1983) Noarlunga & Willunga Embayments
				Waldeila Formation		
			Fulham/Semaphore Sand	Ngankipari Sand	Fulham/Semaphore Sand	Semaphore Sand
			St Kilda Formation		St Kilda Formation	
			Lipson Formation		Lipson Formation	
		Upper mottled gravelly clay	Pooraka Clay	Christies Beach Formation	Pooraka Clay	Pooraka Formation
			Glanville Formation		Glanville Formation	
Travertine & Marl	Travertine Limestone		Hindmarsh Clay	Taringa Formation	Bridgewater Formation Ripon Calcrete	Keswick Clay
Recent Clay	Mottled green fine sandy clay			Ngaltinga Clay	Keswick Clay	
Pleistocene Clay	Reddish-brown fine sand & gravel	Middle pink coarse gravel		Kurrajong Formation	Hindmarsh Clay	Hindmarsh Clay
				Ochre Cove Formation		
	Mottled green & brown fine sandy clay	Lower reddish-buff clay		Seaford Formation		
Lower Pliocene calcareous sands and marly limestone					Burnham Limestone	Burnham Limestone
	Coarse sand, iron cemented		Hallett Cove Sandstone/ Dry Creek Sands	Hallett Cove Sandstone	Hallett Cove Sandstone	Hallett Cove Sandstone

Table 1.1: Correlation of Late Cainozoic stratigraphic units from previous studies in eastern parts of the St Vincent Basin

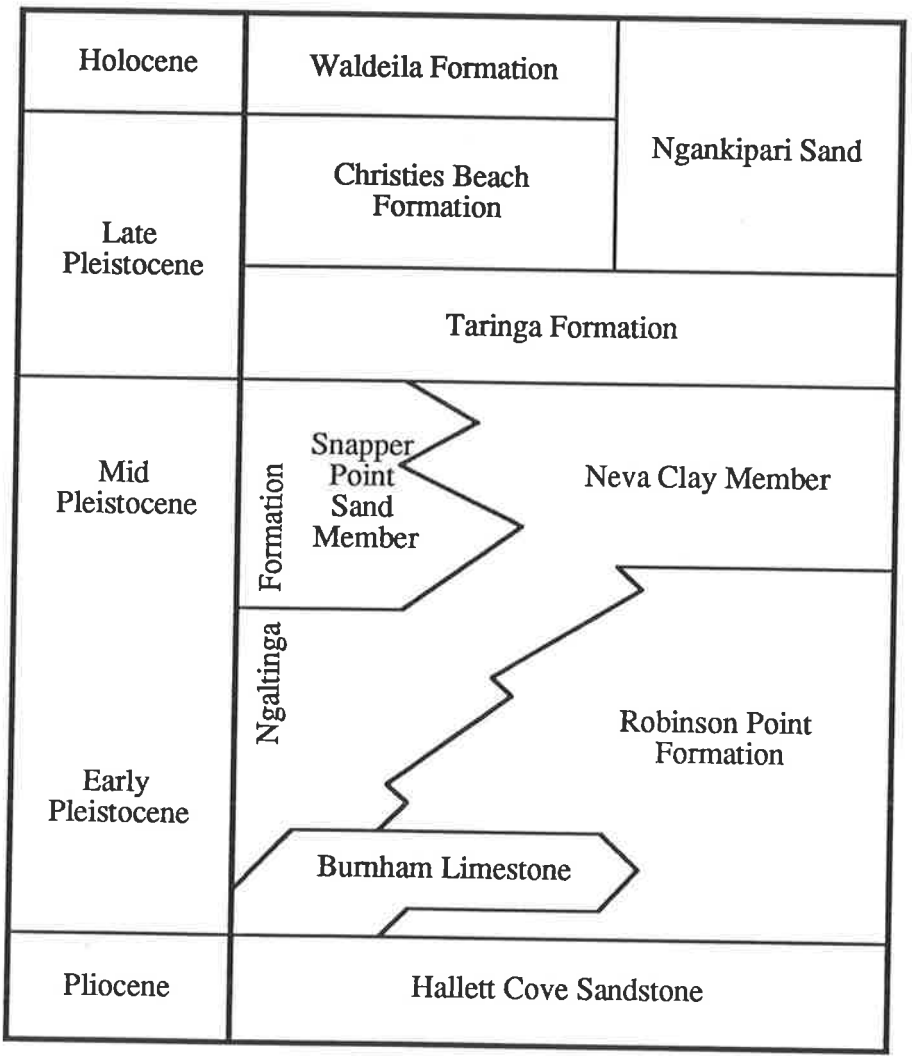

Table 3.1: Late Cainozoic stratigraphy proposed for the Noarlunga and Willunga Embayments.

(Note that the time scale is tentative and provided only as a guide.)

Table 4.1 XRD Peak Positions for Samples where Smectite Identified

Sample	Location	(001) Peak (Å)	(002) Peak (Å)	(003) Peak (Å)	(004) Peak (Å)	Illitic Component (%)
Calculated Data		17.8	8.9	5.93	4.45	0
RM248	MB	18.4	9.25	5.87	4.48	20
RM249	MB	17.88	9.13	5.87	4.52	20
RM250	MB	17.8	8.9	nd	4.46	5
RM294	OT	17.6	8.99	5.91	4.47	5
RM295	OT	17.7	~9.0	5.87	4.46	5
RM296	OT	17.9	~8.9	~5.85	nd	5-10
RM299	OT	17.9	8.99	5.91	nd	0
RM301	OT	17.6	9.06	~5.84	nd	20
RM302	OT	17.6	9.25	5.86	nd	20
RM303	OT	17.6	~9.25	5.87	nd	20
RM304	OT	17.7	8.91	nd	nd	5
RM305	OT	17.8	9.01	nd	nd	10
RM306	OT	17.7	8.94	nd	nd	5
RM307	OT	17.4	8.78	nd	nd	5-10
RM54	PW	19.0	~9.6	nd	nd	?
RM73	PW	18.7	~9.5	nd	~4.52	20
RM75	PW	19.0	~9.6	nd	~4.47	20
RM76	PW	19.2	~9.7	nd	~4.52	20
RM104	SB	18.5	~9.5	~5.87	~4.54	20
RM105	SB	18.4	~9.3	nd	nd	?
RM391	CG	19.0	~9.5	nd	~4.51	20
RM392	CG	19.0	~9.6	nd	~4.51	20
RM119	WB	18.4	9.2	nd	nd	0
RM133	RP	18.8	~9.4	nd	~4.47	5-10
RM155	OC	18.1	9.17	nd	nd	10
RM158	AR	18.7	9.3	nd	4.6	5-10
RM181	RB	18.2	9.23	nd	nd	10-15

Note: All samples Mg saturated and glycerol solvated.
nd = peak not detected or exact position obscured by other minerals.
MB = Maslin Bay, OT = Onkaparinga Trig, PW = Port Willunga, SB = Sellicks Beach, CG = Chinaman Gully, WB = Witton Bluff, RP = Robinson Point, OC = Ochre Cove, AR = Ardrossan, RB = Redbanks.

Table 5.1: Previously reported occurrences of alunite in South Australia

Author	Location	Host sediment
Jack (1914)	Carrickalinga	Cambrian slates and limestones
Jack (1915)	Napperby	Shale of uncertain age, ?Precambrian
Ward (1917)	Stuart's Range opal field	Alunite enclosed by opal
Dickinson (1943)	Angepena Station	Weathered Precambrian shales
King (1953)	Pidinga	Tertiary clay
Crawford (1965)	Yorke Peninsula - numerous sites	Tertiary-Quaternary clays
Ward (1966)	Seaford	Pliocene sandy clay
Lindsay (1970)	Tickera	Oligo-Miocene fossiliferous sand
Callen (1976)	Lake Frome	Tertiary sediments
Lindsay & Williams (1977)	Hartley	Oligocene clayey sand

Table 5.2: Bulk mineralogy of samples containing alunite and/or halloysite determined from XRD.

Sample	Location	Mineralogy
RM141	Onkaparinga Trig	Quartz, 7Å+10Å halloysite, alunite
RM142	Onkaparinga Trig	Alunite, quartz
RM209	Onkaparinga Trig	Quartz, 7Å halloysite, halite, feldspar, alunite
RM210	Onkaparinga Trig	Quartz, 7Å halloysite, halite, feldspar
RM408	Onkaparinga Trig	10Å+7Å halloysite, quartz, feldspar, halite, alunite
RM412	Onkaparinga Trig	Alunite, quartz, halite, 7Å halloysite, feldspar
RM135	Seaford	Alunite, 10Å halloysite
RM138	Seaford	Alunite, 10Å+7Å halloysite, quartz, feldspar
RM388	Onkaparinga River	Alunite, quartz, halite
RM389	Onkaparinga River	Alunite, quartz, halite, clays
RM120	Port Noarlunga	Quartz, 7Å+10Å halloysite, alunite
RM149	Witton Bluff	Alunite, quartz, clays
RM126	Port Stanvac	Alunite, quartz, feldspar, 7Å halloysite
RM127	Port Stanvac	Alunite, quartz, feldspar, 7Å halloysite
RM174	Stanvac Railway Cutting	Alunite, quartz, feldspar
RM175	Stanvac Railway Cutting	Quartz, feldspar, alunite
RM177	Field River	Alunite, quartz
RM179	Field River	Alunite, quartz
RM385	Hallett Cove	Alunite, quartz, halite, 7Å halloysite, feldspar
RM386	Hallett Cove	Alunite, quartz, halite, clays
RM180	Redbanks	Alunite, quartz
RM63	Port Moorowie	Alunite, quartz, 10Å+7Å halloysite
RM64	Port Moorowie	10Å halloysite, quartz
RM160	Port Moorowie	Quartz, 10Å+7Å halloysite, feldspar
RM165	Port Moorowie	Alunite, 10Å halloysite
RM166	Port Moorowie	10Å halloysite, quartz, alunite
RM167	Port Moorowie	10Å halloysite, alunite

Note: Mineralogy given in order of decreasing abundance as estimated from XRD peak intensity.

Table 5.3: Si and Al concentrations in ammonium oxalate extractions

Sample	Mineralogy	% Si	% Al	Field Test
RM63	alunite + halloysite	0.026	0.072	*
RM120A	alunite + minor halloysite	0.014	0.170	*
RM120B	minor halloysite + trace alunite	0.012	0.100	-
RM135	alunite + trace halloysite	n.d.	0.034	-
RM138A	alunite + halloysite	n.d.	0.078	-
RM142	alunite	n.d.	0.044	-
RM165	alunite + halloysite	0.012	0.116	*
RM167	halloysite + trace alunite	0.028	0.178	*

* indicates positive field test for reactive aluminium using 0.02M NaF
n.d. indicates silica not detected in this extract

Table 5.4: Mineralogical details for iron-rich samples from mottled intervals

Sample	Location	Description	Dominant iron mineral (XRD)	Goethite (110) peak (Å)	Peak width	Goethite (111) peak (Å)	Al substitution	Hematite (110) peak width	%Fe2O3 (XRF)	Ratio goethite (110) to hematite (110)	Munsell colour	Other minerals (XRD)
RM24	Sellicks Beach	Unmottled							1.67			K,M,Q,F
RM25	Sellicks Beach	Mottle	goethite=hematite	4.184	0.4	nd	None	0.6	9.94	1.18	10R 3/6	K,M,Q,F,H
RM28-1	Sellicks Beach	Unmottled							2.18			M,K,Q,F
RM28-2	Sellicks Beach	Mottle	goethite=hematite	4.177	0.5	nd	None	0.3	22.79	1.04	10R 4/6	M,K,F,Q
RM31	Mitcham	Mottle	goethite	4.175	0.3	2.441	2-5 mole%	0.3	26.88	2.82	7.5YR 6/8	K,M,Q,F
RM32-1	Mitcham	Unmottled							2.70			K,M,Q,F
RM32-2	Mitcham	Mottle	goethite=hematite	4.18	0.3	nd	None	0.4	11.53	1.11	2.5YR 4/8	K,M,Q,F
RM37-1	Blackwood	Yellow mottle	goethite	4.175	0.7	2.446	2 mole%	0.7	17.90	2.26	10YR 6/8	K,Q,F
RM37-2	Blackwood	Red mottle	hematite	4.179	0.3	nd	None	0.4	15.00	0.56	10R 3/6	K,Q,F
RM40	Ochre Point	Mottle	goethite=hematite	4.18	0.6	2.448	None	0.4	25.42	1.73	10R 3/6	K,M,Q,F
RM41	Ochre Point	Mottle	goethite=hematite	4.167	0.5	2.446	2-6 mole%	0.4	27.37	1.59	10R 4/6	K,M,Q,F
RM62-1	Port Moorowie	Unmottled							1.73			M,K,Q,F,A,H
RM62-2	Port Moorowie	Mottle	hematite	4.177	?	nd	None	0.6	45.64	0.03	7.5R 2/2	Q,M,K,F
RM168	Port Moorowie	Mottle	hematite	4.163	0.3?	2.437	~8 mole%	0.7	38.71	0.32	7.5R 3/6	Q,Ha,F,A
RM220N	Snapper Point	Unmottled										K,M,Q,F,H
RM220M	Snapper Point	Mottle	hematite	4.18	?	nd	None	0.7		0.80	5YR 6/4	K,M,Q,F,H
RM264	Maslin Bay	Mottle	hematite	4.185	0.6	nd	None	0.7		0.83	10R 6/3	K,M,Q,F,H
RM327N	Onkaparinga Trig	Unmottled										K,M,Q,F,H
RM327M	Onkaparinga Trig	Mottle	hematite	nd		nd		0.7		<<0.1	10R 4/6	K,M,Q,F,H

NOTE: Peak widths in °2θ, measured at half height
K = kaolinite, M = mica, Q = quartz, F = feldspar, H = halite, A = alunite, Ha = halloysite
nd = not detected

Table 5.5: Mineralogical information for samples containing calcite and dolomite from the Neva Clay Member and the Burnham Limestone

Sample	Location	Stratigraphic unit	Calcite d(104) (Å)	Dolomite d(104) (Å)	Ca:Mg ratio in dolomite	Ratio of calcite to dolomite	Other minerals
RM1	Sellicks Beach	BLS	3.030	2.897	Dolomite	>>25	Q
RM2	Sellicks Beach	BLS	3.029	2.898	Dolomite	>>25	Q,C,F
RM4	Sellicks Beach	BLS	3.032	2.909	55:45	3.0	Q,C
RM6	Sellicks Beach	BLS	3.030	2.903	50:50	6.4	Q,C,F
RM8	Sellicks Beach	BLS	3.034	2.906	55:45	7.8	Q,C,F
RM21	Sellicks Beach	BLS	3.030	None			Q,C,F
RM23	Sellicks Beach	CO_3 above BLS	None	2.897	Dolomite		Q,C,H,F
RM170	Snapper Point	NCM	3.027	2.905	50:50	0.5	Q,C,F
RM171A	Snapper Point	NCM	3.027	2.906	55:45	0.5	Q,C,F
RM171B	Snapper Point	NCM	3.033	2.907	55:45	2.0	Q,C
RM228	Snapper Point	NCM	None	2.894	Dolomite		Q,C
RM230	Snapper Point	NCM	3.031	2.909	55:45	1.2	Q,C
RM231	Snapper Point	NCM	3.034	2.909	55:45	>>25	Q,C
RM243	Snapper Point	CO_3 above BLS	None	2.909	55:45		Q,C,F
RM244	Snapper Point	CO_3 above BLS	3.024	2.900	50:50	<<0.1	Q,C,F
RM246	Snapper Point	BLS	3.025	2.903	50:50	0.3	Q,C
RM51	Port Willunga	BLS	3.030	None			Q,C
RM52	Port Willunga	CO_3 above BLS	None	2.909	55:45		Q,C,H
RM53	Port Willunga	CO_3 above BLS	None	2.903	50:50		Q,C,H,F
RM70	Port Willunga	CO_3 above BLS	None	2.900	50:50		Q,H
RM71	Port Willunga	CO_3 above BLS	None	2.903	50:50		Q,H,F
RM72	Port Willunga	CO_3 above BLS	None	2.908	55:45		Q,C,H,F
RM74	Port Willunga	BLS	3.030	None			Q,C
RM390	Chinaman Gully	BLS	3.032	None			Q,C,F
RM110	Tortachilla Trig	BLS	3.026	None			Q,H,G,C
RM147	Onkaparinga Trig	NCM	None	2.896	Dolomite		Q,C,H
RM317	Onkaparinga Trig	NCM	None	2.900	50:50		Q,C,H
RM319	Onkaparinga Trig	NCM	3.031	2.906	55:45	>>25	Q,C,H
RM321	Onkaparinga Trig	NCM	3.025	None			Q,C
RM191	Onkaparinga River	NCM	3.030	2.886	Dolomite	>>25	Q
RM150	Hallett Cove	CO_3 mottles. BLS?	None	2.891	Dolomite		Q,F,H

NOTE: For pure calcite d(104) = 3.035Å and pure dolomite d(104) = 2.886Å.
Expected Ca:Mg ratio in dolomite is 51:49.
Q = Quartz, C = Clay minerals, F = Feldspar, H = Halite, G = Goethite.

Table 6.1 Summary of Clay Minerals Identified in Soils from the Adelaide Region (after Norrish & Pickering 1983)

Area	Major Components (>20%)	Minor Components
Barossa Valley (23 soils)	Illite, Kaolin, RIM	V, RIM, T, K, H/Go, I
Adelaide Plains and Lower North (55 soils)	Illite, Kaolin, RIM, Smectite (1 soil)	K, H/Go, C, V
Mt Lofty Ranges and Fleurieu Peninsula (31 soils)	Illite, Kaolin, RIM (9 soils), Chlorite (1 soil)	RIM, H/Go, Vi, G, T

Note that certain clay minerals (eg Illite, RIM) occur as major components in some soils but as minor components in other soils from the same area.

RIM = Randomly interstratified clays
V = Vermiculite
T = Talc
K = Kaolinite
H/Go = Hematite and/or goethite
I = Illite
C = Chlorite
Vi = Chloritised vermiculite
G = Gibbsite

APPENDICES

APPENDIX 1: DETAILS OF SAMPLES COLLECTED

Location	Sample number	Stratigraphic unit	Height above datum	Description
Sellicks Beach, 1.05 km south of boat ramp				
	RM1	BLS		Soft, white calcareous sediment
	RM2	BLS		Hard, white calcareous sediment
Ochre Cove				
	RM3	BPM		White to green, porous and silicified clay
Sellicks Beach, section through Burnham Limestone, 1.1 km south of boat ramp				
	RM4	BLS	1.5 m above Tertiary	White friable limestone with orange mottling
	RM5	RPF	2.5 m	Grey-black non-calcareous clay
	RM6	BLS	1.7 m	White friable limestone, fossiliferous
	RM7	RPF	2.7 m	Black clay
	RM8	BLS	2.0 m	Hard white limestone
	RM9	RPF	2.9 m	Black clay with inclusions of white carbonate
	RM10	RPF	0.75 m	Orange-grey sand
	RM11	BLS	1.3 m	White limestone
Sellicks Beach, section through Burnham Limestone, 1.05 km south of boat ramp				
	RM12	RPF	2.2 m above Tertiary	Black-grey clay above Burnham Limestone
	RM13	RPF	2.0 m	Grey-orange sand above Burnham Limestone
	RM14	RPF	1.2 m	Grey sandy clay
	RM15	RPF	0.6 m	White-grey sandy clay above gravel layer
	RM16	RPF	0.3 m	Chocolate to grey clay below gravel layer
Sellicks Beach, section immediately above Burnham Limestone, 1.12 km south of boat ramp				
	RM17	RPF	1.45 m above BLS	Sandy orange-grey clay immediately below gravel layer
	RM18	RPF	1.1 m	Grey-green clay
	RM19	RPF	0.75 m	Grey-green clay with orange mottles and small carbonate pods
	RM20	RPF	0.1 m	Calcareous grey clay with minor black inclusions
	RM21	BLS	0 m	Friable white limestone
	RM22	RPF	1.6 m	Red-grey clay with sand and grit-sized clasts above gravel layer

Sellicks Beach, small gully, 1.15 km south of boat ramp			
	RM23	RPF	1.7 m above BLS	White clay immediately above gravel layer
	RM24	RPF	3.5 m	White-grey sandy clay within iron mottled interval
	RM25	RPF	3.5 m	Bright red sandy clay from iron-rich mottle
Sellicks Beach, up gully, 1.1 km south of boat ramp			
	RM26	RPF	4.0 m above BLS	White-grey sandy clay from orange-coloured broadly mottled interval
	RM27	RPF	11.0 m	White-grey clayey sand from orange mottled interval
Sellicks Beach, upper part of cliffs along access path, 0.6 km south of boat ramp			
	RM28-1	RPF	3.5 m below top of cliff	White-grey gravelly and sandy clay from within iron mottled interval
	RM28-2	RPF	3.5 m	Hard red mottled sandy clay
	RM29	NF	2.0 m	Grey-green clay with sand and gravel-sized clasts, minor orange mottling
Mitcham Quarry, south west of Old Belair Road			
	RM30	HC		Grey unmottled sandy clay
	RM31	HC		Bright red mottled clay to sandy clay
	RM32-1	HC		Grey sandy clay with minor gravel clasts from iron mottled zone
	RM32-2	HC		Red mottled sandy clay
Hallett Cove, near top of Quaternary sequence, 25 m north of The Amphitheatre			
	RM33	NF		Green friable clay
Ochre Cove, adjacent to Lennard Drive			
	RM34	RPF		Red-yellow clayey sand near top of RPF
	RM35	NF		Grey-green clay with minor sand-sized clasts from base of NF
	RM36	RPF		Ferruginised sand from upper part of RPF
Blackwood railway cutting, west of Coromandel Pde			
	RM37-1	Tertiary?		Soft yellow mottle from sandy clays
	RM37-2	Tertiary?		Hard red to purple mottle above RM37-1
	RM38	Tertiary?		Silicified root-like cylindrical features, upper surface of Tertiary sediments
Ochre Point			
	RM39	RPF		Red and yellow mottled sandstone
	RM40	SPSM		Hard red mottle within white sandy lens
	RM41	SPSM		Soft red mottle immediately above RM40
	RM42	HCSS		Yellow-orange sandy ferruginous conglomerate overlying bedrock
	RM43	NCM		Green-grey clay, minor yellow-brown mottles, scattered sand-sized clasts

RM44	SPSM	Red-green sandy clay between RM41 and overlying calcrete
RM45-1	SPSM	Red-brown clay immediately below calcrete
RM45-2	SPSM	White carbonate mottle surrounded by red-brown clay
RM46	NCM	Green-grey clay immediately above RPF
Port Willunga, cliffs immediately south of kiosk		
RM47	SPSM	Hard calcareous nodules in green clay below calcrete, 30 m south of kiosk
RM48	SPSM	Calcareous clay immediately below calcrete, 200 m south of kiosk
RM49	SPSM	Carbonate pod in grey-green clay below calcrete, 240 m south of kiosk
RM50	SPSM	Carbonate mottle 10 cm above RM49
RM51	BLS	Hard nodular cream limestone, 35 m south of kiosk
RM52	NCM	Soft rubbly carbonate 20 cm above BLS within green clay, above RM51
RM53	NCM	Equivalent to RM52, but sampled 2 m to the north
RM54	NCM	Green clay immediately below RM53 but above BLS
Bradbury, (Max Bradbury's quarry)		
RM55	Precambrian	Soft white weathered shale from base of quarry face, Woolshed Flat Shale
RM56	Precambrian	Soft white weathered shale, minor iron staining, 2 m above RM55
Port Julia, Yorke Peninsula, opposite jetty		
RM57	Quaternary	Reddish sandy clay from base of cliffs
RM58	Quaternary	Light brown sandy, calcareous sediment 40 cm below lower calcrete
RM59	Quaternary	Hard white calcrete
RM60	Quaternary	Light brown calcareous sand 60 cm below upper calcrete
RM61	Quaternary	Hard nodular calcrete
Port Moorowie, Yorke Peninsula, 100 m east of boat ramp		
RM62-1	Quaternary	Grey sandy clay immediately above mottled Permian sediments
RM62-2	Quaternary	Red mottle adjacent to RM62-1
RM63	Quaternary	Grey clay, columnar structure, mottled, immediately below halloysite layer
RM64	Quaternary	White halloysite from thin upper bed within brown clay
RM65	Quaternary	Brown sandy clay between halloysite layers and calcrete
RM66	Quaternary	Carbonate nodules in brown silt at base of calcrete
Port Moorowie, Yorke Peninsula, adjacent to boat ramp		
RM67	Quaternary	Brown sandy clay from just below calcrete
RM68	Quaternary	Nodules of carbonate within brown silt at base of calcrete
Seaford, 500 m north of Moana boat ramp		
RM69	RPF	White alunite from narrow band in sand at base of cliffs

Port Willunga, 40 m south of kiosk

RM70	NCM	15.65 m below cliff top	Thin white friable carbonate layer above BLS, hard skin
RM71	NCM	15.70 m	Soft white carbonate from centre of layer within clays above BLS
RM72	BLS	15.85 m	Soft carbonate mixed with green clay, minor manganese coating
RM73	NCM	15.80 m	Green clay between BLS and overlying carbonate layer
RM74	BLS	15.90 m	Rubbly carbonate mixed with green clay at top of BLS
RM75	BLS	16.50 m	Green sandy clay filling hollows within BLS
RM76	BLS	16.70 m	Green sand and nodules of carbonate from within BLS
RM77	NCM	15.40 m	Green clay above carbonate layer, slickensides common
RM78	NCM	13.30 m	Green clay, minor orange mottling and isolated sandy pockets
RM79	NCM	10.40 m	Green sandy clay, minor orange mottling
RM80	NCM	9.80 m	Green-grey sandy clay, minor gravel clasts, common ferruginous mottles
RM81	SPSM	8.60 m	Red and yellow mottled sandy clay
RM82	SPSM	8.40 m	Grey-green clay with minor red mottling
RM83	SPSM	6.40 m	Grey-green clay, small red mottles, slickensides common
RM84	SPSM	4.00 m	Dark grey-green clay with minor small red mottles
RM85	SPSM	3.80 m	Grey-green sandy clay, rare calcareous pods, manganese staining

Aldinga Beach, road cutting on Esplanade, 100 m south of Morgan St

RM86	NF	0.2 m above base of section	Red mottled grey-green sandy clay from base of exposure
RM87	NF	0.2 m	Large red vertical mottle adjacent to RM86
RM88S	NF	0.7 m	White sand from patch within mottled sandy clay, 0.5 m above RM86
RM88M	NF	0.7 m	Red mottle with yellow alteration on margins, adjacent to RM88S
RM89	NF	1.1 m	Red and yellow mottled white sand from top of sandy unit
RM90	NF	2.1 m	Grey-green clayey sand with broad orange-yellow mottles
RM91	NF	3.0 m	Soft white carbonate from base of 0.3 m thick carbonate layer
RM92	NF	2.9 m	Grey-green sandy clay from contact with overlying carbonate
RM93	NF	3.4 m	Green-grey clay immediately above carbonate, minor carbonate nodules
RM94	NF	3.3 m	Top surface of carbonate, white rubbly material
RM95	NF	3.3 m	Hardened clast of carbonate 10 cm diameter
RM96	NF	4.3 m	Orange mottled clayey sand, minor carbonate nodules
RM97	NF	5.3 m	Non calcareous orange sand just below main calcrete interval

Sellicks Beach, section through interval containing BLS, 1.1 km south of boat ramp

RM98	RPF	0.1 m above Tertiary	Grey to dark brown clay
RM99	RPF	0.4 m	Grey sandy clay with small orange mottles
RM100	RPF	0.65 m	Grey gravelly clay with orange mottles
RM101	RPF	1.05 m	Gritty grey sand with large orange patches, immediately below BLS
RM102	RPF	2.0 m	Grey clay with minor soft calcareous clasts, 10 cm above BLS
RM103	RPF	2.2 m	Dark grey clay with minor small orange mottles
RM104	RPF	2.6 m	Grey clay with occasional yellow-white laminations of sand
RM105	RPF	2.9 m	Grey-brown sand with several small patches of soft white carbonate
RM106	RPF	3.0 m	Reddish clay with common gravel and sand-sized clasts

Tortachilla Trig

RM108	RPF	Thin bed of soft white alunite 1.2 m above BLS
RM109	RPF	Black manganese staining sands 1 m above BLS
RM110	BLS	Yellow-brown to white clayey limestone
RM111	HCSS	White, shelly sand
RM112	TLS	Green fossiliferous clay

Railway cutting, immediately south of O'Sullivan Beach Road

RM113	RPF	Grey clay from base of section immediately above Precambrian rocks
RM114	RPF	White-grey sand from base of central sandy unit
RM115	RPF	Red-yellow mottle from adjacent to RM114
RM116	RPF	Grey sand, weakly mottled yellow from top of sandy unit
RM117	NF	Grey-green sandy clay from transitional zone above sandy unit
RM118	NF	Grey-green clay from base of upper clay unit

Port Noarlunga, 150 m north of jetty

RM119	RPF?	Green clay below alunite interval and above Tertiary sediments
RM120A	RPF	White alunite from hard thin bed
RM120B	RPF	Grey sandy alunite from same thin bed as RM120A
RM121	RPF	Soft white alunite from layer 15 cm above RM120

Christies Beach, south end of beach

RM122	BPM	Soft white siliceous material
RM123	BPM	Green clay immediately above RM122, white siliceous laminations
RM124	BPM	Green clay from below RM122 with occasional Turritella fossils
RM125	BPM	Hard fossiliferous sandy limestone several metres below RM122

Port Stanvac Refinery, cliffs in front of holiday camp		
	RM126	HCSS
	RM127	HCSS
Seaford, 200 m north of Robinson Point		
	RM128	NCM
	RM129	SPSM
	RM130	SPSM
	RM131	SPSM
	RM132	SPSM
Robinson Point, just north of the Point		
	RM133	RPF
	RM134	RPF
	RM135	RPF
	RM136	RPF
	RM137	RPF
	RM138A	RPF
	RM138B	RPF
	RM139	SPSM
	RM140	SPSM
Onkaparinga Trig, 200 m south of trig point		
	RM141A	RPF
	RM141B	RPF
	RM142	RPF
	RM143	RPF
	RM144	RPF
	RM145	RPF
	RM146	RPF
	RM147	NCM
	RM148	SPSM
Witton Bluff		
	RM149	RPF
Hallett Cove, immediately east of The Sugarloaf		
	RM150	BLS
	RM151	NF

Soft white alunite immediately below hard calcareous sandstone of HCSS
Soft white alunite forming round pods immediately above HCSS

Grey-green clay from base of Ngaltinga Formation
Green clayey sand, base of sand unit in central part of Ngaltinga Formation
Brown clay with manganese staining immediately below calcrete
Vertical white carbonate mottle extending into brown clay below calcrete
Vertical white carbonate mottle 50 cm north of RM131

Sandy clay from base of cliffs, just above alunite interval
Red and yellow mottled sand from centre of RPF
Small white pod of alunite within yellow and pink coloured sand
Brown-red sand immediately above Tertiary limestone, base of cliffs
Banded pink, yellow and white sand immediately below alunite interval
White friable alunite forming skin of small pod
Cream waxy alunite forming core of small pod
Horizontal 10 cm band of carbonate within brown clays just below calcrete
White carbonate forming vertical mottle 0.5 m above RM139

White powdery alunite from band immediately above Tertiary
Dark grey waxy material from same band as RM141A
White nodular alunite in green clay filling solutional hollow in Tertiary
Yellow-dark brown sand partly indurated, 0.5 m above RM142
Green clay immediately above Tertiary BPM and below alunite beds
Red-pink sand from centre of alunite-rich interval
Yellow-dark brown indurated sand from top of alunite interval
Soft white carbonate from 10 cm interval within green clays
Vertical carbonate mottle within sandy clay immediately below calcrete

White alunite from thin band within upper sands of RPF

White carbonate from 15cm band within grey sandy clay 70cm above HCSS
Brown clay from immediately below calcrete

Witton Bluff		
	RM152	NF
	RM153	NF
	RM154	NF
Ochre Cove, adjacent to Lennard Drive		
	RM155	BPM
	RM156	BPM
Ardrossan, Yorke Peninsula, north side of jetty		
	RM157	Quaternary
	RM158	Quaternary
	RM159	Quaternary
Port Moorowie, Yorke Peninsula, 1 km east of boat ramp		
	RM160	Quaternary
	RM161	Quaternary
	RM162	Quaternary
	RM163	Quaternary
	RM164	Quaternary
Port Moorowie, Yorke Peninsula, 100 m east of boat ramp		
	RM165	Quaternary
	RM166	Quaternary
	RM167	Quaternary
	RM168	Quaternary
Aldinga Beach, 150 m north of car park		
	RM169	NF
Snapper Point, 400 m south of point		
	RM170	NCM
	RM171	NCM
	RM172	SPSM
	RM173	SPSM
Stanvac railway cutting, 600 m south of Field River		
	RM174	SPSM
	RM175	P
Coastal cliffs, 1 km south of mouth of Field River		
	RM176	HCSS
	RM177	RPF

Hard carbonate layer at base of red-brown clay 2.5 m below cliff-top
Soft white carbonate within red-brown clay 50 cm above RM152
Red-brown clay immediately above RM153

Green speckled clay immediately below sand and alunite of Quaternary
White siliceous fossiliferous sediment from immediately below RM155

Mottled red and white clay from upper part of cliffs below calcrete
Clayey sand near base of cliffs just below gravel lens, small yellow mottles
Red cross-bedded sands and gravels, 25 cm above RM158

Green clay from central part of cliffs, manganese staining
Soft white carbonate pods from upper part of green clay just below calcrete
Soft carbonate in basal part of carbonate blanket 40 cm above RM161
Green clayey sand from base of cliffs
Green clay sampled 90 cm above RM163

White nodular alunite from basal band of alunite interval
Waxy nodule from upper white band of alunite interval 30 cm above RM165
Soft waxy material from central band between RM165 and RM166
Hard red mottle within sandy clays just above Permian sediments

Thin 30 cm layer of white carbonate in green-brown clay

White carbonate from 2 m interval within clays halfway up cliffs
Soft white carbonate 50 cm above RM170
Hard white-buff sand from cross-bedded lens 2.5 m above RM171
Uncemented white sand from adjacent to RM172

White pods of alunite within brown sandy clay just below calcrete
Well-bedded grey clay, Fe-mottled. Probable Permian sediments

Calcareous gravelly sandstone, ferruginous below Quaternary sediments
Off-white alunite from thin bed just above RM176

RM178	RPF		Softer white alunite from thin bed 2 m south of RM177
RM179	RPF		Hard white alunite with gravel clasts 1 m south of RM178
Redbanks, River Light, southeast of Mallala, Adelaide Plains Sub-Basin			
RM180	Quaternary		White alunite within grey-yellow sand 0.5 m above Tertiary? limestone
RM181	Quaternary		Chocolate brown clay between RM180 and underlying limestone
RM182	Quaternary		Green sandy clay firm small pockets interbedded? with limestone
Dry Creek adjacent to Bridgeway Hotel, Adelaide Plains Sub-Basin			
RM183	Quaternary		Grey clay from immediately below Pooraka Formation. Hindmarsh Clay?
Onkaparinga River Mouth, storm water gully opposite Berwick Street			
RM184	SPSM	6.5 m above RPF	Brown clay immediately below calcrete, rare nodules of carbonate
RM185	SPSM	6.0 m	Brown clay with manganese staining
RM186	SPSM	5.5 m	Mottled grey sandy clay. Mottles red-brown coloured
RM187	SPSM	5.0 m	Mottled grey sand from laterally extensive thin lens
RM188	SPSM	6.7 m	Vertical white carbonate mottle adjacent to brown clay of RM184
RM189	SPSM	4.2 m	White-grey silty sand with numerous tubular burrow? structures
RM190	NCM	3.5 m	Green-grey clay, columnar structure, slickensides, rare red mottles
RM191	NCM	2.5 m	White carbonate from 40 cm interval within clays
RM192	NCM	0.2 m	Grey sandy clay with small red and yellow mottles
Ochre Point			
RM193	HCSS		Ferruginous sand from interval containing fossiliferous conglomerate
Snapper Point, 400 m south of point			
RM194	HCSS		Preserved roots (calcified) on upper surface of HCSS, on shore platform
Witton Bluff			
RM195	BPM		Possible preserved (silicified) root on upper surface of BPM
RM196	RPF		Pink sand from within alunite interval at base of RPF
Onkaparinga River Mouth, storm water gully opposite Berwick Street, samples collected for microfossil study			
RM197	RPF		Yellow-red sandy and gravelly sediment
RM198	NCM		Grey-green clay, 1 m above RPF
RM199	NCM		Grey-green clay between carbonate and SPSM. Equivalent to RM190
RM200	SPSM		Grey silty sand. Equivalent to RM189
RM201	SPSM		Grey sand. Equivalent to RM187
RM202	SPSM		Red-brown clay. Equivalent to RM185
Onkaparinga Trig, 200 m south of trig point, samples collected for microfossil study			
RM203	RPF		Grey fine silty sand just above alunite interval. Equivalent to RM293
RM204	NCM		Green clay from adjacent to carbonate interval. Equivalent to RM322

RM205	RPF		Laminated yellow, pink and white sand from just below alunite interval
Tortachilla Trig			
RM206	BLS		Soft mottled carbonate from upper part of probable BLS
RM207	BLS		Similar white mottled carbonate 150 m further south
Onkaparinga Trig, 200 m south of trig point, samples collected for spectroscopic study by A.Gabel, CSIRO, Sydney			
RM208	RPF		White alunite from clay-filled hollow in Tertiary. Equivalent to RM142
RM209	RPF		White sandy alunite from basal layer of alunite interval
RM210	RPF		Pink-white sandy and waxy alunite/halloysite. Equivalent to RM141B
Snapper Point, 400 m south of point			
RM211	SPSM	14.1 m above BLS	Calcareous brown sandy clay
RM212	SPSM	14.1 m	Soft white carbonate mottle adjacent to RM211
RM213	SPSM	13.6 m	Sandy green clay
RM214	SPSM	13.6 m	Hard white pod of carbonate within clay of RM213
RM215	SPSM	13.1 m	Green clay slightly sandy, minor small orange-red mottles
RM216	SPSM	12.6 m	Green clay with scattered sand-sized grains, minor orange-red mottles
RM217	SPSM	12.35 m	Green sandy clay with red-orange mottles
RM218	SPSM	12.1 m	Green-yellow sand with large red mottles
RM219	SPSM	11.6 m	Green sand with red mottles
RM220	SPSM	11.1 m	Green sandy clay with some red mottles
RM221	SPSM	10.6 m	Horizontally bedded buff sand with some small orange mottles
RM222	SPSM	10.1 m	White sand, red-orange mottles
RM223	SPSM	9.6 m	White sand with broad pink-red mottles
RM224	NCM	9.1 m	Green clay with rare small yellow-orange mottles
RM225	NCM	8.6 m	Green clay with small orange mottles
RM226	NCM	8.1 m	Dark green clay, massive
RM227	NCM	7.6 m	Green clay, small orange mottles and manganese staining
RM228A	NCM	7.1 m	Green clay with rare small orange mottles
RM228B	NCM	7.1 m	Blotches of soft white carbonate associated with clay, top of carbonate zone
RM229	NCM	6.6 m	Green clay with small orange mottles within carbonate zone
RM230	NCM	6.1 m	Large mottles of soft white carbonate in green clay
RM231A	NCM	5.6 m	Green clay with small orange mottles and manganese staining
RM231B	NCM	5.6 m	Small blotches and mottles of soft white carbonate, base of carbonate zone
RM232	NCM	5.1 m	Green clay, very rare orange mottles
RM233	NCM	4.6 m	Green clay, minor orange-yellow mottles
RM234	NCM	4.1 m	Green clay with small orange mottles

RM235	NCM	3.6 m	Green clay with small orange mottles
RM236	NCM	3.1 m	Green clay with small orange mottles
RM237	NCM	2.6 m	Green clay with small orange mottles
RM238	NCM	2.1 m	Green clay with small orange mottles
RM239	NCM	1.6 m	Green clay with small orange mottles
RM240	NCM	1.1 m	Green clay with small orange mottles and some manganese staining
RM241	NCM	0.7 m	Green clay with small orange mottles and some manganese staining
RM242	NCM	0.4 m	Green clay with small red-brown mottles and manganese staining
RM243	NCM	0.2 m	White carbonate from small vertical mottle within clays
RM244	NCM	0.2 m	Hard carbonate mottle from adjacent to RM243
RM245	NCM	0.0 m	Green clay with small red-brown mottles
RM246	BLS		Soft carbonate from rubbly BLS, 0.2 m below RM245
Maslin Bay, 200 m north of toilet block			
RM247	BLS	0.0 m above top of BLS	White carbonate forming large mottles within yellow-orange sand
RM248	RPF	0.35 m	White-green sand interbedded with orange sand
RM249	RPF	0.7 m	White-yellow-orange clayey sand
RM250	RPF	1.0 m	Yellow-green sandy clay with extensive manganese staining
RM251	RPF	1.4 m	Yellow-green sandy clay with rare interbeds of pink-red clay
RM252	RPF	1.8 m	Small 20 cm pocket of white sand within RM253
RM253	RPF	1.8 m	Yellow-green and pink-red sand to sandy clay
RM254	RPF	2.3 m	Pink-red sandy clay
RM255	RPF	2.7 m	10 cm layer of pink-white waxy sediment within pink-red sandy clay
RM256	RPF	3.0 m	Grey sandy alunite/halloysite as 10 cm band within pink-red sandy clay
RM257	RPF	3.5 m	Grey sandy and waxy sediment forming thin band in pink-red sandy clay
RM258	RPF	4.0 m	Grey-white sandy clay with small red mottles
RM259	RPF	4.5 m	Grey-white sand with small red mottles
RM260	RPF	5.0 m	Grey-white clayey sand with red mottles
RM261	RPF	5.5 m	Grey-white clayey sand with red mottles
RM262	RPF	6.0 m	Soft grey-white sandy clay with large hard red vertical mottles
RM263	RPF	6.5 m	White clayey sand
RM264	RPF	6.5 m	Large indurated red sandy mottle from adjacent to RM263
RM265	RPF	7.0 m	Indurated white sand
RM266	RPF	7.4 m	White sand from upper part of indurated interval
RM267	RPF	8.0 m	Soft white sandy clay
RM268	RPF	8.5 m	Grey-white clayey sand

RM269	RPF	9.0 m	Grey-white sand
RM270	RPF	9.5 m	Grey-white sand
RM271	RPF	10.0 m	Grey-white sand
RM272	RPF	10.5 m	Grey-white sand with small red mottles
RM273	RPF	11.0 m	Grey-white sandy clay
RM274	RPF	11.5 m	Grey-white sandy clay from 0.7 m clay-rich bed, minor red-brown mottling
RM275	RPF	11.9 m	Grey-white clay from same interval as RM274
RM276	RPF	12.4 m	Grey-white clayey sand, minor red mottles
RM277	RPF	12.9 m	Grey-white clayey sand, minor yellow-red mottles
RM278	NF	13.5 m	Green clay with some yellow-orange mottles
RM279	NF	14.0 m	Green clay, minor red mottling
RM280	NF	14.5 m	Green clay
RM281	NF	15.0 m	Green clay
RM282	NF	15.5 m	Green clay
RM283	NF	16.0 m	Green clay with rare red mottles
RM284	NF	16.5 m	Green clay with rare red mottles
RM285	NF	17.0 m	Green clay with red and orange mottles
RM286	NF	17.5 m	Green clay with some small yellow orange mottles
RM287	NF	18.0 m	Green clay with rare orange mottles and minor manganese staining
RM288	NF	18.5 m	Green clay with rare small white carbonate blotches
RM289	NF	19.5 m	Dark green clay with rare white carbonate mottles penetrating clay
RM290	NF	20.5 m	Brown clay with numerous small mottles and blotches of white carbonate
Onkaparinga Trig, 200 m south of trig point			
RM291	RPF	0.8 m above Tertiary seds	Pink-orange sand from top of alunite-rich interval
RM292	RPF	1.0 m	Yellow sand
RM293	RPF	1.4 m	Green sandy clay with minor orange mottles
RM294	RPF	1.6 m	Grey-green clay with small red mottles
RM295	RPF	1.8 m	Grey clay with small yellow-orange mottles, evidence of bioturbation
RM296	RPF	2.0 m	Grey sandy clay, small yellow-orange mottles, bioturbated, palaeosol
RM297	RPF	2.0 m	Oriented sample of palaeosol for thin section studies
RM298	RPF	2.3 m	Red gritty sand
RM299	RPF	2.45 m	Grey silty clay with small yellow-orange mottles, palaeosol
RM300	RPF	2.65 m	Cross-bedded red grits and gravels
RM301	RPF	2.9 m	Red-grey clay
RM302	RPF	3.15 m	Grey-yellow silty clay, mottled yellow-orange, bioturbated, palaeosol

RM303	RPF	3.8 m	Grey silty clay, minor red and yellow mottles
RM304	RPF	4.3 m	Red to grey sandy clay
RM305	RPF	4.8 m	Yellow-grey silty clay with red mottles
RM306	RPF	5.3 m	Yellow-grey silty clay with red mottles
RM307	RPF	5.8 m	Yellow-grey silty clay with a few red mottles
RM308	NCM	6.7 m	Massive green clay with minor small red mottles
RM309	NCM	7.2 m	Green clay with small red mottles
RM310	NCM	7.7 m	Green clay with small red mottles
RM311	NCM	8.2 m	Green clay with small red mottles
RM312	NCM	8.7 m	Green clay with rare small red mottles
RM313	NCM	9.2 m	Green clay with small red mottles
RM314	NCM	9.7 m	Green clay with small red mottles
RM315	NCM	10.2 m	Green clay with small red mottles
RM316	NCM	10.5 m	Green clay with small blotches of carbonate, base of carbonate interval
RM317	NCM	10.5 m	Blotches of soft white carbonate adjacent to RM316
RM318	NCM	11.0 m	Dark green clay with small carbonate blotches, minor manganese staining
RM319	NCM	11.5 m	Soft white carbonate forming mottles within green clay
RM320	NCM	12.0 m	Green clay with numerous small carbonate blotches
RM321	NCM	12.0 m	Soft white carbonate adjacent to RM320
RM322	NCM	12.5 m	Green clay from immediately above carbonate-rich interval
RM323	NCM	13.0 m	Green clay
RM324	NCM	13.5 m	Green clay
RM325	NCM	14.0 m	Green clay
RM326	SPSM	14.3 m	Grey-white silty sand
RM327	SPSM	14.8 m	White sand with yellow-orange mottles
RM328	SPSM	15.3 m	Grey clayey sand with some red mottles
RM329	SPSM	15.8 m	Grey sandy clay, minor red mottling
RM330	SPSM	16.3 m	Grey sandy clay, minor red mottling
RM331	SPSM	16.8 m	Grey-brown sandy clay, minor red mottling
RM332	SPSM	17.3 m	Chocolate sandy clay, minor manganese staining
RM333	SPSM	17.8 m	Chocolate-red sandy clay
RM334	SPSM	18.3 m	Chocolate-red sandy clay
RM335	SPSM	18.8 m	Red sandy clay, rare carbonate inclusions
RM336	SPSM	19.3 m	Red calcareous sandy clay
RM337	SPSM	19.8 m	Red calcareous sandy clay with small white carbonate mottles

Hallett Cove, along gully 25 m north east of Sugarloaf

RM338	RPF	0.0 m above HCSS	Green-yellow sand immediately above isolated remnant of HCSS
RM339	RPF	0.5 m	Green sand from thin gravel layer
RM340	RPF	1.0 m	Green-yellow clay with minor orange mottles
RM341	RPF	1.5 m	Green clay with minor small orange mottles
RM342	RPF	2.0 m	Green clay with minor small orange mottles
RM343	RPF	2.5 m	Green clay with small red and orange mottles
RM344	RPF	3.0 m	Green clay with small red and orange mottles
RM345	RPF	3.5 m	Green clay with larger red mottles
RM346	RPF	4.0 m	Green silty clay with large red mottles
RM347	RPF	4.5 m	Grey sandy clay with red mottles
RM348	RPF	5.0 m	White indurated sand
RM349	RPF	5.0 m	Large indurated red mottle from adjacent to RM348
RM350	RPF	5.5 m	Indurated white sand
RM351	RPF	6.0 m	Indurated white sand
RM352	RPF	6.5 m	Indurated white sand
RM353	RPF	6.5 m	Large indurated red mottle from adjacent to RM352
RM354	RPF	7.0 m	Indurated white sand
RM355	RPF	7.5 m	Indurated white sand
RM356	RPF	8.0 m	Soft white sand with large soft red mottles
RM357	RPF	8.5 m	Grey sand with small red mottles
RM358	RPF	9.0 m	Grey sand with small red mottles
RM359	RPF	9.5 m	Grey clayey sand with small red mottles
RM360	RPF	10.0 m	Grey clayey sand with small red mottles
RM361	RPF	10.5 m	Grey sand with small red-brown mottles
RM362	RPF	11.0 m	Grey sand with small red-brown mottles just below small gravel lens
RM363	RPF	11.5 m	Grey sand with minor small red-brown mottles
RM364	NF	12.0 m	Green clay with minor small red mottles
RM365	NF	12.5 m	Green clay with minor small red mottles
RM366	NF	13.0 m	Green to red clay
RM367	NF	13.5 m	Green clay with small red mottles
RM368	NF	14.0 m	Green clay with small red mottles
RM369	NF	14.5 m	Green clay with small red mottles
RM370	NF	15.0 m	Green clay with small red mottles

RM371	NF	15.5 m	Green clay with small red mottles
RM372	NF	16.0 m	Green clay with small red mottles
RM373	NF	16.5 m	Green clay with small red mottles
RM374	NF	17.0 m	Green clay with small red mottles
RM375	NF	17.5 m	Green clay with rare small red mottles
RM376	NF	18.0 m	Green clay with minor small red mottles
RM377	NF	18.5 m	Green clay with minor small red mottles
RM378	NF	19.0 m	Green clay with rare orange-red mottles
RM379	NF	19.5 m	Brown-green sandy clay with minor small white carbonate inclusions
Hallett Cove, adjacent to The Amphitheatre			
RM385	RPF		Soft white alunite from base of RPF, south end of Amphitheatre
RM386	RPF		White alunite from thin band at base of RPF, north end of Amphitheatre
RM387	RPF		Hard sandy white alunite from 0.5 m above RM386
Onkaparinga River, along River Rd, 0.5 km east of New Rd intersection			
RM388	NMS		Small round pod of alunite in roadside cutting
RM389	NMS		Long thin bed of soft white alunite adjacent to RM388
Chinaman Gully, exposure immediately south of gully			
RM390	BLS		White, sandy limestone from top of BLS
RM391	NCM		Thin bed of green sand interbedded with green clay immediately above BLS
RM392	NCM		Green clay from 15 cm above RM391
RM393	SPSM		Pale yellow material coating red mottle at base of SPSM. Probable jarosite
Blanche Point, immediately south of point			
RM394	NF		Yellow-green clay from about 3 m above BLS
RM395	NF		Green clay with minor red mottles about 3 m below overlying calcrete
Onkaparinga Trig, section through mottled carbonate interval from NCM, 200 m south of trig point			
RM397	NCM	0.2 m from base of carbonate	Soft white carbonate from small 3 cm thick pod
RM398	NCM	0.25 m	Soft white carbonate from 6 cm by 10 cm mottle
RM399	NCM	0.3 m	Soft white carbonate from base of large 10 cm thick by 40 cm wide mottle
RM400	NCM	0.4 m	Soft white carbonate from top of same mottle as RM399
RM401	NCM	0.05 m	Soft white carbonate from 5 cm thick elongate mottle
RM402	NCM	0.65 m	Soft white carbonate from base of 25 cm thick by 15 cm wide mottle
RM403	NCM	0.7 m	Soft white carbonate from same mottle as RM402
RM404	NCM	0.85 m	Soft white carbonate from top of same mottle as RM402 and RM403
RM405	NCM	1.05 m	Indurated clast of carbonate surrounded by softer white material
RM406	NCM	0.25 m	Green clay forming small pod within carbonate mottle

Onkaparinga Trig, section through alunite interval at base of cliffs, 200 m south of trig point

RM407	RPF	0.3 m above Tertiary PWF	Indurated clast of limestone within yellow-green clay
RM408	RPF	0.6 m	Base of waxy pod of halloysite 16 cm by 24 cm within yellow-pink sand
RM409	RPF	0.7 m	Upper portion of same pod as RM408
RM410	RPF	1.0 m	Thin band of white alunite/halloysite within tough pink-red clayey fine sand
RM411	RPF	0.75 m	White alunite from 25 cm long pod 3 cm thick in yellow-pink clayey sand, 50 cm south of RM408
RM412	RPF	0.65 m	Soft white alunite from 7 cm by 3 cm pod immediately below RM411

NOTE: RM107 collected in NSW and not related to present study
RM380 to RM384 collected in NSW and not related to present study
RM396 collected in Adelaide Hills but not related to present study

SPSM = Snapper Point Sand Member
NCM = Neva Clay Member
NF = Ngaltinga Formation
RPF = Robinson Point Formation
HC = Hindmarsh Clay
BLS = Burnham Limestone
HCSS = Hallett Cove Sandstone
PWF = Port Willunga Formation
BPM = Blanche Point Marls
TLS = Tortachilla Limestone
NMS = North Maslin Sand
P = Permian

APPENDIX 2: PARTICLE SIZE DATA

Snapper Point

Sample	Height (m)	Crse Sand (%)	Fine Sand (%)	Silt (%)	Clay (%)	Cs/Fs
RM215	13.1	14.5	18.7	17.6	49.2	0.78
RM216	12.6	18.9	20.3	15.8	45.0	0.93
RM217	12.35	23.6	23.0	14.1	39.3	1.02
RM218	12.1	36.8	28.9	9.2	25.2	1.27
RM219	11.6	26.7	23.9	11.5	37.9	1.12
RM220	11.1	23.6	22.5	14.2	39.7	1.05
RM221	10.6	33.3	37.4	10.5	18.8	0.89
RM222	10.1	26.0	47.3	7.2	19.5	0.55
RM223	9.6	31.9	36.2	7.1	24.8	0.88
RM224	9.1	3.0	5.7	23.6	67.7	0.53
RM225	8.6	1.2	4.8	21.5	72.5	0.25
RM226	8.1	2.1	2.5	21.9	73.5	0.83
RM227	7.6	0.8	2.4	21.1	75.7	0.33
RM228A	7.1	0.4	1.2	18.5	80.0	0.30
RM229	6.6	0.4	1.7	20.6	77.3	0.23
RM231	5.6	0.8	2.8	21.2	75.2	0.28
RM232	5.1	0.7	2.5	24.7	72.1	0.26
RM233	4.6	0.6	2.6	21.2	75.6	0.23
RM234	4.1	0.5	2.3	20.7	76.5	0.23
RM235	3.6	0.7	3.2	28.4	67.7	0.22
RM236	3.1	0.5	2.1	20.6	76.8	0.23
RM237	2.6	0.8	2.7	21.2	75.3	0.29
RM238	2.1	0.7	2.6	21.6	75.2	0.28
RM239	1.6	0.7	2.8	21.2	75.2	0.26
RM240	1.1	0.4	1.9	20.4	77.2	0.23
RM241	0.7	0.4	2.0	20.5	77.1	0.19
RM242	0.4	0.3	0.9	19.8	79.0	0.30
RM245	0	1.5	6.9	18.8	72.8	0.22

Maslin Bay

Sample	Height (m)	Crse Sand (%)	Fine Sand (%)	Silt (%)	Clay (%)	Cs/Fs
RM248	0.35	19.9	31.9	19.6	28.7	0.62
RM249	0.7	19.2	25.4	15.4	40.0	0.76
RM250	1	25.1	38.7	16.2	20.0	0.65
RM251	1.4	18.6	24.5	8.0	48.9	0.76
RM252	1.8	72.5	22.4	1.1	4.0	3.23
RM253	1.8	15.5	59.4	9.7	15.5	0.26
RM254	2.3	17.6	19.4	12.1	50.9	0.91
RM255	2.7	34.3	18.5	17.2	30.0	1.86
RM256	3	20.7	40.6	13.8	25.0	0.51

Sample	Height (m)	Crse Sand (%)	Fine Sand (%)	Silt (%)	Clay (%)	Cs/Fs
RM257	3.5	32.6	30.5	7.9	29.0	1.07
RM258	4	18.8	45.7	9.5	26.0	0.41
RM259	4.5	24.2	38.4	8.5	28.9	0.63
RM260	5	26.6	34.4	12.1	27.0	0.77
RM261	5.5	33.6	36.5	10.9	19.0	0.92
RM262	6	10.4	11.4	31.9	46.3	0.92
RM263	6.5				35.6	
RM265	7				14.6	
RM266	7.4				11.2	
RM267	8				22.8	
RM268	8.5	15.8	31.2	27.8	25.3	0.51
RM269	9	14.2	32.5	26.3	27.0	0.44
RM270	9.5	18.3	28.4	29.4	24.0	0.64
RM271	10	18.6	33.2	28.5	19.8	0.56
RM272	10.5	19.7	29.5	24.8	26.0	0.67
RM273	11	15.5	35.2	22.3	27.0	0.44
RM274	11.5	16.3	29.3	16.5	38.0	0.56
RM275	11.9	5.8	10.9	25.8	57.5	0.54
RM276	12.4	7.9	47.6	20.2	24.3	0.17
RM277	12.9	23.3	37.5	18.2	21.0	0.62
RM278	13.5	1.7	5.6	27.4	65.3	0.30
RM279	14	0.3	2.0	27.5	70.3	0.13
RM280	14.5	0.5	3.0	27.6	68.9	0.16
RM281	15	0.5	3.4	27.3	68.8	0.16
RM282	15.5	0.6	3.7	27.2	68.6	0.16
RM283	16	1.4	5.7	26.9	66.0	0.25
RM284	16.5	1.3	6.0	26.5	66.3	0.21
RM285	17	2.3	7.2	26.5	64.0	0.32
RM286	17.5	3.4	10.3	25.8	60.5	0.33
RM287	18	2.9	10.3	26.2	60.5	0.28
RM288	18.5	3.8	9.9	25.8	60.5	0.38
RM289	19.5	3.4	9.7	26.0	60.9	0.35
RM290	20.5	3.7	10.7	25.9	59.8	0.34

Onkaparinga Trig

Sample	Height (m)	Crse Sand (%)	Fine Sand (%)	Silt (%)	Clay (%)	Cs/Fs
RM144	0	1.0	41.0	8.0	50.0	0.02
RM291	0.8	16.9	67.2	4.9	11.0	0.25
RM292	1	1.3	86.8	4.4	7.5	0.01
RM293	1.4	3.0	60.0	10.9	26.1	0.05
RM294	1.6	1.3	18.3	31.7	48.6	0.07
RM295	1.8				39.0	
RM296	2				30.0	
RM298	2.3	66.7	18.1	5.2	10.0	3.68
RM299	2.45				32.0	
RM300	2.65	71.0	4.9	6.7	17.4	14.58

Sample	Height (m)	Crse Sand (%)	Fine Sand (%)	Silt (%)	Clay (%)	Cs/Fs
RM301	2.9				38.0	
RM302	3.15				29.0	
RM303	3.8				34.5	
RM304	4.3				37.0	
RM305	4.8				36.0	
RM306	5.3	1.1	5.2	54.0	39.7	0.22
RM307	5.8	0.6	7.9	53.5	38.0	0.08
RM308	6.7	0.2	1.5	27.7	70.5	0.16
RM309	7.2	0.2	1.4	28.4	70.1	0.14
RM310	7.7	0.5	2.5	29.3	67.8	0.19
RM311	8.2	0.5	2.7	24.3	72.5	0.17
RM312	8.7	0.9	4.3	24.6	70.2	0.21
RM313	9.2	1.4	5.9	27.0	65.7	0.24
RM314	9.7	1.4	5.4	25.7	67.5	0.26
RM315	10.2	1.8	6.2	27.4	64.6	0.29
RM316	10.5	0.9	2.8	25.3	71.0	0.32
RM318	11	1.2	3.5	26.1	69.3	0.34
RM320	12	1.9	4.1	18.6	75.4	0.45
RM322	12.5	2.0	5.1	26.6	66.3	0.40
RM323	13	1.5	4.9	26.0	67.7	0.30
RM324	13.5	3.0	6.4	29.8	60.8	0.47
RM325	14	2.1	5.0	26.0	66.9	0.42
RM326	14.3	6.1	26.1	30.9	37.0	0.23
RM327	14.8	25.4	50.4	7.4	16.8	0.50
RM328	15.3	17.1	31.2	15.5	36.2	0.55
RM329	15.8	23.1	27.7	13.2	36.1	0.83
RM330	16.3	20.9	25.6	16.2	37.4	0.81
RM331	16.8	21.6	25.6	16.0	36.8	0.84
RM332	17.3	14.6	21.3	18.1	46.1	0.69
RM333	17.8	10.5	18.0	21.8	49.7	0.58
RM334	18.3	8.0	13.3	24.1	54.6	0.60
RM335	18.8	11.3	30.0	20.2	38.6	0.38
RM336	19.3	12.5	34.9	16.0	36.6	0.36
RM337	19.8	11.8	30.6	17.5	40.1	0.39

Hallett Cove

Sample	Height (m)	Crse Sand (%)	Fine Sand (%)	Silt (%)	Clay (%)	Cs/Fs
RM338	0	25.8	30.0	11.6	32.6	0.86
RM339	0.5	33.3	21.0	5.2	40.5	1.58
RM340	1	12.3	5.3	30.0	52.5	2.34
RM341	1.5	7.2	4.0	24.7	64.2	1.79
RM342	2	4.0	4.3	22.6	69.0	0.93
RM343	2.5	5.3	6.5	24.3	64.0	0.81
RM344	3	7.8	8.1	24.1	60.0	0.96
RM345	3.5	7.1	9.7	29.9	53.3	0.74

Sample	Height (m)	Crse Sand (%)	Fine Sand (%)	Silt (%)	Clay (%)	Cs/Fs
RM346	4	16.8	19.2	14.3	49.7	0.88
RM347	4.5	15.7	19.4	14.5	50.3	0.81
RM348	5	22.0	24.7	21.2	32.0	0.89
RM350	5.5				21.0	
RM351	6				16.0	
RM352	6.5				18.0	
RM354	7				23.0	
RM355	7.5				17.0	
RM356	8	19.2	32.0	18.8	30.0	0.60
RM357	8.5	17.6	29.6	20.8	32.0	0.60
RM358	9	18.7	28.7	12.8	39.8	0.65
RM359	9.5	15.3	28.3	13.2	43.2	0.54
RM360	10	14.7	27.8	13.4	44.1	0.53
RM361	10.5	13.3	25.2	14.0	47.5	0.53
RM362	11	15.8	29.5	12.9	41.8	0.54
RM363	11.5	19.2	32.5	12.1	36.2	0.59
RM364	12	13.0	21.2	14.6	51.2	0.61
RM365	12.5	2.6	7.0	22.6	67.7	0.38
RM366	13	6.4	11.7	19.3	62.5	0.55
RM367	13.5	8.6	14.8	20.7	56.0	0.58
RM368	14	8.3	14.8	20.7	56.2	0.56
RM369	14.5	7.5	13.3	22.2	57.0	0.57
RM370	15	5.6	10.3	25.8	58.3	0.54
RM371	15.5	5.3	9.6	26.4	58.7	0.55
RM372	16	6.4	12.4	25.2	56.0	0.52
RM373	16.5	7.6	13.7	24.4	54.3	0.56
RM374	17	5.0	9.9	25.5	59.6	0.51
RM375	17.5	4.0	7.3	28.2	60.5	0.54
RM376	18	4.1	7.7	27.8	60.4	0.54
RM377	18.5	5.1	10.3	24.9	59.8	0.49
RM378	19	8.2	19.5	19.2	53.1	0.42

Port Willunga

Sample	Height (m)	Crse Sand (%)	Fine Sand (%)	Silt (%)	Clay (%)	Cs/Fs
RM73	1.2	4	28	8	60	0.14
RM75	0.5	17	26	9	48	0.65
RM76	0.3	5	58	1	36	0.09
RM77	1.6	4	32	3	61	0.13
RM78	3.7	7	12	11	70	0.58
RM79	6.6	17	30	10	43	0.57
RM80	7.2	15	44	13	28	0.34
RM81	8.4	27	35	9	29	0.77
RM82	8.6	9	29	9	53	0.31
RM83	10.6	5	16	7	72	0.31
RM84	13	7	26	7	60	0.27
RM85	13.2	7	28	6	59	0.25

Sellicks Beach

Sample	Height (m)	Gravel (%)	Crse Sand (%)	Fine Sand (%)	Silt (%)	Clay (%)	Cs/Fs
RM98	0.1	2	2	7	6	83	0.33
RM99	0.4	trace	13	36	16	31	0.36
RM100	0.65	1	32	30	7	27	1.07
RM101	1.05	5	52	22	1	19	2.36
RM102	2		trace	5	5	88	0.08
RM103	2.2		trace	6	10	82	0.05
RM104	2.6		3	37	18	43	0.08
RM105	2.9		18	37	9	32	0.49
RM106	3	10	5	21	23	42	0.24

Aldinga Beach

Sample	Height (m)	Crse Sand (%)	Fine Sand (%)	Silt (%)	Clay (%)	Cs/Fs
RM86		36	23	3	38	1.57
RM88S		41	37	5	16	1.11
RM88M		32	28	4	37	1.11
RM89		56	29	2	14	1.93
RM90		36	35	1	29	1.03
RM92		22	31	2	43	0.70
RM93		14	36	4	45	0.38
RM96		34	37	trace	29	0.93
RM97		31	51	trace	17	0.60

Robinson Point

Sample	Stratigr Unit	Crse Sand (%)	Fine Sand (%)	Silt (%)	Clay (%)	Cs/Fs
RM136	RPF	41	48	3	9	0.85
RM137P	RPF	2	79	3	15	0.03
RM137Y	RPF	6	81	2	11	0.08
RM133	RPF	6	54	4	33	0.11
RM134	RPF	35	50	trace	15	0.70
RM128	NCM	2	18	10	67	0.12
RM129	SPSM	35	46	3	16	0.74
RM130	SPSM	19	34	5	40	0.57

Onkaparinga River Mouth

Sample	Stratigr Unit	Crse Sand (%)	Fine Sand (%)	Silt (%)	Clay (%)	Cs/Fs
RM192	RPF	13	54	6	26	0.24
RM190	NCM	2	15	9	73	0.16
RM189	SPSM	2	50	17	31	0.03
RM187	SPSM	20	50	4	23	0.40

Sample	Stratigr Unit	Crse Sand (%)	Fine Sand (%)	Silt (%)	Clay (%)	Cs/Fs
RM186	SPSM	13	34	6	46	0.37
RM185	SPSM	11	35	8	45	0.32
RM184	SPSM	9	32	9	49	0.28

Railway Cutting, O'Sullivan Beach Road

Sample	Stratigr Unit	Crse Sand (%)	Fine Sand (%)	Silt (%)	Clay (%)	Cs/Fs
RM113	RPF	4	21	11	58	0.17
RM114	RPF	68	23	trace	8	2.99
RM115	RPF	45	41	1	12	1.08
RM116	RPF	53	35	2	9	1.52
RM117	RPF	34	34	2	28	0.99
RM118	NF	24	28	5	41	0.86

Port Moorowie

Sample	Stratigr Unit	Crse Sand (%)	Fine Sand (%)	Silt (%)	Clay (%)	Cs/Fs
A. Boat Ramp Site						
RM62	Lower clay	11	28	15	47	0.41
RM63	Mottled clay	6	16	10	70	0.35
RM65	Upper clay	5	26	14	55	0.21
B. 1km East of Boat Ramp						
RM163	Lower sand	10	65	3	21	0.16
RM160	Centre clays	4	27	9	61	0.16
RM164	Upper clay	11	28	8	50	0.40

APPENDIX 3A. MINERALOGY OF FINE SAND FRACTIONS USING X-RAY DIFFRACTION

LOCALITY	STRATIGRAPHIC UNIT	MINERALOGY
Sellicks Beach		
RM99	Robinson Point Formation	Quartz dominant, minor K-felds, plag
RM100	Robinson Point Formation	Quartz dominant, minor K-felds, plag
RM104	Robinson Point Formation	Quartz dominant, minor K-felds, plag, calcite
RM105	Robinson Point Formation	Quartz dominant, minor K-felds, trace plag
Aldinga Beach		
RM90	Ngaltinga Formation	Quartz dominant, minor K-felds
Port Willunga		
RM73	Neva Clay Member	Quartz dominant, minor K-felds, plag
RM75	Neva Clay Member	Quartz dominant, minor K-felds, plag, calcite, trace dolomite
RM76	Neva Clay Member	Quartz dominant, minor K-felds, trace plag
RM77	Neva Clay Member	Quartz dominant, minor K-felds
RM78	Neva Clay Member	Quartz dominant, minor K-felds, plag
RM79	Neva Clay Member	Quartz dominant, minor K-felds, plag
RM80	Neva Clay Member	Quartz dominant, minor K-felds, plag
RM81	Snapper Point Sand Member	Quartz dominant, minor K-felds, plag
RM82	Snapper Point Sand Member	Quartz dominant, minor K-felds, plag, trace hematite
RM83	Snapper Point Sand Member	Quartz dominant, minor K-felds, plag, trace dolomite
RM84	Snapper Point Sand Member	Quartz dominant, minor K-felds, trace plag
RM85	Snapper Point Sand Member	Quartz dominant, minor K-felds, plag
Ochre Point		
RM39	Robinson Point Formation	Quartz dominant, minor K-felds, trace plag
Seaford		
RM128	Neva Clay Member	Quartz dominant, minor K-felds, plag
RM129	Snapper Point Sand Member	Quartz dominant, minor K-felds, plag
RM130	Snapper Point Sand Member	Quartz dominant, minor K-felds, plag
Hallett Cove		
RM33	Ngaltinga Formation	Quartz dominant, minor K-felds, plag
O'Sullivan Beach Road Railway Cutting		
RM113	Robinson Point Formation	Quartz dominant, minor K-felds, plag
RM114	Robinson Point Formation	Quartz dominant, minor K-felds, trace plag
RM118	Ngaltinga Formation	Quartz dominant, minor K-felds, plag, trace hematite

APPENDIX 3B. MINERALOGY OF COARSE SAND FRACTIONS FROM ONKAPARINGA TRIG.

Sample	Quartz	Feldspar	Tourmaline	Rutile	Muscovite	Iron Oxides	Epidote	Barite	Rock Fragments	Staurolite
RM144	P	R								
RM291	P	F	R	R					T	T
RM292	P	F	T							
RM293	P	R								
RM294	P		T	T						
RM295	P		R		F					
RM296	P									
RM298	P	F	F			R				
RM299	P		F		R					
RM300	P	R								R
RM301	P		R		F	R				
RM302	P		F		F	R				
RM303	P		F		F					
RM304	P		F		F					
RM305	P	F	R		O	R				
RM306	P				T	R				
RM307	P		T							
RM308	P	R	T							
RM309	P	R				R				
RM310	P	R				F				
RM311	P	R				F				
RM312	P	R				R				
RM313	P	R								
RM314	P					F				
RM315	P	R	T			R	R	T	T	
RM316	P		R			R				
RM318	P									
RM320	P	R	T	T		T				
RM322	P	T	T			T				
RM323	P									
RM324	P	R		T		T				
RM325	P	R					T		T	T
RM326	P		R	T	F	R				
RM327	P	R	F	R	O	F		T	R	R
RM328	P	R	R		F	F			R	
RM329	P	R	F			O				R
RM330	P	F	F	T		O			R	R
RM331	P	R	F	T		O			R	R
RM333	P	F	F	T		F			R	R
RM334	P	F	R	T		R			R	
RM335	P	R	F			F			R	R
RM336	P	R	R			F			R	T
RM337	P	R	R			F				

NOTE: P= >50%, A= 20-50%, C= 10-20%, S= 3-10%, O= 1-3%, F= 0.1-1%, R= 2-10 grains, T= 1 grain

Sample	Ilmenite	Biotite	Sillimanite	Garnet	Leucoxene	Corundum	Pyroxene	Anatase	Amphibole	Pyrite Pseudomorph
RM144										
RM291										
RM292										
RM293										
RM294										
RM295										
RM296										
RM298										
RM299										
RM300										
RM301										
RM302										
RM303										
RM304										
RM305										
RM306										
RM307										
RM308										
RM309										
RM310										
RM311										
RM312										
RM313										
RM314										
RM315										
RM316										
RM318										
RM320										
RM322										
RM323										
RM324				T						
RM325										
RM326	R	R								
RM327	T	R	R							
RM328	R	R				T				
RM329						T	T			
RM330										
RM331				T				T	T	T
RM333										
RM334	T			T						
RM335	R				R					
RM336			T							
RM337			T							

APPENDIX 3C: MINERALOGY OF HEAVY MINERAL CONCENTRATE FOR EIGHT SAMPLES FROM MASLIN BAY AND ONKAPARINGA TRIG

Sample	RM259	RM262	RM265	RM304	RM312	RM323	RM326	RM334
Location	MB	MB	MB	OT	OT	OT	OT	OT
Iron Oxides	F	A	O	O	P	C	A	A
Tourmaline	A	A	A	F	F	A	S	A
Sillimanite	A	S	A			F	O	
Staurolite	S	O	O	O	T	F	S	O
Garnet						A	O	S
Rutile	R	R	R	R	T	F	F	F
Mica				A			A	
Ilmenite					T	O	S	S
Kyanite		F	S	R			R	R
Barite				A	F	F		
Zircon			R			T	R	
Amphibole							T	R
Spinel								T
Corundum								R
Andalusite	R	T						
Rock Fragments		C	F	F				
Leucoxene			F					

NOTE: P= >50%, A= 20-50%, C= 10-20%, S= 3-10%, O= 1-3%, F= 0.1-1%, R= 2-10 grains, T= 1 grain

APPENDIX 4. CLAY MINERAL DATA

Snapper Point

Sample	Height (m)	CEC (mequiv %)	K2O (%)	Measured K/I	<2μm (%)	Kaolin (%)	Halloysite (%)	Illite (%)
RM215	13.1	53	2.91	0.70	49.2	20-30		40-50
RM216	12.6	51	2.94	0.95	45.0	30-40		30-40
RM217	12.35	52	2.78	0.96	39.3	30-40		30-40
RM218	12.1	48	2.34	0.86	25.2	30-40		30-40
RM219	11.6	57	2.04	1.20	37.9	30-40		20-30
RM220	11.1	44	2.02	2.00	39.7	40-50		20-30
RM221	10.6	48	2.26	1.90	18.8	40-50		20-30
RM222	10.1	40	1.96	2.27	19.5	50-60		20-30
RM223	9.6	37	1.61	2.25	24.8	30-40	20-30	20-30
RM224	9.1	54	2.86	0.33	67.7	10-20		50-60
RM225	8.6	54	3.11	0.33	72.5	10-20		50-60
RM226	8.1	53	3.00	0.33	73.5	10-20		50-60
RM227	7.6	57	2.93	0.32	75.7	10-20		50-60
RM228A	7.1	55	3.12	0.42	80.0	15-25		40-50
RM229	6.6	56	3.05	0.53	77.3	20-30		40-50
RM231	5.6	54	2.96	0.50	75.2	20-30		40-50
RM232	5.1	56	2.92	0.50	72.1	20-30		40-50
RM233	4.6	56	2.96	0.55	75.6	20-30		40-50
RM234	4.1	54	3.07	0.49	76.5	20-30		40-50
RM235	3.6	54	3.12	0.48	67.7	20-30		40-50
RM236	3.1	55	2.84	0.49	76.8	20-30		40-50
RM237	2.6	51	2.78	0.53	75.3	20-30		40-50
RM238	2.1	50	2.86	0.51	75.2	20-30		40-50
RM239	1.6	52	2.92	0.51	75.2	20-30		40-50
RM240	1.1	54	3.03	0.58	77.2	20-30		40-50
RM241	0.7	56	3.00	0.54	77.1	20-30		40-50
RM242	0.4	51	3.00	0.54	79.0	20-30		40-50
RM245	0	51	3.22	0.50	72.8	20-30		40-50

Maslin Bay

Sample	Height (m)	CEC (mequiv %)	K2O (%)	Measured K/I	<2μm (%)	Kaolin (%)	Halloysite (%)	Illite (%)
RM248	0.35	69	1.40	0.60	28.7	15-25		30-40
RM249	0.7	72	1.47	0.55	40.0	10-20		30-40
RM250	1	60	2.30	1.12	20.0	30-40		20-30
RM251	1.4	38	1.00	1.15	48.9	40-50		30-40
RM252	1.8	17	0.15		4.0	35-45	55-65	0
RM253	1.8	20	1.18	0.93	15.5	30-40	30-40	25-35
RM254	2.3	45	1.77	1.38	50.9	40-50		30-40
RM255	2.7	19	1.05	1.35	30.0	30-40	30-40	20-30
RM256	3	22	1.08	1.33	25.0	30-40	30-40	25-35
RM257	3.5	18	1.02	1.74	29.0	40-50	25-35	20-30
RM258	4	40	1.40	1.75	26.0	40-50	0-10	20-30
RM259	4.5	35	1.70	2.50	28.9	50-60	Tr	20-30
RM260	5	31	2.36	2.40	27.0	55-65	Tr	20-30
RM261	5.5	36	2.08	1.85	19.0	50-60		20-30

Sample	Smectite (%)	Interstratified (%)	Expandible layers (%)	Collapse on heating?	Peak width Kaolin (001)	Peak width Illite (001)	Other minerals
RM215		30-40	30	No	0.4	0.9	Q,F
RM216		30-40	30	No	0.45	1	Q
RM217		30-40	15	No	0.5	1	Q,F,Go
RM218		20-30	20	No	0.45	0.9	Q
RM219		30-40	40	No	0.5	0.9	Q,F
RM220		20-30	30-40	No	0.5	1.1	Q
RM221		20-30	20-30	No	0.5	1	Q,F
RM222		20-30	15	No	0.55	1	Q,F
RM223		15-25	20	Yes	1.3	1.8	Q
RM224		25-35	20	No	0.5	1	Q
RM225		20-30	20	No	0.45	1	Q,Go
RM226		20-30	20-30	No	0.45	1	Q
RM227		30-40	20	No	0.45	1	Q
RM228A		30-40	20	No	0.4	1	Q
RM229		30-40	20	No	0.4	0.9	Q,Go,Do
RM231		25-35	20-30	No	0.4	0.9	Q,Go,Do
RM232		30-40	20	No	0.4	0.85	Q
RM233		30-40	20	No	0.4	0.9	Q,Go
RM234		25-35	20	No	0.4	0.9	Q
RM235		30-40	20-30	No	0.45	0.85	Q
RM236		30-40	20	No	0.4	0.85	Q
RM237		20-30	20	No	0.4	0.85	Q,Go
RM238		20-30	20-30	No	0.4	0.9	Q
RM239		20-30	20	No	0.4	0.75	Q
RM240		30-40	20	No	0.45	0.9	Q
RM241		30-40	20	No	0.4	0.75	Q
RM242		20-30	20	No	0.45	0.7	Q
RM245		20-30	20-30	No	0.45	0.9	Q

Maslin Bay

Sample	Smectite (%)	Interstratified (%)	Expandible layers (%)	Collapse on heating?	Peak width Kaolin (001)	Peak width Illite (001)	Other minerals
RM248	40-50			Yes	0.4		Q,Go
RM249	45-55			Yes	0.45		Q,Go
RM250	35-45			Yes	0.6		Q,F,Mn
RM251		15-25	40	Yes	0.5	0.7	
RM252		0					
RM253		0					He
RM254		20-30	20	Yes	0.55	0.9	He
RM255		0					Q
RM256		0					
RM257		0					
RM258		20-30	10-20	Yes	0.6	0.9	Q
RM259		10-20	10-20	Yes	0.6	1	Q,F
RM260		10-20	10	Yes	0.5	0.85	Q,F
RM261		10-20	10	Yes	0.55	1	Q,F

Sample	Height (m)	CEC (mequiv %)	K2O (%)	Measured K/I	<2µm (%)	Kaolin (%)	Halloysite (%)	Illite (%)
RM262	6	45	2.77	0.68	46.3	30-40		40-50
RM263	6.5	48	2.72	0.83	35.6	30-40		30-40
RM265	7	30	1.64	0.92	14.6	40-50		40-50
RM266	7.4	26	2.31	0.50	11.2	20-30		65-75
RM267	8	35	2.65	0.70	22.8	30-40		50-60
RM268	8.5	35	2.23	0.83	25.3	30-40		40-50
RM269	9	40	2.15	1.10	27.0	40-50		30-40
RM270	9.5	38	2.00	1.18	24.0	40-50		30-40
RM271	10	33	2.33	1.36	19.8	45-55		30-40
RM272	10.5	35	1.84	1.64	26.0	50-60		30-40
RM273	11	36	1.90	1.84	27.0	50-60		20-30
RM274	11.5	42	1.47	2.35	38.0	50-60		20-30
RM275	11.9	45	2.10	1.35	57.5	40-50		30-40
RM276	12.4	34	1.61	1.75	24.3	50-60		25-35
RM277	12.9	28	1.45	1.77	21.0	50-60		30-40
RM278	13.5	55	2.30	0.53	65.3	20-30		40-50
RM279	14	57	2.56	0.49	70.3	20-30		40-50
RM280	14.5	59	2.52	0.55	68.9	20-30		40-50
RM281	15	60	2.44	0.65	68.8	20-30		30-40
RM282	15.5	60	2.61	0.60	68.6	20-30		35-45
RM283	16	61	2.70	0.67	66.0	20-30		30-40
RM284	16.5	58	2.75	0.55	66.3	20-30		40-50
RM285	17	53	2.64	0.58	64.0	20-30		40-50
RM286	17.5	54	2.81	0.50	60.5	20-30		40-50
RM287	18	55	3.39	0.40	60.5	15-25		40-50
RM288	18.5	57	3.30	0.30	60.5	10-20		50-60
RM289	19.5	55	3.10	0.25	60.9	10-20		50-60
RM290	20.5	51	3.19	0.24	59.8	10-20		60-70

Onkaparinga Trig

Sample	Height (m)	CEC (mequiv %)	K2O (%)	Measured K/I	<2µm (%)	Kaolin (%)	Halloysite (%)	Illite (%)
RM144	0	50	2.18	0.46	50.0	20-30		40-50
RM291	0.8	20	0.50	1.70	11.0	30-40	45-55	10-20
RM292	1	19	0.40	1.80	7.5	30-40	45-55	10-20
RM293	1.4	50	2.34	1.30	26.1	35-45		25-35
RM294	1.6	36	1.72	1.75	48.6	50-60		20-30
RM295	1.8	38	1.55	1.35	39.0	40-50		30-40
RM296	2	36	1.56	1.25	30.0	40-50		30-40
RM298	2.3	25	1.20	1.58	10.0	50-60		30-40
RM299	2.45	40	1.41	1.90	32.0	45-55		20-30
RM300	2.65	30	1.15	1.75	17.4	50-60		30-40
RM301	2.9	38	1.71	1.81	38.0	45-55		20-30
RM302	3.15	35	2.15	1.60	29.0	45-55		30-40
RM303	3.8	40	1.84	1.71	34.5	40-50		20-30
RM304	4.3	48	1.90	2.06	37.0	40-50		20-30
RM305	4.8	47	1.85	1.90	36.0	40-50		20-30
RM306	5.3	46	1.77	2.04	39.7	40-50		20-30
RM307	5.8	48	1.64	1.88	38.0	40-50		20-30
RM308	6.7	45	2.56	0.95	70.5	30-40		30-40

Sample	Smectite (%)	Interstratified (%)	Expandible layers (%)	Collapse on heating?	Peak width Kaolin (001)	Peak width Illite (001)	Other minerals
RM262		20-30	50	No	0.45	0.6	Q,F
RM263		20-30	50	Yes	0.45	0.45	Q,F,Go
RM265		5-15	20	Yes	0.4		Q
RM266		0-10					Q,F
RM267		10-20	20	Yes	0.45	0.5	Q,F
RM268		10-20	20-30	Yes	0.4	0.4	Q,F
RM269		15-25	30	Yes	0.4	0.35	Q,F
RM270		10-20	10-20	Yes	0.5	0.5	Q,F
RM271		10-20	20-25	Yes	0.45	0.5	Q,F
RM272		10-20	30-40	Yes	0.4	0.4	Q,F
RM273		10-20	30	Yes	0.5	0.6	Q,F
RM274		20-30	30-40	Yes	0.5	0.6	Q,F
RM275		20-30	30-40	No	0.5	0.4	Q,F
RM276		10-20	10-20	Yes	0.6	0.45	Q,F
RM277		10-20	10-20	Yes	0.65	0.7	Q,F
RM278		30-40	30	No	0.4	0.7	Q
RM279		30-40	30-40	No	0.4	0.8	Q
RM280		30-40	30-40	No	0.4	0.75	Q
RM281		30-40	20-30	No	0.4	0.7	Q
RM282		30-40	30	No	0.4	0.8	Q
RM283		30-40	30	No	0.4	1	Q,F
RM284		30-40	30	No	0.4	1	Q
RM285		20-30	20-30	No	0.4	1.2	Q
RM286		25-35	30	No	0.4	0.9	Q
RM287		30-40	25	No	0.4	1	Q
RM288		25-35	20	No	0.35	1.2	Q
RM289		20-30	20	No	0.4	1	Q,Do,Ca
RM290		20-30	20	No	0.4	1	Q,Ca,Do

Onkaparinga Trig

Sample	Smectite (%)	Interstratified (%)	Expandible layers (%)	Collapse on heating?	Peak width Kaolin (001)	Peak width Illite (001)	Other minerals
RM144		30-40	40-50	Yes	0.45	0.8	Q
RM291		0-10					Q
RM292		0-10					
RM293		25-35	20-30	Yes	0.4	0.75	Q
RM294	15-25			No	0.4	0.55	Q,Go
RM295	20-30			Yes	0.4	0.4	Q,Go,F
RM296	15-25			Yes	0.4		Q,Go
RM298	0-10				0.6		Q,Go
RM299	20-30			Yes	0.4	0.5	Q,Go,F
RM300	10-20			Yes	0.5		Q,Go
RM301	20-30			Yes	0.4	0.45	Go,Q
RM302	10-20			Yes	0.4	0.4	Q,Go
RM303	20-30			Yes	0.4	0.35	Q,Go
RM304	25-35			Yes	0.4	0.35	Q,Go
RM305	20-30			Yes	0.4	0.4	Q,Go,F
RM306	25-35			Yes	0.4	0.35	Q,Go,F
RM307	25-35			Yes	0.4	0.35	Q,Go,F
RM308		20-30	30-40	No	0.4	0.55	Q

Sample	Height (m)	CEC (mequiv %)	K2O (%)	Measured K/I	<2μm (%)	Kaolin (%)	Halloysite (%)	Illite (%)
RM309	7.2	49	2.35	0.97	70.1	30-40		30-40
RM310	7.7	47	2.48	0.85	67.8	30-40		30-40
RM311	8.2	50	2.60	0.82	72.5	30-40		30-40
RM312	8.7	49	2.42	0.81	70.2	30-40		35-45
RM313	9.2	51	2.42	0.75	65.7	25-35		35-45
RM314	9.7	49	2.51	0.83	67.5	30-40		30-40
RM315	10.2	52	2.68	0.90	64.6	30-40		30-40
RM316	10.5	48	3.30	0.31	71.0	10-20		50-60
RM318	11	49	3.24	0.34	69.3	15-25		50-60
RM320	12	51	3.20	0.32	75.4	10-20		50-60
RM322	12.5	49	3.24	0.30	66.3	10-20		50-60
RM323	13	47	3.47	0.35	67.7	15-25		50-60
RM324	13.5	46	3.30	0.44	60.8	20-30		50-60
RM325	14	47	3.24	0.34	66.9	15-25		50-60
RM326	14.3	35	2.10	1.79	37.0	50-60		25-35
RM327	14.8	27	2.38	1.36	16.8	50-60		30-40
RM328	15.3	34	2.90	1.00	36.2	40-50		40-50
RM329	15.8	50	2.43	1.17	36.1	30-40		30-40
RM330	16.3	47	2.66	1.40	37.4	40-50		25-35
RM331	16.8	51	2.80	1.22	36.8	30-40		30-40
RM332	17.3	55	2.89	0.91	46.1	30-40		30-40
RM333	17.8	57	3.20	0.79	49.7	20-30		30-40
RM334	18.3	52	3.12	0.63	54.6	20-30		40-50
RM335	18.8	57	2.88	0.75	38.6	20-30		30-40
RM336	19.3	57	2.67	0.64	36.6	20-30		35-45
RM337	19.8	54	2.82	0.50	40.1	20-30		40-50

Hallett Cove

Sample	Height (m)	CEC (mequiv %)	K2O (%)	Measured K/I	<2μm (%)	Kaolin (%)	Halloysite (%)	Illite (%)
RM338	0	64	2.70	0.67	32.6	20-30		30-40
RM339	0.5	62	2.44	0.78	40.5	20-30		30-40
RM340	1	48	2.51	0.93	52.5	30-40		30-40
RM341	1.5	47	2.48	0.96	64.2	30-40		30-40
RM342	2	46	2.44	0.96	69.0	30-40		30-40
RM343	2.5	43	2.49	1.04	64.0	30-40		30-40
RM344	3	42	2.36	1.36	60.0	40-50		30-40
RM345	3.5	40	2.31	1.39	53.3	40-50		30-40
RM346	4	41	2.52	1.36	49.7	40-50		30-40
RM347	4.5	41	2.62	1.10	50.3	35-45		30-40
RM348	5	37	2.45	1.25	32.0	40-50		30-40
RM350	5.5	30	2.12	1.15	21.0	30-40		50-60
RM351	6	30	2.12	1.11	16.0	40-50		40-50
RM352	6.5	29	1.97	1.06	18.0	40-50		40-50
RM354	7	26	1.46	1.50	23.0	50-60		30-40
RM355	7.5	27	1.64	1.67	17.0	50-60		30-40
RM356	8	45	2.28	1.24	30.0	40-50		30-40
RM357	8.5	50	2.04	1.46	32.0	40-50		20-30
RM358	9	48	2.14	1.59	39.8	40-50		20-30
RM359	9.5	47	2.17	1.85	43.2	40-50		20-30

Sample	Smectite (%)	Interstratified (%)	Expandible layers (%)	Collapse on heating?	Peak width Kaolin (001)	Peak width Illite (001)	Other minerals
RM309		20-30	30-40	No	0.4	0.6	Q
RM310		20-30	20-30	No	0.45	0.7	Q
RM311		20-30	30	No	0.45	0.7	Q
RM312		20-30	30	No	0.45	0.55	Q
RM313		25-35	30	No	0.4	0.75	Q
RM314		20-30	30	No	0.4	0.7	Q
RM315		30-40	20-30	No	0.45	0.75	Q
RM316		20-30	20-30	No	0.45	1.2	Q,Do
RM318		20-30	20-30	No	0.45	1.2	Q
RM320		20-30	20-30	No	0.45	1.1	Q
RM322		20-30	20	No	0.4	0.9	Q
RM323		20-30	20	No	0.4	1	Q
RM324		20-30	20	No	0.45	0.8	Q
RM325		20-30	20	No	0.45	0.9	Q
RM326		10-20	20	No	0.45	0.6	Q
RM327		5-15	30		0.4	0.45	Q
RM328		10-20	30-40	No	0.4	0.4	Q
RM329		25-35	30-40	No	0.4	0.6	Q
RM330		20-30	30	No	0.45	0.8	Q
RM331		30-40	30-40	No	0.45	0.85	Q
RM332		30-40	30	No	0.4	0.8	Q
RM333		30-40	30	No	0.4	0.8	Q,Ca
RM334		25-35	30	No	0.45	0.85	Q,Ca
RM335		30-40	30	No	0.4	0.8	Q,Ca,Do
RM336		30-40	30	No	0.5	0.8	Q,Ca,Do
RM337		25-35	20-30	No			Q,Ca,Do

Hallett Cove

Sample	Smectite (%)	Interstratified (%)	Expandible layers (%)	Collapse on heating?	Peak width Kaolin (001)	Peak width Illite (001)	Other minerals
RM338		40-50	40-50	Yes	0.5	0.9	Q
RM339		35-45	20-30	Yes	0.5	0.8	Q
RM340		20-30	30-40	Yes	0.5	0.6	Q,F
RM341		20-30	30	Yes	0.5	0.5	Q
RM342		20-30	20-30	Yes	0.5	0.6	Q
RM343		20-30	30	Yes	0.45	0.45	Q,F
RM344		20-30	20-30	Yes	0.65	0.75	Q
RM345		20-30	20-30	Yes	0.6	0.65	Q
RM346		20-30	20	Yes	0.5	0.45	Q,F
RM347		20-30	30-40	Yes	0.45	0.4	Q,F
RM348		10-20	20	Yes	0.55	0.4	Q,F
RM350		5-15	20	Yes	0.5	0.4	Q,F
RM351		5-15	20	Yes	0.5	0.4	Q
RM352		5-15	20	Yes	0.5	0.4	Q,F
RM354		0-10					Q
RM355		5-15					Q
RM356		20-30	40-50	Yes	0.45	0.5	Q,F
RM357		30-40	40	Yes	0.45	0.5	Q,F
RM358		20-30	30-40	Yes	0.4	0.45	Q,F
RM359		20-30	30-40	Yes	0.45	0.45	Q,F

Sample	Height (m)	CEC (mequiv %)	K2O (%)	Measured K/I	<2μm (%)	Kaolin (%)	Halloysite (%)	Illite (%)
RM360	10	45	2.25	2.25	44.1	45-55		20-30
RM361	10.5	50	2.30	1.79	47.5	40-50		20-30
RM362	11	46	2.18	1.97	41.8	40-50		20-30
RM363	11.5	47	2.19	1.90	36.2	40-50		20-30
RM364	12	46	2.02	1.46	51.2	40-50		20-30
RM365	12.5	48	2.60	0.91	67.7	30-40		30-40
RM366	13	48	2.82	0.61	62.5	20-30		40-50
RM367	13.5	49	2.70	0.60	56.0	20-30		40-50
RM368	14	52	2.44	0.81	56.2	30-40		30-40
RM369	14.5	55	2.60	0.54	57.0	20-30		40-50
RM370	15	53	2.65	0.57	58.3	20-30		40-50
RM371	15.5	53	2.57	0.58	58.7	20-30		40-50
RM372	16	52	2.77	0.58	56.0	20-30		40-50
RM373	16.5	49	3.01	0.53	54.3	20-30		40-50
RM374	17	47	2.75	0.67	59.6	25-35		40-50
RM375	17.5	48	3.24	0.41	60.5	20-30		50-60
RM376	18	49	3.14	0.41	60.4	20-30		50-60
RM377	18.5	50	3.28	0.40	59.8	20-30		50-60
RM378	19	52	3.46	0.27	53.1	10-20		50-60

NOTE: Q = Quartz, F = Feldspar, Do = Dolomite, Ca = Calcite, Go = Goethite, He = Hematite
Mn = Manganese Oxide

Sample	Smectite (%)	Interstratified (%)	Expandible layers (%)	Collapse on heating?	Peak width Kaolin (001)	Peak width Illite (001)	Other minerals
RM360		20-30	30	Yes	0.45	0.45	Q,F
RM361		30-40	40-50	No	0.45	0.6	Q,F
RM362		20-30	20-30	Yes	0.45	0.45	Q,F
RM363		20-30	20-30	Yes	0.45	0.45	Q,F
RM364		25-35	40-50	No	0.45	0.6	Q
RM365		20-30	40-50	No	0.45	0.6	Q
RM366		20-30	30	No	0.4	0.65	Q
RM367		20-30	30	No	0.4	0.7	Q
RM368		30-40	40-50	No	0.45	0.75	Q
RM369		30-40	30-40	No	0.45	0.85	Q
RM370		25-35	30	No	0.45	0.85	Q
RM371		30-40	30	No	0.4	0.85	Q
RM372		25-35	30-40	No	0.4	0.7	Q
RM373		20-30	30	No	0.4	0.85	Q
RM374		20-30	30	No	0.4	0.8	Q
RM375		20-30	30	No	0.4	0.85	Q
RM376		20-30	30	No	0.4	1	Q
RM377		20-30	30	No	0.4	0.9	Q
RM378		20-30	20	No	0.45	1.1	Q

APPENDIX 5. CLAY MINERAL DATA FOR SIZE FRACTIONATED SAMPLES

Sample	Location	Stratigraphic Unit	Size Fraction	Measured K/I	Kaolin (%)	Illite (%)	Smectite (%)
RM259	Maslin Bay	RPF	<20µm	1.63	50-60	30-40	
			<5µm	1.58	50-60	30-40	
			<2µm	1.50	40-50	30-40	
			<0.2µm	1.15	30-40	30-40	
RM262	Maslin Bay	RPF	<20µm	0.53	20-30	40-50	
			<5µm	0.56	20-30	40-50	
			<2µm	0.57	20-30	40-50	
			<0.2µm	0.92	20-30	20-30	45-55
RM265	Maslin Bay	RPF	<20µm	0.44	20-30	50-60	
			<5µm	0.44	20-30	50-60	
			<2µm	0.41	20-30	50-60	
			<0.2µm	0.27	10-20	50-60	
RM304	Onkaparinga Trig	RPF	<20µm	0.87	30-40	40-50	20-30
			<5µm	0.81	25-35	30-40	30-40
			<2µm	1.20	20-30	20-30	40-50
			<0.2µm	2.55	20-30	5-15	60-70
RM312	Onkaparinga Trig	NCM	<20µm	0.56	20-30	40-50	
			<5µm	0.45	20-30	50-60	
			<2µm	0.54	20-30	40-50	
			<0.2µm	0.32	10-20	40-50	
RM323	Onkaparinga Trig	NCM	<20µm	0.21	10-20	60-70	
			<5µm	0.20	10-20	60-70	
			<2µm	0.20	10-20	50-60	
			<0.2µm	0.14	5-15	50-60	
RM326	Onkaparinga Trig	SPSM	<20µm	0.91	35-45	40-50	
			<5µm	0.92	30-40	35-45	
			<2µm	1.23	40-50	30-40	
			<0.2µm	0.78	30-40	40-50	
RM334	Onkaparinga Trig	SPSM	<20µm	0.36	15-25	45-55	
			<5µm	0.40	15-25	45-55	
			<2µm	0.45	15-25	45-55	
			<0.2µm	0.22	10-20	50-60	

NOTE: Q = Quartz, F = Feldspar, H = Halloysite, A = Alunite, Go = Goethite
RPF = Robinson Point Formation
NCM = Neva Clay Member
SPSM = Snapper Point Sand Member

Sample	Interstratified (%)	Expandible layers (%)	Collapse on heating?	Peak width Kaolin (001)	Peak width Illite (001)	Other Minerals
RM259	10-20	20	Yes	0.5	0.55	Q,F,H
	10-20	20	Yes	0.55	0.55	Q,F,H
	15-25	20	Yes	0.5	0.65	Q,F,H,A
	25-35	30	Yes	0.75	0.85	Q
RM262	20-30	40	Yes	0.45	0.45	Q,F,H
	20-30	40	Yes	0.45	0.5	Q,F,H
	20-30	50	Yes	0.45	0.45	Q,F,H
			Yes	0.6	0.75	
RM265	10-20	20	Yes	0.4	0.45	Q,F,H
	10-20	20	Yes	0.4	0.5	Q,F,H
	20-30	40	Yes	0.45	0.55	Q,F,H
	25-35	40	Yes	0.55	0.8	
RM304			Yes	0.4	0.4	Q,F,Go
			Yes	0.4	0.4	Q,F,Go
			Yes	0.4	0.4	Q,F,Go
			Yes	0.65	0.6	Go
RM312	20-30	20	No	0.45	0.6	Q,F
	20-30	20	No	0.45	0.65	Q,F
	30-40	30	No	0.4	0.65	Q
	35-45	30	No	0.6	1.15	
RM323	20-30	25	No	0.4	0.75	Q,F
	20-30	25	No	0.4	0.7	Q,F
	25-35	25	No	0.4	0.75	Q,F
	35-45	25	No	0.5	0.9	Q
RM326	10-20	20	Yes	0.4	0.45	Q,F
	20-30	25	Yes	0.4	0.5	Q,F
	10-20	25	Yes	0.4	0.65	Q,F
	10-20	25	No	0.65	0.9	Q
RM334	25-35	30	No	0.4	0.7	Q,F
	25-35	30	No	0.4	0.8	Q,F
	25-35	30	No	0.4	0.8	Q,F
	30-40	30	No	0.6	1.15	Q

APPENDIX 6
DESCRIPTION OF THIN SECTIONS

RM34, Ochre Cove, Robinson Point Formation

Porous sandy sediment with sand-sized grains comprising up to 80% of sample and voids up to 20%.

Framework Grains

Quartz with very rare opaques and tourmaline. Size is generally between 0.2 and 0.4 mm with rare grains to 0.6 mm. Sample is well sorted with grains rounded to sub-rounded.

Matrix

Mostly red-orange iron oxides with rare grey-yellow clays. Forms coating around many grains with minor laminations observed. Iron oxides very rarely fill intergranular pores.

RM40, Ochre Point, Snapper Point Sand Member

Ferruginous, sandy sediment with sand-sized grains forming 70 to 80% of sample.

Framework Grains

Dominantly sub-rounded to rounded quartz grains with rare feldspar and tourmaline. Most grains are 0.3 to 0.5 mm in size with rare grains to 0.8 mm. Sample is well sorted with many grains showing corroded edges.

Matrix

Red iron oxides which coat framework grains and fill some intergranular space. Voids make up about 10% of sample. Iron oxides impregnate fine fractures in quartz grains where small crystallites up to 10 μm can be seen.

RM41, Ochre Point, Snapper Point Sand Member

Sandy, ferruginous sediment with sand-sized grains forming 70% of sample. About 10% of sample comprises voids with remainder being iron oxides.

Framework Grains

Dominantly quartz with some composite grains and very rare feldspar, tourmaline and opaques. Moderately well sorted with most grains between 0.2 and 0.4 mm in size and some grains up to 1 mm. Grains are rounded to sub-angular with many showing corroded edges. Some silt-sized quartz grains occur within ferruginous matrix and have angular shapes.

Matrix

Mostly dark red iron oxides which coat framework grains and fill some intergranular space. Iron oxides also impregnate small fractures within quartz grains. Several small patches of grey-yellow clay occur within ferruginous matrix which show development of tiny areas (up to 0.05 mm) where iron has replaced clays.

RM62-2, Port Moorowie, Quaternary sediments

Sandy clay which is mostly ferruginous. Sand-sized grains comprise 30 to 40% of sample with few voids.

Framework Grains

Mostly quartz grains from 0.1 to 0.3 mm in size with some grains to 0.5 mm. Occasional mica laths to 0.15 mm in size. Poor to moderate sorting with sub-angular grains which show etching and corrosion. Some silt-sized, angular quartz grains observed within clay-rich matrix.

Matrix

Dominantly red to black iron oxides which fills all intergranular space. On margins of ferruginous material there is some yellow-grey clay. Tiny patches of red iron oxide replace clays in some parts and often coalesce to larger patches up to 0.2 mm in size. Iron also impregnates elongate fractures within clay. Clay tends to show bi-directional extinction (bimasepic).

RM69, Seaford, Robinson Point Formation

Fine grained sediment with less than 1% of sand-sized grains in alunitic parts of the sample but approximately 10% in clay-rich sections.

Framework Grains

Sub-angular to sub-rounded quartz grains averaging 0.5 mm in size but with several grains up to 4 mm. In clay-rich zones there are also numerous silt-sized grains <0.1 mm in size.

Matrix

Alunite-rich sections have very low birefringence and also show a speckled pattern. Several patches occur where a second phase of alunite has filled fractures and displays a different orientation to the surrounding matrix.

Clay-rich zones are yellow to orange in colour with low birefringence and occur in elongate patches up to 4 mm wide which are surrounded by alunitic material. The contact between the two matrix materials is sharp. The clay often shows a bi-directional pattern of striations at right angles (bimasepic after Brewer). Isolated small patches of alunite up to 0.1 mm in diameter also occur within the clays.

RM80, Port Willunga, Neva Clay Member

Sandy clay with approximately 60% sand-sized grains. Intervening areas are filled by clays with very few voids.

Framework Grains

Mostly quartz with very rare feldspar and tourmaline. Most grains are 0.2 to 0.3 mm in size with some to 0.5 mm. Common silt-sized quartz grains as well. Grains are sub-rounded to sub-angular showing minor solution and embaying.

Matrix

Very fine clays showing low birefringence. Commonly oriented, particularly around framework grains and along fractures. Patches of yellow and red iron oxides are common and appear to replace clay minerals. Size of these patches varies from 0.1 to 3 mm in diameter with shape being irregular but with some tendency toward elongation, possibly along old fractures.

RM105, Sellicks Beach, Robinson Point Formation

Calcareous sandy clay with sand-sized grains comprising 50 to 60% of sample. Very few voids are present with carbonate or clay filling most intergranular spaces.

Framework Grains

Mostly quartz with very rare opaques and tourmaline. The sub-rounded to sub-angular grains are generally 0.2 to 0.5 mm in size with rare grains up to 1 mm. Moderate sorting is observed.

Matrix

Fine-grained highly birefringent carbonate fills most intergranular pores. Minor yellow-grey clay forms a thin coating around many framework grains and also occurs as rare, isolated patches within the carbonate.

RM113, O'Sullivan Beach Road Railway Cutting, Robinson Point Formation

Sandy clay with approximately 25% of sample comprising sand-sized grains.

Framework Grains

Quartz grains with size mostly in the range 0.2 to 0.3 mm. Rare grains to 0.6 mm are observed. Grains are sub-angular to sub-rounded and scattered randomly through the clay-rich matrix. Some silt-sized quartz grains to 0.05 mm in size also occur.

Matrix

Grey-yellow clay which shows orientation around framework grains. Remainder of clay matrix often shows bi-directional extinction. Isolated patches of red-orange iron oxides to 0.1 mm with some elongate patches along fractures through the clay.

RM120A, Port Noarlunga, Robinson Point Formation

Very fine grained sediment with <20% comprising sand-sized grains. These occur mostly in several thin bands. Fine grained areas include <5% sand-sized grains.

Framework Grains

Sub-angular to sub-rounded quartz with very rare feldspar. Most grains are between 0.2 and 0.3 mm in size with some grains to 0.6 mm. Minor silt-sized quartz is also present.

Matrix

Grey, very low birefringent material which is sometimes almost isotropic comprises most of sample (probable alunite, identified by XRD). Large patches up to 0.5 mm in diameter

extinguish together as a block. These are cut by thin, elongate zones displaying different orientation which represent a second phase of alunite. Minor yellow-brown (clay?) forms laminations on margins of some rounded pores within the sediment which are up to 1 mm in diameter.

RM120B, Port Noarlunga, Robinson Point Formation

Sandy sediment with sand-sized grains forming approximately 70% of sample. Framework grains often form thin bands up to 3 mm thick. Matrix fills most intergranular space.

Framework Grains

Mostly quartz with about 5% feldspar and rare tourmaline, opaques and rutile. Grains are sub-rounded and generally 0.2 to 0.4 mm in size. Some grains to 1 mm are observed with generally poor sorting. Minor embaying shown by larger grains with smaller silt-sized grains being angular to sub-angular. Silt-sized mica laths are common.

Matrix

Colourless material showing very low birefringence; a mix of halloysite and alunite. Some yellowish clay forms thin laminae along elongate fractures. No iron oxides observed.

RM121, Port Noarlunga, Robinson Point Formation

Fine grained sediment with less than 5% comprising sand-sized grains.

Framework Grains

Sub-angular to sub-rounded quartz grains with very rare rounded grains. Most grains are between 0.2 and 0.4 mm in size with rare grains to 1 mm and also some silt-sized grains. Sorting is poor and the quartz grains are generally scattered randomly through the sample.

Matrix

Fine, greyish material which has very low birefringence and displays a patchy, undulose extinction pattern. A second phase of material having a different orientation fills very thin, elongate fracture zones which cut across the matrix. Several small mica laths about 0.1 mm in size show individual layers being forced apart by the alunitic material crystallising between them.

RM134, Robinson Point, Robinson Point Formation

Sandy sediment with approximately 90% comprising sand-sized grains. Considerable porosity with fine matrix forming coatings around larger grains and joining grains with meniscus-like cements.

Framework Grains

Mostly quartz with rare feldspar, tourmaline and opaques. Grains are sub-angular to sub-rounded and well sorted with size mostly in the range from 0.2 to 0.3 mm.

Matrix

Mostly a yellow-orange colour and is a mix of very fine clay and iron oxides. Some brighter red iron-rich patches. Occasional evidence of layering of matrix around framework grains, particularly where meniscus-like deposits join several grains.

RM135, Robinson Point, Robinson Point Formation

Fine grained sediment with approximately 5% sand-sized material.

Framework Grains

Mostly sub-angular to sub-rounded quartz with very rare feldspar. Size of grains averages 0.2 mm but with rare grains up to 0.4 mm. Grains are scattered randomly through the sample.

Matrix

Very low birefringent cryptocrystalline material which displays undulose extinction patterns in some areas. Other parts of the sample show a speckled pattern and these are thought to be alunite-rich.

RM137, Robinson Point, Robinson Point Formation

Sandy sediment with approximately 80% sand-sized grains. Minor yellow and pink patches of iron oxides.

Framework Grains

Mostly quartz grains with rare feldspar, opaques and tourmaline. Grains are sub-rounded and rarely sub-angular. Size is mostly between 0.2 and 0.3 mm with some grains to 0.6 mm. Rare mica laths to 0.1 mm. Mostly moderately well sorted with common small pores (to 0.3 mm size) between grains.

Matrix

Low birefringent clays form thin coatings around many grains but rarely fill intergranular pores. Isolated patches of yellow-orange iron oxides varying in size from 0.1 to 1 mm replace clays coating framework grains and filling pore space. These patches are sometimes elongate.

RM138B, Robinson Point, Robinson Point Formation

Fine grained sediment with approximately 5% sand-sized grains.

Framework Grains

Sub-rounded to rounded quartz grains which are mostly between 0.1 and 0.2 mm in size but with some grains up to 0.6 mm. Sand-sized grains are scattered randomly through the sample.

Matrix

Very low birefringent material which often shows a speckled pattern, most probably due to tiny alunite crystals. Other sections show an undulose extinction pattern. A second phase of

alunite occurs along thin fractures several cm long and displays a different orientation from the surrounding matrix.

RM141B, Onkaparinga Trig, Robinson Point Formation

Sandy sediment with approximately 80% sand-sized grains.

Framework Grains

Sub-angular to sub-rounded quartz grains with rare feldspar. Grains are mostly 0.1 to 0.3 mm in size with some to 0.6 mm and rare silt-sized micas.

Matrix

Very low birefringent clays which are almost isotropic in places (halloysite?) and fill most intergranular spaces, coating many grains. Minor porosity is present. Clays exhibit wavy, undulose extinction in places with some areas showing cumulate textures and others being fibrous in nature.

RM142, Onkaparinga Trig, Robinson Point Formation

Fine grained sediment with less than 2% comprising sand-sized grains.

Framework grains

Rare sub-rounded quartz grains which are scattered randomly through the matrix. Average size of grains is 0.1 mm.

Matrix

Very low birefringent to isotropic cryptocrystalline alunite which often shows undulose extinction over large areas. Numerous elongate fractures averaging 0.05 mm wide are filled with a second phase of alunite which has a completely different orientation.

RM166, Port Moorowie, Quaternary sediments

Fine grained sediment with less than 2% sand-sized grains.

Framework Grains

Sub-rounded to rounded quartz grains up to 0.5 mm in size. Quartz is more common in clay-rich zones compared with alunitic/halloysitic areas.

Matrix

Fine grained, almost isotropic material (probable halloysite) makes up most of matrix. Tiny lozenge-shaped grains (<20 μm in size) are scattered through some sections and probably represent alunitic material.

Small patches of clay up to 5 mm in size occur on the edge of the sample and also embedded within the alunite-rich areas. Some preferred orientation of the clay occurs around the edges of quartz grains. Thin cracks through the clay are filled with nearly isotropic material which is similar to the halloysite-rich matrix.

RM167, Port Moorowie, Quaternary sediments

Fine grained sample with scattered sand-sized quartz grains comprising approximately 5% of the sample.

Framework Grains

Sub-rounded quartz grains averaging 0.2 mm in size but with some grains to 0.4 mm. Silt-sized grains are common and are more angular than larger grains.

Matrix

Very fine grained material with very low birefringence which often displays a mottled to undulose extinction pattern. A second phase of this material exhibiting different orientation fills thin fracture zones through the matrix. A colourless material with low birefringence showing bimasepic clay-like extinction patterns occurs in some areas and is thought to be halloysite which has replaced other clay minerals but retaining previous textures.

RM170, Snapper Point, Neva Clay Member

Fine clay with abundant carbonate. Sand-sized grains comprise less than 10% of sediment.

Framework Grains

Rare sub-angular grains of quartz up to 0.3 mm in size. Occasional round, nodular carbonate masses up to 0.15 mm in size and surrounded by clays. These may be reworked into sediment from carbonate mottles formed elsewhere in the clay-rich sediment.

Matrix

Mostly very fine carbonate. Some pockets of grey to yellowish clay which are completely surrounded by carbonate. These may vary in size from 0.5 to 10 mm and appear to be unaltered by invasion of carbonate. A second stage of carbonate has precipitated in voids and fractures as much larger crystals up to 10 μm in size. Elongate patches of yellow and red iron oxides are often seen along margins of fractures in the sediment.

RM172, Snapper Point, Snapper Point Sand Member

Sandy sediment with sand-sized grains comprising approximately 80% of sample. Grey, very low birefringent clays form coatings on grains and fill some voids. Sediment has moderate porosity (up to 20%).

Framework Grains

All grains observed are quartz with most being sub-rounded but with rare sub-angular grains. Size of grains is up to 1 mm but with most between 0.2 and 0.4 mm. Sediment is well sorted.

Matrix

Clays fill some voids and form coatings around most grains, including some meniscus-like coatings which join adjacent grains. No iron oxides observed.

RM217, Snapper Point, Snapper Point Sand Member

Sandy clay with 50 to 60% sand-sized grains, scattered randomly through the sample.

Framework Grains

Quartz with very rare feldspar. Grains are sub-rounded to rounded and well sorted. Most grains are between 0.2 to 0.4 mm with some to 0.6 mm.

Matrix

Low birefringent clay fills all intergranular space and is oriented around some framework grains and along elongate fractures. Isolated patches of yellow-orange iron oxides up to 0.05 mm in size replace clays with redder patches developed on edges of framework grains and along fractures.

RM220, Snapper Point, Snapper Point Sand Member

Clayey sand with 60 to 70% sand-sized grains.

Framework Grains

Sub-angular to sub-rounded quartz grains with rare feldspar and opaques. Moderate sorting with grains mostly between 0.2 and 0.4 mm in size. Some grains to 1 mm in size. Frequent sub-angular silt-sized quartz grains scattered randomly through the matrix.

Matrix

Clay fills most pore space with some orientation around framework grains and along fractures. Many small patches of red iron oxides from 0.05 to 0.1 mm in size replace clays. Some elongate zones of iron along fractures with larger areas to 0.5 mm size developed through coalescing of smaller patches.

RM238, Snapper Point, Neva Clay Member

Clay-rich sediment with approximately 5% sand-sized grains in a clay-rich matrix.

Framework Grains

Sub-angular to sub-rounded quartz grains scattered randomly through the matrix. Size is mostly between 0.2 and 0.4 mm with rare grains showing embayed edges. About 20% of sample comprises sub-angular silt-sized quartz grains.

Matrix

Fine clay which is commonly oriented to produce a striated birefringence pattern (bimasepic, after Brewer 1964). Clay is also oriented along fractures running through the sediment. Can often observe small silt-sized mica grains (up to 5 μm in size) within the matrix. Rare, round carbonate masses occur within the matrix and are up to 60 μm in size. Smaller masses up to 20 μm appear concretionary and have a highly birefringent centre with thick outer walls.

RM250, Maslin Bay, Robinson Point Formation

Clayey sand with approximately 75% sand-sized grains. Black manganese oxides form thin bands through the sample.

Framework Grains

Sub-rounded to sub-angular quartz grains with rare feldspar. Size is mostly between 0.2 and 0.5 mm with some grains to 1 mm and numerous silt-sized grains of 0.05 mm. Sorting is moderate.

Matrix

Clay fills most voids and coats framework grains. Minor lamination of clay is seen along margins of several cross-cutting fractures. About 10% of sample comprises black, isotropic manganese oxides (identified using XRF) which form elongate, parallel zones varying from 0.3 to 2 mm width. Manganese oxides replace clays in pore space in these zones with yellow-orange iron oxides (goethite) forming small, isolated zones adjacent to the manganese oxide.

RM264, Maslin Bay, Robinson Point Formation

Iron-rich mottle from sandy interval. Sand-sized grains form approximately 70% of the sample with clay or iron oxides filling many intergranular voids. Section shows transition from iron-rich mottle to unmottled sediment.

Framework Grains

Mostly quartz grains with rare feldspars. Rare composite quartz grains and some which show undulose extinction. Grains are sub-rounded to rounded and mostly between 0.3 to 0.5 mm in size. Some grains up to 1 mm are observed as well as many small, silt-sized grains which tend to be more angular than larger grains. Embaying of grains is uncommon in unmottled part of sediment but common in mottled parts. Feldspars are often considerably etched and corroded in mottled portions with replacement of grains by iron oxides.

Matrix

In unmottled portions, low birefringent clay forms thin oriented coatings around framework grains and joins grains by way of meniscus cements. Numerous voids are up to 0.2 mm in diameter. Colourless, isotropic material with high relief is probably opal and fills some voids, coats grains and partially replaces some quartz grains.

In mottled portions, red to black iron oxides have almost completely replaced clays filling all intergranular space and coating larger grains. Replacement of quartz grains and feldspars by iron oxides is common. In places, small pockets of yellow-grey clay remain and are completely enclosed by dark iron oxides. Opal is only rarely observed in mottled areas.

In transitional portions, red to orange iron oxides replace some clay, occurring as small blotches and in elongate zones along fractures in sediment.

RM293, Onkaparinga Trig, Robinson Point Formation

Fine sandy clay with approximately 70% of sample comprising sand-sized grains.

Framework Grains

Dominantly quartz with very rare opaques, garnet and rutile. Average grain size is 0.1 mm with some grains to 0.2 mm and also <0.05 mm (silt). Most grains are sub-angular and well sorted.

Matrix

Yellow-green to grey clay fills many intergranular spaces and coats framework grains. No orientation of clay is noted. Rare tiny patches of red iron oxides (mostly <0.05 mm) within the clay matrix. Voids form about 10 to 20% of sample. Many are rounded in shape but with some being elongate and up to 4 mm in size. These may be biogenic in origin.

RM297, Onkaparinga Trig, Robinson Point Formation

Silty sediment, from palaeosol horizon. Clay forms approximately 30% of sample with remainder being silt and sand-sized grains.

Framework Grains

Mostly quartz but with some feldspar and micas. Quartz and feldspar are mostly sub-angular and 50 to 100 μm in size with rare grains to 0.5 mm. Micas are mostly muscovite but with some biotite and generally 20 to 50 μm in size.

Voids

Some circular to oval-shaped voids up to 0.2 mm in diameter are observed. These are coated by dark black-brown organic-rich clays which tend to be laminated. These probably represent burrows of soil organisms.

Matrix

Yellow-grey clay coats larger grains and partially fills voids. Little orientation of clays is observed compared with other samples from this study. Yellow-orange iron oxides form small patches up to 0.2 mm in diameter replacing clays and silt-sized micas.

RM319, Onkaparinga Trig, Neva Clay Member

Clay-rich sediment with abundant carbonate. Less than 10% of the sediment comprises sand-sized grains.

Framework Grains

Quartz grains up to 0.4 mm in size scattered randomly through the sample. Grains are sub-angular to sub-rounded. Some round carbonate masses up to 0.2 mm in size are noted completely surrounded by clay.

Matrix

Mostly very fine carbonate with rare patches of grey-yellow clay up to 1 mm in size. Secondary carbonate with crystals up to 10 μm in size fills some voids and fractures.

RM349, Hallett Cove, Robinson Point Formation

Red, iron-rich mottle from indurated sandy unit. Sand-sized grains form approximately 60% of the sample.

Framework Grains

Mostly quartz with minor feldspar and mica. Grains are sub-angular to sub-rounded, mostly about 0.25 mm in size but with some grains to 1 mm. There are a significant number of small, more angular, silt-sized grains approximately 0.05 mm in size. Many grains, particularly the smaller ones show embaying of margins.

Matrix

Mostly very dark red to black iron oxides which replace clays and fill all intergranular voids. Where iron has replaced margins of quartz grains, very small crystallites up to 2 μm are observed. Some isolated pods of fine-grained clay-rich material up to 4 mm in diameter occur. These contain small patches of orange-red iron oxides and silt-sized quartz grains. On edges of the mottled area, minor opal is observed filling some pores.

RM353, Hallett Cove, Robinson Point Formation

Red clayey sand forming mottle with approximately 60% of sample comprising sand-sized grains.

Framework Grains

Sub-rounded to rounded quartz with very rare opaques and rutile. Moderate sorting with most grains between 0.3 and 0.5 mm in size. Some grains to 1 mm and also many silt-sized grains <0.5 mm.

Matrix

Clay forms small part of matrix and where present fills intergranular space, coats framework grains and shows orientation around some larger grains. In mottled zone, red to black iron oxides completely replace clays and also margins of some quartz grains. Fractures in many framework grains also filled by iron oxides. Transition from clay to iron oxides is relatively sharp and takes place over a 2 mm zone. Small patches of iron oxides within clay frequently coalesce particularly along elongate fracture zones. Yellowish (goethitic?) iron oxides are often present on margins of red mottled areas.

APPENDIX 7: XRF DATA

1. Major Element Geochemistry <2um Fraction

Sample	Location	Fe2O3 %	MnO %	TiO2 %	CaO %	K2O %	SiO2 %	Al2O3 %	MgO %	SiO2:Al2O3
RM144	OT	8.9	0.013	0.43	0.06	2.18	49.9	21.7	2.1	2.30
RM219	SP	9.2	0.016	0.81	0.40	2.01	50.3	22.3	3.3	2.26
RM221	SP	3.0	0.003	0.69	0.11	1.14	26.7	15.8	2.9	1.69
RM226	SP	9.0	0.019	0.84	0.35	3.41	53.0	22.3	3.1	2.38
RM238	SP	8.9	0.020	0.83	0.16	3.02	50.0	21.4	3.0	2.34
RM249	MB	18.4	0.067	0.35	0.20	1.23	45.2	12.3	4.3	3.67
RM259	MB	5.9	0.009	0.88	0.08	1.42	44.7	25.3	3.5	1.77
RM262	MB	2.9	0.002	0.82	0.09	1.22	29.5	18.4	4.3	1.60
RM266	MB	1.9	0.004	1.17	0.32	1.77	53.8	13.4	4.1	4.01
RM269	MB	6.9	0.013	1.46	0.35	2.18	51.3	21.8	4.3	2.35
RM282	MB	8.7	0.021	0.86	0.18	2.61	50.6	21.5	3.1	2.35
RM291	OT	2.7	0.004	0.16	0.09	0.49	32.3	25.7	8.2	1.26
RM293	OT	9.4	0.017	0.62	0.10	2.34	46.4	21.0	4.4	2.21
RM294	OT	10.0	0.012	1.07	0.07	1.48	49.5	21.0	2.9	2.36
RM296	OT	6.0	0.006	0.48	0.26	0.74	29.7	16.2	5.1	1.83
RM298	OT	7.6	0.012	0.46	0.22	1.01	31.1	14.3	4.5	2.17
RM299	OT	9.7	0.015	1.03	0.07	1.33	45.0	20.3	4.0	2.22
RM300	OT	7.0	0.023	0.79	0.51	1.46	34.0	16.6	4.5	2.05
RM301	OT	10.3	0.020	0.80	0.10	1.33	36.8	20.0	2.9	1.84
RM302	OT	8.5	0.012	0.61	0.09	1.33	29.7	16.6	3.0	1.79
RM303	OT	7.4	0.014	0.98	0.13	1.44	41.4	18.8	4.1	2.20
RM304	OT	9.4	0.020	1.09	0.13	1.55	44.5	22.4	2.6	1.99
RM312	OT	8.0	0.018	0.86	0.10	2.58	50.3	23.8	2.1	2.11
RM315	OT	8.2	0.008	0.74	0.14	2.58	36.4	22.4	1.2	1.63
RM316	OT	7.9	0.022	0.68	2.16	3.22	50.2	20.1	4.3	2.50
RM318	OT	7.7	0.021	0.70	0.51	3.24	49.6	20.7	3.4	2.40
RM320	OT	8.4	0.025	0.70	0.85	3.28	50.9	21.5	3.0	2.37
RM327	OT	3.1	0.007	0.38	0.25	1.02	27.8	36.5	2.5	0.76
RM332	OT	9.3	0.028	0.73	0.14	2.55	48.0	21.4	3.5	2.24
RM341	HC	9.7	0.023	0.83	0.12	2.45	47.3	23.2	1.8	2.04
RM350	HC	2.3	0.005	0.76	0.17	1.24	37.5	23.0	2.5	1.63
RM361	HC	9.7	0.016	0.80	0.10	1.77	49.1	22.6	2.2	2.17
RM362	HC	5.4	0.013	1.14	0.06	1.95	51.9	25.8	1.9	2.01
RM368	HC	9.5	0.020	0.84	0.11	2.27	52.0	21.9	2.1	2.37
RM369	HC	9.0	0.021	0.86	0.08	2.44	51.3	21.5	2.0	2.39

NOTE All clays Mg saturated
OT = Onkaparinga Trig
SP = Snapper Point
MB = Maslin Bay
HC = Hallett Cove

APPENDIX 7: XRF DATA

2. Low dilution analyses of the <2μm fraction

Sample	Location	SiO2 %	Al2O3	Fe2O3 %	MgO %	CaO %	Na2O %	K2O %	TiO2 %
RM259	MB	42.6	24.7	5.7	5.2	0.06	0.12	1.39	0.92
RM282	MB	43.3	19.4	7.7	4.5	0.20	0.16	2.32	0.80
RM294	OT	44.2	19.8	9.2	4.4	0.04	0.17	1.35	1.01
RM304	OT	40.7	21.0	9.0	5.2	0.06	0.19	1.43	1.06
RM312	OT	44.3	22.3	7.1	3.3	0.06	0.13	2.35	0.80
RM318	OT	44.3	19.4	7.0	4.9	0.48	0.18	3.06	0.66
RM327	OT	38.4	19.7	6.2	7.9	0.13	0.19	1.80	0.81
RM332	OT	42.5	19.8	8.3	5.1	0.07	0.18	2.33	0.70

Sample	Location	P2O5 %	MnO %	Cu ppm	Zn ppm	Sr ppm	Zr ppm	Ni ppm	Rb ppm
RM259	MB	2.33	0.008	70	34	40	186	32	144
RM282	MB	1.22	0.016	39	36	71	145	23	114
RM294	OT	1.29	0.010	122	61	46	196	25	118
RM304	OT	4.30	0.015	115	82	56	243	32	147
RM312	OT	1.00	0.014	43	47	42	155	35	120
RM318	OT	1.68	0.017	33	40	77	137	41	123
RM327	OT	6.60	0.015	98	65	89	190	38	107
RM332	OT	2.20	0.023	65	64	69	146	37	113

Sample	Location	Ba ppm	V ppm	Cr ppm	La ppm	Ce ppm	Pb ppm	Y ppm	Co ppm
RM259	MB	128	70	122	51	<10	18	19	7
RM282	MB	174	108	98	18	<10	17	15	9
RM294	OT	120	94	127	17	<10	31	16	8
RM304	OT	185	108	126	25	27	49	25	14
RM312	OT	166	75	97	21	<10	27	14	14
RM318	OT	120	43	116	12	<10	35	15	13
RM327	OT	130	76	114	78	18	48	19	10
RM332	OT	147	109	95	36	50	39	47	9

Sample	Location	Ga ppm	U ppm	Th ppm	Ignition Loss %	Sum %
RM259	MB	30	5	7	18.7	83.1
RM282	MB	25	<5	<5	21.0	79.7
RM294	OT	35	5	6	21.6	81.6
RM304	OT	38	<5	14	21.7	83.1
RM312	OT	27	<5	7	20.3	81.5
RM318	OT	23	<5	<5	20.7	81.8
RM327	OT	28	<5	13	21.8	81.9
RM332	OT	24	<5	11	20.7	81.3

NOTE All clays Mg saturated and with some residual Calgon (phosphate)
MB = Maslin Bay
OT = Onkaparinga Trig

APPENDIX 7: XRF DATA

3. Analyses of various bulk samples

Sample	Location	Description	Na2O	MgO	Al2O3	SiO2	P2O5	SO3
A. MOTTLED ZONES								
RM24	Sellicks Beach	Pallid	2.4	0.96	17.27	59.9	0.03	0.09
RM25	Sellicks Beach	Mottle	1.9	0.74	13.35	60.5	0.08	0.03
RM28-1	Sellicks Beach	Pallid	0.9	0.62	11.71	73.3	0.03	tr
RM28-2	Sellicks Beach	Mottle	0.8	0.63	9.75	54.0	0.15	0.01
RM30	Mitcham	Pallid	0.5	0.70	18.25	65.4	0.02	nd
RM31	Mitcham	Mottle	0.4	0.49	11.98	47.7	0.13	0.01
RM32-1	Mitcham	Pallid	0.6	0.61	15.71	67.8	0.03	0.01
RM32-2	Mitcham	Mottle	0.7	0.50	13.90	61.3	0.03	0.05
RM40	Ochre Point	Hard mottle	0.4	0.18	2.32	67.0	0.09	0.03
RM41	Ochre Point	Soft mottle	0.8	0.30	3.15	60.8	0.08	0.01
RM62-1	Port Moorowie	Pallid	1.4	0.90	10.18	71.1	0.02	nd
RM62-2	Port Moorowie	Mottle	0.9	0.82	6.69	35.1	0.14	0.01
B. SEDIMENTS								
RM33	Hallett Cove	NCM	1.3	1.45	15.33	55.5	0.06	0.14
RM34	Ochre Cove	RPF	1.6	0.46	3.51	84.8	0.36	0.04
RM35	Ochre Cove	NCM	1.2	0.91	8.84	72.3	0.02	0.08
RM42	Ochre Point	HCSS	0.4	0.20	1.56	88.2	0.08	0.02
RM43	Ochre Point	NCM	0.9	0.93	13.83	67.5	0.02	nd
RM44	Ochre Point	SPSM	1.2	1.02	10.89	73.8	0.02	0.03
RM45	Ochre Point	SPSM	2.0	1.85	13.02	62.8	0.03	0.05
RM46	Ochre Point	NCM	1.7	1.34	17.15	56.2	0.02	0.07
RM63	Port Moorowie	Alunite interval	1.6	1.09	42.01	40.3	0.21	
RM64	Port Moorowie	Halloysite	1.5	0.38	45.75	52.4	0.01	nd
RM120A	Port Noarlunga	Alunite interval	3.2	0.75	38.61	48.7	0.24	
RM142	Onkaparinga Trig	Alunite	1.3	0.30	60.88	2.9	0.24	

NOTE All values are percentages
Samples RM63, RM64, RM120A, RM142 prepared as ignited samples. Sulphur not recorded for alunite-rich samples due to ignition losses.
NCM = Neva Clay Member
SPSM = Snapper Point Sand Member
RPF = Robinson Point Formation
HCSS = Hallett Cove Sandstone
tr = present in trace amounts
nd = not detected

Sample	K2O	CaO	TiO2	MnO	Fe2O3	Ignition Loss	Total
A. MOTTLED ZONES							
RM24	2.63	0.05	1.02	0.01	1.67	13.67	100.7
RM25	2.52	0.05	0.97	0.01	9.94	10.03	100.1
RM28-1	2.71	0.16	1.00	tr	2.18	7.24	99.8
RM28-2	2.11	0.14	0.80	0.01	22.79	8.81	100.0
RM30	2.33	0.30	1.23	tr	2.05	9.22	100.0
RM31	1.74	0.24	0.84	0.01	26.88	9.44	99.8
RM32-1	2.30	0.23	1.34	tr	2.70	8.52	99.9
RM32-2	2.04	0.22	1.27	0.01	11.53	8.63	100.2
RM40	0.44	0.08	0.13	0.01	24.08	5.29	100.0
RM41	0.55	0.07	0.26	0.01	24.85	9.20	100.1
RM62-1	3.34	0.11	0.98	0.01	1.73	9.66	99.5
RM62-2	1.95	0.16	0.46	0.02	45.64	8.32	100.2
B. SEDIMENTS							
RM33	2.62	0.35	0.70	0.02	7.22	15.71	100.4
RM34	0.76	0.12	0.55	tr	3.27	5.64	101.1
RM35	1.49	0.18	0.75	0.01	4.35	10.52	100.7
RM42	0.47	0.12	0.12	0.02	7.52	2.38	101.1
RM43	1.39	0.11	0.75	0.01	4.40	11.87	101.7
RM44	1.02	0.06	0.48	0.01	3.12	10.00	101.6
RM45	1.88	0.11	0.51	0.05	4.52	15.12	101.9
RM46	1.86	0.12	0.84	0.02	5.92	16.78	102.0
RM63	8.52	0.24	0.29	0.01	2.73	Note	97.0
RM64	0.09	0.29	nd	tr	0.11	Note	100.5
RM120A	6.15	0.07	0.04	nd	0.38	Note	98.1
RM142	16.47	0.06	0.03	tr	0.58	Note	82.8